Research & Technology 1992

National Aeronautics and Space Administration

Lewis Research Center
Cleveland, Ohio 44135

TM-105924

Introduction

The NASA Lewis Research Center has moved forward in a great number of areas during 1992. One of the most significant accomplishments was the new Strategic Plan. The Strategic Plan clearly sets out a course that Lewis will follow both organizationally and technically. It is required reading for anyone interested in the direction of our technical programs. In conjunction with the Strategic Plan, Total Quality Management has been targeted as an essential component of Lewis' future success in an increasingly competitive environment

The 1992 Research & Technology report is organized so that a broad cross section of the community can readily use it. A short introductory paragraph begins each article and will prove to be an invaluable reference tool for the layperson. The approximately 200 articles summarize the progress made during the year in various technical areas and portray the technical and administrative support associated with Lewis technology programs. If additional information is desired, the reader is encouraged to contact the authors identified in the articles.

The principal purpose of this report is to give a brief but comprehensive review of the technical accomplishments of the Center during the past year. It is a testimony to the dedication and competence of all the employees, civil servants and contractors, who make up the staff.

The Lewis Research Center is a unique facility, located in an important geographic sector, with a long and distinguished history of performing research and technology development in support of NASA's mission and the Nation's needs.

L J Ross

Lawrence J. Ross
Director

Inquiries regarding this report can be addressed to the Office of Interagency and Industry Programs, Mail Stop 3–7. The telephone number is (216) 433–5382.

ORIGINAL PAGE
BLACK AND WHITE PHOTOGRAPH

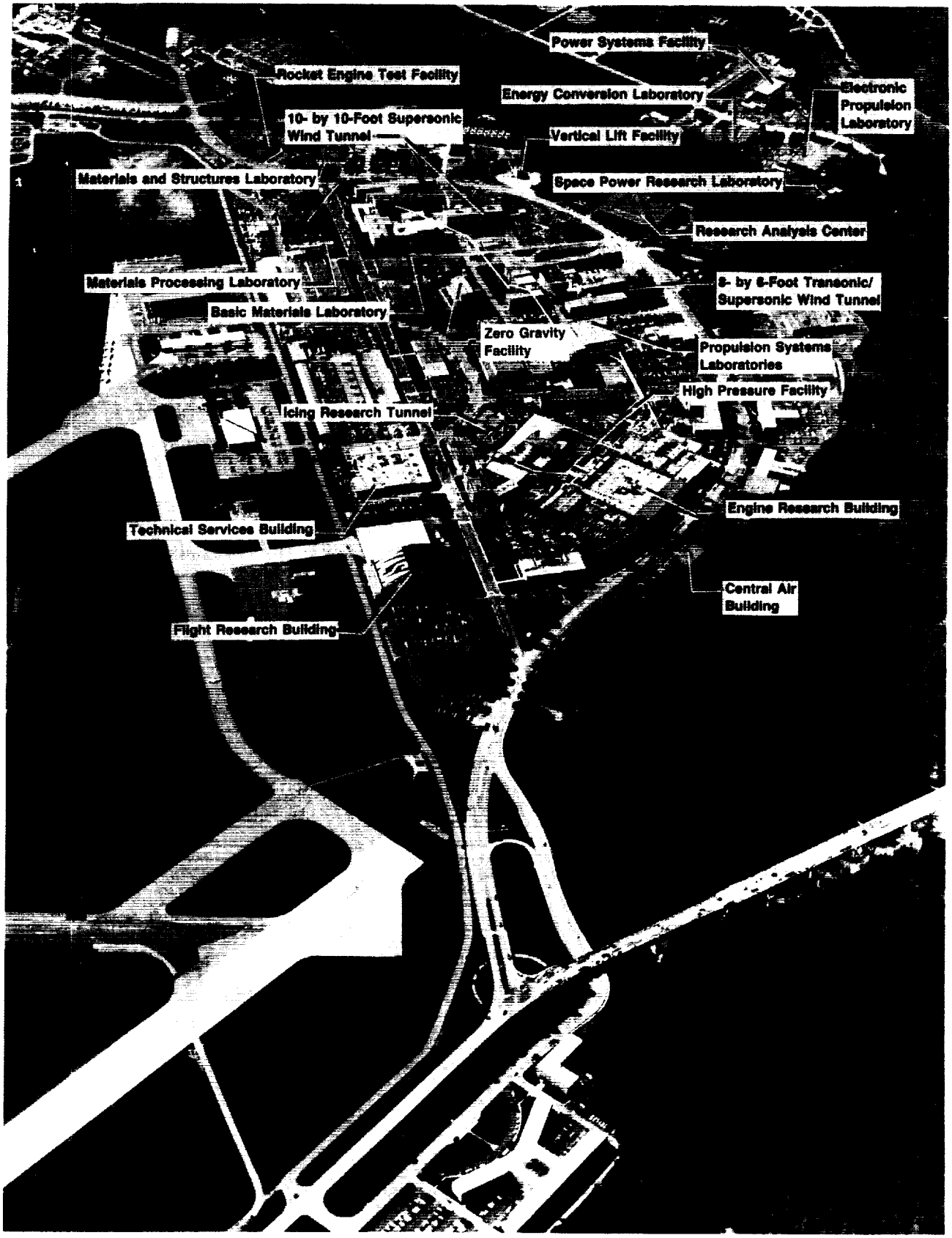

Lewis Research Center, Cleveland, Ohio

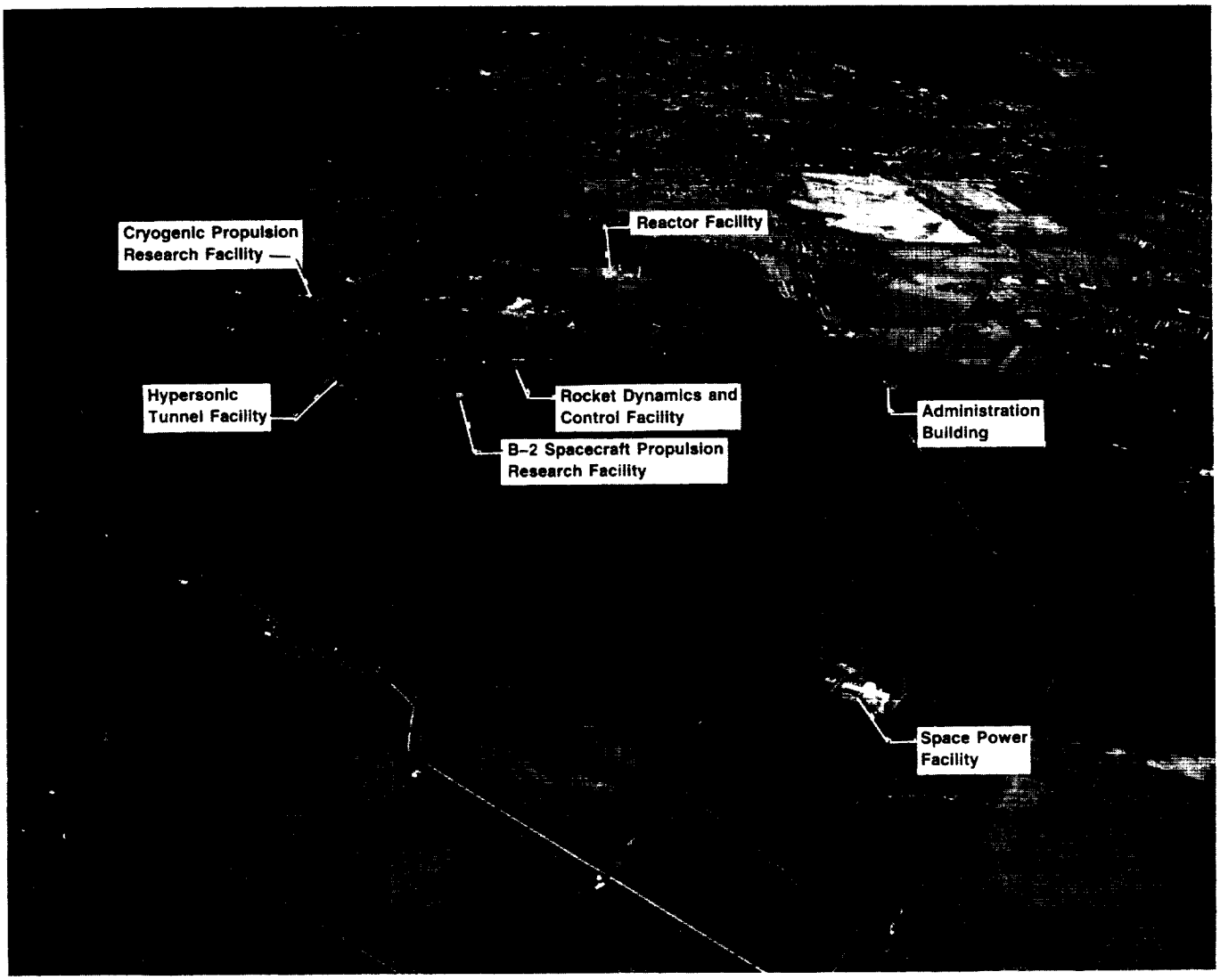

Plum Brook Station, Sandusky, Ohio

NASA Lewis Research Center

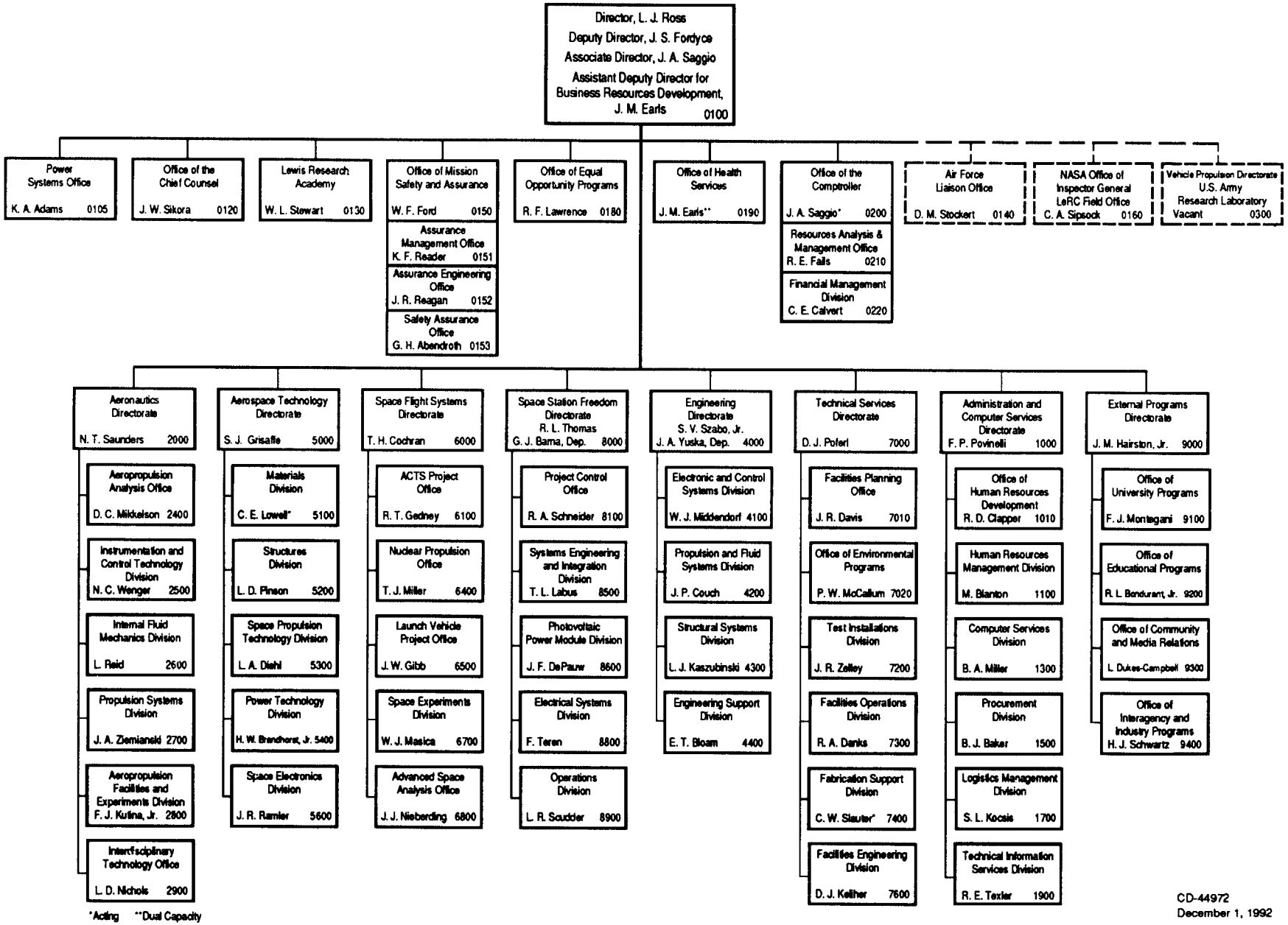

*Acting **Dual Capacity

CD-44972
December 1, 1992

Contents

Aeronautics

Aeropropulsion Analysis

Integrated Propulsion/Airframe Analysis System Optimizes Aircraft Design

An integrated system for the multidisciplinary analysis and optimization of airframe and propulsion design parameters is being developed in the NASA Lewis Aeropropulsion Analysis Office. The integrated propulsion/airframe analysis system (IPAS) significantly reduces the time required to optimize an advanced aircraft design and to assess the potential benefits of advanced propulsion concepts and technologies.

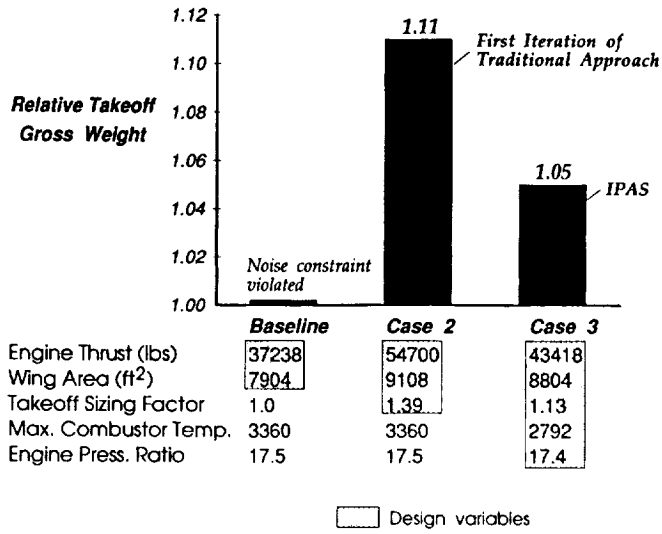

Traditional mission analysis versus IPAS.

In the traditional method of analysis, engine cycles are loosely coupled to their respective airframes and missions. This process includes several steps. First, a thermodynamic cycle analysis is done to establish a plausible propulsion system. Next, a mission analysis is performed to determine the overall performance of this propulsion system on a predefined aircraft. The mission analysis does allow for variations of the basic airframe design parameters. Therefore, the optimum airframe can be determined for a given fixed engine cycle. Then, in order to determine the best combination of propulsion system and airframe, it is necessary to iterate on the key propulsion design parameters until an overall optimum solution has been achieved. This process is time consuming and labor intensive. However, it must be done because the results that drive the propulsion system design selection can only be obtained by performing a mission analysis.

In IPAS the propulsion system, airframe, and mission are closely coupled. The propulsion system analysis code is directly integrated into the mission analysis code. This allows the propulsion design parameters to be optimized along with the airframe and mission design parameters, thereby significantly reducing the time required to obtain an optimized solution.

The capabilities of IPAS were demonstrated on a Mach 2.4 high-speed civil transport problem. The objective was to determine the minimum takeoff gross weight for an aircraft subject to the constraints of a takeoff field length of 11,000 ft and Federal Aviation Regulations (FAR) 36 stage III noise requirements. Three cases were run. The first case was used as a baseline. It was run with the airframe design parameters allowed to vary but the propulsion system design parameters fixed at values that were initially thought to yield the optimum solution. The noise constraint was not taken into account. The result was an aircraft that was well over the FAR 36 stage III noise requirements.

The second case was run to show what overall results the initial engine design guess gave when the noise constraint was considered. Once again the engine design parameters were fixed and the airframe design parameters were allowed to vary. The latter included the takeoff sizing factor, which represents how much the engine must be oversized so that it can be throttled back at takeoff to reduce the jet noise. This time the noise constraint was met. However, because the engine design was fixed, the only way to meet this constraint was to oversize the engine by 39 percent. The resulting poor match between the cycle, airframe, and mission yielded a weight penalty of 11 percent. This case represents the first step in the traditional iterative process.

The third case was run to determine the overall optimum results of using IPAS. All of the engine and airframe design parameters were now allowed to vary. The noise constraint was met through a combination of oversizing the engine and lowering the maximum combustor temperature. This

optimum combination of cycle, airframe, and mission yielded a weight penalty of only 5 percent. The engineer would eventually achieve this result by the traditional method. However, it would require many iterations to approach this solution, taking about five days. Using IPAS, an optimized solution can be obtained in only one run, taking about one day (6 hours of CPU time), a time saving of approximately 80 pecent.

Lewis contact: Thomas M. Lavelle, (216) 977-7042
Headquarters program office: OAST

Broad-Speed-Range Engines Proposed for Advanced High-Speed Tilt Rotor Transports

Advanced tilt rotor transports may help alleviate airport overcrowding without building new larger airfields. This aircraft takes off and lands vertically with the rotors in a horizontal position. It then tilts its rotors into the vertical plane and cruises as a fixed-wing turboprop aircraft. With appropriate propulsion systems this aircraft can cruise efficiently at speeds greater than 400 knots (Mach 0.65).

Takeoff and landing require a high-subsonic rotor tip velocity. However, for quiet, efficient cruise operation the sum of the rotor tip speed due to rotation and that due to forward velocity must remain subsonic. The rotor, now acting as a propeller, must rotate as much as 50 percent slower than during takeoff and landing. Reducing the engine rotational speed to do this would result in 18 percent larger engines with 20 percent worse specific fuel consumption (SFC).

The solution is to develop new engine systems that can run efficiently at both high and low speeds while operating a full power—the broad-speed-range engine. As part of contracted efforts Allison Gas Turbine Division of General Motors and General Electric studied several concepts. Three concepts proved to be the most attractive:

- The reduced-stage-loading power turbine adds stages to the turbine and has airfoils capable of running well with angles of incidence from −45° to 60°. Here the engine size increase required is only 4 percent and the SFC penalty is only 6 percent.

- The counterrotating turbine offers the greatest improvement. Here the increase in engine size is only 1 percent and the SFC penalty is just 2 percent. The power turbine in this engine operates like a conventional turbine during takeoff and landing. During cruise the turbine "stators" are unlocked and rotate in the opposite direction of the turbine rotor, thus

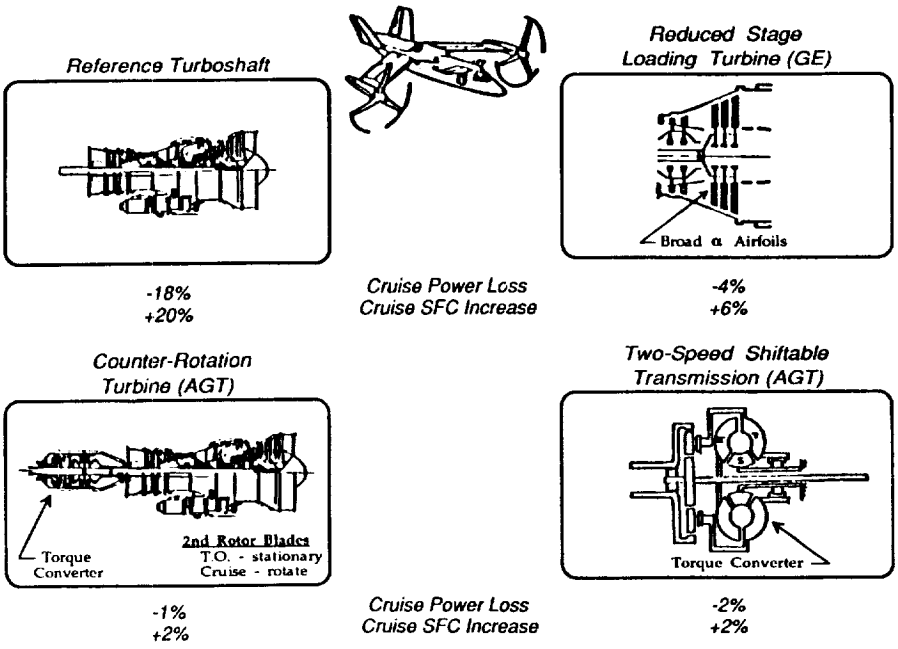

Broad-speed-range engines for advanced high-speed tilt rotor transports (Mach 0.65).

becoming a counterrotating turbine. In this mode the shaft speed to the rotor/propeller is half of that during takeoff. A gearbox and a torque converter are required to combine power from both shafts and ensure a smooth transition between modes. The torque converter would be emptied of fluid after mode shifting is completed in order to avoid heat loss into the fluid.

- The two-speed shiftable transmission offers improvements close to that of the counterrotating turbine and requires no modifications to the engine itself. Here the engine would have to be only 2 percent larger with a 2 percent penalty in SFC. A two-speed transmission is combined with a torque converter similar to that described previously for shifting between modes.

Each concept will incur some weight penalties because of the extra equipment required (torque converter, etc.), but these penalties are expected to be modest and will be far outweighed by the improved SFC. These engine systems do require some technical developments—aerodynamic and structural design of broad-speed-range turbine airfoils, a torque converter having 10 times the current power capacity, and a lockup device for counterrotating turbines.

Lewis contact: Joseph D. Eisenberg, (216) 977-7027
Headquarters program office: OAST

Instrumentation and Control Technology

Four-Spot, Time-of-Flight Laser Anemometer Used in Small Centrifugal Compressor Research

Computer codes are being developed to model the complex, highly turbulent flow fields within centrifugal compressors. The computational fluid dynamics models require benchmark data to compare with their predictions and to validate the assumptions used. The blade passages within the centrifugal compressor impeller are relatively shallow, from 64 mm at the inlet to 17 mm at the diffuser. A nonintrusive optical diagnostic is required for measuring the complex flow field within the impeller passages. The demanding requirements of the centrifugal compressor necessitate the use of a laser anemometer with special qualities.

The four-spot, time-of-flight anemometer (TOFA) is a hybrid laser anemometer system specifically designed to facilitate measurements in the demanding environment of centrifugal compressors. The probe volume coding scheme employs two pairs of partially overlapping, elliptical spots. The overlapping spots are orthogonally polarized so that light scattered by particles can be distinguished from each spot. An argon ion laser operating in the multiple-line mode is used to generate blue (488 nm) and green (514.5 nm) spot pairs with a higher light flux in the probe volume than a single-color system. The elliptical spots accommodate the large variation in particle trajectories caused by high turbulence levels. The elliptical spots are 50 μm high by 10 μm wide and separated by 100 μm, yielding an acceptance angle of ±30°. The small width of the spots provides high spatial selectivity, which enables the detector to discriminate against background noise and therefore allows measurements close to surfaces. The high light flux in the probe volume enables the use of small seed particles that will accurately follow the flow.

The overlapping spot pairs in the four-spot TOFA simplify the signal-processing requirements. The signals obtained from the overlapping spot pairs generate optimum-shaped bipolar pulses that are independent of velocity, which minimizes the measurement error and eliminates electronic delay circuitry. The velocity is calculated from the known spot spacing and the measured pulse-to-pulse particle transit time. A custom signal-processing module was designed and built that contains a standard counterprocessor timer module for measuring the particle transit time. The timer module uses a commercial host computer interface.

The single-component, four-spot TOFA is used to measure the two-dimensional flow velocity vector by orienting the spot pairs to three different angles to the mean flow angle with an image rotator and recording a velocity histogram at each orientation. The estimated mean velocities at the

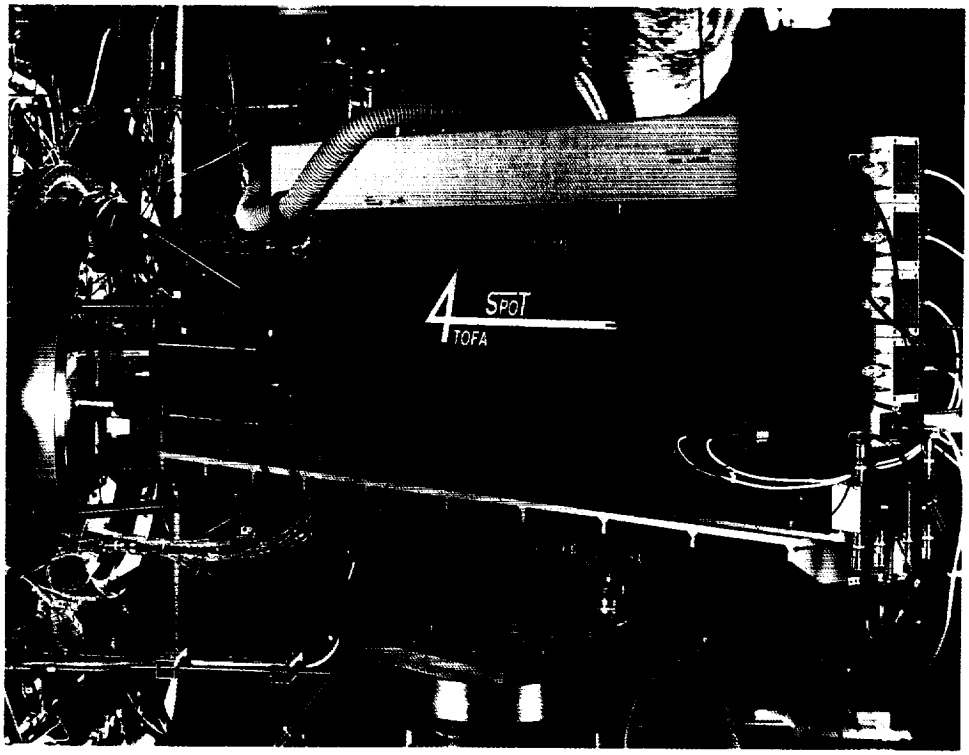

Four-spot, time-of-flight laser anemometer.

different spot orientation angles are used to calculate the two-dimensional velocity vector's magnitude and angle.

The compressor facility was seeded with 0.7-μm-diameter polystyrene latex spheres. Sixteen viewing ports, located along the shroud from the impeller inlet to the diffuser, enabled optical access for the velocity measurements. Fifteen spanwise velocity surveys were completed; the survey range varied depending on the window size and the impeller surface contour. Several of the surveys ranged from 5 to 95 percent of span.

Lewis contact: Dr. Mark P. Wernet, (216) 433–3752
Headquarters program office: OAST

Optical Strain Measurements Made Possible on Fibers and Wires

Strong, lightweight structural materials being developed for high-temperature aeronautical and astronautical applications have pushed test measurement requirements beyond traditional measurement techniques. Therefore, optical strain measurement systems have been developed to measure strain on small-diameter wires and fibers used in state-of-the-art, high-temperature composite materials. These optical strain measurement systems meet the stringent requirements of being noncontacting, being able to make pinpoint measurements on minute specimens, operating at high temperatures, and requiring no surface preparation. The research and development work for this technique was done for NASA Lewis through a contract with Sverdrup Technology, Inc. An application of this work has provided a custom-built strain measurement system for a fiber research laboratory at NASA Lewis, and this system is currently being installed.

These strain measurement systems use the speckle-shift technique, which detects the movement of laser speckle patterns generated at a measurement point on a test specimen. Laser speckle appears as mottled lighting and is a random interference effect that occurs when spatially coherent light reflects off an optically rough surface (any nonmirrored surface). The speckle patterns move at the detector array because of surface strains as well as rigid body motions of the specimen. During the measurement the

speckle movements due to rigid body motions are cancelled mathematically by using two symmetrical laser beams to make two absolute measurements; only the desired strain term then remains. This automatic cancellation of rigid body motion is a great advantage over some other optical techniques, which require tedious postprocessing procedures to recover the strain data.

Tests of systems developed at Lewis have demonstrated both one- and two-dimensional strain measurements on flat bar specimens at temperatures beyond 750 °C. These are among the highest temperatures at which strains have ever been measured. Recent testing has demonstrated accurate strain and Young's modulus measurements on ceramic fibers as small as 22 μm in diameter at room temperature (these fibers are thinner than a human hair). Accurate strain measurements have been made on polycrystalline aluminum oxide, sapphire, and silicon carbide fibers and on tungsten-rhenium, palladium-chromium, and platinum wires. In the process of investigating any high-temperature limits on the technique, speckle pattern stability has been demonstrated at temperatures beyond 2000 °C, indicating that strain measurements are feasible in this high-temperature regime. The speckle-shift technique also can measure small translations and rotations of objects, in lieu of strain. The technique's features, including the ability to unobtrusively measure strain on a wide variety of specimen materials, make it a powerful research tool for many of today's high technology applications.

Bibliography

Lant, C.T.: Advanced One-Dimensional Optical Strain Measurement System—Phase IV. (Sverdrup Technology, Inc., NASA Contract NAS3-25266). NASA CR-190760, 1992.

Oberle, L.G.; et al.: An Application of the Speckle-Shift Technique to Measuring Strain in Fibers. HITEMP Review 1991: Advanced High Temperature Engine Materials Technology Program. NASA CP-10082, 1992, pp. 66-1 to 66-8.

Lewis contacts: Christian T. Lant, (216) 433-6360; Dr. John P. Barranger, (216) 433-3642; Lawrence G. Oberle, (216) 433-3647; Lawrence C. Greer III, (216) 433-8770

Headquarters program office: OAST

Silicon Carbide Epilayers and PN Junction Diodes Greatly Improved

The High Temperature Integrated Electronics and Sensors (HTIES) Program is currently developing a new family of silicon carbide (SiC) semiconductor devices for use in high-temperature, high-power, and/or high-radiation conditions where conventional semiconductors (such as silicon) cannot operate. These devices have numerous important applications within the aerospace areas of propulsion control, power control, radar and communications, and radiation-hardened circuits. A family of hostile-environment integrated electronics and sensors would also find numerous important spinoff applications in the Earth-bound commercial power and automobile industries.

SiC occurs in many different crystal structures (called polytypes), each having its own unique electrical and optical properties. 3C-SiC and 6H-SiC are the two most common polytypes that have been investigated to date. The electrical performance of 6H-SiC devices has been far superior to that of 3C-SiC devices, entirely because growth techniques for producing 6H-SiC substrates and epitaxial films are more advanced.

The purity and quality of the semiconductor crystal are naturally critical limiting factors for semiconductor devices. The NASA Lewis HTIES group has recently developed a new chemical vapor deposition (CVD) growth process that consistently and reproducibly yields the highest purity single-crystal SiC epilayers (both 3C and 6H) reported to

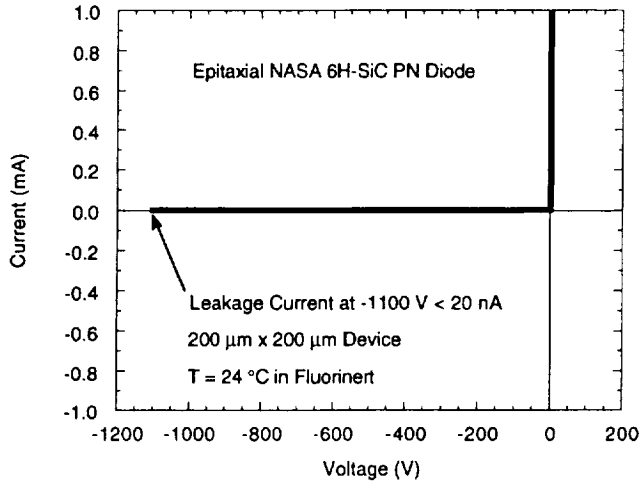

6H-SiC PN diode current-voltage characteristics.

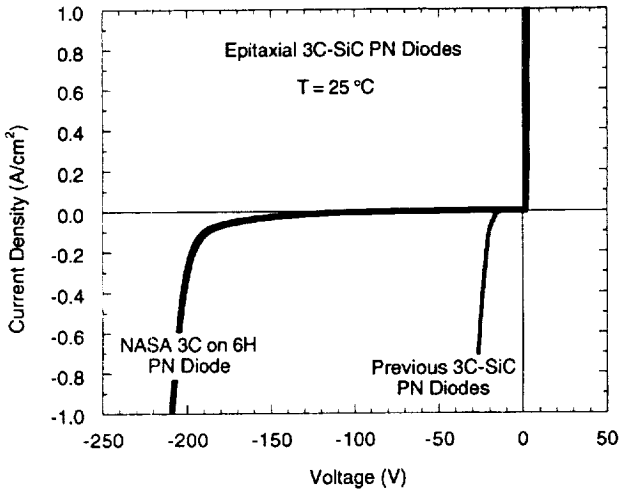

3C-SiC PN diode current-voltage characteristics.

date. The new technique has been employed to fabricate 3C- and 6H-SiC PN junction diodes that exhibit record-shattering electrical performance characteristics.

The reverse breakdown voltage of an epitaxial 6H-SiC PN junction diode exceeded our 1100-V measurement capabilities. To the best of our knowledge the 20-nA leakage current represents the lowest room-temperature leakage current density (<50 $\mu A/cm^2$) ever reported in a semiconductor diode at an applied reverse bias above 1 kV.

The 3C polytype diode blocked current at a 200-V reverse bias. This diode represents a greater than fourfold improvement in reported 3C-SiC PN junction rectification voltage. When placed under sufficient forward bias the 3C diodes emitted a bright green-yellow light. To the best of our knowledge, this work represents the first report of a significantly bright 3C-SiC light-emitting diode.

As evidenced by the record-setting diode characteristics, the improved-quality SiC offered by the NASA Lewis growth techniques should enhance the electrical performance of most SiC-based devices and circuits.

Lewis contacts: Dr. David J. Larkin, (216) 433–8718; Dr. Philip G. Neudeck, (216) 433–8902
Headquarters program office: OAST

Expert System Diagnoses Rocket Engine Faults

Performance goals for the Space Shuttle and future reusable rocket engines include significant reduction in overall operating cost, increased flight rates, improved performance, and extended engine life. Achieving these goals will require engine controllers to have integrated diagnostic capabilities that will diagnose anomalous operation, implement accommodating closed-loop control to extend engine life, and maximize available system performance. These are the goals of the Intelligent Control System (ICS) Project (ref. 1) at NASA Lewis.

A diagnostic system that is compatible with an intelligent control system has several unique requirements. Detection and isolation of failures must be performed in real time. The diagnosis must be able to address emergency conditions and critical failures on a priority basis. The diagnostic system must take advantage of many diverse types of analytical processing to determine the health of individual engine components and subsystems and must combine these sources of information with knowledge of the engine physics and failure modes to diagnose faults. The diagnostic system must be able to interface with an external expert system residing in the intelligent controller. Finally, because the physical engine and knowledge of its operation are constantly changing, the diagnostic system must be easily updated and expanded.

The architecture of the reusable rocket engine diagnostic system (ReREDS) has been developed (ref. 2) with these requirements in mind and to have a versatile user-interface that allows the diagnostic process to be carefully monitored and interrogated. The ReREDS system architecture has three layers of information processing: the condition-monitoring layer, the fault-detecting layer, and the expert system layer. The structure places the low-intelligence analytical processing functionality at the bottom of the hierarchy and the most abstract reasoning functionalities at the top of the hierarchy.

The ReREDS condition-monitoring functions validate the sensor channels through voting, determine the relative sensor state (against the expected normal operating conditions), and assess bearing health through spectral analysis. Each fault detector checks a particular sensor

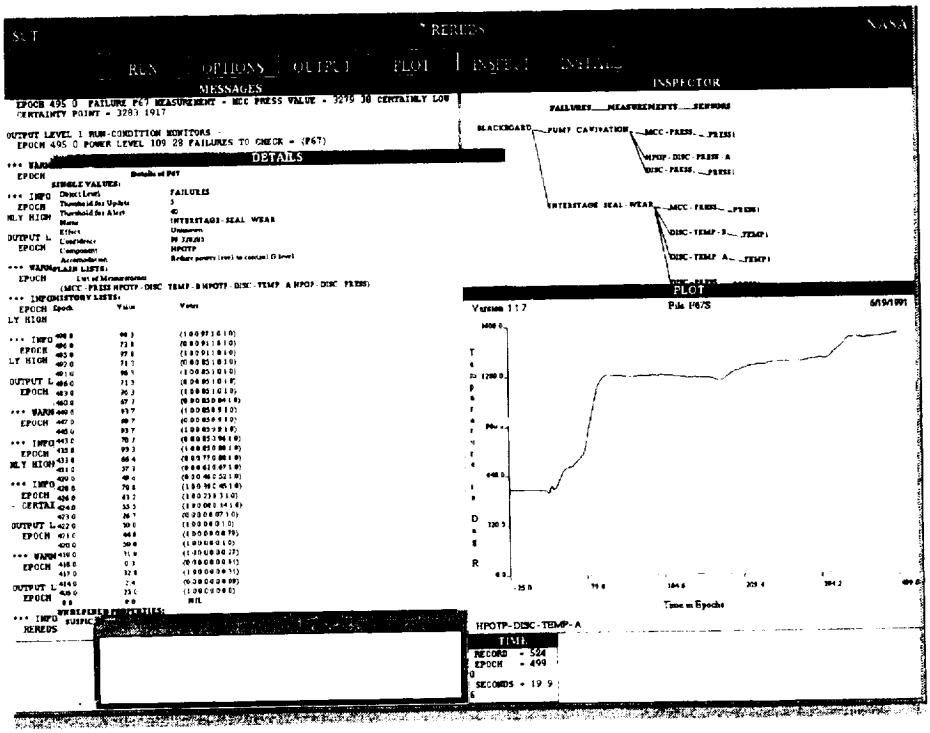

ReREDS display.

pattern of selected faults that has been obtained by interviewing field rocket engine experts. The expert system layer of the hierarchy coordinates the fault detectors. It contains knowledge of fault mode propagation, the expected correlation between the fault detectors, and the relative priority of the fault modes. The expert system uses this knowledge to resolve conflicting reports from the fault detectors, to maintain a record of the engine health status, and to produce a failure report, which is passed to the intelligent controller. The fault report contains the current engine health status in terms of diagnosed faults, confidence levels for the diagnosis, and an estimate of the severity of the faults.

ReREDS is a menu-driving system. It is implemented in a hierarchical and decentralized blackboard design by using Common Lisp.

References

1. Merrill, W.C.; and Lorenzo, C.F.: A Reusable Rocket Engine Intelligent Control. AIAA Paper 88–3114, 1988.
2. Anex, R.P.; Russel, J.R.; and Guo, T.H.: Development of an Intelligent Diagnostic System for Reusable Rocket Engine Control. AIAA Paper 911–2533, 1991.

Lewis contact: Ten-Huei Guo, (216) 433–3734
Headquarters program office: OAST

Modified Government Baseline Engine Control System Tested in Altitude Facility

The performance of the propulsion system for the National Aerospace Plane (NASP) will be crucial to the successful flight of the X–30 NASP vehicle. The NASP propulsion system will require an advanced digital control system in order to achieve its maximum performance. In support of the NASP program a series of tests were completed this year in the NASA Lewis PSL–4 facility on a generic hydrogen-fueled ramjet called the modified government baseline engine (MGBE). This

type of engine is being considered for the NASP. The objectives of the tests were to investigate the performance, dynamics, and control of such engines and provide data to the NASP program.

The PSL–4 facility was modified by adding hydrogen-air preheaters to allow testing at Mach 3.44. The MGBE is a subscale engine, about 55 in. long with a minimum (throat) cross section of 2 by 3 in. During the tests supersonic facility airflow was captured and compressed by the engine's mixed-compression inlet, and fuel was added in the subsonic combustor and expanded through the variable-area exhaust nozzle. Primary MGBE features included throat bleeds, shoulder bleed, a movable cowl flap, multiple fuel injection locations, a movable exhaust nozzle flap, and an upstream flow-disturbance-generator system. A digital control system, which commanded fuel flow, cowl position, and nozzle flap position, was designed for the engine. A number of high-temperature dynamic pressure sensors were installed throughout the engine duct to provide control system feedback signals. The objectives of the MGBE controls tests were to demonstrate a feedback control system that would provide closed-loop combustor pressure control for enhanced engine stability and automatic restart control in the event of an inlet unstart. The control logic was implemented on a microprocessor-based control computer, the CIM (control, interface, and monitor) unit. The control logic in the CIM modulated fuel flow and nozzle area to keep the combustor pressure within specified limits and moved the cowl flap to accomplish engine restarts. An alternative version of the control logic was also tested, in which an estimate of the internal normal-shock position, instead of the combustor pressure, was computed and regulated by the control.

The MGBE tests in PSL–4 successfully demonstrated a closed-loop control system for the engine. Typical tests were run to prove-out the control: (1) step input tests—perturbing the engine and verifying that the control produced well-behaved engine output responses; (2) throttle responses—showing that the control caused engine thrust to follow throttle commands; and (3) unstart tests—unstarting the engine and having the control sense the unstart and automatically perform a restart. The test results provide a data base for ramjet control design and analysis for NASP-type engines in the supersonic flight regime.

Lewis contact: Dr. Bruce Lehtinen, (216) 433–3746
Headquarters program office: OAST

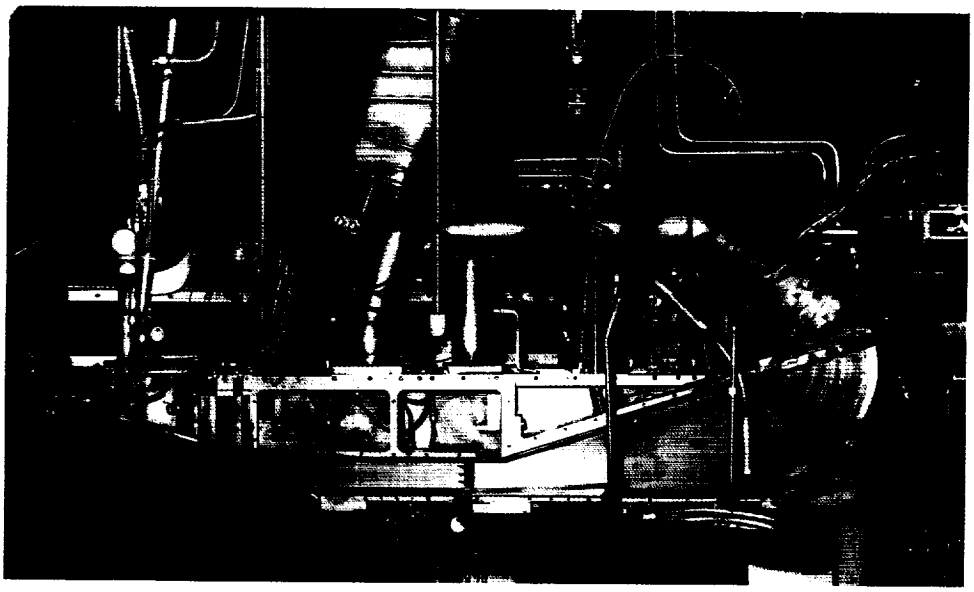

Government baseline engine installed in PSL–4 for controls testing.

Wave Rotor Core Modeled

The wave rotor is presently being investigated for use as a core gas generator for multiple-spool gas turbine engines in order to achieve high peak cycle temperatures and pressures. The device uses unsteady waves to transfer energy directly to and from the working fluid through which the waves travel. It consists of a series of constant-area passages (tubes) that rotate about an axis. Through rotation the ends of the tubes are periodically exposed to various circumferentially arranged ports in which the flow is steady but which initiate unsteady waves within the tubes. Because of the unsteady nature of the device, each tube of the wave rotor is periodically exposed to both hot and cold flow over roughly equal time periods. The mean temperature of the rotor material may therefore be expected to remain considerably below the peak cycle temperature. This characteristic and the anticipated low rotational speed for a given mass flow give the wave rotor several potential advantages over conventional gas generators.

Analyzing wave rotor behavior is difficult because the model that is used must integrate time-dependent (e.g., hyperbolic) equations of motion, often with shock waves present. Because closed-form solutions of these equations do not generally exist, numerical methods must be used. An effort is presently under way to develop such a model. The model follows a single tube of the wave rotor as it is exposed to the various ports at either end. The tube is assumed to have uniform properties at any cross section (i.e., one-dimensional flow), and the gas is assumed to be calorically perfect. As the tube rotates, running sums of the mass, momentum, and energy fluxes in the ports are recorded. These are then used to calculate the steady averaged flow properties in the ports.

The model has been favorably compared with several simplified wave rotor experiments designed to demonstrate the principle of work by using unsteady waves. With these benchmark comparisons as a validation for the model, the next phase of the work will be to use the model to design a full wave rotor gas generator core and to analyze its behavior in the full engine environment.

Lewis contact: Daniel E. Paxson, (216) 433–8334
Headquarters program office: OAST

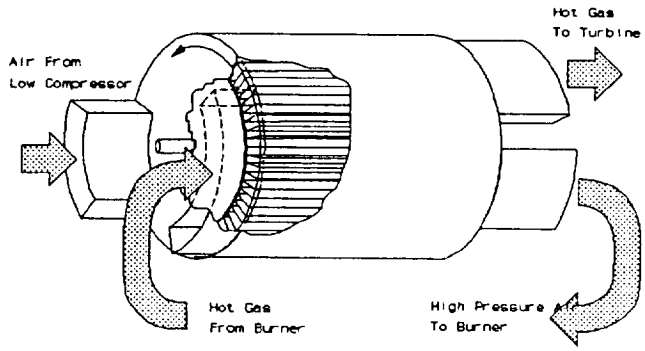

Wave rotor core model.

Internal Fluid Mechanics

Hierarchically Structured Euler/Navier-Stokes Solver Speeds Grid Generation

Of the many goals promised for the future of computational fluid dynamics, perhaps the two most important are accuracy and geometric flexibility. Geometric flexibility is a pacing item because for complicated geometries generating a grid (upon which the solution is desired) can often take many work hours, and for a realistic geometry, is a formidable task. Once a grid is generated, the accuracy of the solution may be suspect, unless refinement of the grid shows that all important flow features are manifested and well resolved. NASA Lewis is working to address both of these goals: geometric flexibility through the use of unstructured grids, and accuracy by locally adaptive mesh refinement.

Only through proper formulation and matching of the solution algorithm and computational data structures can unstructured grids yield accurate solutions for complex geometries. The approach relies upon a hierarchical description of the unstructured grid and is based upon a finite-volume, Godunov-based scheme. The grid generation is entirely automatic. As the grid is generated, the hierarchy of the process is stored in a binary data tree. The data tree inherently contains important geometric data simply by its construction and allows all connectivity to be obtained by logical tree traversals. By use of

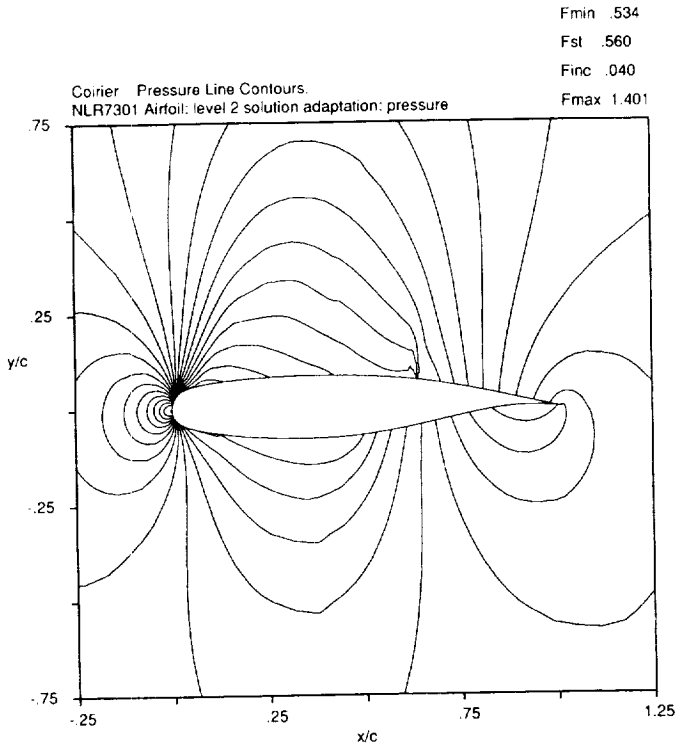

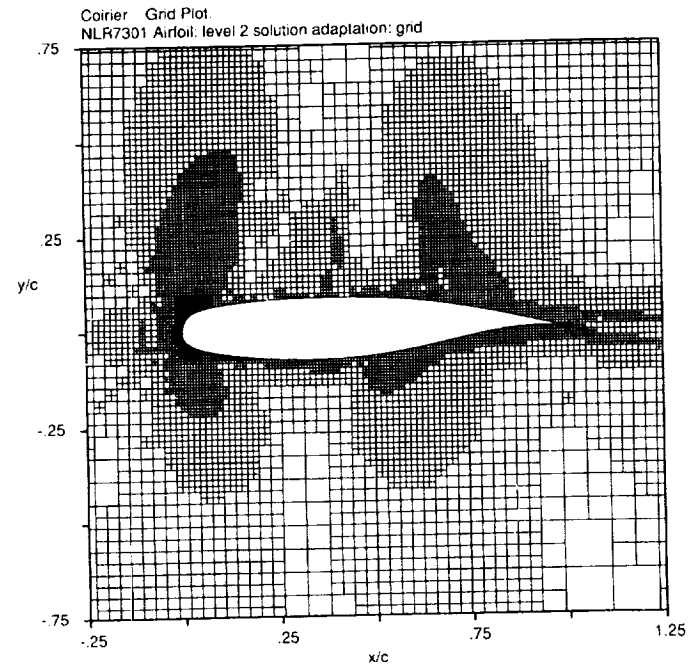

Adaptively refined grid and pressure line contours about a supercritical airfoil at near-design conditions.

Cartesian cells the resulting grid is highly isotropic in regions away from bodies. At boundaries of bodies the cells are actually cut from the background Cartesian mesh into irregularly shaped cells. The solution in each cell is reconstructed in a K-exact fashion and is used to compute the fluxes through the cell boundaries by an approximate Riemann solver (Roe's scheme). Monotonicity is obtained by using a limiting procedure that is similar to a minimum-modulus scheme. Accuracy of the resulting scheme is enhanced by automatically adapting the grid around important flow features. The adaptation is keyed to a cell-size-weighted statistical description of the local velocity divergence and velocity curl.

Shown here is a calculation of an isolated, supercritical airfoil at near-design conditions. A base grid was generated (automatically), upon which a flow solution was obtained. On the basis of this solution the grid was refined and coarsened in regions dictated by the adaptation criteria, and then a new flow solution was obtained. This process (from initial grid generation to solution to adaptation) is completely automatic. The plots show the resulting grid and pressure line contours after two levels of adaptive mesh refinement.

The work is being performed in-house and in collaboration with the University of Michigan Aerospace Engineering Department while the author is performing research for his Ph.D. dissertation.

Lewis contact: William J. Coirier, (216) 433–5764
Headquarters program office: OAST

Turbulent Flow Solved Over Backward-Facing Step

When considering internal flow for an engineering calculation, one often encounters a turbulent flow separation. Examples include flow in a curved duct, flow over a ramped injector, and flow in a turbine blade cooling passage. Thus, in order to predict the recirculating flow field by using a Navier-Stokes calculation, an efficient turbulence modeling technique must be used. Many state-of-the-art flow solvers have implemented the energy-dissipation model, or k-ε model, as a compromise between accuracy and efficiency. No one turbulence model has been demonstrated to accurately predict all of the characteristics of turbulence encountered in an engineering environment. However, a particular class of flow phenomenon can often be adequately predicted

by an appropriate choice of turbulence model. Separated flow stretches the predictive capabilities of the k-ε technique, often resulting in an error of 12 percent in the reattachment length. However, one particularly efficient implementation has been shown to yield the best possible results for the energy-dissipation model when flow separation is encountered.

In this study four different low-turbulent-Reynolds-number k-ε models were compared against the standard, or high-turbulent-Reynolds-number formulation. All five forms were based on the isotropic eddy viscosity assumption. The major difference between the two techniques lies in the resolution of the near-wall flow. The low-turbulence-Reynolds number model sets a boundary condition at the wall and fully resolves the near-wall gradients in the velocity and turbulence components. This implies a fine mesh spacing near all no-slip boundaries. The high-turbulent-Reynolds-number model determines an interior location near the edge of the viscous sublayer for imposing a turbulent boundary condition, thus avoiding the need to numerically resolve the near-wall gradients. Although this results in a gain in efficiency, it is often argued that one surrenders a certain degree of accuracy. The surprising conclusions of this research for separated flow over a backward-facing step demonstrate that the more efficient technique also yields the more accurate result. This is stictly a fortuitous situation because the boundary conditions used for the high-turbulent-Reynolds-number technique are not valid for separated flow.

The calculations were compared against the experimental data of Driver and Seegmiller (ref. 1). Results include velocity, static pressure coefficient, friction coefficient, and turbulent stress components. The two formulations generally agree in all but the friction coefficient data, where the high-turbulent-Reynolds-number data are clearly in better agreement with the experimental findings.

This research is being completed in-house and is presently being compiled into a NASA Technical Memorandum.

Reference

1. Driver, D.M.; and Seegmiller, H.L.: Features of a Reattaching Turbulent Shear Layer in Divergent Channel Flow. AIAA J., vol. 23, no. 2, 1985, pp. 163–171.

Lewis contact: Christopher J. Steffen, (216) 433–8508
Headquarters program office: OAST

Parallel Turbomachinery Codes Made Portable

Computer simulations of multidisciplinary, grand-challenge problems, such as airflow through the blade passages of aircraft engine turbomachinery, involve considerable programming effort and computing time. Simulation time and cost can be achieved by computing portions of the simulation simultaneously, using parallel computers. Many different parallel computers are available, each having a unique programming environment that takes significant time to learn. In the future these problems may be solved in a distributed, heterogeneous, computing environment, which complicates the programming effort even more. A programming approach based on the application portable parallel library (APPL) is intended to minimize the learning curve and programming effort required to move application codes to different and/or networked machines.

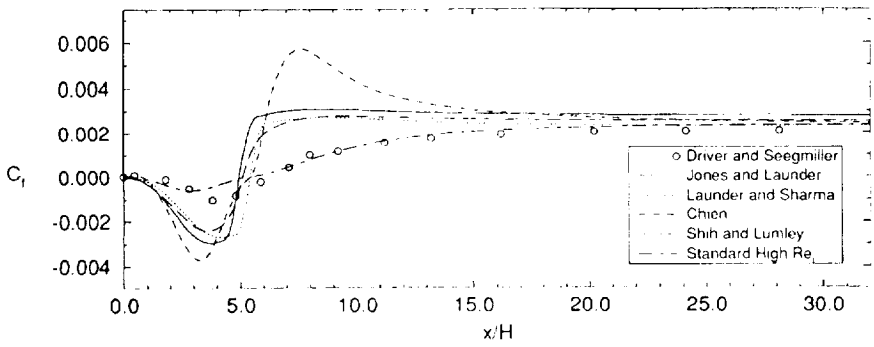

Friction coefficient along stepside wall, downstream of separation point.

In the APPL approach an application program is developed by the user thinking in terms of communicating processes rather than a particular hardware physical architecture. The processes execute in parallel on separate processors and exchange information as needed. Basic message-passing primitives, making up the APPL, are used to communicate between processes. The primitives are the same, regardless of the machine, thus making the application program port-able. Once the application is developed, the user has the freedom of mapping it to a particular hardware configuration by specifying a process definition file. A special initiator task takes care of initializing the environment and loading the executable code.

Two parallel turbomachinery codes have been developed by using APPL. The first is an inviscid code, called ISTAGE (ref. 1), which is configured to solve for the flow within a single blade passage. The performance of the parallel version of ISTAGE was determined for three different parallel computers, as shown in a log-log plot of time spent for 20 iterations of the code versus number of processors. The Intel iPSC/860 and Delta machines are commercial parallel computers. The Hypercluster is an in-house, parallel-processing testbed (ref. 2). The performance of the same code was also determined on a single processor of the Cray Y/MP. The best performance was achieved when compiler and algorithm optimization were applied to the iPSC/860 version of ISTAGE. Roughly half of the single-processor Y/MP performance was achieved with this code by using 32 processors on the iPSC/860.

The second code is a viscous code called MSTAGE (ref. 3). The test case here was a two-stage compressor (four blade rows). APPL was used to compute, in parallel, the flows within each individual blade row. This code has been tested on the Hypercluster and a network of IBM RS6000 workstations. The Hypercluster times were determined for 15 cycles, and the IBM RS6000 times for 45 cycles. The IBM RS6000 version of the code yielded 30 percent of the performance of a

Number of processors	Hypercluster		RS6000		Cray Y/MP time, sec
	Time (15 cycles), sec	Speed-up	Time (45 cycles), sec	Speed-up	
1	40,185	------	20,660	------	1,714
2	20,231	1.99	10,912	1.89	-------
4	10,272	3.91	6,038	3.42	-------

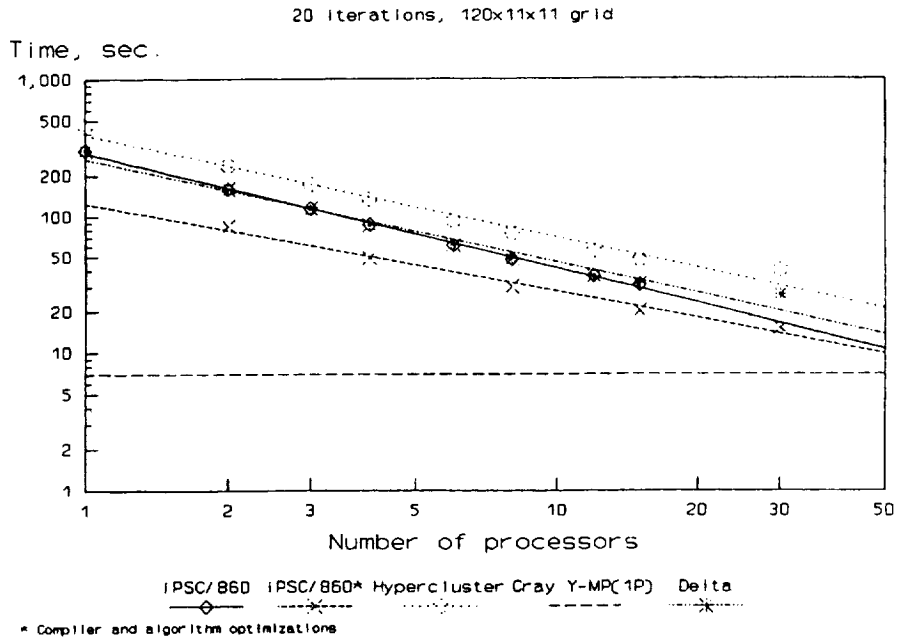

Parallel ISTAGE performance.

single-processor Cray Y/MP. The low cost of the workstations, relative to the Cray, results in a performance/price ratio that is roughly four times that of a Cray Y/MP. Plans include development of a more massively parallel version of MSTAGE and comparisons of its performance on networked workstations and other parallel computers.

References

1. Celestina, M.L.; et al.: A Numerical Simulation of the Inviscid Flow Through a Counterrotating Propeller. J. Turbomach., vol. 108, Oct. 1986, pp. 187–193.
2. Cole, G.L.; Blech, R.A.; and Quealy, A.: Initial Operating Capability for the Hypercluster Parallel Processing Test-Bed. NASA TM–101953, 1989.
3. Adamczyk, J.J.; et al.: Simulation of Three-Dimensional Viscous Flow Within a Multistage Turbine. J. Turbomach., vol. 112, no. 3, July 1990, pp. 370–376.

Lewis contacts: Angela M. Quealy, (216) 826–6642; Richard A. Blech, (216) 433–3657
Headquarters program office: OAST

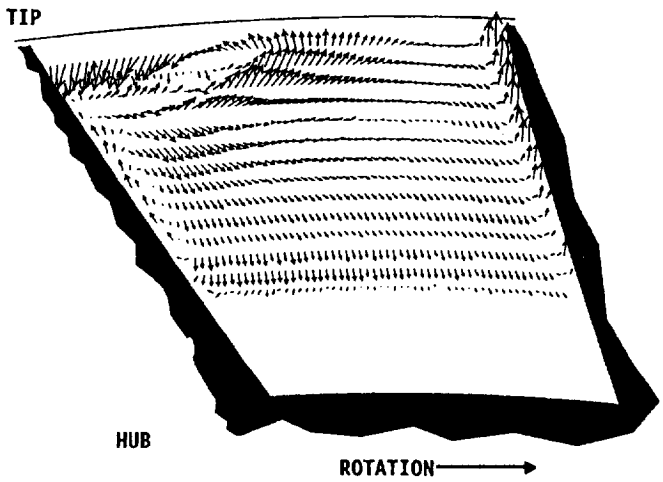

Sample solution for the NASA Lewis Large, Low-Speed Multistage Axial Compressor.

accommodated. The solution provides preliminary flow information that is useful in setting up more sophisticated simulations.

Lewis contact: Dr. Eric R. McFarland, (216) 433–5915
Headquarters program office: OAST

Rapid Multistage Turbomachinery Analysis Method Developed

A typical gas turbine engine includes multiple stages of rotating and stationary blades. Existing numerical methods used in the design of these machines require an enormous amount of computer time to directly account for the interaction of the flow disturbance caused by one blade row on the adjacent downstream rows. In order to analyze these effects more efficiently, a computer code has been developed that can rapidly calculate multiple-blade-row flows on a two-dimensional, blade-to-blade surface of revolution.

In this code, inviscid compressible equations are solved in the absolute frame of reference by using an integral technique. The potential flow effects of relative motion between blade rows are included in the solution. No computational grid is required.

Speed and ease of use make this procedure a potentially useful design tool. Variations in blade geometry and engine configuration are easily

Flow Physics Studied for Multistage Axial Compressor

As turbine engine requirements continue to push back the limits on axial compressor performance, basic understanding of the flow behavior in the multistage environment becomes more essential. Continued flight envelope expansion and fuel burn reductions drive compressor designs far beyond current design experience. The current multistage design approaches are based on time-averaged axisymmetric flow-field representations, but the actual flow field is asymmetric and unsteady. As part of a program to expand the understanding of multistage effects at NASA Lewis, a new experimental Large Low-Speed Multistage Axial Compressor Facility is now in operation. The low-speed multistage experiments are being conducted to execute detailed experiments in order to identify relevant flow physics, to provide interaction between detailed experiments and emerging average-passage and Navier-Stokes computational fluid dynamics (CFD) methods, and to provide data for the development of flow models required by the CFD codes.

Preliminary tests in the new four-stage compressor facility have been completed. The measured performance of the machine compares well with the design intent.

Lewis contact: Dr. Michael D. Hathaway, (216) 433–6250
Headquarters program office: OAST

Engineering Computational Models Being Developed for Film Cooling

There is a growing tendency to use higher temperatures at the inlet to a gas turbine in an effort to improve the thermal efficiency and increase the specific power output. This calls for increasingly effective means of cooling the turbine blades. One cooling technique presently receiving wide application is film cooling. Currently, the design of a film-cooling configuration relies primarily on empirical information. The ability to accurately simulate the film-cooling process with computational fluid dynamics computer codes would allow the designer much more flexibility. With this in mind a comprehensive program is being established with the goals to investigate the basic physics of the flow interactions involved in film cooling, to develop the turbulence models needed to describe these flow interactions, and to develop the engineering models needed to accurately account for film cooling in the turbine heat transfer design process.

Preliminary attempts to use a three-dimensional Navier-Stokes code for computing heat transfer to a film-cooled airfoil have been successful.

Lewis contact: Dr. Vijay K. Garg, (216) 433–6788
Headquarters program office: OAST

Centrifugal Compressor Flow Physics Studied

Centrifugal compressors are used in relatively small propulsion systems for vehicles such as helicopters and small business jets. These compressors are attractive in small engines because of their potential for higher performance, greater reliability, and lower initial cost than small axial compressors. However, centrifugal compressors generally have lower efficiency than axial compressors. Research is currently aimed at improving the efficiency levels of centrifugal compressors.

The flow field within centrifugal compressors is extremely complex and includes flow features such as thick blade surface, hub, and casing boundary layers; strong secondary and tip leakage flows; shock waves in the inducer region of high-speed compressors; and strong unsteady flow interactions between the rotating impeller blades and the stationary diffuser vanes. These flow features currently limit the efficiency of centrifugal compressors. Successful management of these features is the key to improving centrifugal compressor performance.

Centrifugal compressor flow fields are being studied at NASA Lewis through a tightly coupled experimental and numerical research analysis program in order to develop insight that can be used to improve the design of new centrifugal compressors. Experiments are being performed in small, high-speed compressors and in a large, low-speed compressor. Numerical analysis tools that solve the full three-dimensional, viscous Navier-Stokes equations are also being used to predict the measured flow fields. These predictions are being used to guide the experimental measurements.

Laser-based instrumentation has been used to study the three-dimensional flow field in a large, low-speed centrifugal compressor. The inlet diameter of the impeller is about 3 ft and the exit diameter is 5 ft. The rotor blade height varies from about 9 in. at the inlet to about 6 in. at the exit. This large size allows detailed measurements of all three velocity components within the blade passage. Viscous flow effects, which are confined to thin regions near the blade surfaces, have been successfully measured for the first time in this unique facility, providing the most detailed data of this kind available. Currently, engine manufacturers are beginning to use advanced computer programs to predict the complex flows occurring in turbomachines. In order to fully profit from the capability of these codes, the designers must have confidence that the results obtained adequately describe the physics involved. By using the data obtained on the large, low-speed centrifugal compressor to assess the computer code, the designer can determine to what extent results of the computer code can be

relied upon. By utilizing computer codes that have been extensively tested against data such as that obtained on this centrifugal compressor, engine manufacturers will be able to improve the performance of modern aircraft engines.

Lewis contact: Dr. Anthony J. Strazisar, (216) 433-5881
Headquarters program office: OAST

Experimental Data Taken on a Hydrogen Planar Shear Layer

We have all watched flames and been fascinated by the intricate patterns produced as the fuel and air gases mix and burn, adding color to the flow. Patterns of mixing exist in high-speed flow as well. Although some studies had been performed on high-speed combustion, understanding of the physical phenomenon was incomplete. Not enough data existed to back up theories and numerical models for the compressible subsonic combustion of gas turbine and rocket flow. The goal of the Planar Reacting Shear Layer Experiment was to gain additional physical insight into the flow field and to provide quantitative benchmark data to calibrate and improve the numerical models.

If two streams of flow with different flow speeds are brought together, vortices are introduced into the shear layer and mixed. A shear layer is one of the most fundamental flow phenomena inside a combustor. In a planar reacting shear layer experiment in combustion research, the fuel stream and the oxidizer stream with different flow speeds are brought together. There are two competing factors: the chemical reaction time (the combustion) and the mixing time. At low speed the mixing is much slower than the chemical reaction so that as soon as the fuel and the oxidizer mix, they react. At high speeds the mixing and the chemical reaction compete and interact, with combustion affecting the mixing.

A fine grid of measurement points was needed to provide detailed mapping of the flow structures. A specially designed continuous-flow facility was constructed to acquire the extensive amount of data and to meet the severe test requirements, which include high gas temperatures and pressures, hydrogen fuel, and special fluids for flow visualization (e.g., titanium tetrachloride).

Data have been obtained for a reacting and a nonreacting hydrogen shear layer at high subsonic Mach numbers. Flow visualization and quantitative measurements of velocity, turbulence, and temperature were made for the same conditions with and without chemical reaction. These data will be used for benchmark verification of computer codes.

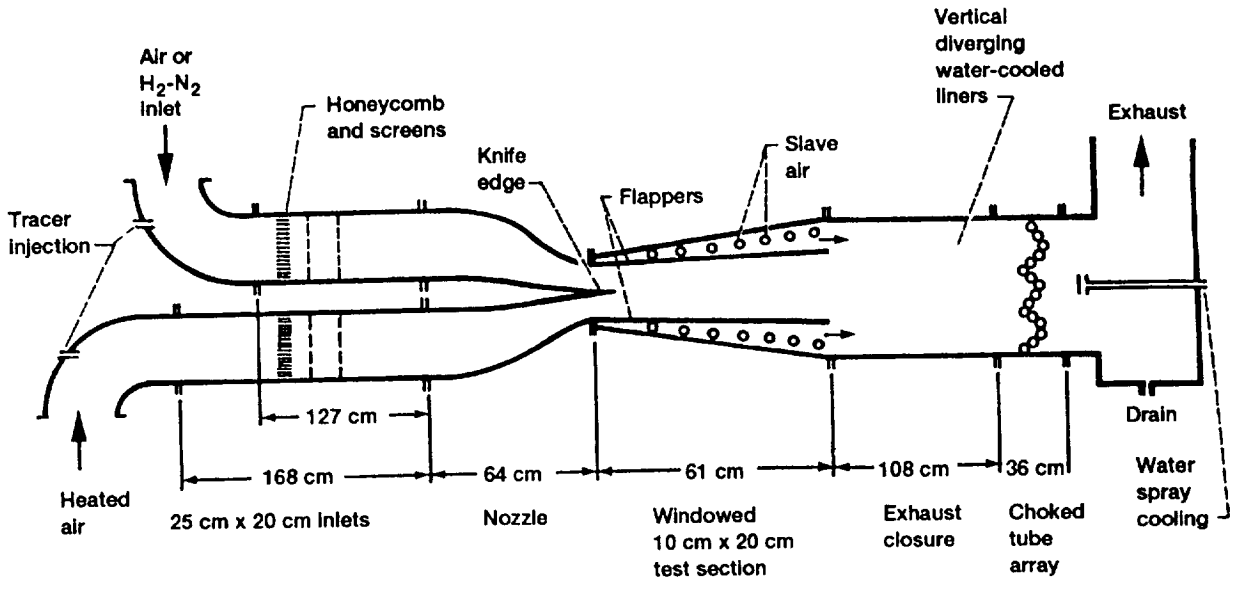

Schematic of Planar Reacting Shear Layer Facility.

The heated air enters the test section at 800 K at Mach 0.7 and the upper stream, either air or a combination of hydrogen and nitrogen gas, enters at 340 K and Mach 0.4. The two streams mix and react with hydrogen to produce thrust. The difficulty is to determine the degree of uniformity in the mixed shear layer.

The velocity, turbulence, and temperature profiles were measured downstream of the mixing (knife) edge. The initial and boundary conditions were well documented. An error function fit the nonreacting and reacting velocity profiles well. It also fit the nonreacting temperature profile. The reacting velocity shear layer was only slightly wider than the nonreacting case. It may be that the turbulence of the nonreacting layer can be used to predict the amount of combustion at high speeds. In other words at high speeds the flow field is not greatly affected by the heat release due to combustion.

More data are needed over a wider range of conditions to substantiate these conclusions. The current data set has been provided to the computational researchers for verification of an advanced computation code called RPLUS.

Lewis contact: Dr. C. John Marek, (216) 433–3584
Headquarters program office: OAST

Diffusing S-Duct Flow Physics Studied

Many aircraft employ bending circular duct geometries (S-ducts) as part of the inlet for the propulsion system. Often, the cross-sectional area of the S-duct increases downstream to decelerate the flow and achieve higher static pressure at the engine compressor. In order to achieve maximum engine performance and avoid engine stall, the S-duct should minimize flow-field total pressure losses throughout the duct as well as total pressure distortion at the duct exit. Curvature of the duct centerline gives rise to cross-stream pressure gradients that result in significant secondary flows within the duct. Additionally, the adverse streamwise pressure gradient caused by increasing cross-sectional area can lead to flow separation. Often, the aircraft designer faces a difficult dilemma. Size and weight restrictions encourage the use of shorter S-ducts. However, the greater centerline curvature and adverse pressure gradients of short ducts increase the risk of unacceptable duct performance.

Researchers at NASA Lewis are developing computational fluid dynamic (CFD) methods to aid in the design and analysis of aircraft propulsion components and systems. The highly three-dimensional and perhaps separated flow in a diffusing S-duct presents a substantial challenge to CFD. A careful comparison of numerical predictions with detailed experimental data is

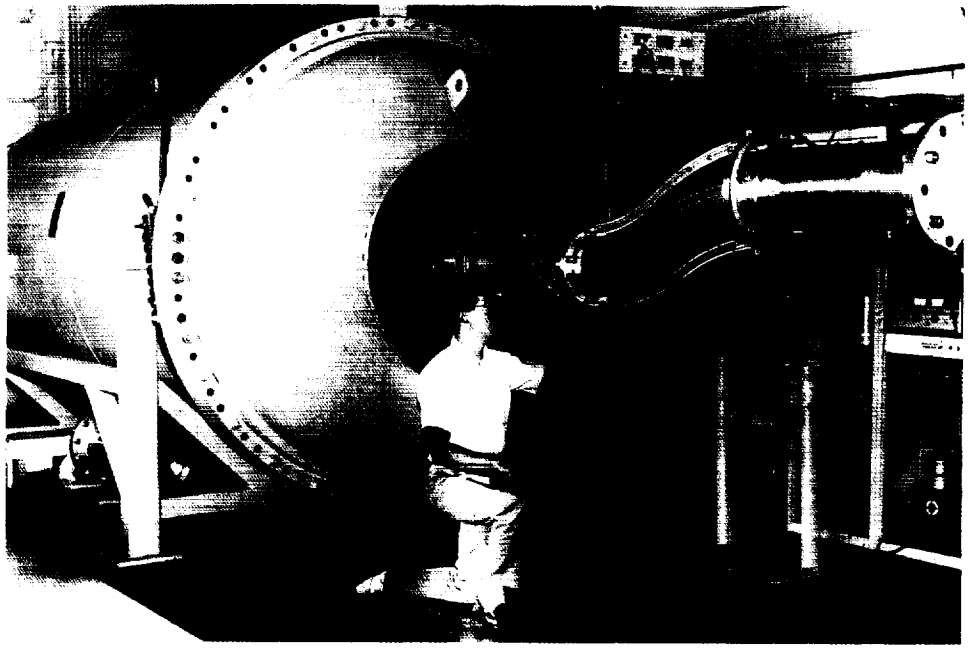

Diffusing S-duct experiment in Internal Fluid Mechanics Facility.

necessary to establish and improve the numerical accuracy. Therefore, a detailed experimental program is investigating the fundamental flow physics within a diffusing S-duct. The detailed data sets will be used to validate the numerical methods.

The experiments are being conducted in the Internal Fluid Mechanics Facility over of range in duct mass flows. The duct being studied has an inlet diameter of about 8 in., an exit diameter of about 10 in., and a diffuser area ratio of 1.52. The duct was intentionally designed to have a separated flow region near the first bend. Calculating the location and extent of this separation region presents a particular challenge to the CFD methods. Complete flow surveys of all three velocity components have been made at several streamwise stations within the duct. In addition, several different vortex generator designs have been used to control the flow separation region. Future experiments will include an investigation of the effect of inlet swirl on the flow characteristics within the duct.

Bibliography

Harloff, G.J.; Reichert, B.A.; and Wellborn, S.R.: Navier-Stokes Analysis and Experimental Data Comparison of Compressible Flow in a Diffusing S-Duct. AIAA Paper 92-2699, June 1992. (Also NASA TM-105683.)

Lewis contact: Dr. Bruce A. Reichert, (216) 433-8397
Headquarters program office: OAST

Space-Time Solution Element Method Improves CFD

An algorithm development effort that is based on a new numerical approach for solving conservation laws, the space-time solution element (STSE) method, is under way. Unlike the established numerical methods, the STSE method is based on flux conservation in a space-time integral formulation. The immediate goal of this effort is to develop faster and more accurate algorithms with much improved physical modeling capabilities for the direct solution of the Navier-Stokes equations. The long-term goal is to implement one or more of the newly developed algorithms into a new state-of-the-art computational fluid dynamics code for internal flow fields, the STS Duct code.

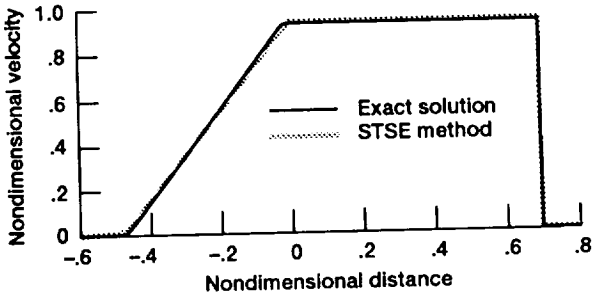

STSE method calculations for shock-tube problem.

Recently, explicit schemes based on the STSE method have been developed for the solution of Burgers equation and the one-dimensional, unsteady Euler equations. Computations for moving-shock problems have shown these schemes to be highly accurate, with only small phase and dispersion errors. An implicit scheme for the direct numerical solution of the steady, compressible Navier-Stokes equations has also been developed. Applying this scheme to fully developed channel flow has demonstrated the ability of the scheme to solve viscous flow fields on a coarsely spaced uniform grid. Solution times required to predict the fully developed velocity profile are less than 1 sec on a scientific workstation.

Bibliography

Chang, S-C.; and To, W-M.: A New Numerical Framework for Solving Conservation Laws—The Method of Space-Time Conservation Element and Solution Element. NASA TM-104495, 1991.

Chang, S-C.; and To, W-M.: A Brief Description of a New Numerical Framework for Solving Conservation Laws—The Method of Space-Time Conservation Element and Solution Element. NASA TM-105757, 1992.

Lewis contact: Dr. James R. Scott, (216) 433-5863
Headquarters program office: OAST

Fluid Flow Investigated for a Row of Jets in Crossflow

Turbulent flows similar to jets in crossflows can be found in many engineering applications including aerospace propulsion systems. A numerical investigation of a row of jets in a confined crossflow has been completed (ref. 1) by using the Reynolds-averaged Navier-Stokes equations with

a multiple-time-scale turbulence model. Analysis of this computational result can lead to a clearer understanding of this complex flow problem.

A side view of three-dimensional particle trajectories shows that the fluid particles near the jet edge carry less momentum. Hence, these particles are quickly entrained to the helical vortices in the wake region of the jet, large-eddy mixing occurs in the wide region of the jet edge, and the fluid particles in the center region of the jet do not mix easily with the crossflow. The primary vortex is formed by the jet, which acts as an internal blockage for the crossflow. In this regard the fluid flow behind the jet is similar to two-dimensional flows over circular cylinders. However, the nature of the primary vortex is quite different from that of flows over circular cylinders because the primary vortex is a helical vortex. The jet is split into two symmetric parts by the reversed flow of the primary vortex at downstream locations.

The surface streaklines for a simulated oil flow on the bottom wall were obtained by tracking the particle trajectories confined on the $z/D = 0.004$ plane, which is one grid point away from the wall. A line of coalescence in the forward region of the jet was caused by the horseshoe vortex, a ring of reversed flows, located along the circumference of the jet exit, and one in the wake region was caused by the viscous force exerted by the external fluid flow. A horseshoe vortex was generated by the strong adverse pressure gradient formed by the jet in crossflow. Previous numerical investigations of jets in crossflow by using k-ε turbulence models failed to predict the horseshoe vortex. The accurate numerical results obtained in the present investigation are attributed to the capability of the multiple-time-scale turbulence equations to resolve the inequilibrium turbulence phenomena. A theoretical analysis of the multiple-time-scale turbulence equations was performed to model the cascade of turbulent kinetic energy (ref. 2). The calculated flow and concentration fields for a circular jet in crossflow were in good agreement with the measured data.

A topological analysis showed that a number of critical points are developed by the separated and recirculating complex three-dimensional fluid flow. The critical points are defined as a spatial location at which velocity gradients vanish, and hence each critical point represents a separation or a reattachment location. The type and location of each critical point were in correct agreement with those observed in experiments.

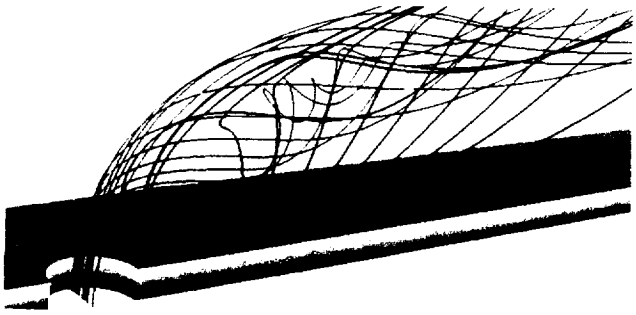

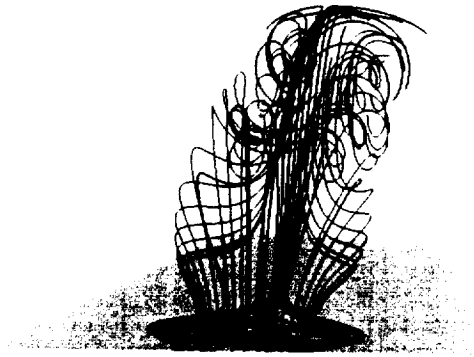

Side and front views of particle trajectories.

References

1. Kim, S.W.; and Benson, T.J.: Fluid Flow of a Row of Jets in Crossflow—A Numerical Study. AIAA Paper 92–0534, 1992.
2. Kim, S.W.; and Benson, T.J.: Calculation of a Circular Jet in Crossflow With a Multiple-Time-Scale Turbulence Model. NASA TM–104343, 1991.

Lewis contact: Dr. Sang-Wook Kim, (216) 433–2606

Headquarters program office: OAST

Aerodynamic Inverse Design and Analysis Performed for a Full Engine

The use of parallel processing with advanced supercomputers is permitting the attempt of computational tasks that only a few years ago would have seemed unreasonable. Present parallel computing capabilities make perfectly reachable the aerodynamic design of a full, multistage turbine engine by direct simulation of the Euler equations. Loss models can then be incorporated for additional viscous effects.

A computer program called Numerical Engine Simulation by Parallel Processing (NESPP) is being developed in-house. This approach should result in an efficient method of enlarging the design data base for turbomachinery blading. This capability has been demonstrated for blade sections, and the goal is to extend it to fully three-dimensional, multistage configurations. The method incorporates in one single procedure the three classic steps of aerodynamic blade design: preliminary design, blade geometry generation, and aerodynamic analysis. The procedure delivers aerodynamic blade and passage shapes as well as the corresponding flow solution.

Using this design tool effectively requires its implementation on a parallel machine. A 25-MFLOPS processor per passage seems a reasonable hardware environment for this problem. A typical engine may require at least 32 processors. To experiment with this idea, a cluster of seven IBM RISC/6000-550 powerstations was used to run a parallel version of the code. Parallel Virtual Machine (PVM) is used as message passage language, and the processors communicate through the Ethernet. Four RISC/6000-550 processors performed in the equivalent time of one Y/MP processor for a coarse-grid test case. With a medium-size grid and enhanced vectorization the ratio of IBM to Y/MP processors is 6, and with a fine grid the ratio is 8.

Two CRAY Y/MP's were later added as nodes to the cluster. The host RISC/6000 handled this heterogeneous cluster perfectly.

Bibliography

Sanz, J.; Pischel, K.; and Hubler, D.: The Engine Design Engine. A Clustered Computer Platform for the Aerodynamic Inverse Design and Analysis of a Full Engine. NASA TM-105838, 1992.

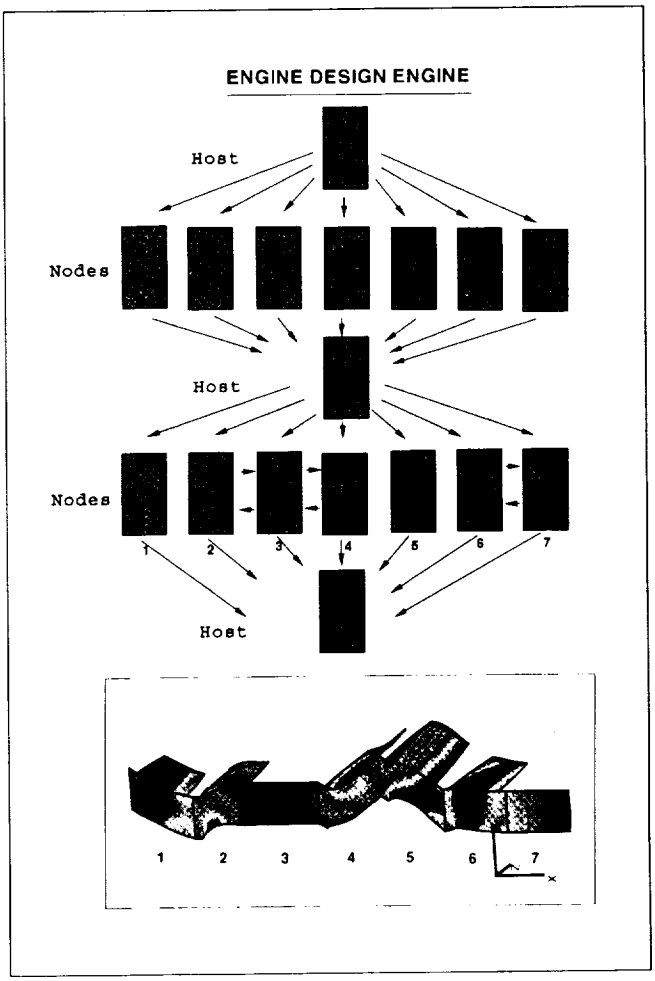

Schematic of parallel cluster running one compressor stage and one and a half turbine stages with simultaneous use of Y/MP and RISC/6000 processors.

Lewis contact: Dr. Jose M. Sanz, (216) 433-5917
Headquarters program office: OAST

Karman Vortex Street Breakdown Simulated

An on-going effort at NASA Lewis is directed to developing a high-resolution, fixed-stencil finite difference scheme suitable for studying complex flow physics. A program has been developed with high temporal (up to fourth order) and spatial (up to fourth order) accuracy. It is an implicit scheme with an explicit-like structure, and it is equipped with arbitrary mesh numbering (blocking) capability. The program is designed to be used on flows with complex geometries, and it can also be easily modified to suit the advanced architecture of modern computers.

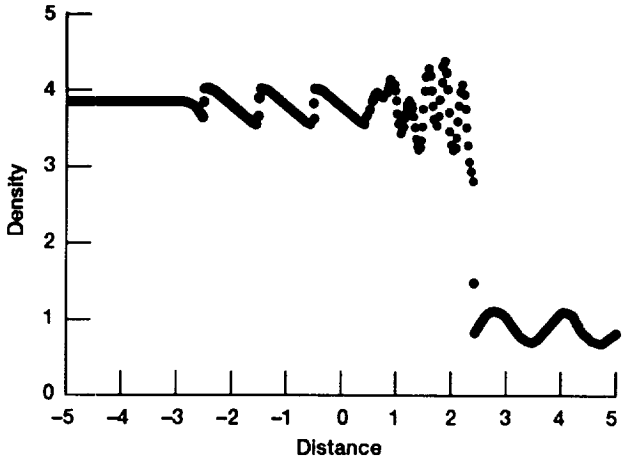

Mach 3 shock wave interacting with spatially changing medium.

The applications effort, to date, consists of two major parts. The first is solving continuous, unsteady Navier-Stokes equations. The adequacy of the scheme in this regard is illustrated by the study described in reference 1. The second part of the effort is to properly represent the weak solution of the Euler equations and to adequately capture the physics of the interacting strong-weak Navier-Stokes solutions. A representative result of this effort showed the interaction of a Mach 3 shock wave propagating into a stationary, spatially changing medium with sinusoidally varying density.

Reference

1. Chen, S.-C.: Breakdown of the Karman Vortex Street Due to Forced Convection and Flow Compressibility. NASA TM-105853, 1992.

Lewis contact: Dr. Shu-cheng Chen, (216) 433-8640
Headquarters program office: OAST

Propulsion Systems

Ceramic Turbine Stage Components Tested to 2500 °F

In order to exploit the high-temperature performance potential of the gas turbine engine without using strategic materials or exotic hot-section cooling techniques, NASA Lewis is working to develop a ceramic component technology base. As part of the U.S. Department of Energy's Automotive Gas Turbine Program, the Advanced Turbine Technology Applications Project (ATTAP) is developing structural ceramic hot-flow-path component technology for advanced small gas turbine engines. These engines, designed to operate at temperatures to 2500 °F, have the potential for significantly less fuel consumption than either metal turbine engines or conventional piston engines. In addition, the turbine engines operate with reduced emission levels that meet the current and proposed Federal standards.

Technology development contracts are in place with the Allison Gas Turbine Division of General Motors Corporation and with the Garrett Auxiliary Power Division of the Allied-Signal Aerospace Company. Each contract relies on the strong support of the U.S. ceramics industry for component development.

Testing has progressed from the proof test of single ceramic components and subassemblies to the evaluation of an all-ceramic gasifier turbine stage consisting of a rotor, a scroll, nozzle vanes, and support and spacing rings. The ceramic components, which meet engine dimensional and strength requirements, are tested in rigs over the full range of engine operating conditions from idle to full power.

During the past year a major project milestone was accomplished. An axial-flow turbine stage with a monolithic silicon nitride rotor, scroll, and nozzle vanes was successfully tested for 100 hours at temperatures to 2500 °F. Test rig conditions included startup, steady state, and transient operation to simulate a vehicle duty cycle.

Preparations are under way for a 300-hour durability test of an all-ceramic turbine stage to 2500 °F. In addition to ceramic component evaluation, fiscal year 1993 activities include development of low emissions combustor

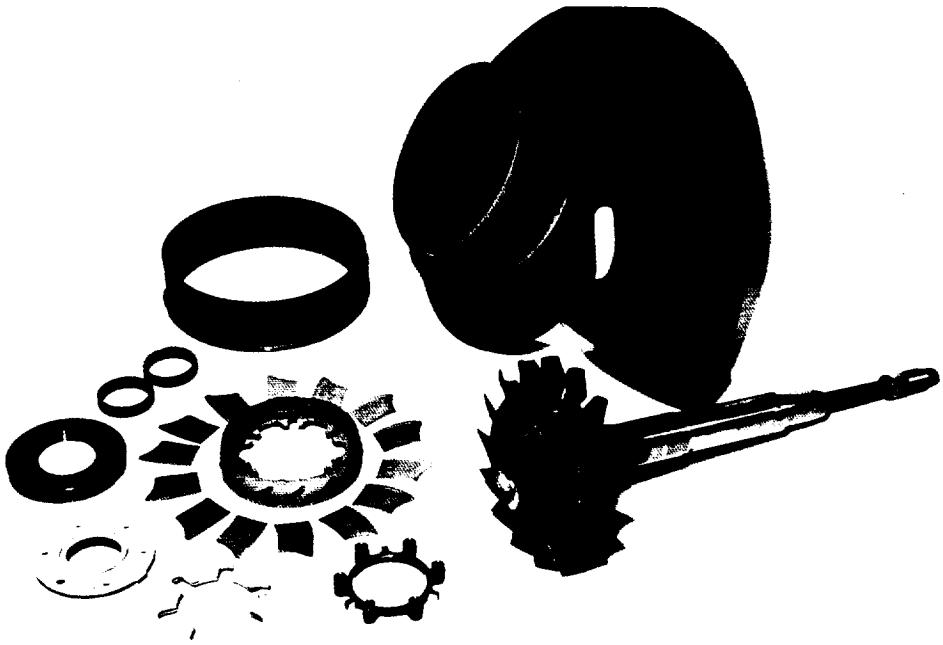

Ceramic components for axial-flow turbine stage.

technology and an improved-performance regenerative heat exchanger subsystem.

Bibliography

Haley, P. J.: Progress on the Advanced Turbine Technology Applications Project (ATTAP), and Automotive Gas Turbine Outlook. ASME Paper 92-GT-292, 1992.

Smyth, J. R.: ATTAP Ceramic Gas Turbine Technology Development. ASME Paper 92-GT-381, 1992.

Lewis contact: Paul T. Kerwin, (216) 433-3409
Headquarters program office: OAST

Focused Schlieren Diagnostics Technique Used for Fuel Injection Studies

A focused schlieren diagnostic technique has been used at NASA Lewis to study the fuel/air mixing effectiveness of a fuel injection concept. A simple, inexpensive diagnostic technique, focused schlieren supplies a qualitative and quantitative description of the flow field, as well as a time-history of the flow field to 10,000 frames per second, using a high-speed motion picture camera.

A xenon lamp supplies light to multiple slits in the "grid." A Fresnel lens focuses this light onto a plane of interest within the test section. A spherical lens collects the image and sends it through the negative grid and another Fresnel lens, which focuses it onto a frosted glass plate where it is photographed by a high-speed 16-mm camera. A digitization system transfers these images to a computer for analysis. In this system a high-resolution video camera transfers the images to a personal computer's frame-grabber board. Image-processing software is then used to produce color-enhanced images that define regions of low- and high-density gradients.

A method of extracting quantitative information from these color-enhanced images was devised. Vertical lines are drawn at different axial stations in the flow. Along each line the mean and standard deviation of the image pixel intensities are found. A relatively low standard deviation is produced when there is little change in density gradients along the line. When a line cuts across a region of intense mixing, a higher standard deviation is produced. As the mixing is completed, a line crosses a more uniform flow field and its standard deviation is lower. This method can be used to quantitatively compare degree of mixedness at various axial locations.

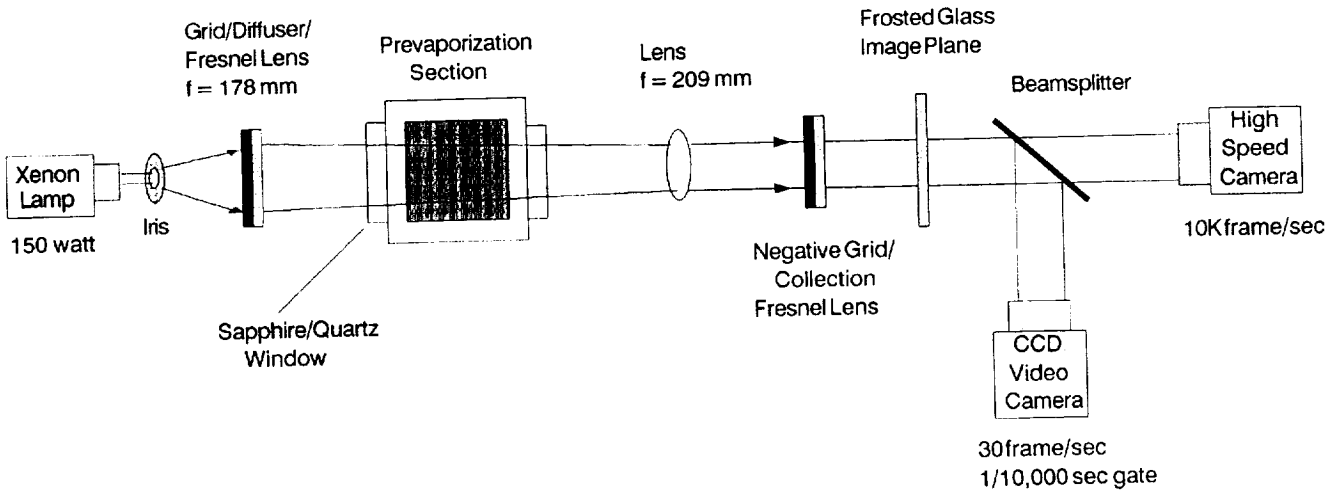

Focused schlieren diagnostics.

Bibliography

Lee, C.-M.; Bianco, J.; and Deur, J.: Nitric Oxide Formation in Lean Premixed-Prevaporized Jet A/Air Flame Tube: An Experimental and Analytical Study. NASA TM–105722, 1992.

Lewis contact: Richard W. Niedzwiecki, (216) 433–3407
Headquarters program office: OAST

Shed-Ice Impact Energy Measurement System Developed

The NASA Lewis aircraft icing group has developed a shed-ice impact energy measurement system (IEMS) to characterize the impact force or energy associated with ice particles shed from a rotating system, such as a propeller or a helicopter main rotor. This system was developed in response to a stated industry need for a data base of impact forces and energies associated with shed-ice particles to use in predicting potential airframe damage from shed-ice impacts. The system consists of an array of force-sensing resistors (FSR's) used in conjunction with high-speed imaging equipment. The FSR's record the force-time trace of the impact, and the high-speed imaging yields information about ice particle size, velocity, and trajectory before the strike. The IEMS was successfully used in a model rotor icing test in the NASA Lewis Icing Research Tunnel (IRT) where over 300 shed-ice impacts were recorded. These data are currently being examined at NASA Lewis.

The FSR's, manufactured by Interlink Electronics, have never been used in this way before. An FSR is a sensing device that has a resistance change as a function of force. The resistance change is repeatable and can be calibrated. The FSR sensing array can be mounted on any rigid flat surface and requires a power supply yielding a constant 8 V. A single FSR can have 22 by 22 in. of sensing area. Because the behavior of the sensor is the same throughout its sensing area, the researcher does not have to be concerned with location effects on the sensor. A 0.032-in. 6061–T6 aluminum overlay was used to protect the sensors from damage. Calibration was done with the overlays attached to the sensors so that the overlay effect on the force readings was calibrated for. The two high-speed cameras were mounted so as to provide the orthogonal viewing planes needed to fully characterize the incoming particle's trajectory. Information about the trajectory, mass, and velocity of the incoming particle is needed to convert the force-time trace into impact energy. The FSR plate was mounted vertically to the tunnel wall. A mirror was used for one of the high-speed cameras mounted outside the tunnel. The second camera was mounted inside the tunnel downstream from the FSR plate.

The proof of concept of the IEMS was developed through a grant with the University of Toledo. All of the concept testing was done in their ice gun facility, which can control the particle size and velocity. This facility is currently being used to take a set of IEMS validation data for comparison with data taken in the IRT.

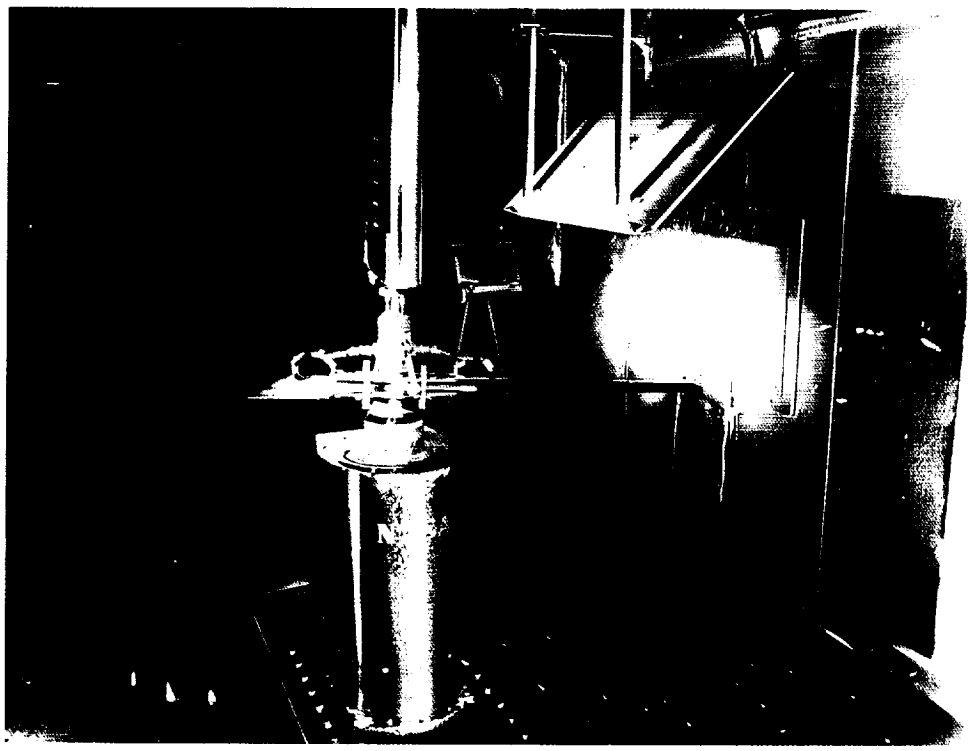

Test setup in IRT, showing IEMS sensor plate mounted to tunnel wall underneath overhead mirror.

Lewis contacts: John J. Reinmann, (216) 433–3900; Randall K. Britton, (216) 891–2237
Headquarters program office: OAST

Code Developed for Optimizing Gearbox Design

In current aircraft transmissions the service life between overhauls is affected mainly by the life of the bearings that support the gears. One reason is that transmissions are designed by choosing gears for the required power transfer and then sizing the bearings and support shafts to accommodate these gears. With a computer code for optimization, however, a different approach can be used whereby the lives of the gears and the bearings, as well as the weight of the components, can all be considered concurrently, to obtain an optimal design for the complete gearbox. For aircraft transmissions the optimal design is lightweight, quiet, and highly reliable and has a long service life.

An optimizer code named SEEK has been developed and coupled with different analytical codes to determine transmission component and system life, permitting concurrent optimization. An optimizer code considers many combinations of the important design variables, looking to find the combination that produces the best result. This result could be the longest life, or lightest weight, or some other desired characteristic. The design can be subject to many constraints, such as a maximum tooth bending stress, a maximum contact stress, and minimum clearances.

By using a modified feasible directions algorithm, SEEK varies the values of the independent design variables, looking for the largest gradient in the value of the desired characteristic (e.g., gear fatigue life). By noting the constraints that have been exceeded, the algorithm changes the parametric values so that the design is placed within required limits. It then proceeds in a feasible direction to improve the design until the optimal design is reached, where the desired characteristic is either maximum or minimum (e.g., maximum fatigue life or minimum weight).

The computer program BOX couples SEEK with analytical routines that describe a single spur-gear mesh transmission. Another program, SBOX, does the same thing for a single spiral-bevel mesh transmission. The angle between the shafts and the gear spiral angle are additional design parameters.

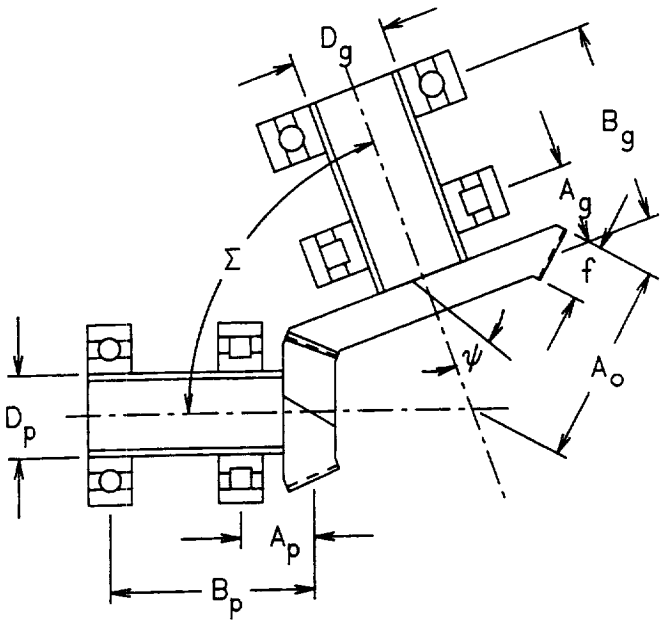

Spiral-bevel gear reduction parameters.

The significance of this new software, developed through a grant with the University of Akron, is that it presents optimal designs for different gear arrangements and permits transmissions to be compared on the basis of fatigue life or total weight or dynamic loading, before commitment to any hardware. This optimization procedure can save money by keeping expensive testing to a minimum. With concurrent optimization of bearing, gearing, and shaft design the best overall system can be obtained, rather than a system comprising optimized individual components.

Bibliography

Savage, M.; et al: Optimal Design of Compact Spur Gear Reductions. NASA TM–105676, 1992.

Savage, M.; et al.: Maximum Life Spiral Bevel Reduction Design. NASA TM–105790, 1992.

Lewis contact: Harold H. Coe, (216) 433–3971
Headquarters program office: OAST

Novel Face Gears Proved Feasible for Advanced Rotorcraft Transmissions

The Advanced Rotorcraft Transmission Program is an Army-funded, joint NASA/Army program to develop and demonstrate lightweight, quiet, and durable drivetrains for next-generation rotorcraft. One contract team participant (McDonnell Douglas Helicopter Company/Lucas Western Incorporated) developed a novel design with a projected weight saving of 40 percent over a conventional design. The new design consisted of face gears in a split-torque arrangement never before used in rotorcraft transmissions. Prototype face gears were tested in the NASA Lewis Gear and Transmission Laboratory to demonstrate their feasibility in a high-speed, high-load application.

A major reason for the reduced weight of the advanced transmission is the first stage, where the torque is split by using face gears. Face gears have significant advantages as a tradeoff for conventionally used spiral-bevel gears. The input pinion is a common involute spur gear, which is simpler in design and cheaper to manufacture than a spiral-bevel gear. Also, the split-torque arrangement (power through the drivetrain is split between two parallel paths) allows smaller, lighter gears to be used because the load transmitted per gear is lower.

Face gears have had widespread use in low-power applications but have been sparingly used in high-power applications. Up to this time the theory of face-gear drives had not been developed sufficiently to meet the demands of high-speed and high-load requirements in helicopter transmissions. Thus, an extensive analysis of face-gear design and geometry was conducted with the University of Illinois (ref. 1). Topics included tooth generation, limiting inner and outer radii, tooth contact analysis, contact ratio, gear eccentricity, and structural stiffness. Valuable insight on face-gear design and manufacturing was gained from this work.

To further the possible use of face gears in helicopter transmission applications, an experimental program to test the feasibility of using face gears in a high-speed and high-power environment was conducted at NASA Lewis (ref. 2). Four face-gear sets were tested in the NASA Spiral Bevel Gear Facility at pinion rotational speeds to 19,100 rpm and to 271 kW (364 hp). The test gear sets were one-half scale of the advanced

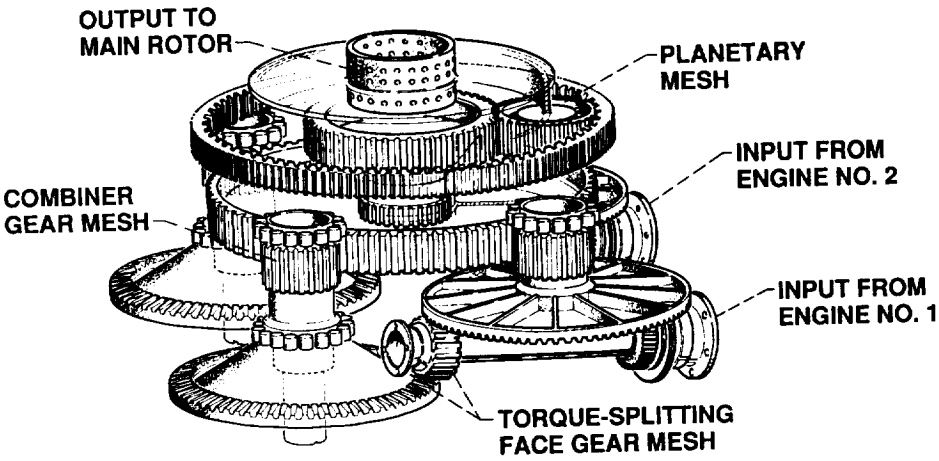

Advanced rotorcraft transmission.

transmission design gear set. The gears were tested at one-eighth power, which resulted in slightly greater bending and compressive stresses than for the full-scale design. All four sets of gears successfully ran at 100 percent of design torque and speed for 30 million pinion cycles, and two sets successfully ran at 200 percent of torque for an additional 30 million pinion cycles. The results demonstrated the feasibility of using face gears for high-speed, high-load applications.

References

1. Litvin, F.L.; et al.: Application of Face-Gear Drives in Helicopter Transmissions. NASA TM–105655, 1992.
2. Handschuh, R.F.; Lewicki, D.G.; and Bossler, R.: Experimental Testing of Prototype Face Gears for Helicopter Transmissions. NASA TM–105434, 1992.

Lewis contacts: David G. Lewicki, (216) 433–3970; Robert F. Handschuh, (216) 433–3969
Headquarters program office: OAST

Mach 0.3 Free-Jet Acoustic Test Capability Developed

A major issue associated with the environmental acceptability of the proposed High Speed Civil Transport (HSCT) is its ability to meet noise standards, currently assumed to be Federal Aviation Regulations (FAR) 36 stage III levels now applied to newly designed subsonic transports. In response to this concern NASA has begun programs to investigate the low-speed performance and takeoff noise characteristics of advanced low-noise nozzle concepts for use on the HSCT. Until recently the 9- by 15-ft Low Speed Wind Tunnel (LSWT) was the only test facility at NASA Lewis capable of acoustically testing these new low-noise nozzles. However, the LSWT is limited to near-field noise measurements and is also in heavy demand by other research programs. The Nozzle Acoustic Test Rig (NATR) was developed in-house to provide the additional test capabilities needed for HSCT nozzle programs. The NATR allows nozzle concepts to be acoustically assessed for far-field (approximately 50 ft) noise characteristics under conditions simulating forward flight.

The NATR is a large free-jet facility (free-jet diameter, 4.25 ft) with a design Mach number of 0.30. It is located inside a geodesic dome, adjacent to the existing Powered Lift Facility (PLF). The total airflow required to operate at Mach 0.30 is achieved by employing an ejector. The primary nozzle (a circular array of 30 nozzles) of the ejector is supplied with 100 lb/sec and must entrain approximately 300 lb/sec of ambient air, a pumping ratio of 3. As a result of the momentum exchange and the streamwise vortices in the annular mixing region, the two flows mix into one subsonic stream. The mixed flow then expands through an annular diffuser and into a settling chamber. Once inside the settling chamber the flow passes through a honeycomb/screen combination intended to remove large disturbances and provide uniform flow. The flow then accelerates through an elliptical contraction, where it achieves a free-jet Mach number of 0.30.

In order to verify the ejector's pumping performance and determine its sensitivity to various parameters (e.g., primary nozzle position, inlet

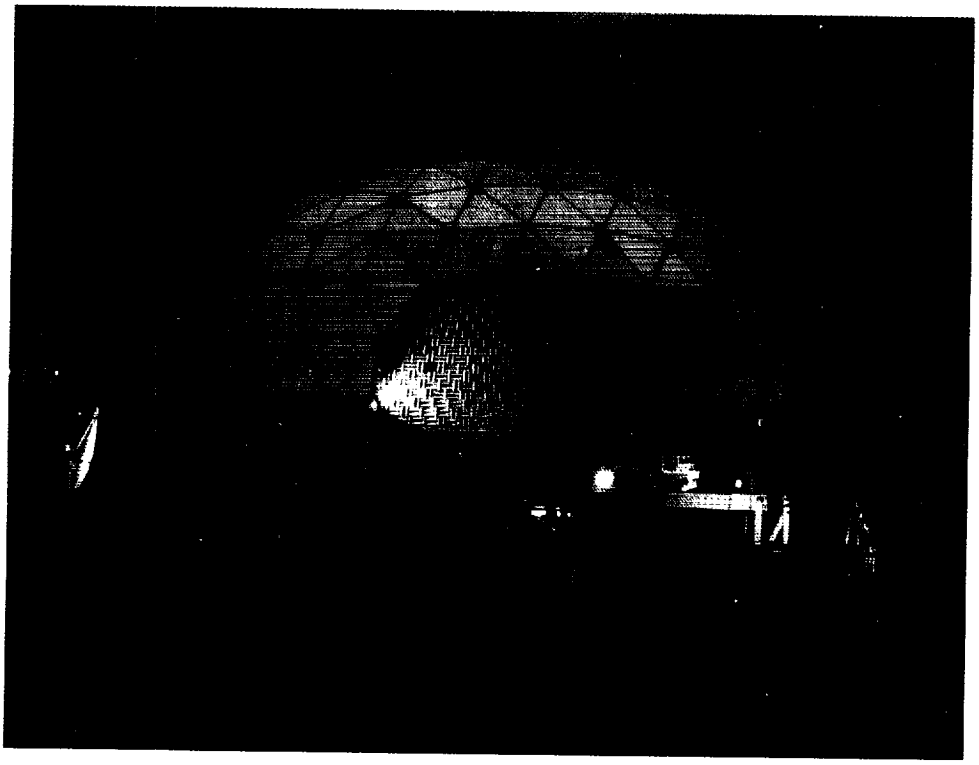

Nozzle Acoustic Test Rig located inside geodesic dome.

blockage, and backpressure levels), a 1/5-scale model of the NATR was fabricated in-house and tested. The model was designed by scaling (geometrically) the dimensions of the full scale by 0.20. The model verified that the required pumping levels were achieved and indicated little system sensitivity to the axial position of the primary nozzles. However, the ejector system was found to be extremely sensitive to vertical and angular misalignment of the primary nozzle array. The effect of inlet blockage on the ejector pumping performance was minimal. The 1/5-scale NATR model provided valuable information for the installation and operation of the full-scale facility. As expected the full-scale NATR achieved the pumping ratio required to attain a free-jet Mach number of 0.30.

Lewis contacts: Mary Jo Long, (216) 433-8708; Rayond S. Castner, (216) 433-5657
Headquarters program office: OAST

Mixer-Ejector Nozzle Tested for Aerodynamic Performance and Noise Suppression

The High Speed Civil Transport is a proposed supersonic transport capable of carrying 300 passengers on transoceanic routes. Such an aircraft must meet Federal noise regulations to be acceptable to communities surrounding airports. Although the only operating supersonic transport, the Concorde, has been granted an exemption from Federal Aviation Administration (FAA) noise standards, such waivers probably will not be given to future supersonic transports. However, the high thrust needed to boost these aircraft to supersonic speeds implies high jet velocities and thus high noise levels. As part of the High Speed Research (HSR) Program, NASA and Pratt & Whitney are working together to develop technology that will reduce the noise produced by these engines while maintaining thrust levels. The engine concepts under study in the HSR program will require a 20-dB suppression in jet noise relative to an unsuppressed nozzle to reach FAA noise regulations.

A promising concept for reducing jet noise is the mixer-ejector nozzle. The mixer-ejector reduces noise by mixing the hot, high-velocity exhaust

from the engine core with low-velocity air drawn from the atmosphere to produce a cooler, lower-velocity exhaust. The mixer is a nozzle with a convoluted or lobed exit cross section. The lobes cause the jet plume to have a large surface area so that it can mix with the surrounding air. The ejector draws in air to mix with the plume and acts as a shield to contain the noise produced during the mixing process. Acoustic treatment applied to the inside ejector surfaces absorbs the mixing noise.

NASA Lewis and Pratt & Whitney have tested a two-dimensional mixer-ejector nozzle in the NASA Lewis 9- by 15-ft Low Speed Wind Tunnel. Two mixer designs, several ejector configurations, and two acoustic liner designs were studied. Testing was performed at conditions representing takeoff and approach.

The NASA Lewis jet exit rig, designed for nozzle testing with hot combustion products, supplied the nozzle with heated air to 2000 °R. A force balance in the jet exit rig measured forces on the model while an array of microphones arranged in a 100° arc to the side of the model measured the nozzle acoustic emissions. Surveys of the flow at the ejector exit were used to study the mixing characteristics of the nozzle configurations.

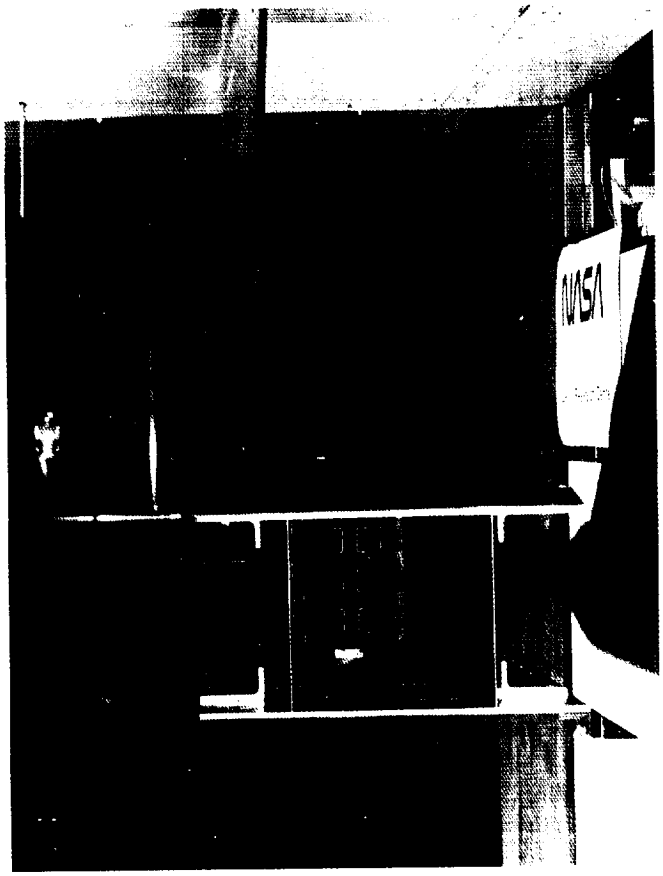

HSR mixer-ejector nozzle in NASA Lewis 9- by 15-ft Low Speed Wind Tunnel.

Previous tests of a similar mixer-ejector configuration had demonstrated that this concept showed promise for jet noise suppression. However, the mixing of the jet exhaust and the ejector flow was incomplete. The more recent test was designed to make use of the lessons learned from the earlier tests to improve the mixing in the nozzle. The results showed greater mixing and progress toward the HSR noise reduction goals.

Lewis contact: John D. Wolter, (216) 433–3941
Headquarters program office: OAST

Computational Fluid Dynamics Being Used to Assess Candidate Supersonic Transport Nozzles

A 300-passenger supersonic transport could be operable by the year 2005, but several issues concerning the aircraft's impact on the environment must first be addressed. One of these issues is the potentially large amount of noise generated at takeoff by the propulsion system. Work at NASA Lewis under the High Speed Research (HSR) Program is aimed at developing an exhaust nozzle that would suppress this noise while still maintaining the high level of thrust required. Several candidate noise-suppressing nozzle concepts have been developed. Computational fluid dynamics (CFD) is currently being used to assess these designs and to guide future nozzle designs.

One of the current designs being studied is a rectangular mixer-ejector nozzle developed by the General Electric (GE) Company under a contract from NASA Lewis. This nozzle is designed to entrain large amounts of external (secondary) flow. This flow is drawn through an array of lobed chutes. These chutes create a set of streamwise vortices that rapidly mix the entrained flow with the high-velocity (primary flow) jet. This mixing reduces the total velocity at the nozzle exit and results in lower noise. At the

same time high thrust is maintained owing to the mass augmentation provided by the secondary flow.

At NASA Lewis the PARC3D CFD code is being used to analyze the aerodynamic characteristics of the nozzle. The PARC code solves the Reynolds-averaged Navier-Stokes equations, using either an algebraic or k-ε turbulence model. This analysis gives insight into both the thrust performance of the nozzle and the mixing effectiveness of the two flows. GE has used the NASA Lewis results from initial studies to help design a series of configurations for experimental testing. Two of these test configurations have been analyzed. The investigation has given good insight into the complex flow field of these nozzles. And the computational results compare well with data obtained through the experiments. The results indicate that the current designs operate overexpanded and thus give lower thrust performance. Stagnation temperature contours at the nozzle exit plane show that large areas of high-temperature primary flow remain and have migrated to the top of the nozzle. This indicates that the mixing process is incomplete. Current efforts using the PARC code are focused on identifying an improved configuration that will provide optimal thrust performance.

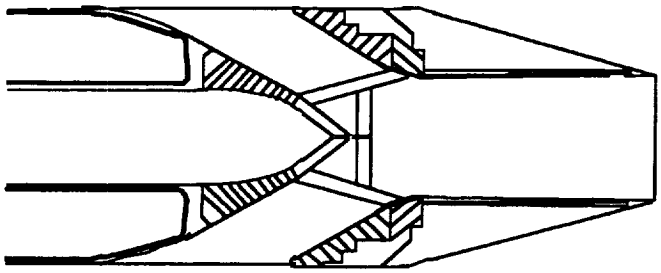

NASA/GE mixer-ejector nozzle.

Bibliography

DeBonis, J.R., Full Navier-Stokes Analysis of a Two-Dimensional Mixer/Ejector Nozzle for Noise Suppression. AIAA paper 92-3570, 1992. (Also NASA TM-105715.)

Lewis contact: James R. DeBonis, (216) 433-6581
Headquarters program office: OAST

Data Base Compiled for Internal Reversing Flow System

Supersonic short-takeoff-and-vertical-landing (SSTOVL) aircraft are within technical reach of meeting future military requirements. Several proposed SSTOVL powered-lift concepts are based on blocking the cruise exhaust nozzle and redirecting engine gas forward to lift thrusters during landing or hover flight. In every case the available lift is directly reduced by the pressure loss in the tailpipe offtakes and ducts leading to the thrusters. The flow patterns causing pressure loss are known to be extremely complex.

One of the technology goals of this program is to determine if the flow behavior in various exhaust configurations can be modeled and predicted successfully with computational fluid dynamics (CFD) programs. This approach has been extended to a generic tailpipe offtake configuration in an ongoing joint program with the McDonnell Aircraft Company. The main test objective was to collect data to compare with the performance predicted for the same configuration by a computational fluid dynamics analysis. A one-third-scale model was built and tested at the NASA Lewis Powered Lift Facility. It retained all the essential features of an SSTOVL aircraft with this type of powered-lift system, except for lift thrusters. The model consisted of a tailpipe with twin elbows, offtake ducts, and flow-control nozzle, plus a small ventral nozzle and a blind flange to simulate a blocked cruise nozzle. Performance tests were made with unheated air at tailpipe-to-ambient pressure ratios up to 5.

Important test results are as follows:

- Total pressure loss in the offtake ducting, as high as 15.5 percent of the tailpipe total pressure, was greater than predicted.
- Nearly all the pressure loss occurred in turning the flow from the tailpipe into and through the elbows.
- No significant recurring pressure fluctuations were measured at the offtake openings or at the blocked end of the tailpipe.
- Flow patterns at the offtake openings were complex.

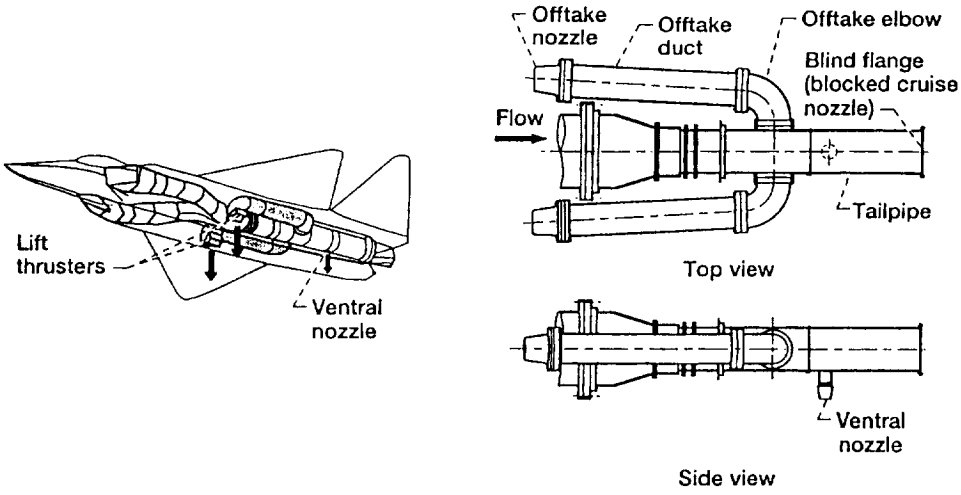

STOVL offtake duct model.

The application of these results to flight hardware design is as follows:

- Turning aids at the offtake openings, such as rounded edges or guide vanes, are needed to reduce offtake pressure loss.
- Turning vanes may have to be tailored to variations in flow approach angles at the tailpipe openings.
- Offtake ducts should be long to promote flow uniformity.

Lewis contact: Jack G. McArdle, (216) 433–3962
Headquarters program office: OAST

Flow Field Measured in High-Speed Centrifugal Compressor

The development and use of advanced computer codes as tools for centrifugal compressor design have become common in the past few years. The codes provide detailed predictions of flow-field behavior within the rotating blade row of a compressor, as well as estimates of compressor performance. What is not as common is the ability to obtain detailed measurements of flow fields in high-speed compressors. These measurements are needed to verify the accuracy of the computer codes. Laser anemometry is normally used to measure internal flow fields, but even this technique is difficult to use in a centrifugal compressor because of the small size and complex shape of the flow path. Therefore, a development program was undertaken at NASA Lewis to obtain flow-field mapping capability for centrifugal compressors.

Historically, two types of laser anemometers have had widespread use: the laser fringe anemometer and the two-spot, time-of-flight anemometer. Each type has features that make it desirable for specific applications. Normally, in centrifugal compressor research the two-spot anemometer has been selected because the small measurement volume provides greater resolution in the blade passage at the centrifugal compressor exit. This feature is traded off against the ability of the laser fringe anemometer to provide high data rates with a large acceptance angle. A new type of laser anemometer called a four-spot, time-of-flight anemometer was developed. This system combines the best features of the two-spot and laser fringe anemometers.

An experimental investigation of the flow fields in a centrifugal compressor with a 4:1 pressure ratio was completed using the four-spot anemometer. Measurements were obtained at 10 spanwise locations for each of 17 chordwise stations in the impeller and the vaneless diffuser. All measurements were taken at the peak efficiency point along the design-speed operating line. These are the first flow-field measurements to be obtained

in a high-speed centrifugal compressor with splitter blades. The impeller was also analyzed with the Dawes Code, a three-dimensional viscous flow code. Prior to laser surveys the impeller performance was mapped at design conditions and at conditions that included variations in scaling parameters.

Lewis contact: Gary J. Skoch, (216) 433-3396
Headquarters program office: OAST

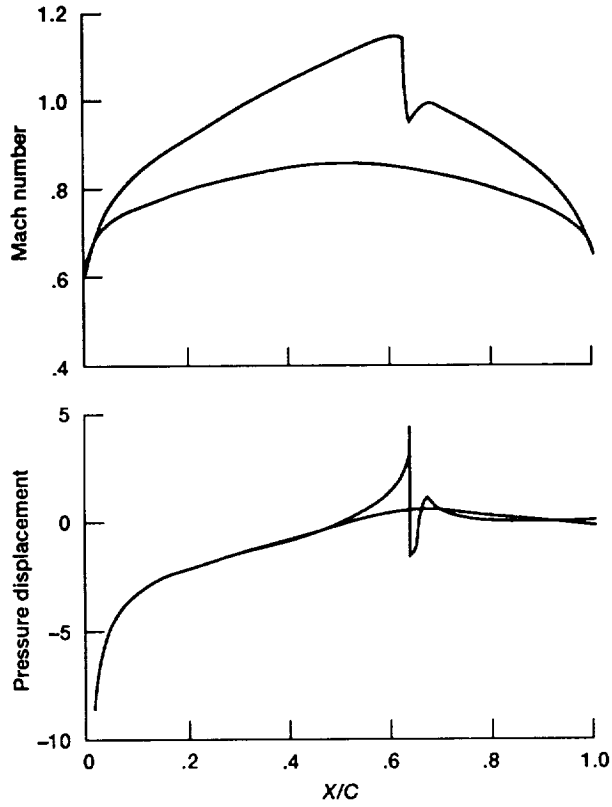

Calculation of blade surface Mach number using SFLOW and pressure-displacement function using LINFLO.

Steady and Unsteady Aerodynamic Analysis Developed for Turbomachinery Aeroelasticity

Turbomachinery aeroelasticity studies aim to predict blade stress levels resulting from structurally and aerodynamically induced vibrations. These vibrations, which result from the blade interacting with the surrounding flow, are typically classified as either flutter or forced response behavior. In flutter the aerodynamic forces are dependent on the blade vibration, and the energy can be extracted from the flow in such a manner as to sustain the vibration. In forced response the aerodynamic forces are independent of the blade motion. The source of the aerodynamic excitation can be wakes from upstream blade rows, variations in the static pressure (acoustic waves) entering the blade row from upstream or downstream, or both. A key to predicting aeroelastic behavior is the ability to determine how blade geometry and steady loading affect the unsteady pressure acting on a blade surface as a result of prescribed blade motion or aerodynamic excitation. A set of algorithms have been developed at NASA Lewis to predict the aeroelastic behavior of an isolated blade row.

The unsteady aerodynamic model was developed by the United Technologies Research Center (UTRC) (ref. 1). The model assumes that the inviscid unsteady behavior is a perturbation to the nonuniform, inviscid, isentropic, and irrotational steady flow. The unsteady flow is thus governed by a linear set of equations with variable coefficients that depend on the background steady flow. The unsteady model thus incorporates the effect of blade geometry and steady loading into the unsteady aerodynamic prediction. This algorithm, referred to as LINFLO (for linearized inviscid flow), can predict the unsteady response for an isolated blade row resulting from prescribed blade motion, variations in total temperature and total pressure (entropy and vorticity waves) at the inlet, and variations in static pressure (acoustic waves) at the inlet and exit of the blade row. Because the unsteady model is dependent on the background steady flow, a companion algorithm referred to as SFLOW (for steady flow) has been constructed to work with LINFLO. The steady algorithm solves a nonlinear equation set for the velocity potential. The SFLOW program is a NASA in-house effort that is being coordinated with UTRC personnel to ensure compatibility with LINFLO.

The LINFLO code is currently being extended to couple a viscous layer analysis to both the steady and linearized unsteady models. SFLOW is being extended to include transonic flow capability. Unsteady responses predicted by SFLOW and LINFLO for subsonic flow have compared well with experimental data and with predictions from

both unsteady Euler and linearized unsteady Euler codes (ref. 2). Because the SFLOW and LINFLO codes are based on a velocity potential formulation, the run times are considerably shorter than those for corresponding Euler calculations. The steady and unsteady transonic response is currently being compared with the calculations from the Euler code described in reference 3. Results for a limited number of cases show good agreement between the two predictions. Validation studies for the transonic capability are continuing. Upon completion of the viscous layer capability, comparison with Navier-Stokes calculations and, when available, experimental data will be undertaken. Because both the SFLOW and LINFLO computer codes permit an efficient and economical prediction of the unsteady response to prescribed blade motion and aerodynamic excitation, they are implemented on a computer workstation and thus are suitable for incorporation into an aeroelastic design prediction system.

References

1. Verdon, J.M.: Linearized Unsteady Aerodynamic Theory. AGARD Manual on Aeroelasticity in Axial Flow Turbomachinery, Vol. 1: Unsteady Turbomachinery Aerodynamics, M.F. Platzed and F.O. Carta, eds., AGARD-AG-298, Ch. 11, Mar. 1987.

2. Manwaring, S.R.; and Wisler, D.C.: Unsteady Aerodynamics and Gust Response in Compressors and Turbines. ASME Paper 92-GT-422, 1992.

3. Huff, D.L.; Swafford, T.W.; and Reddy, T.S.R.: Euler Flow Predictions for an Oscillating Cascade Using a High Resolution Wave-Split Scheme. NASA TM-104377, 1991.

Lewis contact: Dr. Daniel Hoyniak, (216) 433-3789
Headquarters program office: OAST

Turbine Endwall Heat Transfer Predicted With Three-Dimensional Viscous Code

Gas turbine engine efficiency can be improved by increasing the turbine inlet temperature or by decreasing the amount of cooling air. Using either approach requires understanding the physics of the heat transfer process in turbine blade passages. To that end, a three-dimensional viscous flow analysis code was used to calculate endwall heat transfer in a linear turbine cascade at two flow speeds.

The cascade was tested experimentally at NASA Lewis by using a liquid crystal technique to map the endwall heat transfer at various flow conditions (ref. 1). It was found that the inlet boundary layer thickness had little effect on the overall heat transfer (Stanton number) patterns. However, two distinctly different heat transfer patterns were seen at low and high flow speeds (Reynolds numbers).

The RVC3D (for rotor viscous code three-dimensional) turbomachinery analysis code developed at NASA Lewis (ref. 2) was used to compute the flow at two flow conditions. The code is a three-dimensional, explicit finite difference code. A new algebraic turbulence model was developed for the heat transfer analysis. The model is based on the Cebeci-Smith boundary layer model but uses unique integral parameters to provide turbulent length and velocity scales. The code was run on a Cray Y/MP computer using a computational grid with about 300,000 points. Computer time was two to four hours, depending on the case.

Computed endwall heat transfer contours for the low-speed case (chord Reynolds number of 78,000), expressed as a dimensionless Stanton number, show the heat transfer augmentation around the leading edge and the increasing heat transfer as the flow accelerated through the passage. The high-speed contours (not shown) exhibit a distinctly different heat transfer pattern. Both patterns agree fairly well with the experimental results.

Development and testing of the RVC3D code is continuing. The current code is being used by several U.S. companies and universities and in support of other NASA projects.

References

1. Boyle, R.J.; and Russell, L.M.: Experimental Determination of Stator Endwall Heat Transfer. ASME Paper 89-GT-219, 1989.

2. Chima, R.V.: Viscous Three-Dimensional Calculations of Transonic Fan Performance. CFD Techniques for Propulsion Applications, AGARD CP-510, 1992, pp. 21-1 to 21-19. (Also NASA TM-103800, 1991.)

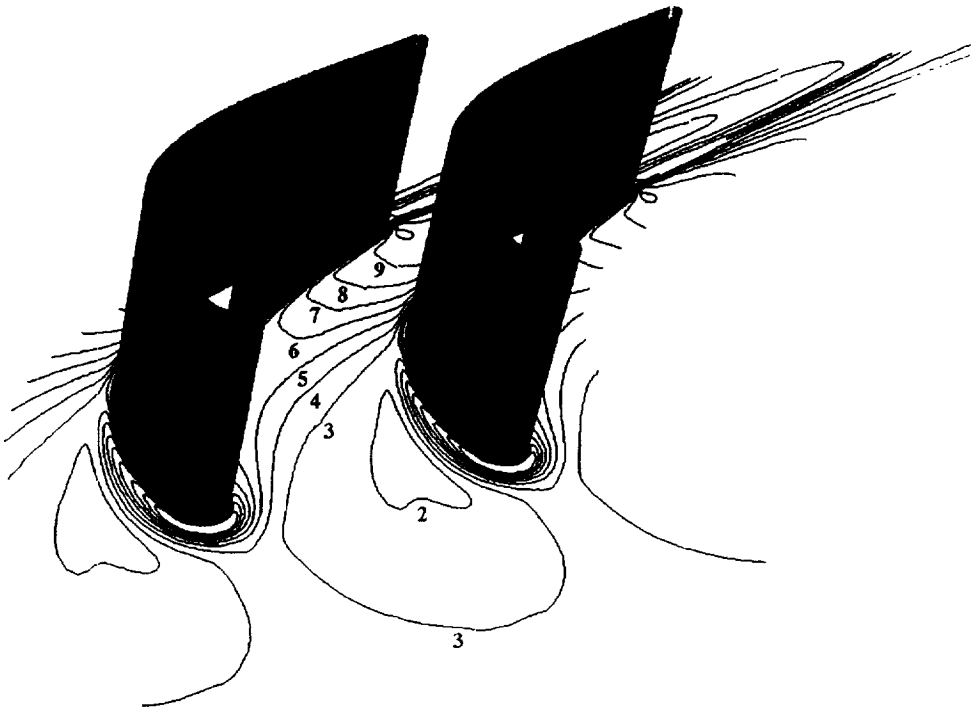

Boyle's linear turbine cascade. Computed Stanton number, ×1000; chord Reynolds number, 78,000.

Lewis contact: Dr. Rodrick V. Chima, (216) 433-5919
Headquarters program office: OAST

Wave Rotor Concepts Studied

A design limitation on jet engines is the maximum temperature of the turbine blades, which in turn limits the temperature of the gas entering the turbine. However, for high efficiency the combustion temperature, and therefore the temperature of the gas entering the turbine, should be as high as possible. Thus, the gas temperature should be high for efficiency, but low for turbine structural integrity. These opposing aims can be partially reconciled if the combustion gas can be cooled by expansion before being sent to the turbine. This can be done in a wave rotor, where the energy extracted from the gas in the expansion is used to compress the incoming gas prior to combustion. The compression and expansion take place in unsteady waves, but the overall flow through the device is steady.

NASA Lewis has begun a program to investigate wave rotors. The wave rotor consists of a rotating bank of passages that move past inlet and outlet ports. A wave is generated whenever a passage is opened to a port. The relative port timing is arranged to enhance the waves. In the NASA Lewis wave rotor there is one inlet port on the right, and two outlet ports on the left. At the high-pressure outlet port the flow is at a higher temperature and pressure than the inlet flow, and at the low-pressure outlet port the flow is at a lower temperature and pressure than the inlet flow. The unit was run for the first time during the last week of August 1992, and generated a temperature of 200 °F in the high-pressure outlet while frost was forming on the low-pressure outlet.

This unit will be used at NASA Lewis to examine the effects of design parameters on wave rotor performance. These design parameters include the gap spacing between the rotor and the endplate at the rotor-port interface (which affects leakage), passage opening time, and passage length-to-width ratio. The experimental results will be used for code validation and for device optimization.

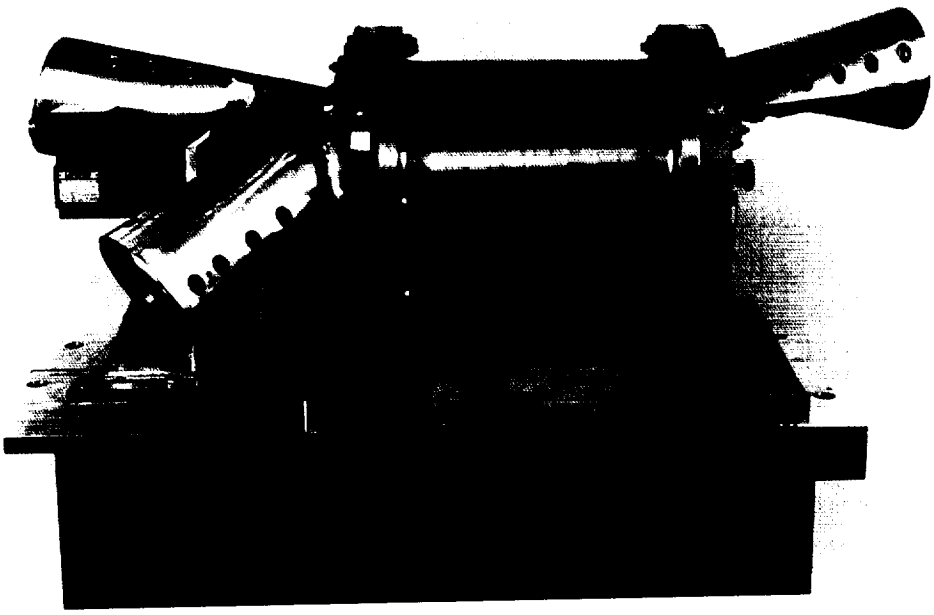

NASA Lewis wave rotor.

Bibliography

Taussig, R.T.: Wave Rotor Turbofan Engines for Aircraft. Mech. Eng., vol. 106, Nov. 1984, pp. 60–64.

Lewis contact: Jack Wilson, (216) 891–2996
Headquarters program office: OAST

LDV Measurments Made on Forward-Swept Propeller

Since the mid-1970's advanced propellers have been investigated as a means of powering aircraft at high subsonic speeds. Advanced propeller models have been tested in wind tunnels in order to quantify the effects of varying such propeller design parameters as blade shape, number of blades, and inflow Mach number on the overall aerodynamic and acoustic properties of both single-rotating and counterrotating configurations. These investigations, which have involved propfan models having blades that sweep back (opposite the flight direction), have demonstrated significant aerodynamic performance advantages of advanced propellers over current turbofans at typical cruise conditions of Mach 0.8 and 35,000-ft altitude.

The counterrotating propellers have proved to be inherently more fuel efficient than the single-rotating propellers because the downstream rotor redirects the swirl generated by the upstream rotor back into the axial direction. Counter-rotating configurations are also inherently noisier. Much of this noise occurs because the downstream rotor operates in the highly unsteady wake of the upstream rotor. Flow-field nonuniformities in the upstream rotor's wake flow can result from viscous wakes, potential field nonuniformities created by the blades, leading-edge and tip vortices, and large-scale flow separation off the blade surfaces. Noise is produced when these phenomena interact with the downstream rotor blades. These nonuniformities, and the noise problems they create, are most severe at takeoff, when the propellers are operating at high power. Making the upstream rotor's wake flow more uniform would tend to decrease the amount of interaction noise produced.

Recently, a test was conducted in the NASA Lewis 9- by 15-ft Low Speed Wind Tunnel to determine if, at takeoff, forward-swept upstream rotor blades might provide a more uniform wake flow than the aft-swept blades normally used in these propellers. Laser Doppler velocimetry (LDV) was used to measure the rotor wake characteristics of both forward-swept and aft-swept upstream rotor

blades. The velocity field created by the aft-swept rotor was measured at low and moderate power levels. Data could only be obtained downstream of the forward-swept blades at low power because they fluttered at higher power conditions.

Because of the flutter the emphasis of the LDV testing shifted from determining the rotor wake flows to measuring the flow field around the forward-swept blades during flutter. A comprehensive set of flow-field data was obtained on the flow within the blade passages. As a comparison with the flutter condition, data were also obtained at a condition where the rotor speeds were decreased to a point where the blades showed no signs of flutter. The LDV data will be used to obtain a better understanding of the flow characteristics during flutter. The data can also be compared with the output of computational fluid dynamic codes being developed to predict flutter.

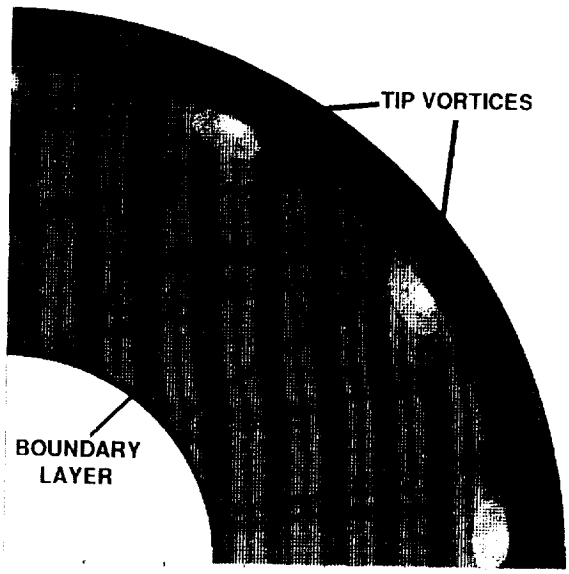

Measured axial velocities downstream of forward-swept propfan.

Lewis contact: Gary G. Podboy, (216) 433–3916
Headquarters program office: OAST

Aeroacoustic Propulsion Laboratory Qualification Tests Are Under Way

Facility checkout tests are under way for the newly completed Aeroacoustic Propulsion Laboratory (APL). The 130-ft-diameter geodesic dome structure provides a hemi-anechoic environment for aeroacoustic testing of aircraft propulsion systems while protecting Lewis' residential neighbors. The completed APL facility houses the new Nozzle Aeroacoustic Test Rig (NATR) as well as the Powered Lift Facility (PLF).

The dome structure, employing an STC–55-rated sandwich panel construction, was designed to reduce noise to acceptable levels in nearby residential communities. The enclosure provides a nearly all-weather semisecure test facility for a variety of test programs, including High Speed Research (HSR) nozzle concept evaluations and short-takeoff-and-vertical-landing activities. Preliminary results of initial transmission loss measurements conducted during NATR checkout tests in the spring of 1992 indicate that the sandwich panels are performing as expected. No noise complaints have been received since the dome construction was completed. Detailed community noise tests will take place in November, using a J85 engine as the sound source.

Fiberglass wedge treatment on the entire interior surface of the dome provides a hemi-anechoic interior environment. Potentially reflective surfaces on internal structures, such as test hardware, facility plumbing, and instrumentation stands, have been covered or shielded with a variety of absorptive materials to ensure the highest quality acoustic environment.

Facility operations and safety systems have been selected, designed, and installed to maintain the research caliber of the acoustic conditions inside the dome structure. A 40,000-ft^3/min fan at the top of the dome provides continuous but quiet ventilation when gaseous hydrogen fuel is burned during HSR testing. Entrained air for the ejector-fed free jet is provided through a noise-attenuating air intake enclosure. The microphone arrays are shielded from radiated self-noise of the ejector by a sealed noise-attenuating (STC–54) structure that surrounds the ejector portion of the NATR. Ejector noise is also attenuated as it travels downstream through the NATR by the Kevlar treatment in the walls of the diffuser and plenum sections.

Necessary facility lighting, camera systems, and facility-monitoring instrumentation systems have all been selected and located to minimize any acoustic interference while ensuring safety and meeting research requirements. New equipment installations and facility modifications are all considered and implemented with regard for their impact on the quality of the acoustic environment.

Extensive checkout tests are now being conducted to evaluate the interior of the dome structure with respect to a number of accepted performance measures, among them the absorption coefficient of the wedge treatment and the observed behavior of sound with respect to the inverse square law of sound propagation. During this evaluation a frequency-versus-spatial-location map of the acoustic quality of the facility's intended microphone array region will be created, using three sound sources and a variety of signal-processing techniques. Any sources of acoustically significant reflections will be identified and solutions proposed.

Lewis contact: Beth A. Cooper, (216) 433–3950
Headquarters program office: OAST

Euler/Navier-Stokes Code Predicts Coupled Internal and External Engine Flow

Current high-bypass-ratio engines tend toward larger diameters and shorter cowls in the quest for larger thrusts and lower drags. These geometric changes created a need for computer analysis tools that would couple the regions within the engine while computing the flow. Although it is possible to analyze the engine one component or one flow path at a time, the strong coupling between components within an engine makes that effort tedious and inefficient. An ongoing engine analysis code development effort, carried out under contract at the Allison Gas Turbine Division of General Motors, has produced a computer program that solves for three-dimensional steady flows through a wide range of engine configurations. The major advance in this code is the ability to simultaneously solve for the flow through the multiple flow paths found in engines (e.g., flow outside the cowl, flow through the fan and bypass duct, and flow through the engine core). Each flow path may contain one or more blade rows.

Allison Gas Turbine has developed several advanced ducted propfan analysis codes (ADPAC). The current version, using the average passage equation system for the blade-to-blade coupling is known as ADPAC–APES. The code is an extension of the Euler/Navier-Stokes code VSTAGE developed by Dr. John Adamczyk at NASA Lewis. With the average passage technique the influence of one blade row on all the others is introduced

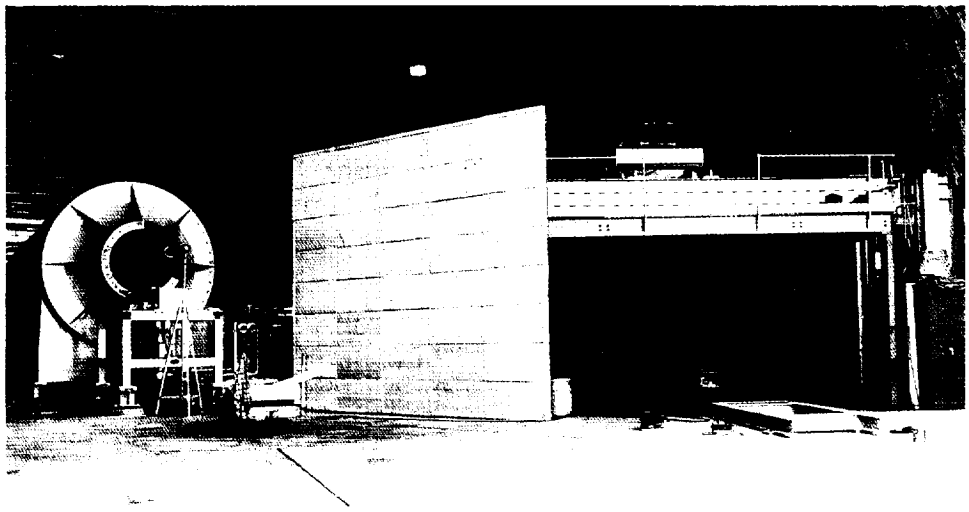

Interior view of hemi-anechoic Aeroacoustic Propulsion Laboratory near completion.

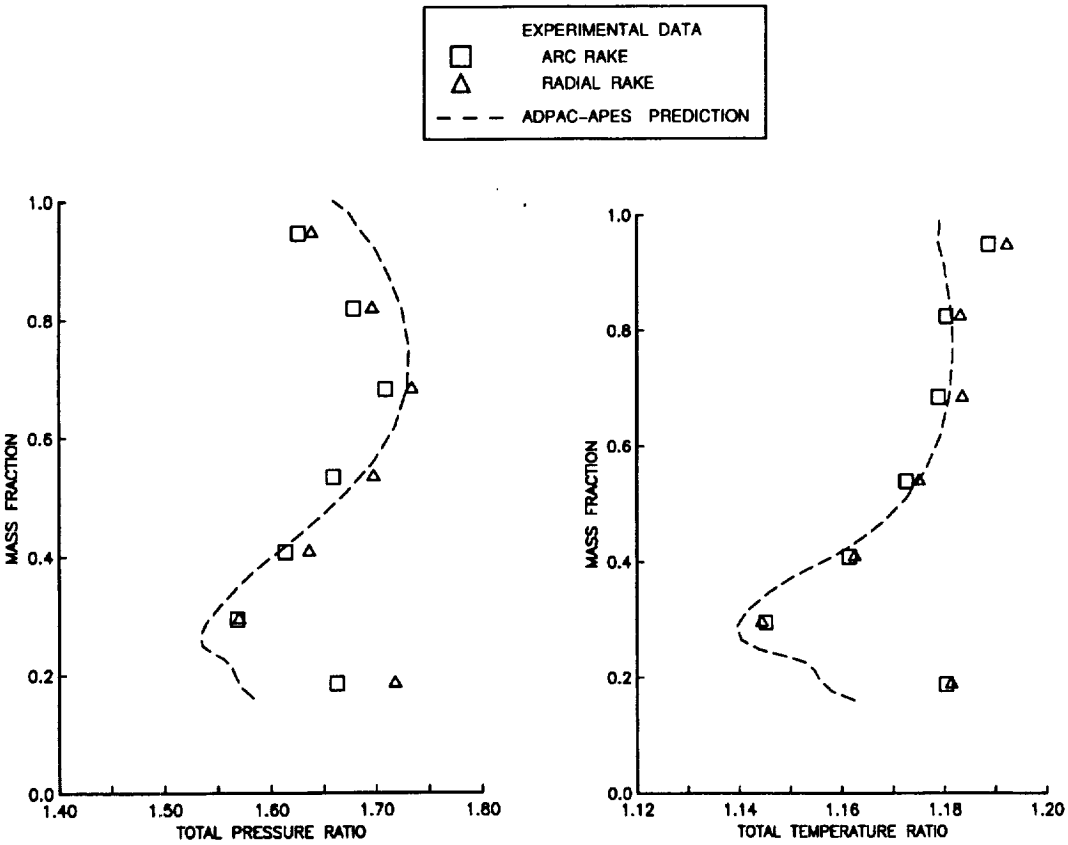

Comparison of predicted and measured total pressure and total temperature as function of (spanwise) mass fraction.

through distributed body forces and blade row blockage. The ADPAC–APES code automatically couples the various flowpaths and blade rows being modeled, allowing for a simpler and more efficient analysis of complex configurations.

Comparisons with test data to validate the code have shown good agreement. The Navier-Stokes results compare better with experimental data than the Euler results, although both require geometry models that include the gap between the fan tip so that the tip leakage flow is also predicted. Experimental data are available for one validation case, NASA's Energy Efficient Engine fan section near its design point. The data points shown are from rakes placed downstream of the fan in the bypass duct. The Navier-Stokes predictions of total pressure and total temperature agree well with data over most of the span. The discrepancy near the hub is attributed to errors in geometry (core inlet guide vane) reducing the core mass flow and hence affecting the hub region of the fan. At the fan tip the coarse grid reduced the accuracy of the tip leakage flow prediction.

NASA and industry are now using the ADPAC–APES flow solver to analyze future engine concepts. Future efforts will couple this flow solver to combustor models to enable the simulation of the entire engine.

Bibliography

Crook, A.J.; and Delaney, R.A.: Investigation of Advanced Counterrotation Blade Configuration Concepts for High Speed Turboprop Systems. Task IV – Advanced Fan Section Aerodynamic Analysis Final Report. NASA CR–187128, 1992.

Lewis contact: Dr. Christopher J. Miller, (216) 433–6719
Headquarters program office: OAST

Jet Noise Prediction Method Improved

A major challenge of the High Speed Research Program is the reduction of jet noise to meet the Federal Aviation Administration's community noise standards. Meeting this challenge will require complex noise suppression devices. Appropriate tools for jet noise prediction are needed to design such devices. Current methods for predicting jet noise are primarily empirical and are not applicable to the complex geometries being considered. To address this issue, NASA Lewis has an ongoing program to enhance jet noise prediction capabilities.

Recently, as part of this Lewis program, improvements have been made to the MGB noise prediction method that will enhance its ability to predict the noise from complex nozzles, such as those being considered for the future High Speed Civil Transport. The MGB method, developed by General Electric under government contract, is based on the acoustic analogy approach to noise prediction. It uses computed flow-field information to determine the noise source strength and how the mean flow affects the propagation of this noise to the far field. This method has the potential to calculate the noise from jets of arbitrary geometry. However, this ability depends on predicting the mean flow. Recently, the MGB method has been modified to accept predicted flow-field information as input and to take advantage of recent advances in computational fluid mechanics methods for mean flow and turbulence intensity predictions. The modification also permits independent grid selection for aerodynamic and acoustic purposes.

Predictions of jet noise from an ideally expanded axisymmetric convergent nozzle have been made using this improved noise prediction method with flow-field input from the PARC Navier-Stokes code with a k-ε turbulence model. Comparisons of predicted and measured levels at the jet condition typical of takeoff for the High Speed Civil Transport show excellent agreement. Further improvements to allow predictions for non-axisymmetric jets are under way.

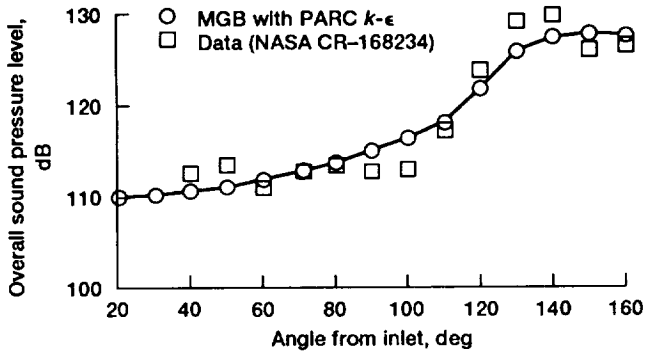

Comparison of measured and predicted jet noise directivity using improved MGB method with PARC k-ε aero input.

Bibliography

Khavaran, A.; et al.: Computation of Supersonic Jet Mixing Noise for an Axisymmetric CD Nozzle Using k-ε Turbulence Model. AIAA Paper 92-0500, 1992. (Also NASA TM-105338, 1992.)

Mani, R.; et al.: High Velocity Jet Noise Source Location and Reduction. Task 2: Theoretical Development and Basic Experiments. Report FAA-RD-76-79-II, 1977.

Lewis contact: Eugene J. Krejsa, (216) 433-3951
Headquarters program office: OAST

Climb/Cruise Performance of Advanced Ducted Propeller Model Measured in Wind Tunnel Tests

With the ever-increasing competition in the world aerospace market, commercial aircraft engine manufacturers are developing technologies to make their products more reliable and maintainable, as well as more economical to operate. One of these advanced technology concepts is the advanced ducted propeller, which attempts to combine the high propulsive efficiency of a propeller with the acoustic attenuating characteristics of a turbofan duct. Current efforts are being directed toward understanding this new technology, and wind tunnel tests being conducted with scale models of advanced ducted propeller designs are helping to provide some answers.

In cooperation with Pratt & Whitney, a division of United Technologies Corporation, an advanced ducted propeller (ADP) model was designed, built, and tested in the NASA Lewis 8- by 6-Foot Supersonic Wind Tunnel to determine the aerodynamic and acoustic performance characteristics at simulated aircraft flight conditions from climb to cruise. Determining the aerodynamic performance characteristics consisted of measuring the forces produced by the fan and the nacelle/stator combination; measuring the model external static pressures on the nacelle; measuring the model

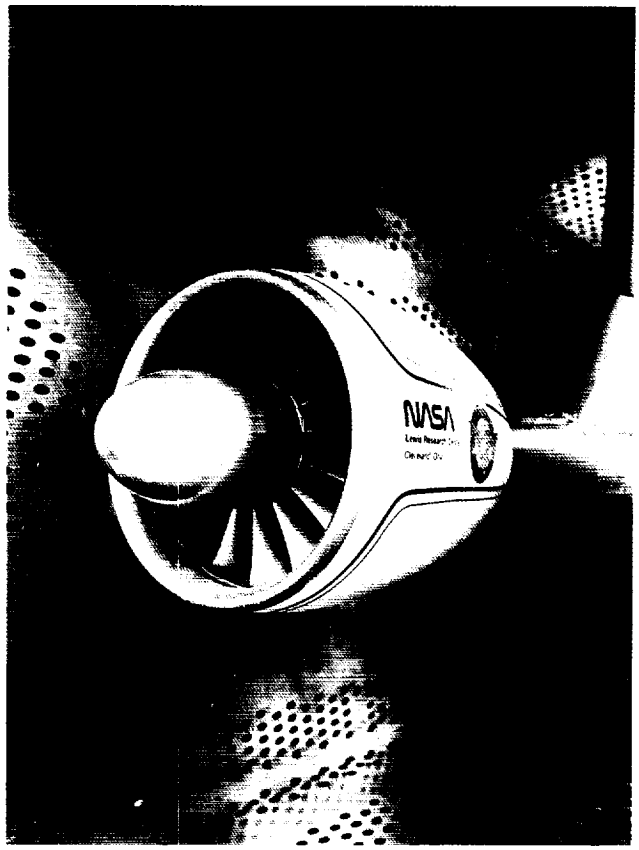

Advanced ducted propeller installed in NASA Lewis 8- by 6-Foot Supersonic Wind Tunnel.

internal static pressures on the inlet duct, fan duct, and nozzle; and measuring the total pressures and total temperatures behind the fan. The fan thrust and torque produced during the test were measured with a two-component rotating force balance. The nacelle/stator combined forces were measured with a unique six-component static force balance. The model noise was measured with a series of pressure transducers mounted on a plate located just above the model.

The ADP model had a 17-in.-diameter fan with 16 fan blades and 22 fan exit guide vane stators. Several different model configurations were investigated, including three inlet duct lengths and seven fan blade angle settings. Each configuration was tested at wind tunnel velocities between Mach 0.40 and 0.85 (265 to 562 knots) and at fan rotation speeds from zero (locked) to 12,000 rpm. Because the engine-out performance characteristics of the engine are of crucial importance to the engine manufacturer, the matrix of test conditions included measurements at different tunnel velocities with the fan both windmilling and locked in place.

Currently, data obtained from the recently completed tests are being analyzed to determine the aerodynamic and acoustic performance characteristics. Results from these tests will be compiled into a data base that will then be used to influence future advanced ducted propeller designs and test programs.

Lewis contacts: Christopher E. Hughes, (216) 433–3924; James H. Dittmar, (216) 433–3921
Headquarters program office: OAST

Forward-Swept Counterrotating Propeller Tested in Wind Tunnel

Testing of a forward-swept counterrotating propeller model was completed in the 9- by 15-Foot Low Speed Wind Tunnel on schedule, July 2, 1992. The purpose of the test was to investigate forward blade sweep as a method of reducing noise at takeoff conditions. The acoustic effects of forward sweep, power level (blade angle), and blade tip geometry on noise were investigated. Blade structure effects on low-speed flutter were extensively investigated, and detailed flow-field measurements were taken with a laser velocimeter system. Overall a large quantity of good aeroelastic, acoustic, and aerodynamic data were recorded, completing a significantly expanded test matrix. The test used the Lewis counterrotation drive rig and blade and hub hardware loaned by General Electric (GE).

Feasibility studies, final design, and fabrication of a forward-swept upstream rotor (F39) were completed by GE on contract with NASA Lewis. The design characteristics of the forward-swept blade were chosen to match an existing blade set (F31/A31). Because the expected difficulties in aeromechanically designing a forward- swept blade that would not structurally diverge under loads did not materialize during the structural analysis, the blades were fabricated with few design iterations. The analytical acoustic effort during the design phase pointed out the need to measure flow-field details including blade wakes, tip vortex strength and size, and vortex trajectory. The predicted aerodynamic effect of forward sweep was favorable, but the predicted acoustic effect remains unknown. A version of the same blade was fabricated with a modified, softer ply

layup that was predicted to structurally diverge (F39D).

Aeroelastic testing quickly became a major part of this tunnel entry when the spar/shell composite forward-swept blades (F39) fluttered at loads below the takeoff design point. The extensive flutter investigation included the softer divergent blade set, F39D; a stiffer blade set, F39S (quickly designed at Lewis and built at GE); blade tip clipping and rounding, blade angle (power level) changes, viscoelastic damping tape, and mismatches of blade tip shape and blade angle.

Acoustic data consisted of recordings of an axial traversing microphone and polar and axial traverses of a polar microphone. The model was set at rotational speeds ranging from below takeoff design to slightly above, and at 0°, ±8°, and ±16° angle of attack (when possible). Data on the aft-swept reference blades (F31/A31) were recorded at low, moderate, and high power for comparison with the forward-swept blades. Configurations tested will allow acoustic evaluation of forward sweep, power level (blade angle), and blade tip geometry.

Extensive unplanned laser Doppler velocimeter (LDV) data were recorded in support of the aeroelastic investigation of low-speed flutter. The LDV data matrix in support of acoustic data and analysis was also expanded. Data documenting the tip vortex and the blade wake were recorded for the original F39 at low blade angles (both below and in the flutter condition and at an acoustic recording point). More extensive flutter data were recorded at higher power for the stiffer F39S blades, and additional data were recorded for acoustics. Reference LDV data on the aft-swept F31 blades were recorded at low, moderate, and high blade angles just as was done for the acoustics.

This accomplishment required commitment from a large number of people (across organizational boundaries) throughout Lewis and quick response from General Electric in fabricating an extra set of blades. The number of configurations tested was nearly double those planned, with 60 percent more tunnel runs. The additional runs concentrated on aeroelastic investigation of flutter and detailed LDV measurements. Although the unducted counterrotation testing is complete, this large set of data will allow continued evaluation of the unexpected flutter that occurred and improvement of the aerodynamic and aeroelastic computer codes needed to design future swept blades.

Lewis contact: Robert J. Jeracki, (216) 433–3917
Headquarters program office: OAST

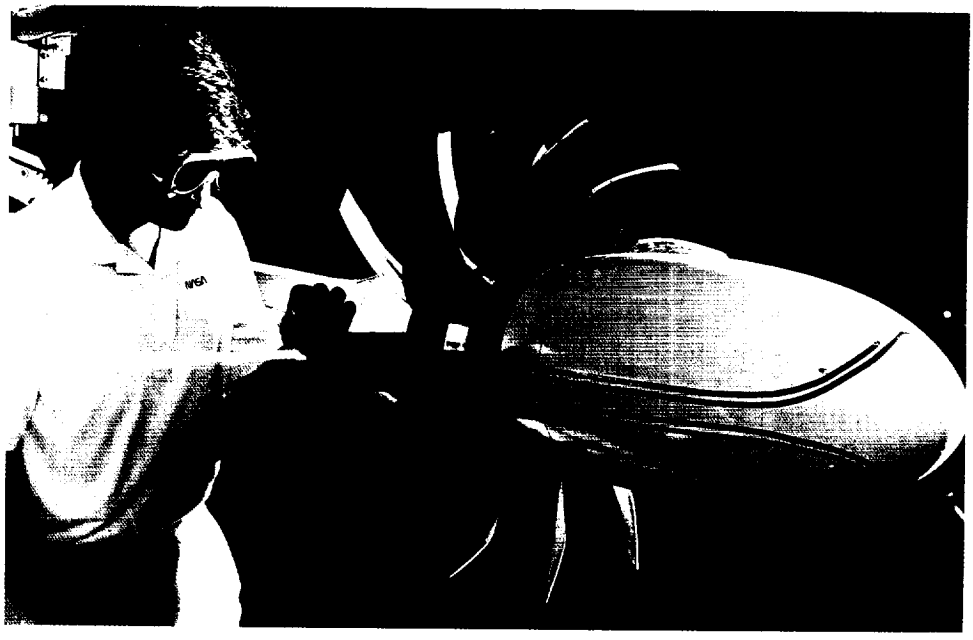

Forward-swept counterrotating propeller model in wind tunnel.

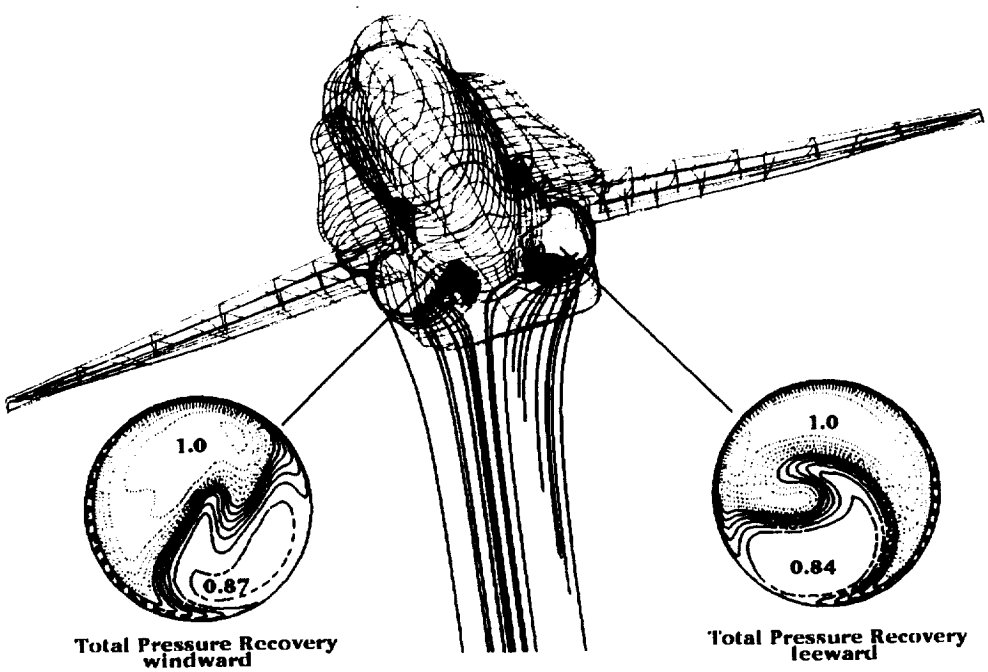

F–18 at high angle of attack and moderate side slip.

F–18 Inlet Flow Calculated at Combination of High Angle of Attack and Moderate Side Slip

NASA Lewis is currently engaged in a research effort as a team member of the High Alpha Technology Program (HATP) within NASA. This program utilizes a specially equipped F–18, the high alpha research vehicle (HARV), in an ambitious effort to improve the maneuverablility of high-performance military aircraft at low-subsonic-speed, high-angle-of-attack conditions. The overall objective of the Lewis effort is to develop inlet technology that will ensure efficient airflow delivery to the engine during these maneuvers. One part of the Lewis approach utilizes computational fluid dynamics codes to predict the installed performance of inlets for these highly maneuverable aircraft.

The PARC3D code, a three-dimensional Navier-Stokes solver, is being used to calculate the flow field ahead of and inside the HARV and a subscale F–18 wind tunnel model. A computational result is presented here for a 19.78-percent scale model at 60° angle of attack and 10° side slip for a free-stream Mach number of 0.20. The particle trajectories indicate vortices developing under the leading-edge extension that are ingested by the inlets, with the stronger vortex being ingested into the leeward inlet. The ingested vortices along with flow separation on the cowl lip and a vortex that develops inside the diffuser duct combine to produce the total pressure profiles shown at the engine face.

These results represent the first predictions of the flow field within F–18 inlets at a high angle of attack and moderate side slip. These and other numerical results will be used to support wind tunnel tests at NASA Lewis and flight tests at NASA Dryden.

Lewis contacts: Richard R. Burley, (216) 433–3605; C. Frederic Smith, (216) 826–6708
Headquarters program office: OAST

Three-Dimensional Rarefied Gas Flow in a Driven Cavity Numerically Analyzed

With space vehicles orbiting the Earth at hypersonic speed, numerical methods to cover all flow regimes (from free molecular flow in space to continuum flow on Earth) become more important. In order to cover all flow regimes, the Boltzmann equation must be used instead of the Navier-Stokes equations. Advances in computer hardware in recent years make methods of solving the Boltzmann equation that are based on the kinetic theory more feasible.

As part of an in-house effort a driven-cavity flow problem has been solved for diatomic gases by applying the discrete ordinate method to the Boltzmann equation with the Bhatnagor-Gross-Krook (BGK) model. A sample of computational results is presented here for velocity profiles along the centerline. The results cover free molecular flow (Knudsen number Kn = 100), slip slow (Kn = 0.1), and nearly continuum flow (Kn = 0.03). They clearly show that the flow slips on the moving surface (y = 1) for free molecular flow and slip flow; that is, the flow velocity on the surface is less than the speed of the moving wall (u_x = 0.1). The velocity on the moving surface is only 0.04 for free molecular flow, or 40 percent of the speed of the moving surface. The velocity on the moving surface for Kn = 0.03 is about 90 percent of the speed of the moving surface. Therefore, the no-slip boundary condition of the Navier-Stokes equation was almost obtained for nearly continuum flow.

The results demonstrate the capability of the method to predict three-dimensional flows ranging from free molecular flow to nearly continuum flow. The method is also a good candidate for use with massively parallel computers because computation can be easily divided into equal pieces for parallel programming.

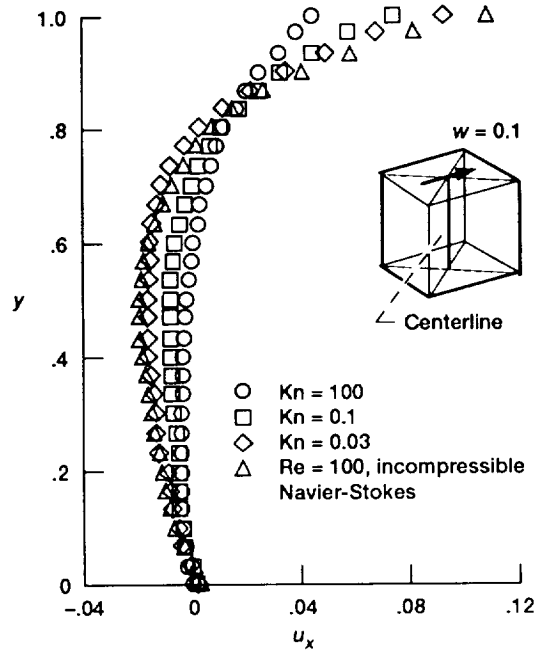

Velocity profiles along centerline.

Bibliography

Hwang, D.P.; and Huynh, T.H.: A Finite Difference Scheme for Three-Dimensional Steady Laminar Incompressible Flow, NASA TM-89851, 1987.

Lewis contact: Dr. Danny P. Hwang, (216) 433–2187
Headquarters program office: OAST

Aeropropulsion Facilities and Experiments

Laser Sheet Flow Visualization System Added to Supersonic Wind Tunnel

The Mach 5 test at the 10- by 10-Foot Supersonic Wind Tunnel marked the first time that laser testing was conducted in a supersonic tunnel at NASA Lewis. This was also the first time for model-mounted, sheet-generating optics and video camera systems in a supersonic tunnel environment at Lewis.

Laser sheet flow visualization capability has been recently added to this facility. The new system utilizes laser light to acquire qualitative data for internal flow-field investigation of wind tunnel inlet models. Such data not only provide an increased ability to understand the local flow phenomena, but are also valuable for calibrating and validating computational fluid dynamics (CFD) analyses.

The Mach 5 inlet wind tunnel model was the first test program to utilize the facility laser sheet flow visualization system. The Mach 5 is a large-scale inlet containing highly complex three-dimensional flow phenomena. Extensive CFD analyses have been performed on this model, but the laser sheet data were extremely valuable in increasing understanding of the three-dimensional flow phenomena due to the shock/boundary layer interactions that are common to inlets of this type.

Mach 5 inlet installed in wind tunnel.

A water-cooled 25-W argon ion laser provides the light source for the laser sheet. The laser is housed in a newly constructed laser room and remotely operated by a computer located in the facility control room. The laser room is near the test section and is large enough to accommodate future expansion of the facility laser system for potential laser Doppler velocimetry (LDV) work. Where it was possible and practical, the design of the laser sheet system allowed for potential adaptation into a full nonintrusive LDV system.

The laser light is transmitted to model-mounted optics through single-fiber, fiber optic cables. Visual data for the laser sheet are obtained through the use of small model-mounted black-and-white charge-coupled device cameras. Laser sheet images are viewed in real time with on-line image enhancement capability.

A tunnel seeding system has been mounted upstream of the test section in the tunnel bell-mouth. Steam is injected into the tunnel flow stream and controlled remotely from the control room. Tunnel seeding can also be accomplished by operating the facility at a higher dewpoint, resulting in condensation in the flow stream.

Lewis contact: Tim W. Schuler, (216) 433–8730
Headquarters program office: OAST

Aerospace Technology

Materials

Advanced High-Temperature Engine Materials Technology Continues Progress

The objective of the Advanced High-Temperature Engine Materials Technology (HITEMP) Program is to generate technology for revolutionary advances in composite materials and their structural analysis that will enable the development of 21st century civil propulsion systems with greatly increased fuel economy, improved reliability, extended life, and reduced operating costs. The primary focus is on fan and compressor materials (polymer matrix composites), compressor and turbine materials (metal and intermetallic matrix composites), and turbine materials (ceramic matrix composites). These composite materials are being developed by in-house researchers and on grants and contracts.

NASA considers this program to be a focused materials and structures research effort that builds upon our basic research programs and will feed results into application-oriented projects, such as NASA's proposed initiatives to develop the technology for advanced subsonic transport engines, for rotorcraft engines, and for a 21st century high-speed civil transport. HITEMP is also closely coordinated with the Department of Defense/NASA Integrated High Performance Turbine Engine Technology (IHPTET) Program and the National Aerospace Plane (NASP) Program. Advanced composite materials from HITEMP may be used in these future applications.

A Lewis-developed polymer matrix composite has been fabricated into an engine fairing and successfully tested in an F110 engine. The fairing performance was excellent, showing little or no visible degradation. Advanced x-ray and x-tomography techniques have been demonstrated as successful methods of guiding the precision machining and structural modeling of metal matrix composite rings for compressor disks. A continuum damage mechanics model has been used to accurately predict the fatigue life of laboratory samples of the metal matrix composite ring materials. Experimental quantities of higher strength alumina fibers have been produced, and an optimized fabrication technique for processing glass ceramic matrix composites has been developed.

The fifth annual review of the HITEMP Program was held October 27 and 28, 1992. Details of research accomplishments are published in a conference report, NASA CP–10104.

Lewis contacts: Dr. Hugh R. Gray, (216) 433–3230; Carol A. Ginty, (216) 433–3335
Headquarters program office: OAST

Materials Program Supports High-Speed Civil Transport

NASA is undertaking a materials research and development program supporting the development of a high-speed (supersonic) civil transport (HSCT) for entry into commercial service by the year 2005.

The objectives of the Enabling Propulsion Materials (EPM) Program are

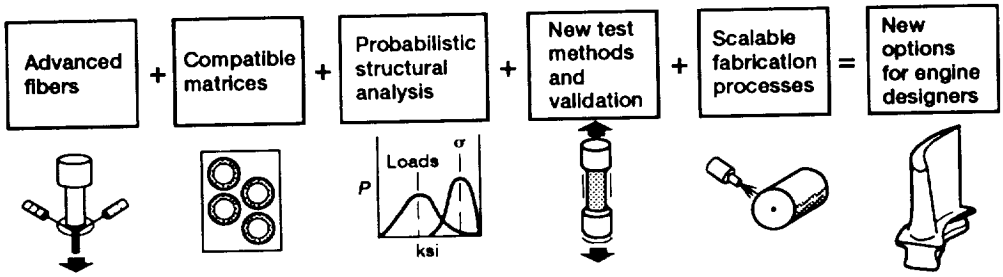

Elements of HITEMP program.

- To develop high-temperature advanced materials including fibers, ceramic matrix composites, and lightweight intermetallic matrix composites/metal matrix composites

- To establish improved processes for fabricating advanced composite components

- To enhance the development of analytical tools for composite and component design, fabrication, and life prediction

- To evaluate composite subcomponent and component reliability and durability in a rig or engine environment. The primary focus is on demonstrating the technology readiness of a combustor liner and an exhaust nozzle for an HSCT propulsion system by 1999.

EPM is primarily a contractual effort involving the two major U.S. aircraft engine manufacturers, Pratt & Whitney (P&W) and General Electric Aircraft Engines (GEAE). In addition, a broad-based subcontractor team includes other engine companies, fiber producers, composite fabricators, testing companies, and academia. Complementing this contractual effort is an NASA Lewis in-house program that will address risk reduction issues.

A unique feature of EPM is the establishment of integrated product development teams for the combustor liner and the exhaust nozzle. These teams consist of representatives from P&W, GEAE, NASA, and subcontractors where appropriate. Members from various disciplines, including engineering expertise in design, processing, materials, structures, and test operations, make up the teams. The major benefit of these teams will be to reduce the materials development risk.

The in-house efforts at NASA Lewis have contributed significantly to materials development for HSCT engines. NASA Lewis' unique ability to conduct environmental durability tests of candidate materials is critical to the overall program. The tests are performed in a high-pressure burner rig that simulates the HSCT combustor environment while thermally cycling the materials as in an actual HSCT mission. Additional in-house research includes studies of environmental degradation mechanisms, ceramic fiber and matrix development and characterization, and development of novel ceramic materials to alleviate the risk involved in HSCT materials development.

The two combustor concepts proposed to meet the low oxides-of-nitrogen (NO_x) requirements of the HSCT engines, the rich burn/quick quench/lean-burn (RQL) and the lean premixed/prevaporized (LPP) combustor, require the use of advanced high-temperature ceramic matrix composite materials. The economic and environmental effects of incorporating advanced materials and processes in low-NO_x combustors were evaluated for a long-range Mach 2.4 HSCT. When evaluated on a 500-aircraft fleet, the EPM combustor materials reduced total NO_x emissions by 174,000 tons (a 28-percent reduction) annually. The material systems selected for development consist of small-diameter, near-stoichiometric silicon carbide (SiC) fibers in an SiC or silicon nitride (Si_3N_4) matrix. These material systems can meet the projected temperature capability, usable strength, elastic modulus, coefficient of thermal expansion, thermal conductivity, and Poisson's ratio. The parabolic oxidation rates of high-purity chemical vapor deposited (CVD) SiC and Si_3N_4 were determined for various operating environments in the 2190 to 2550 °F (1200 to 1400 °C) temperature range. Also, preliminary cyclic oxidation studies in 2730 °F (1500 °C) and 2370 °F (1300°) air failed to reveal any serious scale spallation behavior for either CVD SiC or sintered SiC or Si_3N_4.

Two candidate exhaust nozzle designs have been proposed to meet the dual requirements of noise attenuation and high-temperature durability for the exhaust nozzle. Both designs would use advanced high-temperature composites for the nozzle structure and acoustic liners to attenuate noise. Single-crystal oxide monofilaments were chosen as the fiber reinforcement for these composites because of their creep resistance and thermochemical stability. A current concern for these fibers is their lack of strength at high temperatures. As part of the fiber development program performed under EPM, single-crystal alumina fibers with an average tensile strength of 280 ksi at 2000 °F (1095 °C) have been produced. This represents a 70-percent increase over the original fiber strength. A variety of composite fabrication processes are now being evaluated to incorporate these fibers into high-temperature metal and intermetallic matrices for use in the HSCT exhaust nozzle.

Lewis contact: Joseph R. Stephens, (216) 433–3195
Headquarters program office: OAST

Laser Light Scattering Provides a Clear Vision of the Future

A compact fiber optic probe developed for on-orbit science experiments has been used to detect the onset of cataracts, a capability that could eliminate physicians' guesswork and result in new drugs to dissolve cataracts before surgery is necessary. This probe is a spinoff of an advanced technology development program in laser light scattering at NASA Lewis that has reduced a small roomfull of electronics, detectors, lasers, and associated optics to the size of a briefcase. This progress will permit experiments in microgravity that can quantitatively answer basic science questions about nucleation, critical phenomena, aggregation, diffusion, etc., in an environment unfettered by convection and sedimentation effects. Meanwhile, ground-based spinoffs of this work will be impacting our lives in the near future.

Ansari and Dhadwal have recently (1992) published a paper showing the crystalline size distribution of senile cataracts in human eye lenses of different ages. This characterization work was done using a noninvasive probe about the size of a pencil. This fiber optic probe sends a cone of light into the eye and routes the light scattered back in its direction through an optical fiber to a detector. The signal coming from the detector is then sent to a laptop computer containing a correlator that interprets the information contained in the light scattered by the eye lens. A cataract, which is caused by a change in the chemical composition of the lens, leads to blurred and double vision, sensitivity to light and glare, a less vivid perception of color, and frequent eyeglass prescription changes. Normally cataracts develop over many years but are not readily identifiable at their onset. At present the only treatment is to surgically remove the clouded eye lens and replace it with an artificial lens. With the new ability to detect cataracts early on and to monitor their progression, treatments through diet and medicine may become possible.

This NASA spinoff is a result of instrumentation designed to study a large variety of chemical problems and solutions discussed in the AIAA article. Protein crystals are one of these systems; cataracts are but a small, yet significant, group of proteins. Our recent work with one of the scientists studying protein crystals for NASA (W. Wilson) has shown that this compact non-

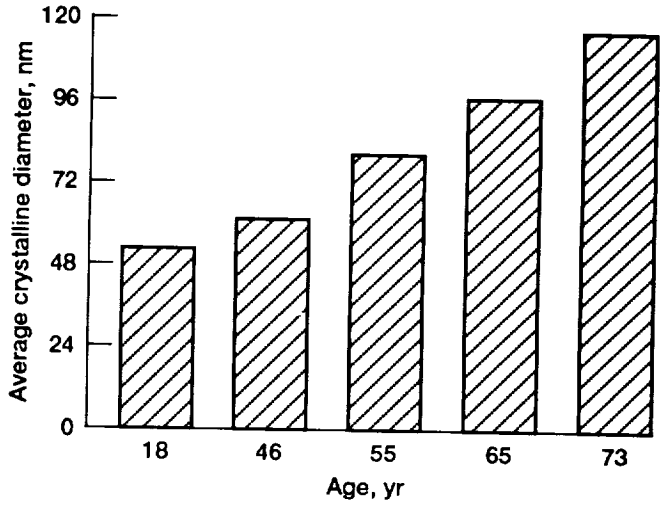

Crystalline size distribution of senile cataract in human eye lenses.

invasive instrument accurately monitors proteins down to a few nanometers in size and works from dilute solutions all the way up to highly concentrated solutions that would not allow a conventional light-scattering instrument to function. This backscatter probe functions over this large range because the scattered light is collected before it passes very far into a concentrated solution and hence before it can multiply scatter the light and corrupt the information this scattered light carries. A conventional system attempting to analyze the light coming through a concentrated medium, which scatters the light many times before it reaches an observer, is much like trying to look through milk or like trying to see the world through eyes that have cataracts.

Bibliography

Ansari, R.R.; and Dhadwal, H.S.: A Fiber Optic Sensor for Ophthalmic Refractive Diagnostics. Fiber Optic Medical and Fluorescent Sensors and Applications; Proceedings of the Meeting, D.R. Mansmann, et al., eds., (SPIE Proceedings, vol. 1648), Society of Photo-Optical Instrumentation Engineers, Bellingham, WA, 1992, pp. 83–105.

Dhadwal, H.S.; Ansari, R.R.; and Meyer, W.V.: A Fiber Optic Probe for Particle Sizing in Concentrated Suspensions. Rev. Sci. Instrum., vol. 62, Dec. 1991, pp. 2963–2968.

Meyer, W.V.; and Ansari, R.R.: A Preview of a Microgravity Laser Light Scattering Instrument. AIAA Paper 91–0779, 1991.

Lewis contacts: William V. Meyer, (216) 433–5011;
Dr. Rafat R. Ansari, (216) 433–5008
Headquarters program office: OSSA

Improved Copper Alloy Developed for Cooled Rocket Engine Combustion Chambers

The combustion chamber of the Space Shuttle main engine (SSME) is cooled by the cold hydrogen fuel that passes through internal passages on its way to being burned. It is made from a copper (Cu) alloy, NARloy-Z, which has greater high-temperature strength than pure cooper while retaining adequate thermal conductivity and resistance to embrittlement by hydrogen. The combined mechanical and thermal stresses nevertheless distort the cooling passages, requiring honing of the inner wall after each flight.

For applications such as SSME the development of advanced copper alloys strengthened by fine Cr_2Nb precipitates was undertaken. The balance of strength and thermal conductivity of an alloy containing 8 at. % chromium and 4 at. % niobium (Cu-8Cr-4Nb) appeared suitable for further investigation. Initially, the fine precipitates were produced by using chill block melt spinning to achieve rapid solidification. In order to scale up production, a powder metallurgy process has been chosen that uses inert-gas powder atomization as the means of rapid solidification. The powders were subsequently consolidated by hot extrusion. Preliminary evaluation shows that alloy Cu-8Cr-4Nb thus produced appears to have an excellent balance of high-temperature strength and thermal conductivity for applications such as the SSME combustion chamber.

Three lots of material produced by commercial sources of inert-gas-atomized powder have been evaluated. The results thus far indicate that the material has good, reproducible properties. The Cu-8Cr-4Nb alloy has much greater mechanical strength than NARloy-Z, particularly at elevated temperatures. The ductility of Cu-8Cr-4Nb is also very good with elongations between 20 and 30 percent and reductions in area between 30 and 50 percent being typical. NASA Marshall Space Flight Center has conducted room-temperature tests of the Cu-8Cr-4Nb alloy in high-pressure hydrogen. Its strength did not change nor was there a decrease in ductility. Therefore, hydrogen embrittlement should not be a problem for this alloy. Testing is currently ongoing to determine the effects of several high-temperature cycles in a high-pressure hydrogen environment on the mechanical properties.

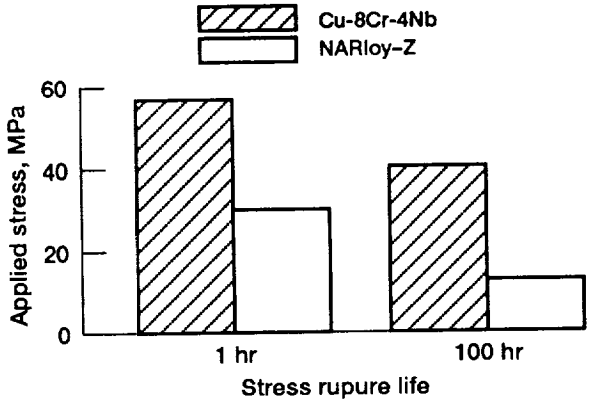

Comparison of stress for 1- and 100-hour stress rupture lives for Cu-8Cr-4Nb and NARloy-Z.

The stress rupture properties of the Cu-8Cr-4Nb alloy at 705 °C (1300 °F) have been examined. Cu-8Cr-4Nb can support approximately twice the stress of NARloy-Z. Alternatively, the life of Cu-8Cr-4Nb is more than 100 times that of NARloy-Z at a given stress level.

Thermal conductivity testing was conducted at Purdue University by using the laser flash technique. Cu-8Cr-4Nb retained 72 to 78 percent of the thermal conductivity of pure copper.

Lewis contact: David L. Ellis, (216) 433–8736
Headquarters program office: OAST

Effect of Matrix Mechanical Properties on SiC/Ti Composite Fatigue Resistance Determined

Titanium and titanium aluminide matrix composites are being considered for advanced aerospace applications requiring high strength and light weight. Beta titanium alloys reinforced by silicon carbide (SiC) fibers could be used in advanced compressor disks of future gas turbine engines and in the airframes of hypersonic vehicles such as the National Aerospace Plane. Although fatigue damage often limits the durability of components in such applications, it is not clear what mechanical properties of the matrix alloy promote satisfactory composite fatigue resistance. NASA Lewis has been studying the effects of these properties on the fatigue resistance of Ti-15-3 beta titanium alloy reinforced with SiC fibers.

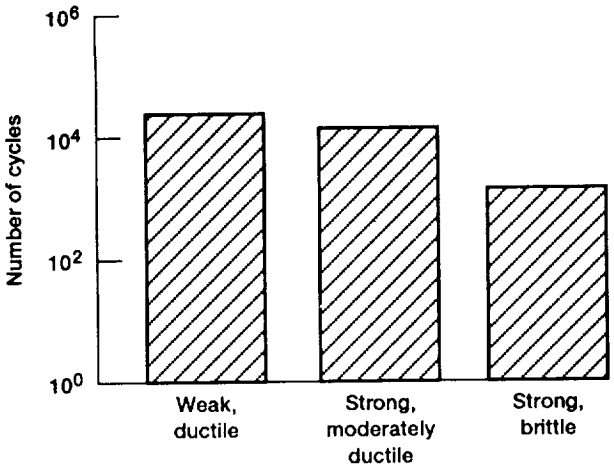

Comparison of SiC/Ti-15-3 crossply composite fatigue lives.

Tests of unreinforced Ti-15-3 matrix alloy indicated that tensile strength, elastic modulus, and ductility could be substantially varied through selective heat treatments. Heat treatments producing weak and ductile, strong and moderately ductile, and strong and brittle matrix alloys were identified. These heat treatments were performed on an SiC/Ti-15-3 "unidirectional" composite reinforced with SiC fibers oriented parallel to the specimen loading axis and on a "crossply" composite reinforced with fibers alternately oriented at 30° and −30° to the loading axis. The composites were then fatigue tested at room temperature to assess their relative fatigue resistances. The fatigue resistance of unidirectional SiC/Ti-15-3 was not strongly affected by the variations in matrix mechanical properties. The large variations in matrix alloy strength, elastic modulus, and ductility only slightly influenced this composite's fatigue life. However, the fatigue resistance of the crossply SiC/Ti-15-3 composite was more affected by the matrix property changes. The weak, ductile matrix and the strong, moderately ductile matrix crossply composite again had essentially the same fatigue life, but the strong, brittle matrix crossply composite had about 10 times lower life.

These results provide some insights on the relative importance of different matrix mechanical properties in these beta titanium matrix composites and also in other metal and intermetallic matrix composites reinforced by continuous ceramic fibers. Matrix properties must allow composite consolidation and must be able to sustain thermal mismatch strains induced by the fibers. But composite fatigue resistance is not necessarily sensitive to matrix modulus and strength and does not demand inordinately high matrix ductility. Satisfactory composite fatigue resistance may be attained with only minimal to moderate matrix ductility, depending on the intended application and component design.

Bibliography

Gabb, T.P.; et al.: The Effect of Matrix Mechanical Properties on SiC/Ti Composite Fatigue Resistance. HITEMP Review 1991: Advanced High Temperature Engine Materials Technology Program, NASA CP-10082, 1991, pp. 38-1 to 38-10.

Gabb, T.P.; et al.: The Effect of Matrix Mechanical Properties on $[0]_8$ Unidirectional SiC/Ti Composite Fatigue Resistance. Scr. Metall. Mater., vol. 24, no. 11, Dec. 1991, pp. 2879–2884.

Lerch, B.A.; Gabb, T.P.; and MacKay, R.A.: Heat Treatment Study of the SiC/Ti-15-3 Composite System. NASA TP-2970, 1990.

Lewis contacts: Dr. Timothy P. Gabb, (216) 433-3272; Dr. John Gayda, (216) 433-3273; Dr. Bradley A. Lerch, (216) 433-5522; Dr. Gary R. Halford, (216) 433-3265
Headquarters program office: OAST

SiC Fiber-Reinforced, Strontium Aluminosilicate, Glass-Ceramic Matrix Composites Tested

Strong, tough, and environmentally stable materials are needed for high-temperature structural applications in advanced high-efficiency, high-performance engines for the aerospace propulsion and power systems of the future. Continuous-silicon-carbide-fiber-reinforced $SrO\text{-}Al_2O_3\text{-}2SiO_2$ (SAS) glass-ceramic matrix composite having monoclinic celsian as the crystalline phase is one such material. Celsian SAS is refractory, oxidation resistant, phase stable from room temperature to the melting point, and thermal shock resistant because of its low thermal expansion coefficient ($\sim 2.7 \times 10^{-6}$ per deg C).

At present, continuous-CVD-SiC-monofilament-reinforced SAS glass-ceramic matrix composites are being processed by using a tape method followed by hot pressing. Composite panels are being hot pressed at various temperatures, pressures, and times in order to optimize the processing parameters. The composites are being tested

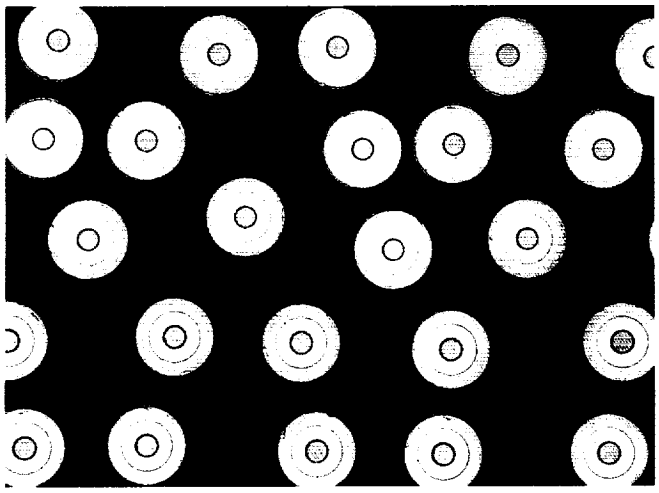

Optical micrograph showing polished and plasma-etched cross section of unidirectional CVD SiC fiber-reinforced SAS glass-ceramic matrix composite.

in three-point bending at room temperature. Strong, tough, and nearly fully dense (~95 to 98 percent) unidirectional composites having first matrix crack stress above 210 MPa and ultimate flexural stress as high as 840 MPa have been fabricated. The fiber/matrix interface was weak, indicating no chemical interaction between the fiber and the matrix during high-temperature processing of the composites. After processing parameters have been optimized, the thermochemical and thermomechanical behaviors of these composites will be characterized under the hostile environments to be encountered in advanced engine applications.

Bibliography

Bansal, N.P.: $SrO.Al_2O_3.2SiO_2$(SAS) Glass-Ceramic Matrix for Fiber-Reinforced Composites. HITEMP Review 1992: Advanced High Temperature Engine Materials Technology Program, NASA CP-10104, 1992, pp. 62–1 to 62–17.

Bansal, N.P.; and Drummond, C.H., III: Kinetics of Hexacelsian to Monoclinic Celsian Phase Transformation in $SrAl_2Si_2O_8$. Presented at 94th Annual Meeting of American Ceramic Society, Minneapolis, MN, Apr. 1992.

Lewis contact: Dr. Narottam P. Bansal, (216) 433–3855

Headquarters program office: OAST

New High-Temperature Reinforcement Fiber Produced

High-temperature structural materials are needed for a variety of component applications in the aerospace, automotive turbine, and power generation industries. These materials should be capable of carrying significant loads at 3000 °F (1650 °C), and higher, under oxidizing conditions. One approach to developing materials that meet these requirements is to focus on refractory oxide composites where oxidation is not a primary consideration for material performance and life.

One approach being considered to meet the strength, toughness, and creep resistance properties required for advanced oxide-based reinforcements is to produce directionally solidified eutectic fibers. The alumina/yttrium-aluminum garnet ($Al_2O_3/Y_3Al_5O_{12}$) eutectic system is chemically, microstructurally, and mechanically stable. There is little or no solid solubility of yttrium-aluminum garnet (YAG) in alumina up to its eutectic temperature, little or no Oswald ripening behavior with exposures up to 1750 °C, and extremely small mismatch in the thermal expansion coefficients. The present work was undertaken to produce the aluminum/YAG directionally solidified eutectic material in continuous fiber form by using a high-thermal-gradient solidification process known as the laser-heated floating zone method.

The first alumina/YAG eutectic fiber was successfully produced at NASA Lewis. The microstructure is aligned in the fiber growth direction and has an aspect ratio on the order of 10 to 1.

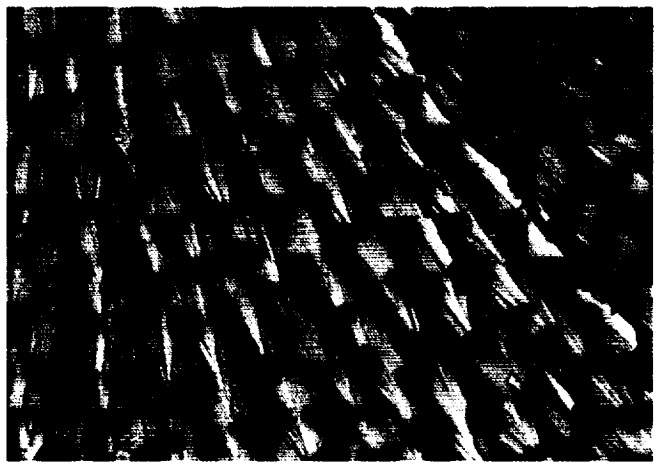

Lamellar microstructure of directionally solidified $Al_2O_3/Y_3Al_5O_{12}$ eutectic fiber.

The fiber's unique lamellar microstructure indicates that the directionally solidified fiber is itself an in-situ composite and therefore should withstand processing damage and carry considerable load at high temperatures. This was demonstrated by tensile strength measurements. The room-temperature tensile strength was 1400 MPa and the 1350 °C tensile strength was 1000 MPa. The strength retention at 1350 °C (relative to room-temperature strength) of 0.7 is quite good in comparison with other single-crystal fibers, which typically retain 0.2 of their room-temperature strength. This unique material is considered to be a potential candidate for NASA's advanced engine programs.

Bibliography

Matson, L.E.; Hay, R.; and Mah, T.: Characterization of Alumina/Yttrium-Aluminum-Garnet and Alumina/Yttrium-Aluminum-Perovskite Eutectics. Ceram. Eng. Sci. Proc., vol. 11, no. 7–8, 1990, pp. 995–1003.

Sayir, A.; and Matson, L.E.: Growth and Characterization of Directionally Solidified $Al_2O_3/Y_3Al_5O_{12}$ (YAG) Eutectic Fibers. HiTEMP Review 1991: Advanced High Temperature Engine Materials Technology Program, NASA CP–10082, pp. 83–1 to 83–13.

Lewis contact: Dr. Ali Sayir, (216) 433–6254
Headquarters program office: OAST

Interface Coatings Identified for Sapphire-Fiber-Reinforced Ceramic Matrix Composites

Achieving high toughness and improved reliability in a ceramic matrix composite requires that a weak interface be maintained between the fiber and the matrix. In an oxide matrix composite reinforced with oxide fibers, it is often necessary to coat the fibers in order to avoid the fiber/matrix interactions that can occur at processing or use temperatures. An effective coating material for an oxide/oxide composite system must be chemically stable within the composite system, oxidation resistant to the intended use temperature, and capable of providing a weak link between the fiber and the matrix in order to achieve low interfacial shear stress.

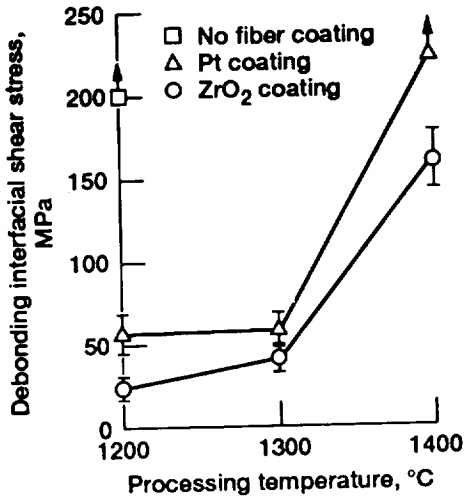

Effects of fiber coatings on debonding interfacial shear stress.

Consequently, the selection of a suitable fiber coating was identified as a critical issue in the development of a tough oxide/oxide composite. In-house efforts at NASA Lewis have involved the evaluation of both platinum and zirconia as interfacial coatings. In order to evaluate the effectiveness of these coating materials, interfacial shear stresses were measured by fiber pushout tests. Low-fiber-volume composites were fabricated by pressureless sintering of composite preforms at 1200, 1300, or 1400 °C for 8 hours in air.

Lower interfacial shear stresses, less than 60 MPa, indicated improved toughness for the composites containing zirconia- or platinum-coated fibers when composite processing temperatures were below 1300 °C. Beyond 1300 °C, increased coating density and grain growth resulted in unfavorably high shear stress of approximately 160 MPa for the zirconia-coated fiber composites. For the platinum-coated fiber composites, shear stress could no longer be measured beyond the 1300 °C processing temperature. The platinum tended to coalesce in an effort to lower surface energy, thus leaving behind uncoated areas of the fiber surface that resulted in strong bonding between fiber and matrix. Because of the strong bonding, matrix and fiber cracking occurred during the fiber pushout attempts.

From these results it is believed that with improved control of the grain growth and porosity the zirconia coatings offer the greatest potential for limiting fiber/matrix bonding to higher temperatures in a sapphire-fiber-reinforced alumina

matrix composite. Therefore, future efforts in the oxide composite area at NASA Lewis will be focused on the fabrication and mechanical evaluation of zirconia-coated sapphire fibers in polycrystalline alumina matrices.

Lewis contact: Martha H. Jaskowiak, (216) 433–5515
Headquarters program office: OAST

VCAP Polyimide Resin Successfully Tested in Hot Section of F110 Engine

Under the HITEMP program polymer research at NASA Lewis has focused on the development of advanced polymers for aircraft engine applications. Studies to improve engine performance indicate that advanced designs will dictate higher thrust-to-weight ratios than present-day levels. Meeting the material demands of the more advanced engine designs will dictate extensive use of high-strength, lightweight polymer matrix composites (PMC's). Although current application of PMC's to engines has resulted in significant weight and cost reductions, the upper use temperature of the most widely used PMC materials (PMR–15 polyimides, which were developed at NASA Lewis) limits PMC applications to 550 °F (288 °C). Further performance improvement requires utilizing PMC's in the hotter sections of the engine.

In response to this need, NASA Lewis has developed high-molecular-weight (HMW) polyimide materials that extend the upper use temperature of PMC's by more than 100 deg F. The most stable of these HMW resins is VCAP–75 polyimide. VCAP–75 composite materials exhibit excellent retention of properties during extended exposure at temperatures as high as 700 °F (370 °C). For these reasons General Electric selected VCAP–75 to replace PMR–15 as the resin used to fabricate a section of the GE–F110–129 improved-performance engine, which exhibited thermal degradation at hot spots.

Under contract to NASA, GE developed an autoclave process for fabricating a VCAP–75/T650–35 graphite-fabric-reinforced fairing. The fairing section survived more than 300 engine cycles (225 hours of engine testing) without degradation of properties. Also, in contrast to the PMR–15 fairing, the VCAP fairing exhibited no microcracking after thermocycling.

Bibliography

McCormack, W. E.: High Molecular Weight Addition Polyimide Composite Process Development. HITEMP Review, 1991: Advanced High Temperature Engine Materials Technology Program, NASA CP–10082, 1991, 11p.

Vannucci, R.D.; Malarik, D.C.; and Waters, J.F.: Autoclavable Addition Polyimides for 371 °C Composite Applications. International SAMPE Technical Conference, 22nd; Proceedings, L.D. Michelove, et al., eds., Society for the Advancement of Material and Process Engineering, Covina, CA, 1990, pp. 175–185.

Lewis contact: Raymond D. Vannucci, (216) 433–3202
Headquarters program office: OAST

Oxidation of Silicon Nitride and Carbide Is Better Understood

High-performance rockets and engines of the future will function at high temperatures and so require materials that resist oxidation better than those now in service. Silicon carbide and nitride

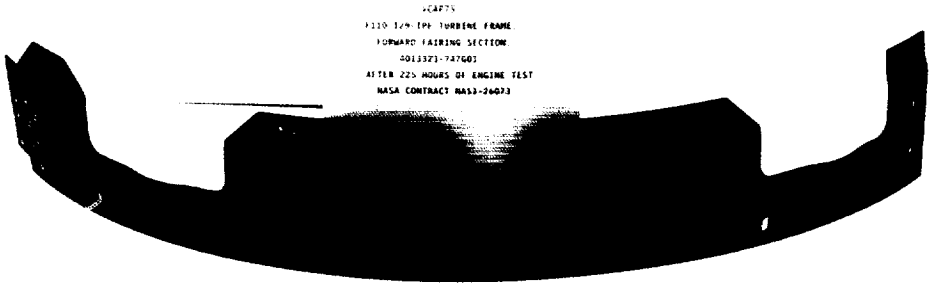

are under serious consideration for this application and will probably be employed in combination (as composites). Among other desirable qualities, they are slow to oxidize. Their oxidation forms an adherent crust of silica (silicon dioxide), which seals their surfaces from further attack by oxygen. Silicon nitride resists oxidation even better than silicon carbide. This advantage is thought to be due to an inner skin of silicon oxynitride beneath the silica crust. (This added buffer is missing with silicon carbide.) Reliable prediction of service life requires detailed knowledge of their oxidation behavior, including the nature of the suboxide inner buffer in silicon nitride and under what conditions that extra protection may be lost.

Investigation of a cross section of partially oxidized silicon nitride indicates that the composition of the suboxide is graded in depth, changing continuously from the fully oxidized top layer down to the unoxidized substrate. This suggests a straightforward atomistic mechanism for silicon nitride oxidation, different from the rather unsatisfactory model heretofore assumed. In the new model oxidation proceeds by simple substitution of oxygen for nitrogen atoms in the crystal structure of silicon nitride, and not by the destruction and reconstruction process that characterizes classical reactions in the solid state. The nitridation of silica follows the exact converse of this process.

Under severe thermal schedules such as may occur in actual service (including sharp temperature cycles and excursions), the silicon oxynitride inner layer is disrupted or lost, rendering silicon nitride no more oxidation resistant than silicon carbide. However, under steady oxidation conditions the inner suboxide is present, and the oxidation rate of silicon nitride is less than one-tenth that of silicon carbide. This correlation lends strong support to the hypothesis that the inner suboxide is responsible for the superior oxidation resistance of silicon nitride.

Bibliography

Ogbuji, L.U.J.T.; and J.L. Smialek: TEM Evidence for Oxynitride Layer in the Oxidation of Silicon Nitride. J. Electrochem. Soc., vol. 138, no. 10, 1991, pp. L51–L53.

Ogbuji, L.U.J.T.: Oxidation Instability of Silicon Carbide and Silicon Nitride Following Thermal Excursions. J. Electrochem. Soc., vol. 138, no. 10, 1991, pp. L53–L56.

Ogbuji, L.U.J.T.: Role of Silicon Oxynitride in the Passive Oxidation of Silicon Nitride. To be published in J. Am. Cer. Soc., 1992.

Lewis contact: Dr. Linus Thomas-Ogbuji, (216) 433–6463
Headquarters program office: OAST

Plasma-Sprayed Ceramic Thermal Barrier Coatings Applied to Smooth Surfaces

Traditional thermal barrier coatings (TBC's) for aircraft gas turbine engines typically consist of an outer layer of a thermally insulating ceramic, such as zirconia-yttria (ZrO_2-Y_2O_3), and an inner layer of an oxidation-resistant metallic bond coat, such as a nickel-chromium-aluminum-yttrium (NiCrAlY) alloy. However, for certain potential new materials, such as NiAl-base alloys, the bond coat layer may be unnecessary because of the inherent oxidation resistance of this material. The bond coat may be undesirable in other applications, such as those involving rotating turbomachinery, where added weight is a concern. Until now, ceramic TBC's could be applied to smooth surfaces only by the electron beam–physical vapor deposition (EB–PVD) process and not by the plasma spray process. A disadvantage of EB–PVD ceramic TBC's is that the thermal conductivity is about twice that of plasma-sprayed TBC's. A method has been developed at NASA Lewis for plasma spraying ceramic TBC's directly onto smooth substrates.

The approach used is to apply a ZrO_2-Y_2O_3 ceramic TBC to the substrate (e.g., NiAl) in two layers. The first layer is deposited onto the

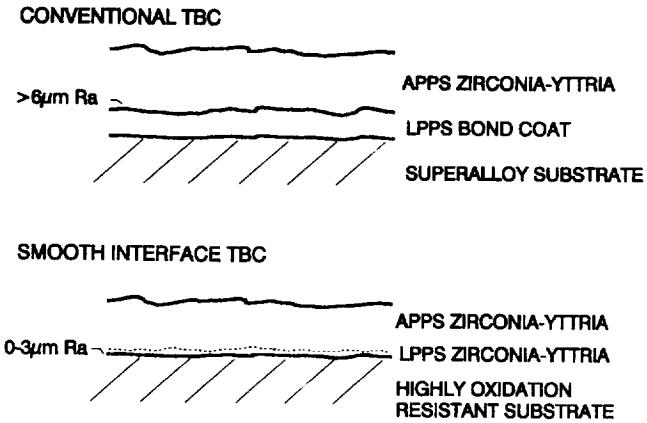

New TBC approach eliminates bond coat.

preheated substrate by low-pressure plasma spraying, and the second is deposited by conventional atmospheric-pressure plasma spraying. The first ceramic TBC layer bonds well even on smooth substrates and has a surface roughness that is sufficient to allow mechanical bonding of the outer layer. This layer eliminates the need for a conventional metallic bond coat. This approach allows the use of ceramic TBC's, without a bond coat, on highly oxidation-resistant substrates and on rotating turbomachinery. Potential applications include thermal barrier coatings for NiAl-based exhaust nozzles and thermal barrier coatings applied directly on pack-aluminide-coated turbine blades. This process may also be extended to other ceramics and substrates. Work on this process is continuing.

Bibliography

Miller, R.A.; and Brindley, W. J.: Plasma Sprayed Thermal Barrier Coatings on Smooth Surfaces. Proceedings of the International Thermal Spray Conference, Orlando, FL, 28 May–5 June 1992, pp. 493–498.

Miller, L.A.; and Doychak, J.: Plasma Sprayed Ceramic Thermal Barrier Coatings for Smooth Intermetallic Alloys. J. Thermal Spray Technol., in press.

Lewis contact: Dr. Robert A. Miller, (216) 433–3298

Headquarters program office: OAST

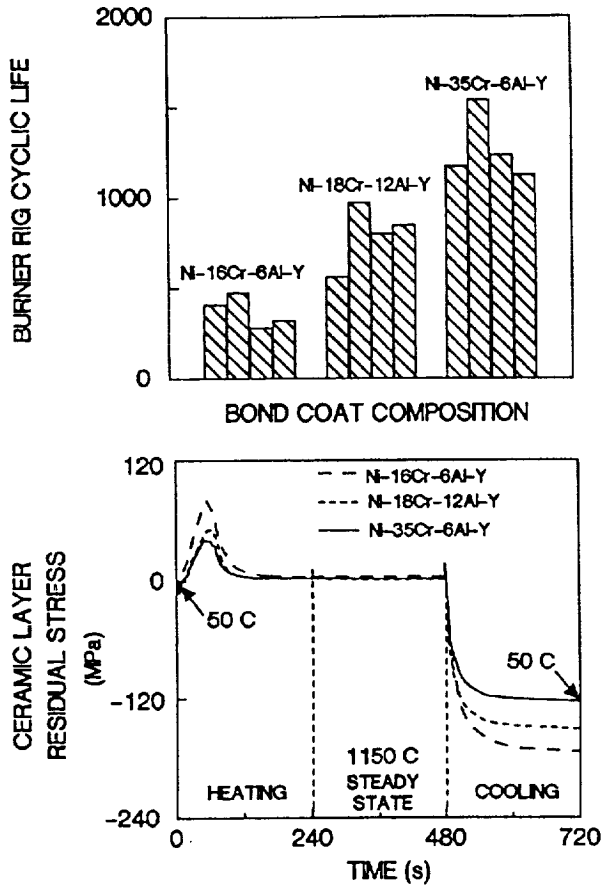

Differences in thermal cycle life of ceramic layer on various bond coats related to differences in residual stress levels during cycling.

Bond Coat Property Effects on Thermal Barrier Coating Life Measured

Plasma-sprayed thermal barrier coatings (TBC's) are used in aircraft gas turbine engines to reduce component temperatures in hot sections. TBC's incorporate a metal-chromium-aluminum-yttrium (MCrAlY) bond coat layer (where "M" stands for nickel, cobalt, iron, or a combination of these elements) and an outer insulating zirconia-yttria (ZrO_2-Y_2O_3) ceramic layer. The MCrAlY bond coat promotes adhesion of the ceramic layer and, more importantly, makes the underlying superalloy component resistant to oxidation. TBC life has been correlated with bond coat oxidation resistance, but recent work has indicated that other bond coat properties must also influence TBC life. A study was conducted on three bond coat compositions to determine which properties of the bond coat, other than oxidation resistance, affect TBC life and to determine the mechanism by which they operate. The results of this comparative study indicate that the coefficient of thermal expansion (CTE) and the stress relaxation behavior of the bond coat are linked to TBC life through their influence on TBC residual stresses.

The bond coat properties thought to be pertinent to TBC life are oxidation behavior, stress relaxation behavior, CTE, and elastic modulus. These properties were measured for Ni-16Cr-6Al-0.3Y, Ni-18Cr-12Al-0.5Y, and Ni-35Cr-6Al-0.95Y (compositions in weight percent). The thermal cycle lives of identical TBC's plasma sprayed on the three different bond coats were also determined. The results of the life and oxidation testing showed that Ni-16Cr-6Al-0.3Y had the lowest oxidation weight gain (the least oxidation) and had the shortest ceramic layer life. Conversely, Ni-35Cr-6Al-0.95Y had the highest weight gain (highest oxidation) and the best TBC life. In this

comparison, then, it is clear that the poorer oxidation resistance of the Ni-35Cr-6Al-0.95Y bond coat was offset by other bond coat properties. The bond coat elastic modulus was ruled out as a contributor to increased life because the moduli of the three bond coats were quite similar. However, the CTE and stress relaxation responses of the three alloys were significantly different.

A model that incorporated the measured stress relaxation and CTE responses was developed for the three bond coats to predict the stress levels of the TBC's during burner rig thermal cycling. The model predicts a residual stress ranking of the alloys (for both tensile and compressive stresses), from lowest to highest stress, of Ni-35Cr-6Al-0.95Y, Ni-18Cr-12Al-0.5Y, and Ni-16Cr-6Al-0.3Y. This ranking holds for lowest to highest stress range also. Because the lowest residual stresses should yield the longest TBC life, this ranking matches the cyclic lives determined in the burner rig. Furthermore, the residual stress is the only factor that correctly ranks TBC life for these three bond coats.

The conclusion that can be drawn from this work is that CTE and stress relaxation behavior, in addition to oxidation behavior, can have a significant effect on TBC life. Continuing work is aimed at tailoring the bond coat CTE and stress relaxation behavior to improve TBC life.

Bibliography

Brindley, W.J.; and Miller, R.A.: Thermal Barrier Coating Life and Isothermal Oxidation of Low Pressure Plasma-Sprayed Bond Coat Alloys. Surf. Coat. Technol., vol. 43/44, 1990, pp. 446–457.

Brindley, W.J.: Bond Coat Property Effects on Thermal Barrier Coating Life. Submitted to Mater. Sci. Eng.

Miller, R.A.; and C.E. Lowell: Failure Mechanisms of Thermal Barrier Coatings Exposed to Elevated Temperatures. Thin Solid Films, vol. 95, 1982, pp. 265–273.

Lewis contact: Dr. William J. Brindley, (216) 433–3274
Headquarters program office: OAST

Thermochemical Limitations Studied for Ceramic Matrix Composites

Silicon-base ceramic matrix composites (CMC's), such as silicon-carbide-fiber-reinforced SiC or silicon nitride (Si_3N_4), are prime candidates for the High Speed Civil Transport (HSCT) combustor liner. In this application the composite will be subjected to high temperatures and reactive gases. A systematic theoretical and experimental program has begun to determine the major thermochemical degradation routes. The particular temperature and gas atmosphere depend on the combustion conditions (i.e., fuel lean to fuel rich). A range of temperatures and gas compositions have been incorporated into the program.

In a typical silicon-base CMC the fibers are coated to prevent fiber bonding to the matrix and to establish optimum composite mechanical properties. In general, thermochemical degradation can be divided into external and internal effects. External effects include oxidation and scale volatility. Internal effects include fiber coating/matrix reactions and oxidation of the fiber coating, the fiber, or both.

The experimental program is obtaining baseline isothermal oxidation rates for pure materials in pure gases, the least aggressive conditions. The effects of more aggressive environments and conditions have also been examined and assessed. These include gas atmosphere effects (e.g., hydrogen, carbon monoxide, or water) and thermal cycling. In addition to oxidation, scale volatility

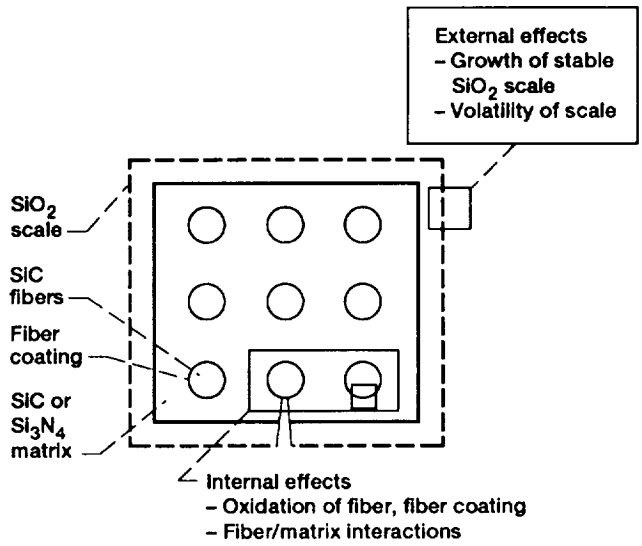

Key thermochemical degradation routes for CMC's.

has been examined both theoretically and experimentally. Except in highly reducing atmospheres it does not appear to be a major issue for silicon-base ceramics.

Current fiber coatings include carbon and boron nitride (BN). These are known to be stable over the short term with SiC fibers in SiC and Si_3N_4 matrices. Experiments were conducted to determine the possibility of reactions over the long times that will be required of these materials. It was found that Si_3N_4 and carbon react to form a thin layer of SiC. Formation of this layer terminates after a short time, and it does not appear to adversely affect the composite. There is some limited evidence of a BN/SiC reaction. This may be an issue for long times at high temperatures. Oxidation of the fiber coating, through porosity or cracking is one of the major thermochemical limitations of composites. Future experimental work is aimed at this critical issue.

Bibliography

Jacobson, N.S.: High Temperature Durability Considerations for HSCT Combustor. NASA TP-3162, 1992.

Lee, K.N.; and Jacobson, N.S.: Fiber Coating/Matrix Reactions in Silicon-Based Ceramic Matrix Composites. Ceram. Eng. Sci. Proc., vol. 13, no. 7-8, July-Aug. 1992, pp. 29-36.

Lewis contacts: Dr. Nathan S. Jacobson, (216) 433-5498; Dr. Elizabeth J. Opila, (216) 433-8904
Headquarters program office: OAST

Plasma-Sprayed Mullite Coatings Protect Silicon-Base Ceramics

Silicon-base ceramics are promising candidate materials for high-temperature structural applications but lack environmental durability in certain conditions, such as when molten salt or hydrogen is present. This drawback can be overcome by applying protective refractory oxide coatings, such as alumina, yttria-stabilized zirconia, or mullite. NASA Lewis is working to develop refractory oxide chemical/thermal barrier coatings to extend the life and temperature range of silicon-base ceramics in hostile environments.

Mullite appears most promising as a base coating because of its close thermal expansion match with silicon-base ceramics. It also has excellent physical and mechanical properties. However, previous work on mullite coatings showed that plasma-sprayed mullite tends to crack on thermal cycling. When molten mullite is rapidly quenched as in plasma spray, crystallization is suppressed and metastable amorphous mullite is formed. The study showed that amorphous mullite crystallizes on subsequent thermal cycling, which is accompanied by volume shrinkage and resultant high residual stress. The crystallization of metastable amorphous mullite at ~1000 °C and the high residual stress were identified as the key contributors to the cracking of plasma-sprayed mullite.

A new approach has been proposed for minimizing the deposition of metastable amorphous mullite: The mullite substrate was heated above the crystallization temperature (1000 °C) during the plasma spraying. A specially designed furnace was used to accurately control the substrate temperature. Preliminary results showed a significant reduction of amorphous mullite phase and a dramatic improvement of bonding at the coating/substrate interface and of thermal shock resistance.

Statistically designed experiments to optimize processing parameters are in progress. Environmental durability tests and the application of overlayer coatings of alumina or yttria-stabilized zirconia will be performed in the future. Alumina or yttria-stabilized zirconia overlayers will further enhance the protective nature of the coating.

Lewis contacts: Dr. Kang N. Lee, (216) 433-5634; Robert A. Miller, (216) 433-3298
Headquarters program office: OAST

Fiber Strength Controls Room-Temperature Tensile Strength of SiC/Ti-24Al-11Nb

The strength of titanium alloy and Ti_3Al matrix composites reinforced with silicon carbide fibers has frequently been found to be lower than predicted by the rule-of-mixtures calculation. To increase our understanding of what controls composite strength, NASA Lewis has investigated

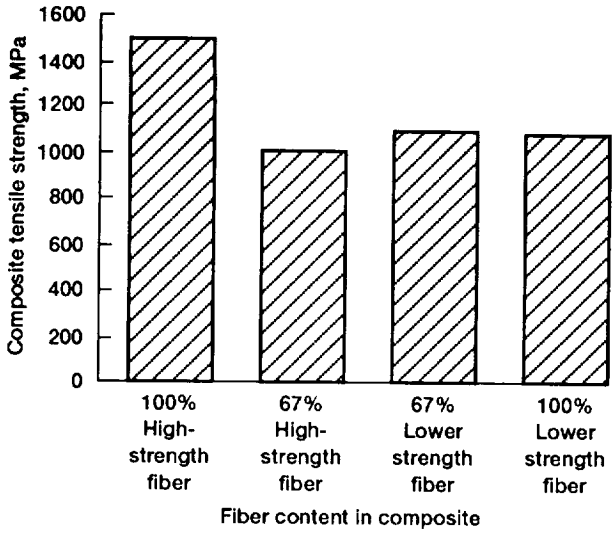

Effect of fiber strength on composite tensile strength.

in-house numerous variables related to processing and microstructure. None of the variables, including fiber, produced a statistically significant effect on the composite ultimate tensile strength (UTS). However, fiber strength can vary from lot to lot, and it was postulated that this variability has the largest influence on composite tensile strength. Fiber strength could also deteriorate during composite fabrication. This effect was assessed by testing fiber that was etched from an SiC/Ti-24Al-11Nb composite (composition in atomic percent). It was found that the powder cloth fabrication process resulted in only a slight degradation of SCS–6 SiC fiber strength. This being established, the next step was to incorporate fiber of known strength into composites and investigate the effect of fiber strength variability on composite UTS. One high-strength and one lower strength lot of SCS–6 SiC fiber were selected for composite fabrication. Composite plates were fabricated so that some contained all high-strength fiber and others contained all lower strength fiber. Two plates were fabricated with mixed fiber lots so that one composite had 67 percent high-strength fiber and the other composite had 67 percent lower strength fiber.

The results showed that the strength of the composite correlated directly with the strength of the as-received fiber, with higher strength fiber resulting in higher strength and larger strain to failure of the composite. The strength of the composite plates containing mixed fiber lots was dominated by the lower strength fiber. Thus, fiber strength was shown to be the most important factor influencing composite tensile strength. Increased accuracy in predicting composite strength may be obtained by monitoring the fiber strength in composites. With the variation in fiber strength minimized, other factors would be expected to influence composite strength. Ongoing research using fiber within one lot has shown that the strength of SiC/Ti-24Al-11Nb does depend on the fiber volume fraction. Reducing the low-strength fiber content in composites would also improve composite strength.

Bibliography

Draper, S.L.; Brindley, P.K.; and Nathal, M.V.: Effect of Fiber Strength on the Room Temperature Tensile Properties of SiC/Ti-24Al-11Nb. Metall. Trans. A, vol. 23A, no. 9, 1992, pp. 2541–2548.

Brindley, P.K.; et al.: Factors Which Influence Tensile Strength of a SiC/Ti-24Al-11NB (at. %) Composite. Fundamental Relationships between Microstructures and Mechanical Properties of Metal Matrix Composites, Proceedings of the Symposium, P.K. Liaw and M.N. Gungor, eds., TMS, Warrendale, PA, 1990, pp. 387–401.

Lewis contacts: Susan L. Draper, (216) 433–3257; Pamela K. Brindley, (216) 433–5529
Headquarters program office: OAST

Structures

Damage and Fracture Simulated in Composite Thin Shells

Lightweight, laminated composite shells are used in many aerospace applications, such as advanced aircraft fuselages and rocket motor cases, because of their high strength and stiffness. In these applications composite shells are required to withstand significant internal pressures. Any inadvertent ply damage, such as transverse cracks and fiber fractures, could weaken their overall strength and durability. It is neither practical nor feasible to design a composite shell to resist inadvertent damage at all times. A more practical approach is to allow for the existence of local defects under service loads and possible overloading. It is therefore useful to quantify the reduction in the overall strength and durability of a composite structure because of preexisting defects.

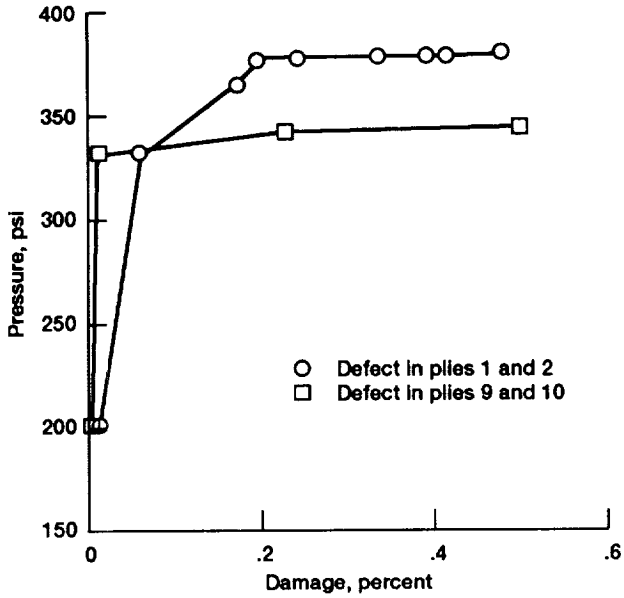

Damage propagation with pressure for composite shell T300/epoxy[$90_2/\pm15/90_2/\pm15/90_2/\pm15/90_2$].

The behavior of laminated composite structures under loading is rather complex, especially when possible degradation with preexisting damage and fracture propagation is to be considered. Therefore, the predictions of damage initiation, damage growth, and propagation to fracture are important in evaluating the load-carrying capacity and reliability of composite structures. Quantification of the structural fracture resistance is also required to evaluate the durability or life of composite structures.

The CODSTRAN computer code has been developed for this purpose. CODSTRAN can simulate damage initiation, damage growth, and fracture in composites under various loading and environmental conditions. The simulation of progressive fracture by CODSTRAN has been verified to be in reasonable agreement with experimental data from tensile tests.

Bibliography

Minnetyan, L.; Chamis, C.C.; and Murthy, P.L.N.: Damage and Fracture in Composite Thin Shells. NASA TM–105289, 1991.

Lewis contacts: Dr. Christos C. Chamis, (216) 433–3252; L. Minnetyan, (315) 268–7741
Headquarters program office: OAST

Hot Composites Analyzed for Adverse Thermal and Structural Loads

In the pursuit of efficient use of materials, technology must develop material combinations that are light and strong yet able to survive in adverse environments. Research over the years has led to such materials. However, innovative ways are necessary to keep these materials cool at elevated temperatures. Therefore, there is a need to assess the high-temperature endurance of these materials. Intricate computer codes are required to appropriately model the complex behavior of such materials.

Over the past two decades NASA Lewis researchers have developed a specialty code called HITCAN (for high-temperature composite analysis). This computer code analyzes structures made of advanced composite materials in aggressive environments. HITCAN is a general-purpose code that predicts the global structural and local stress-strain response of hot, multilayered metal matrix structures both at the constituent level (fiber, matrix, and interphase) and at the structure level, including the fabrication process effects. The types of structures it uses vary from simple beams to builtup structures under axial, bending, or buckling loading. The thermomechanical properties of the constituents are considered to be nonlinearly dependent on several parameters, including temperature, stress, and stress rate. The code's computational procedure is based on an incremental iterative nonlinear approach utilizing a multifactor interaction model.

HITCAN has been used to analyze several typical aerospace components including actively cooled hot composite structures. The many features and analysis capabilities embedded in HITCAN make it a powerful tool for analyzing aerospace structures.

Bibliography

Chamis, C.C.; Murthy, P.L.N.; Singhal, S.N.; and Lackney, J.J.: HITCAN for Actively Cooled Hot-Composite Thermostructural Analysis. NASA TM–103750, 1991.

Lewis contact: Dr. Christos Chamis, (216) 433–3252
Headquarters program office: OAST

Microfracture Simulated in High-Temperature Metal Matrix Composites

Microfracture (fiber/matrix fracture, interface debonding, and interply delamination) in high-temperature metal matrix composites (HTMMC) is critical to assessing their fatigue resistance, durability, impact resistance, and other important properties. Traditionally, researchers have focused on local fracture toughness parameters, such as stress intensity factors at the local level, to characterize fracture initiation and propagation. This is difficult to observe by conventional experiments and is computationally involved. An alternative procedure is to evaluate the global behavior and global strain energy release rates to identify and quantify the microfracture propagation hierarchy.

An ongoing in-house research activity at NASA Lewis is developing computational simulation methods for evaluating microfracture behavior in HTMMC's. The objective of this research activity is also to predict the microfracture propagation, the hierarchy of fracture modes, and the global fracture toughness of HTMMC's. Recent efforts include three-dimensional finite element simulations to evaluate composite microfracture both in unidirectional and crossply laminates when subjected to thermal and mechanical loads. Strain energy release rates and corresponding stiffness reductions for a 30-percent-fiber-volume-ratio SiC/Ti-15 crossply (0/90/0) composite subjected to 3–3 loading show that interface debonding is the only likely fracture propagation mode for this loading case and that the fracture tension test could be a sensitive method of detecting damage. Microfracture propagation is not as sensitive to thermal loading as it is to mechanical loading, or in other words, substantial temperature changes are required for microfracture propagation under thermal loads alone.

Collectively, the results demonstrate that microfracture in HTMMC's can be computationally simulated. Furthermore, global strain energy release rate computations can establish the hierarchy of probable fracture paths following fracture initiation in the fiber, the matrix, or the interface or interply delamination.

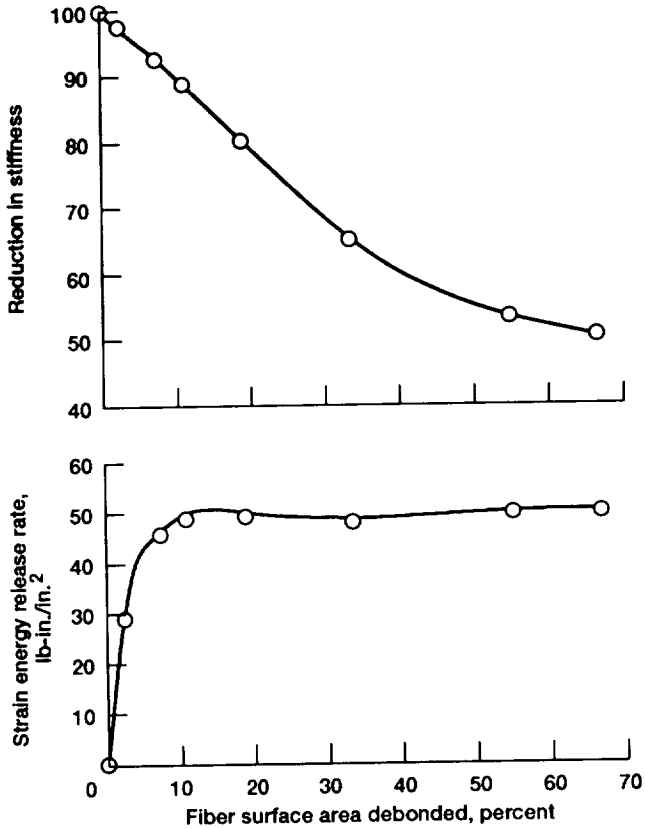

Stiffness reduction and strain energy release rate as function of fiber surface area debonded for 3–3 load.

Bibliography

Mital, S.K.; and Chamis, C.C.: Microfracture in High Temperature Metal Matrix Crossply Laminates. NASA TM–104381, 1991. (Also ICOMP–91–8.)

Lewis contacts: Dr. Christos C. Chamis, (216) 433–3252; Dr. Subodh K. Mital, (216) 433–3261
Headquarters program office: OAST

Composite Micromechanical Modeling Uses Boundary Element Method

Special boundary element methods are used to model three-dimensional thermomechanical behavior of high-temperature composites at micromechanical (constituent) scales. These methods are implemented in a computer-based tool named BEST–CMS (for boundary element solution technology—composite modeling system). The scope of modeling capabilities provided within BEST–CMS includes elastostatic, steady-

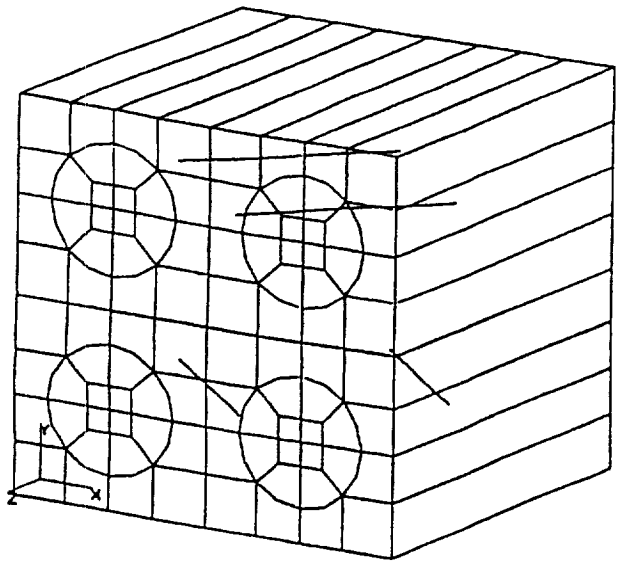

COMGEN–BEM model of $[\pm 45]_{2S}$ laminated composite.

state, and transient heat conduction; steady-state and transient thermoelastic behavior; nonlinear fiber/matrix interfaces, and inelastic matrix constitutive behavior.

In order to facilitate construction of boundary element discretized models for arbitrary composite architectures, an interface to the commercial graphical processing product PATRAN has been created. This interface, named COMGEN–BEM (for composite model generation—boundary element method), enables rapid generation of composite micromechanical models based on simple user-specified parameters, such as fiber volume fraction and fiber diameter. Moreover, COMGEN–BEM provides sufficient flexibility to easily manipulate other model characteristics, such as grid density, material properties, fiber orientation angles, applied loads, and boundary conditions.

Micromechanical models of several metal matrix and ceramic matrix composites have been generated using COMGEN–BEM, and analyses of thermomechanical behavior have been performed using BEST–CMS. Computational results from the special boundary element methods have been compared with results of three-dimensional finite element modeling, approximate analytical modeling, and experimental observations. Overall, the two results exhibited good agreement.

In general, the results achieved to date have demonstrated that the special boundary element methods are accurate and efficient approaches to composite micromechanical modeling. Future work will encompass analyzing the thermomechanical behavior of woven-fabric composites. In addition, the nonlinear behavior of the matrix will be taken into account.

Bibliography

Banerjee, P.K.; Henry, D.P.; Dargush, G.F.; and Hopkins, D.A.: Boundary Element Solution Technology—Composite Modeling System, BEST–CMS Users' Manual, March 1992.

Goldberg, R.K.: COMGEN–BEM: Boundary Element Model Generation for Composite Materials Micromechanical Analysis. NASA TM–105548, 1992.

Lewis contact: Robert K. Goldberg, (216) 433–3330
Headquarters program office: OAST

New Integrated Force Method Developed for Finite Element Analysis

A novel formulation, called the integrated force method (IFM), has been developed for analyzing structures. In this method all the internal forces are taken as independent variables, and the system equilibrium equations are integrated with the global compatibility conditions to form the governing set of equations. In IFM the compatibility conditions are obtained from the strain formulation of St. Venant and no prescription of the redundant load system has to be made, in contrast to the standard force method. This property of the IFM allows the generation of the governing equations to be automated straightforwardly, as it is in the popular stiffness method. The IFM and the stiffness methods were compared relative to the structure of the equations and their conditioning, solution methods, overall computational requirements, and convergence properties as they influence the accuracy of the results.

Overall this new version of the force method produces more accurate results than the stiffness method for comparable computational cost. When the solutions to a plate flexure problem, as obtained by IFM and two stiffness codes (MSC/NASTRAN and ASKA) were graded following MacNeal's scheme (where A = less than 2 percent error), the IFM scored an "A" grade for the first model consisting of four elements only. MSC/NASTRAN required 36 elements to reach "A";

ASKA was unable to achieve an "A" even with 100 elements.

Bibliography

Patnaik, S.N.; Berke, L.; and Gallagher, R.H.: Integrated Force Method Versus Displacement Method for Finite Element Analysis. Comput. Struct., vol. 39, no. 4, 1992, pp. 377–407.

Lewis contacts: Dale A. Hopkins, (216) 433–3260;
Dr. Surya N. Patnaik, (216) 433–8368
Headquarters program office: OAST

Reliability of Space Trusses Obtained by Probabilistic Progressive Buckling

In view of the numerous uncertainties associated with structures in space environments, there is a need to probabilistically describe progressive buckling. Probabilistic structural analysis methods contained in the NESSUS (for numerical evaluation of stochastic structures under stresses) computer code are being used at NASA Lewis. The methods are used to evaluate the reliability of space trusses typical for Space Station *Freedom* by probabilistic progressive buckling.

For any given truss these probabilistic structural analysis methods consider the various uncertainties in a formal quantitative manner rather than as either single values or upper and lower values. Initially, the truss is deterministically analyzed to identify the member or members in which the axial forces exceed the Euler buckling load. Then these members are discretized with several intermediate nodes during the subsequent probabilistic buckling analysis. Margin-of-safety values for specified probability using assumed distributions for applied loads are then calculated. Finally, the buckled member or members are progressively removed from the original truss configuration, and the procedure is repeated until the onset of the collapsed state is reached. Thus, this procedure yields the optimum truss configuration (minimum number of members) for a given loading condition and specified reliability.

Bibliography

Pai, S.S.: Probabilistic Structural Analysis of a Truss Typical for Space Station. NASA TM–103277, 1990.

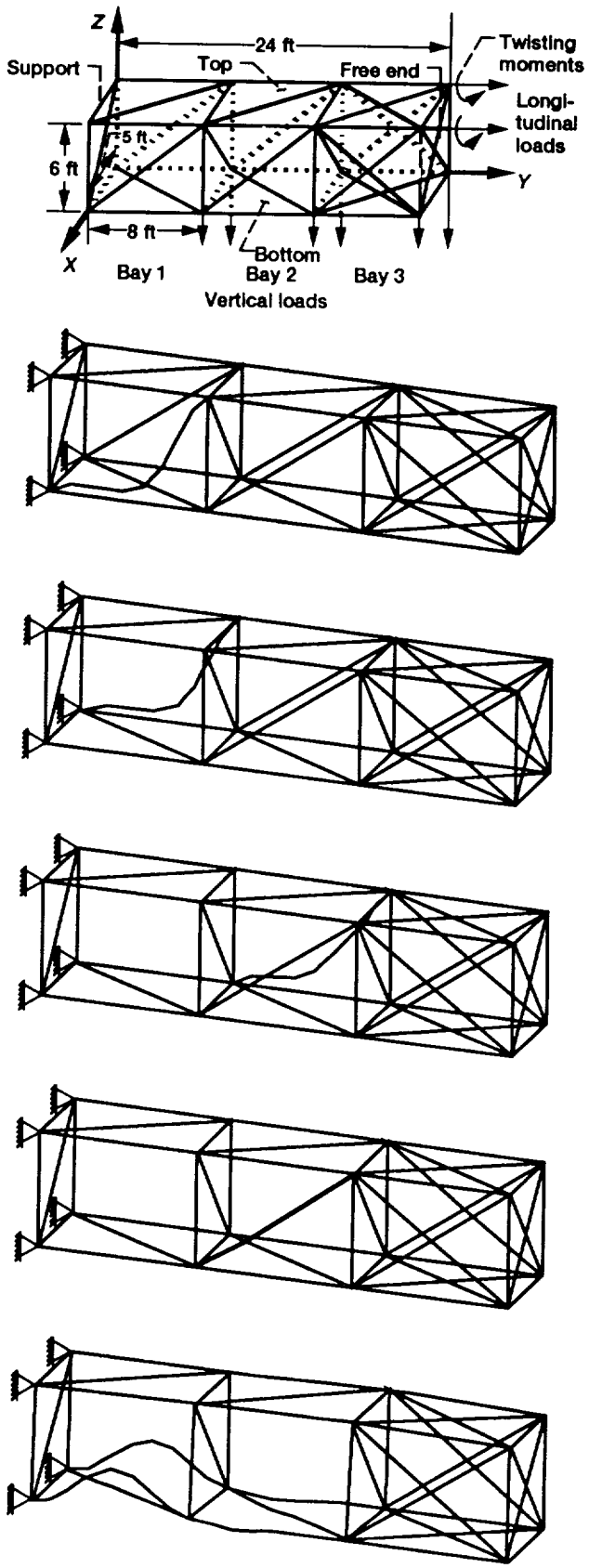

Probabilistic progressive buckling as buckled members are sequentially removed.

Pai, S.S.; and Chamis, C.C.: Probabilistic Progressive Buckling of Trusses. NASA TM–105162, 1991.

Lewis contact: Dr. Shantaram S. Pai, (216) 433–3255
Headquarters program office: OAST

Structural Health-Monitoring System Developed for Composite Aerospace Structures

To reduce operating expenses, airlines are now using the existing fleets of commercial aircraft well beyond their originally anticipated service lives. The repair and maintenance of these "aging aircraft" has become a critical safety issue, both to the airlines and the Federal Aviation Administration. A measurement system is therefore required to continuously monitor the damage and structural degradation of aging airframes that result from the repeated takeoff/landing and pressurization/depressurization cycles that aircraft routinely experience.

An innovative effort has been conducted to develop such a monitoring system. The approach is to monitor the vibration of an in-service structural component and then use a computer-based pattern recognition algorithm to estimate, from these measurements, the extent of damage in the structure. Structural Integrity Associates, Inc., of San Jose, California, recently demonstrated the feasibility of this approach as part of a Small Business Innovation Research contract with NASA Lewis. The results showed that a pattern recognition algorithm could be "trained," by using laboratory test data, to recognize certain characteristic changes in structural frequency response and to infer from those changes the amount of ply delamination, matrix cracking, or both in a composite structural component.

The success of this work has recently brought substantially increased funding from NASA. The hardware and software for a prototype structural health-monitoring system will be developed and demonstrated on a specific aerospace structural component.

Bibliography

Tang, S.S.; Chen, K.L.; and Grady, J.E.: On the Monitoring of Composite Materials Using the Pattern Recognition Method, Presented at the American Society of Composites 7th Technical Conference on Composite Materials, University Park, PA, Oct. 1992.

Lewis contact: Joseph E. Grady, (216) 433–6728
Headquarters program office: OAST

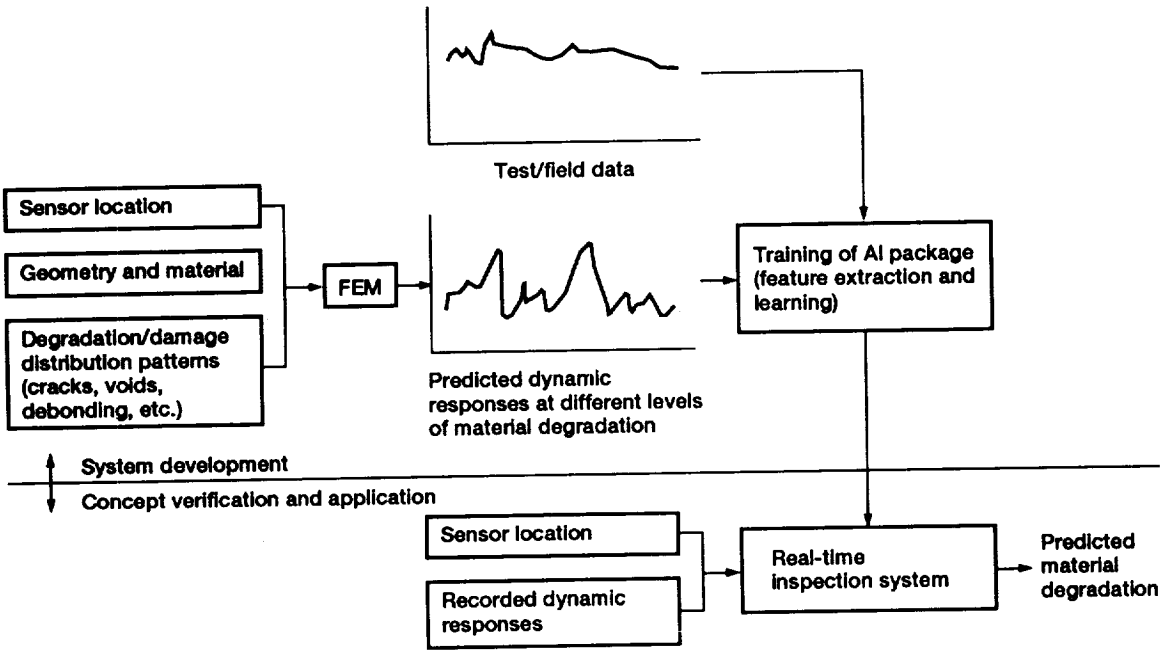

Conceptual design of structural health-monitoring systems.

Novel Mechanics Developed for Damping Analysis of Thick Composite Laminates and Plates

The damping of composite materials is a property receiving attention for its significance in vibration and noise control, fatigue endurance, and impact resistance of flexible lightweight structures. Composites are widely preferred in such high-performance structures for their high specific stiffness and strength. Hence, the higher damping capacity is an added advantage of these materials. Damping is also sensitive to interlaminar and intralaminar stresses and may be an excellent indicator of damage in composites provided that accurate mechanics are available for predicting the damping of the "pristine" material.

As a continuation of previous efforts, novel mechanics for analyzing damping in composite laminates and plates were developed, such as the discrete layer plate theory (DLPT). Assumed discrete displacement fields enable extremely accurate calculation of interlaminar and intralaminar strains and include the effects of interlaminar shear damping. Hence, a unique feature of the DLPT is the capability to simulate the damping in thick composites. A method for exact damped dynamic analysis of thick, simply supported composites plates was also developed.

Comparison of the DLPT with one based on classical laminate plate theory (CLPT) assumptions illustrated the definite superiority of the damping mechanics at higher thicknesses. The damping mechanics also provide significantly improved damping predictions at higher order modes and elevated temperatures and for laminates with significant variation of properties and anisotropy through the composite plies.

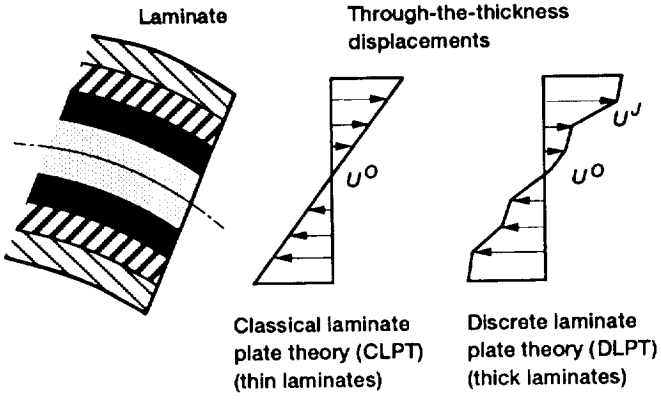

Kinematic assumptions for two composite theories.

Bibliography

Saravanos, D.A.; and Chamis, C.C.: Integrated Mechanics for the Passive Damping of Polymer-Matrix Composites and Composite Structures. NASA TM–104346, 1991.

Lewis contact: Dr. Dimitris A. Saravanos, (216) 433–8466
Headquarters program office: OAST

Complete Potential-Based Thermodynamic Framework Used to Develop Thermoelastic-Viscoplastic Damage Models

In general, the inelastic thermomechanical response of engineering materials is related to irreversible thermodynamic processes. These involve energy dissipations and material stiffness variations due to physical changes in the microstructure. Consequently, thermodynamic arguments have often been used as a foundation on which phenomenological constitutive laws can be formulated: the so-called internal variable formalism. Material descriptions such as elastoplastic, viscoplastic, and continuum-based damage (all falling into this framework) have been subjects of extensive research over the years.

Recently, a "complete" potential-based framework utilizing internal state variables was put forth for the derivation of reversible and irreversible constitutive equations. In this framework the existence of the total (integrated) form of either the Helmholtz free energy or the Gibb complementary free energy is assumed a priori. Two options for describing the flow and evolutionary equations were considered. The first option (the fully coupled form) was shown to be too restrictive. The second option (the decoupled form), however, was shown to provide significant flexibility. With the use of the decoupled form a new operator (the compliance operator) is defined. It provides the missing link between the assumed Gibb's potential and the other complementary dissipation potentials. This missing link allows several modified and new deformation and damage models to be developed with desirable numerical and theoretical features, such as convexity, a variational structure whose properties can be exploited to derive a number of useful material conservation

laws, regularity properties and bonding theorems, and a symmetric material tangent stiffness matrix. Finally, this complete potential-based framework conveniently lends itself to intelligent application of symbolic manipulation systems that facilitate the construction, implementation, and analysis of new deformation and damage models.

Although many theories in the literature do not conform to the general potential framework outlined, it is still possible in some cases, through slight modifications of the employed forms, to restore the complete potential structure. However, the question remains as to whether these modifications will significantly affect the predictive capabilities achieved by the original forms. Consequently, a future objective will be to study the general form and the ensuing restrictions imposed by a complete potential-based viscoplastic formulation in terms of the Gibb's thermodynamic potential, particularly in regard to several of the presently used forms of the flow and evolutionary laws.

Bibliography

Arnold, S. M.; and Kruch, S.: Differential Continuum Damage Mechanics Models for Creep and Fatigue of Unidirectional Metal Matrix Composites. NASA TM–105213, 1991.

Arnold, S. M.; and Saleeb, A. F.: On the Thermodynamic Framework of Generalized Coupled Thermoelastic-Viscoplastic Damage Modeling. NASA TM–105349, 1991.

Lewis contact: Dr. Steven M. Arnold, (216) 433–3334
Headquarters program office: OAST

Secondary Orientation Influences Elastic Response of Nickel-Base, Single-Crystal Superalloy

Single-crystal superalloys are under active consideration as potential blade materials for advanced liquid-propellant rocket engine turbopumps. The mechanical properties of several single-crystal superalloys are being evaluated by materials scientists to find a suitable candidate replacement blade material for the turbopumps of the Space Shuttle main engine (SSME) and other advanced rocket engines. Pratt & Whitney has selected a well-characterized, nickel-base, face-centered-cubic, single-crystal superalloy (PWA 1480 SC) as the blade material for the SSME alternative turbopump development program.

Turbine blades of nickel-base, single-crystal superalloys (including PWA 1480) are directionally solidified along the low-modulus primary [001] crystallographic direction to enhance thermal fatigue resistance. The directional solidification process usually generates a secondary [100] crystallographic direction that is randomly oriented with respect to fixed geometric axes in the turbine blade. Orientation of the secondary crystallographic direction can be controlled by using a seed crystal during solidification. Since single crystals exhibit anisotropic elastic behavior, the general stress-strain response of a turbine blade that is directionally cast along the [001] primary crystal orientation tends to vary with the orientation of the secondary crystallographic direction.

The influence of secondary orientation on the elastic response of [001]-oriented PWA 1480 SC was investigated under mechanical, thermal, and combined loading conditions. A parametric study involving elastic stress analyses and using the MARC finite element code was conducted on a plate model. For this study the stiffness coefficients of PWA 1480 SC were transformed from the crystal to the global coordinate system. The variation in the elastic stiffness coefficients has a periodicity of 90° in the secondary orientation angle. Therefore, a range of 0° to 90° was selected for the parametric study. The magnitudes of the

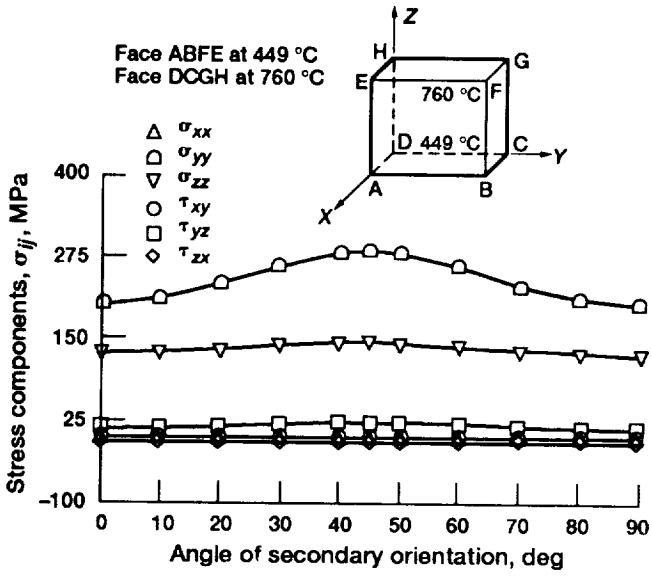

Thermal loading in X-direction: element 445.

individual stress components as well as the normalized stress components showed a substantial variation with the secondary orientation angle under different loading conditions. For example, under thermal loading through the thickness of the plate, the stresses generated at 45° were as much as 40 percent larger than those generated at 0°.

This parametric study quantified the influence of secondary orientation on the stresses developed within a single-crystal turbopump blade material under elastic loading conditions. These elastic stress analyses suggest that, for a given loading condition, it is possible to minimize the stresses developed within a single-crystal turbine blade by selectively orienting the secondary crystallographic direction. Additional research on the influence of primary orientation and the effect of both primary and secondary orientations on the stresses developed within the candidate SSME turbopump blade materials is in progress.

Bibliography

Abdul-Aziz, A.; and Kalluri, S.: Estimation of the Engineering Elastic Constants of a Directionally Solidified Superalloy for Finite Element Structural Analysis. NASA CR–187036, 1991.

Kalluri, S.; Abdul-Aziz, A.; and McGaw, M. A.: Elastic Response of [001]-Oriented PWA 1480 Single Crystal—Influence of Secondary Orientation, SAE Paper Series, No. 911111, presented at the 1991 Aerospace Atlantic Meeting, NASA TM–103782, 1991.

Kalluri, S.; Abdul-Aziz, A.; and McGaw, M. A.: Secondary Orientation Effects in a Single Crystal Superalloy Under Mechanical and Thermal Loads. Proceedings of the Conference on Structural Integrity and Durability of Reusable Space Propulsion Systems, NASA Lewis Research Center, Cleveland, Ohio, NASA CP–10064, May 1991, pp. 197–206.

Lewis contacts: Dr. Sreeramesh Kalluri, (216) 433–6727; Dr. Ali Abdul-Aziz, (216) 433–6729; Dr. Michael A. McGaw, (216) 433–3308

Headquarters program office: OSF

Effect of Fatigue Loading on Interface Properties Determined

Improvements in the toughness and fatigue crack growth resistance of metal matrix composites over monolithic materials rely heavily on fiber-bridging mechanisms. Fiber bridging occurs when cracks propagate in the matrix while leaving the fibers intact in their wake. The load carried by these fibers effectively shields the crack tip from the applied stresses and reduces the crack driving force. For crack bridging to be an effective mechanism the interface must accommodate some degree of fiber-matrix sliding (pullout). In composites with strong interfaces, where fiber-matrix sliding is limited, fiber failure occurs and bridging does not develop. In composites with weak interfaces the load transfer across the interface is limited, and shielding of the crack tip is also limited. Therefore, the mechanical properties of the interface play an important role in determining the effectiveness of the bridging mechanisms, and ultimately in the fatigue life of composite components.

Recent fatigue crack growth testing of titanium-based SCS–6 composites at NASA Lewis indicates that the interface incurs damage during cyclic loading. Therefore, extensive fiber pushout tests were performed to quantify the mechanical properties of the interface (debond and frictional strength). Pushout tests were performed on

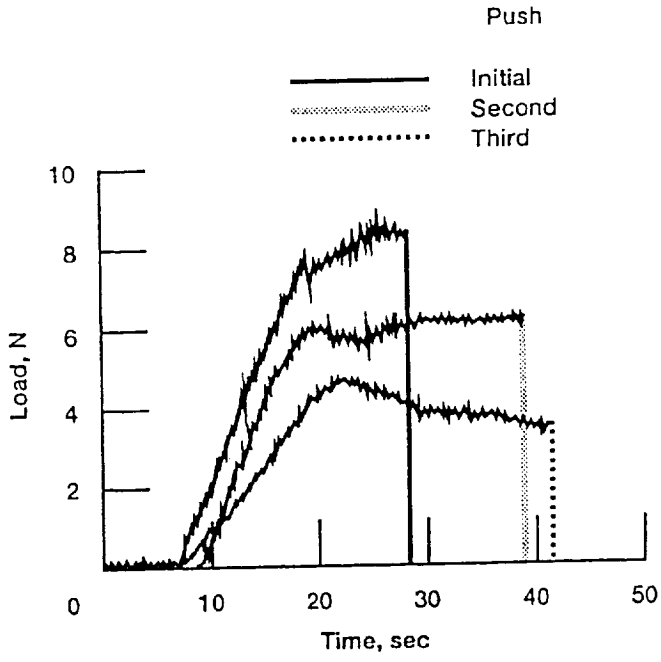

Multiple pushout results.

samples obtained near the fracture surface of specimens previously subjected to cyclic loading, and these results were compared with pushout results for samples in the as-received condition.

The pushout results indicate that the interfaces of these composites are susceptible to fretting damage during fatigue primarily because of the weak outer carbon coatings on the SCS–6 fiber. The frictional strength of the interface decreased about 50 percent during cyclic loading because of fretting damage. The factors governing the interface degradation were identified as the relative magnitude of fiber-matrix sliding, the number of cycles, and the residual clamping stresses.

The decrease in frictional strength of the interface during cyclic loading provides a more realistic baseline and is being used at NASA Lewis for modeling and life prediction methodology.

Bibliography

Ghosn, L. J.; Kantzos, P.; and Telesman, I.: Modeling of Crack Bridging in a Unidirectional Metal Matrix Composite. NASA TM–104355, 1991.

Kantzos, P.; et al.: The Effect of Fatigue on the Interfacial Friction Properties of SCS–6/Ti-15-3 Composites. HITEMP Review, 1991: Advanced High Temperature Engine Materials Technology Program, NASA CP–10082, 1991, 11pp.

Kantzos, P.; and Telesman, I.: Fatigue Crack Growth Study of SCS–6/Ti-15-3 Composite. Int. J. Fatigue, vol. 12, no. 5, Sept. 1990, pp. 409–415.

Kantzos, P.; Telesman, I.; and Ghosn, L: Fatigue Crack Growth in a Unidirectional SCS–6/Ti-15-3 Composite. Composite Materials: Fatigue and Fracture, T.K. O'Brien, ed., (ASTM STP–1110), Vol. 3, ASTM, Philadelphia, PA, 1991, pp. 711–731.

Lewis contacts: Peter T. Kantzos, (216) 433–3303;
Dr. Louis J. Ghosn, (216) 433–3249
Headquarters program office: OAST

High-Temperature Fatigue Crack Growth Modeled in Composites

Metal matrix composites have higher strength-to-density ratios than monolithic materials, particularly at elevated temperatures. However, because of the mismatch in the coefficients of thermal expansion of the metal matrix and the high-strength ceramic reinforcing fibers, small crack-like defects exist in as-fabricated composites. The presence of these defects makes the ability to predict crack growth behavior a vital part of the development of a successful life prediction methodology.

Previous work at NASA Lewis has shown that cracks tend to propagate in the ductile matrices, leaving behind unbroken fibers that bridge the crack surfaces. Crack bridging by the fibers decreases the crack growth rates by decreasing the near-tip crack displacements. Previously, two analytical models were used to successfully model the room-temperature crack growth behavior of composites. In the past year the experimental and analytical work was extended to the high-temperature regime.

High-temperature testing was performed in a specially designed loading stage mounted inside a scanning electron microscope. Use of this facility allows for precise measurements of crack-opening displacements and crack growth rates. The experimental results reveal that crack bridging by fibers controls the high-temperature fatigue crack growth behavior in a manner similar to that of the room-temperature behavior. The main difference is that at high temperatures the crack tip remains closed for a substantial portion of the loading cycle; at room temperature the crack tip remains open over the entire loading cycle.

Two different models were used to analyze the effect of fiber bridging on the crack driving force and crack-opening displacement range. The shear lag model is based on the relative sliding between the fiber and the matrix in the region where the interfacial shear stresses exceed the frictional stresses. The fiber-pressure model, developed at NASA Lewis, assumes that the decrease in the crack driving force due to bridging is proportional to the normal and bending stresses carried by the fibers.

Both models were able to predict the measured crack opening displacements reasonably well. However, the fiber pressure model predicted the fatigue crack growth rates more closely than did the shear lag model.

Bibliography

Lerch, B.A.: Matrix Plasticity in SiC/Ti-15-3 Composite. NASA TM–103760, 1991.

Lerch, B.A.; Melis, M.E.; and Tong, M.: Deformation Behavior of SiC/Ti-15-3 Laminates. Advanced Metal Matrix Composites for Elevated Temperatures, Conference Proceedings, M.N. Gungor, E.J. Lavernia, and S.G. Fishman, eds., ASM, Materials Park, Ohio, 1991, pp. 109–114.

Lerch, B.A.; Melis, M.E., and Tong, M.: Experimental and Analytical Analysis of Stress-Strain Behavior in a (90/0 deg)2s, SiC/Ti-15-3 Laminate. NASA TM–104470, 1991.

Lerch, B.A.; Melis, M.E.; and Tong, M.: Experimental and Numercial Analysis of the Stress-Strain Behavior in a [90/0] 2s, SiC/Ti-15-3 Laminate. HITEMP Review, 1991: Advanced High Temperature Engine Materials Technology Program, NASA CP–10082, 1991, pp. 39.1–39.11.

Lewis contacts: Jack I. Telesman, (216) 433–3310; Dr. Louis J. Ghosn, (216) 433–3249
Headquarters program office: OAST

Aeroelastic Stability Characteristics Assessed for SSME HPOTP Turbine Rotor

A dynamic analysis of the first-stage turbine blade for the Space Shuttle main engine (SSME) high-pressure oxidizer turbopump (HPOTP) was performed wherein the unsteady aerodynamic effect on rotor stability was assessed. Modal dynamic analysis was applied to simulate the coupled blade/fluid system. A three-dimensional finite element model of the blade was used in conjunction with two-dimensional linearized unsteady aerodynamic theory. The aerodynamics were modeled by placing axisymmetric stream-surface strips along the blade span. The blade structural and aerodynamic behaviors were coupled within modal space. A complex eigenvalue problem was solved to determine the stability of the tuned rotor system.

The aeroelastic analysis was applied to the SSME HPOTP first-stage turbine blade operating at 109 pecent of rated power. This blade was modeled by using six axisymmetric stream surfaces along the airfoil span and by retaining the first four normal modes of the turbine blade. The aeroelastic computations using these modes found that the aerodynamic damping levels were low (less than 0.5 percent of critical damping) for all vibration modes. The second normal mode (edgewise mode) was found to be unstable for interblade phase angles from 18° to 221°. This analysis did not consider the effects of mechanical and

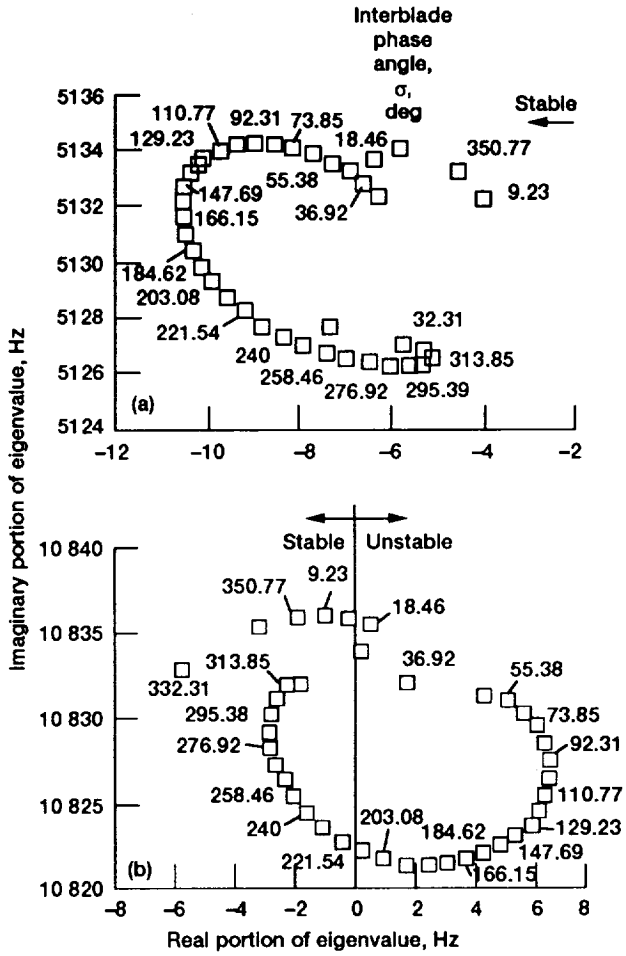

Plot of root locus for tuned HPOTP turbine vibration: (a) first bending motion; (b) first edgewise motion.

material damping on the blade stability. Damping will generally have a stabilizing effect on the blade.

Blade cracking has been a continuing problem during the development of the HPOTP, although not as acute a problem since blade-to-blade friction dampers were introduced at the blade platforms. The results from this analysis indicate that the history of blade cracking may be due to an unstable limit-cycle vibration in the edgewise mode caused by flutter instability.

Lewis contact: Dr. Durbha Murthy, (216) 433–6714
Headquarters program office: OAST

Cryogenic Magnetic Bearing With Permanent-Magnet Bias Tested

The cryogenic turbopumps for pumping liquid hydrogen and liquid oxygen to the Space Shuttle main engines (SSME) have experienced serious rotor vibrations, and the bearings have extremely short life. It appears that the vibration problems and short bearing life can be addressed by using magnetic bearings. A magnetic bearing that utilizes both permanent magnets and electromagnets was tested at room temperature and in liquid nitrogen at -320 °F. The bearing built for this study was 5.25 in. in diameter and 4.5 in. long and weighed 17.4 lb. The bore was 3.03 in. and the air gap was 0.024 in. The radial load capacity of 500 lb could be substantially increased by optimization.

Tests were conducted

- To determine the feasibility of using magnetic bearings in cryogenic turbopumps
- To apply magnetic bearings for controlling the rotordynamics of supercritical rotors such as those found in the SSME turbopumps
- To explore any special problems in applying magnetic bearings to turbopumps

The test rig simulated a rotor and the cold environment of a cryogenic turbopump. It has a unique capability of applying measured forces to the shaft to measure magnetic bearing stiffness and permanent-magnet forces at both room temperature and liquid nitrogen temperature. The rotor, which has a vertical axis, is supported by the magnetic bearing at the bottom and a preloaded duplex ball bearing at the top. The magnetic bearing carries only radial load, but the ball bearing carries both radial and thrust loads. The rotor is driven by an alternating-current motor through a belt-and-pulley speed increaser (2:1 ratio) at speeds up to 14,000 rpm. The rotor has two critical speeds within the operating range. The mode shapes are conical (with some bending) and first bending. The rotor can be unbalanced by placing set screws in one of the disks. For cryogenic operation, liquid nitrogen at -320 °F submerges the magnetic bearing.

The key magnetic bearing components are the ferromagnetic rotor, the rotor laminations, the stator laminations, the stator windings, the samarium cobalt permanent magnet, the pole piece, and the position sensors. The backup bearings at the bottom of the shaft position the rotor when the magnetic bearing is not operating. When the rotor is centered, there is a 0.010-in. radial gap between the rotor and the backup bearings.

A simple proportional, integral, derivative analog controller was designed and used to control the bearing during the tests. The schematic of the

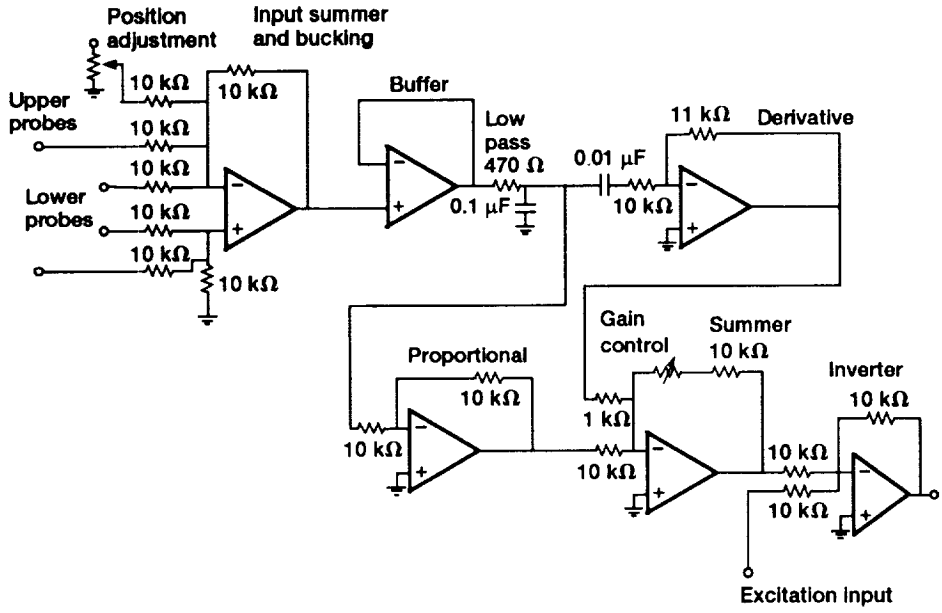

Analog control system for hybrid magnetic bearing.

control circuit for one bearing axis is shown. These component values produced a measured stiffness of 20,000 to 22,000 lb/in. The derivative was limited to a 1.5-kHz bandwidth, and the overall control was limited to a 3-kHz bandwidth by the low-pass filter.

Linear transconductance power amplifiers were used for the tests. The resistive-capacitive feedback circuit, which is required for stability, limits the bandwidth of the amplifier to about 1.5 kHz.

Rotating tests were performed for magnetic bearing stiffnesses from 10,000 to 22,000 lb/in. at room temperature and liquid nitrogen temperature and 46,000 lb/in. at room temperature. The rotor was finely balanced for these tests (i.e., no intentional unbalance was applied). For a magnetic bearing stiffness of approximately 20,000 lb/in., the bearing was operated up to 14,000 rpm, the full speed capability of the rig. Two critical speeds were traversed, a primarily conical mode at 6,300 rpm and a first bending mode at 12,600 rpm.

This magnetic bearing differs from early hybrid designs by avoiding placement of the electromagnets and the permanent magnets in a disadvantageous simple-series magnetic circuit. The particular way in which this is done results in a "homopolar" geometry. An advantage of the homopolar geometry is that the field excursions experienced by the rotor are reduced in frequency and magnitude, reducing rotor heating by magnetic hysteresis and by eddy currents.

These tests have shown that it is feasible to use the hybrid magnetic bearing in the cryogenic environment and to control the rotordynamics of flexible shafts when operating at or above the bending critical speeds.

Although this hybrid magnetic bearing is much smaller and lighter than commercial magnetic bearings, for turbopump applications the size and weight should be reduced further. This can be achieved by optimizing the present design. Also the control system must be developed to improve the stability margin at higher bearing stiffness.

Lewis contact: Eliseo DiRusso, (216) 433–6027
Headquarters program office: OAST

Combined Piezoelectric-Hydraulic, Actuator-Based Active Vibration Control Tested

Utilizing piezoelectric actuators to drive hydraulic actuators was conceived in order to fit an output piston into the small envelope adjacent to a gas turbine engine bearing. The output piston of the hydraulic actuator is employed as the primary actuator in the active vibration control system. Early bench tests using hydraulic fluid and ethylene glycol confirmed the viability of the concept. It was suggested to replace the hydraulic fluids with liquid plastic. The gelatin-like texture of the liquid plastic makes it easy to seal, and liquid plastic is reported to have a high bulk modulus. Many experiment batches of polyvinyl chloride and silicone-based plastics are being developed to operate at 350 °F.

A hydraulic actuator was designed and fabricated for initial tests. Tests have been performed to investigate the effectiveness of the hybrid actuator on an overhung, air-turbine-driven test rig. The piezohydraulic actuators were used in the

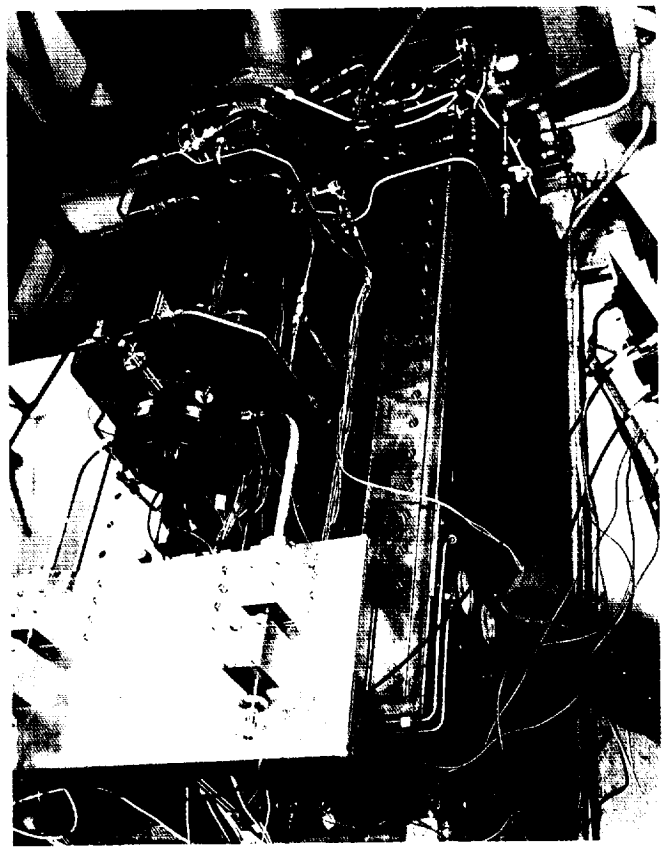

Hybrid actuator installed in air-driven-turbine test rig.

horizontal plane only; piezoelectric actuators were installed in the vertical plane but were turned off for the tests. Tests confirmed the effectiveness of the hybrid actuator, showing significant reductions in vibration through two modes. The hydraulic actuators were filled with polyvinyl-chloride-based liquid plastic for this test. The effectiveness of the actuators was further confirmed by performing transfer function tests on them with both oil and liquid plastic. Future work will include testing smaller-tube-diameter transfer lines, developing high-temperature liquid plastic, and testing the devices in other test rigs.

Lewis contact: Albert F. Kascak, (216) 433–6024
Headquarters program office: OAST

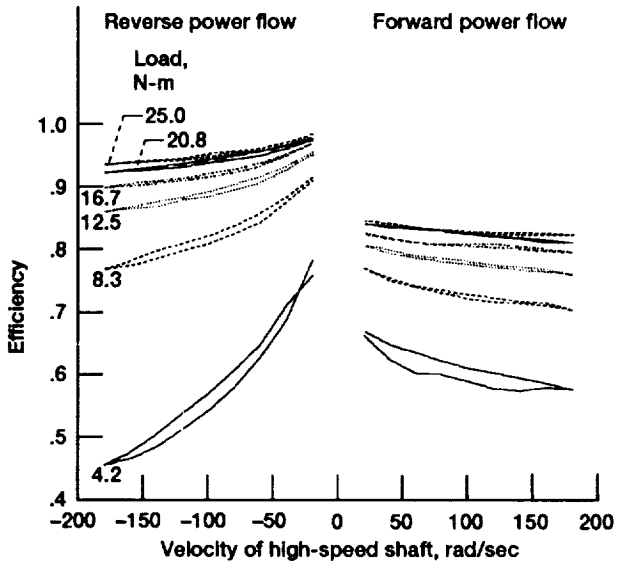

Efficiency of four-planet, 23.2:1 ratio, roller-gear drive with high-speed velocity source and low-speed torque source.

23.2:1 Ratio, Planetary Roller-Gear Robotic Transmission Designed and Tested

Robotic manipulator systems have been proposed for an increasing variety of tasks in space. Like all servomechanism systems, robotic arm actuators require high-performance mechanical power transmissions. Requirements include high efficiency, linearity, low backlash, low torque ripple, and low friction.

A single-axis transmission that utilizes rollers and gears acting in parallel was designed for a robotic manipulator. Traction drives offer the advantages of high efficiency at high ratios, backlash-free operation, low noise, no gear cogging, smooth torque transfer, and back-drivability, but they are torque limited. The maximum tangential force that can be transmitted through a roller contact is a function of the normal load and the available traction coefficient. Where the torque to be transmitted exceeds the capability of a pure traction drive, roller-gear arrangements offer an alternative approach. The gears enhance torque capacity. The rollers provide positioning for the gears, allow the use of multiple planet rows, remove backlash from the torque path, attenuate gear cogging and torque ripple, and support the radial component of gear tooth forces.

The design of a cluster configuration for a traction drive presents a few constraints because an almost infinite array of roller arrangements can be conceived to fit within a given circle. The introduction of gears with finite numbers of teeth to function in parallel with the rollers, however, imposes severe limits on available designs. Solutions for two-planet-row designs are discussed. Gear design must be carefully matched with rollers to ensure good kinematic action. Compromises in tooth design to accommodate mismatching, which occurs in the best of solutions, need to be made.

Roller action in roller-gear drives is such that, at startup before the gears are fully meshed, the compressively loaded rollers transmit torque. "Creep," or loss of motion, occurs in rollers transmitting torque; this causes the gears to "catch up" and assume the burden of torque transmission. Thus, the role played by rollers in torque transmission is transitory.

Iterative calculations of roller torque fraction, normal load, and Hertzian contact are made to determine a feasible level of torque that can be carried through the rollers. In this design a torque fraction of 0.20 was settled upon as reasonable for the rollers.

A two-planet-row, four-planet design was conceived, and two assemblies, one all steel and one containing alternate steel and plastic rollers and gears, were fabricated and tested. Detailed calculations were made of cluster geometry, gear stresses, and gear geometry; and detailed measurement data were taken. Gear tooth geometries necessary for manufacture and data required for inspection were developed.

Measurement data included transmission linearity, static and dynamic friction, inertia, backlash, stiffness, and forward and reverse efficiency. Transmission linearity was measured to within 0.001°. Friction was measured by using reactionless rotating torque transducers as a function of input speed, with the transmission operating both as a speed reducer and as a speed increaser. Inertia was determined through sinusoidal excitation experiments. Backlash was not measurable but was less than 0.001° with respect to the output angle. Stiffness measurements indicated that the transmission behaved as a "stiffening spring," with stiffness increasing with load.

Unusually complete efficiency measurements were taken. The transmission was loaded by controlled actuators at both the high-speed and low-speed shafts. Power transfer efficiency was measured in four regimes: (1) controlled velocity source on the high-speed shaft, controlled torque source on the low-speed shaft, and power flow from high speed to low speed (conventional measurement, speed-reducer operation); (2) controlled velocity source on the low-speed shaft, controlled torque source on the high-speed shaft, and power flow from low speed to high speed (speed-increaser operation); (3) controlled velocity source on the low-speed shaft, controlled torque source on the high-speed shaft, and power flow from high speed to low speed (torque-increaser operation); and (4) controlled velocity source on the high-speed shaft, torque source on the low-speed shaft, and power flow from low speed to high speed (torque reducer operation). An unusual result of the measurements was that the back-driven operating modes of torque reducer and speed increaser resulted in higher efficiencies than the normal "forward" operating modes (speed reducer, torque increaser). The peak efficiency of 98.5 percent occurred at low speed and maximum torque with power flow in the "reverse" direction (from low-speed shaft to high-speed shaft).

Lewis contact: Douglas A. Rohn, (216) 433-3325
Headquarters program office: OAST

High-Temperature Leakage Assessments and Flow Modeling Performed for Hypersonic Engine Panel Seals

Combined-cycle ramjet/scramjet engines being designed for advanced hypersonic vehicles, including the National Aerospace Plane (NASP), require innovative high-temperature dynamic seals to seal the sliding interfaces of the articulating engine panels. New seals are required that will operate hot (1200 to 2000 °F), will seal pressures ranging from 0 to 100 psi, will remain flexible to accommodate significant sidewall distortions, and will resist abrasion over the engine's operational life. NASA Lewis is developing advanced seal concepts and sealing technology to meet these demanding seal challenges. Two seal designs that show promise of meeting the demanding operating conditions of the NASP engine environment and of sealing the gaps between the movable horizontal panels and the vertical splitter walls are the ceramic wafer seal and the braided ceramic rope seal.

Key elements of leakage flow models for each of these seal types have been determined. Flow

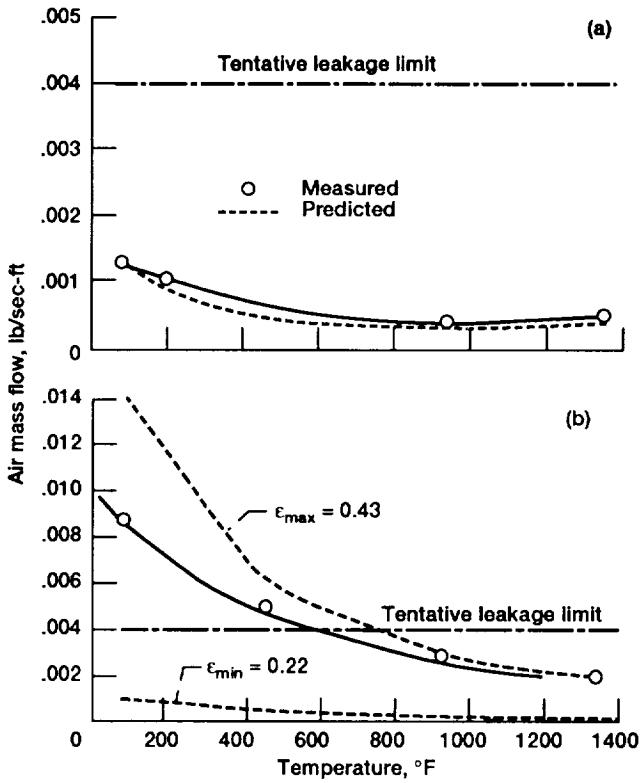

Seal leakage flow modeling for (a) ceramic wafer seal correlation (DP = 40 psi); (b) braided ceramic rope seal correlation (DP = 35 psi).

models such as these help designers to predict performance-robbing parasitic losses past the seals and to estimate purge coolant flow rates. The leakage model developed for the ceramic wafer seal was based on the theory of externally pressurized gas film bearings, which was modified to account for the special features of the seal. The Reynolds flow equation was used as the basis of the flow equations to account for each of the three potential leakage paths: past the nose of the seal; around the back side of the seal; and at temperature, between the wafer elements. The braided rope seal leakage model was based on Kozeny-Carmen relations for flow through porous media. The model treats leakage flow through and around the braided seal structure as a system of flow resistances that are analogous to a series of resistors in an electrical network. These elemental resistances are combined in accordance with their electrical analog to form an overall effective seal resistance that characterizes the seal.

A specially developed high-temperature seal rig was used to collect the required leakage flow rates for validating the seal leakage flow models, as a function of simulated engine temperatures (up to 1350 °F), pressures, and preloads.

The correlation between the measured and predicted leakage rates for the ceramic wafer seal was quite good over the full temperature range examined. The wafer seal met the tentative leakage limit over the measured temperature range. The correlation between the measured and predicted leakage rates for the braided ceramic rope seal was good considering the difficulty in modeling flow through these porous seal structures. At room and moderate temperatures the rope seal model somewhat overpredicted the leakage rate, resulting in a conservative estimate of leakage flow. Work in progress is investigating the effect of preload and engine pressure on seal flow resistance, which may explain part of the discrepancy.

Lewis contact: Dr. Bruce M. Steinetz, (216) 433-3302
Headquarters program office: NASP

Unsteady Aerodynamic Analyses Developed for Turbomachinery Flutter and Forced Response

NASA Lewis is developing theoretical, unsteady aerodynamic models and computer codes for predicting compressible, unsteady, inviscid and viscous flows through the blade rows of axial-flow turbomachines. Such analyses are needed to understand the effect of unsteady aerodynamic phenomena on the structural stability, noise generation, and aerodynamic performance of the blading. They will apply to the prediction of flutter, forced vibration, and the aeroacoustic response of turbomachinery fans, compressors, and turbine blading operating at subsonic and transonic Mach numbers.

Emphasis is being placed on developing theoretical analyses that are based on asymptotic representations of unsteady flow phenomena. Thus, flows that are driven by small-amplitude unsteady excitations in which viscous effects are concentrated in thin layers are being considered. The resulting analyses will apply in most practical situations, will lead to a strong fundamental understanding of the important physical phenomena, and will be computationally efficient. Therefore, they will be appropriate for implementation into turbomachinery aeroelastic and aeroacoustic design prediction systems.

The unsteady aerodynamic behavior of turbomachinery blading is strongly dependent on the underlying steady background flow. Because of loading effects and blade geometry, blade rows operate in nonuniform, steady flow environments. A linearized, inviscid, unsteady aerodynamic analysis, LINFLO, models small unsteady disturbances caused by prescribed blade motions and/or external aerodynamic disturbances that carry energy toward the blade row as first-order or linear perturbations of the mean flow variables.

Under this research program the LINFLO analysis has been extended to predict the unsteady blade loads that are excited by entropic and vortical "gusts." Also, an unsteady viscous-layer analysis and code (UNSVIS) has been extended and coupled to the linearized inviscid analysis to provide a weak viscid/inviscid interaction solution capability for unsteady cascade flows. At present a more accurate inviscid, steady-flow analysis (SFLOW) is being developed to be used in conjunction with LINFLO, and a simultaneous coupling of nonlinear inviscid and viscous-layer

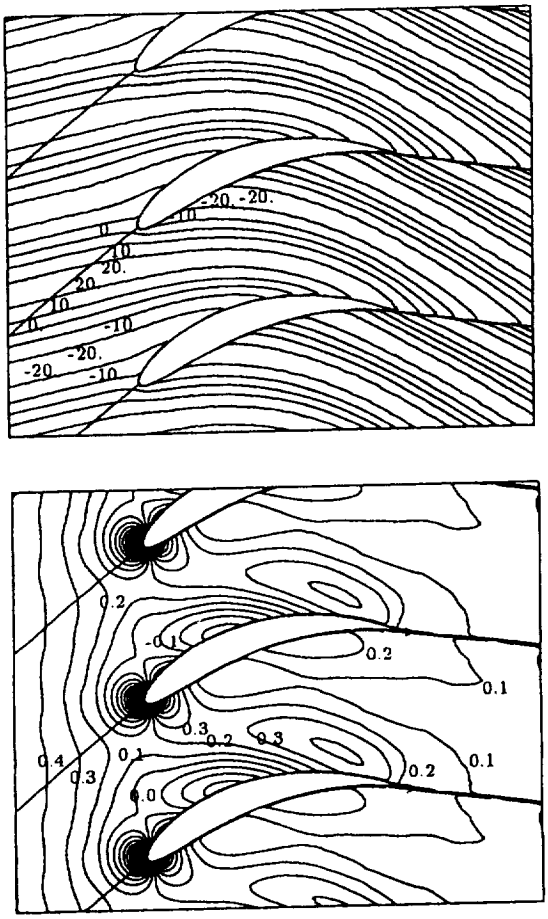

Contours of in-phase components (real parts) of unsteady vorticity and unsteady pressure for EGV cascade subjected to incident vortical gust at reduced frequency of 5 and interblade phase angle of -2π.

analyses is being developed to provide a strong inviscid/viscid interaction capability (SFLOW–IVI) for steady cascade flows. In the future a strong inviscid/viscid interaction analysis will be developed for unsteady cascade flows.

Special consideration must be given to flows in which the unsteady perturbation is due to an entropic or vortical excitation. For subsonic or transonic flows containing weak shocks, the steady background flow can be regarded as irrotational and isentropic. In this case the linearized unsteady equations can be greatly simplified by using a velocity-splitting technique due to Goldstein. A distinct advantage of this formulation is that the unsteady flow can be resolved accurately and with minimal computational effort. This technique was applied to a compressor exit guide vane (EGV) that is excited by a harmonic vortical (wake) excitation at the inlet. The calculated vorticity field and the unsteady pressure response resulting from the interaction of the vortical gust with the EGV blade row were determined. The unsteady pressures acting at the blade surface cause blade vibrations that can eventually lead to high-cycle fatigue failures; those acting upstream and downstream of the blade row can eventually lead to discrete-tone noise. This unsteady calculation required less than 10 sec on a Cray Y/MP.

A comprehensive model for predicting unsteady flows in turbomachinery blade passages must account for viscous effects. Thus, steady and unsteady inviscid/viscid interaction (IVI) analyses are also being developed as part of this research effort. At this point a steady analysis has been developed that will provide the foundation for an unsteady analysis to be constructed in the future. The steady IVI analysis couples the nonlinear potential-flow analysis SFLOW with a finite difference, viscous-layer analysis. The resulting analysis, SFLOW–IVI, can predict flows in which small-to-moderate viscous-layer separations occur. Numerical results were taken for a high-speed compressor cascade. At a Reynolds number of 10^5 the viscous flow separated from each blade suction surface near the trailing edge; the separation bubbles extended over 20 percent of the blade chord.

Because of the large number of controlling parameters involved, an efficient capability for predicting blade-row unsteady aerodynamic responses to structural and external aerodynamic excitations is a crucial prerequisite for improving aeroelastic and aeroacoustic designs. This analytical research is contributing toward meeting this need.

Lewis contact: Dr. Durbha Murthy, (216) 433–6714
Headquarters program office: OAST

Mechanical Properties of High-Temperature Composites Determined From Plate Wave Analysis

Destructive mechanical tests have always played an important part in research aimed at developing materials and structures with improved properties. However, nondestructive evaluation (NDE) techniques that reliably assess the mechanical properties of interest can be of great value.

Whereas destructive test results become available only at the end of specimen life, NDE data can be used to build a history of a material's structural integrity during the processing stages as well as in the testing phase. The NDE technology thus developed can be used to monitor the health of structural components in service.

Ultrasonic velocity has long been used to measure the various moduli in materials and more recently to determine microstructural characteristics, such as porosity and damage, that manifest themselves as microcracks. Acousto-ultrasonics, an NDE technique, appears to be especially suited to interrogating composite structures. In addition to determining relative ultrasonic attenuation, the technique can also be used to perform plate wave analysis (specifically, velocity measurements). This measurement permits the determination of the stiffness moduli in composite panels.

Acousto-ultrasonic measurements employ a two-transducer technique that introduces and receives ultrasound after it passes through a selected part of the specimen. In the plate wave technique individual propagation modes are identified. The measured velocities of these modes have been theoretically related to specific mechanical properties of interest.

The plate wave technique has three advantages:

- Ultrasonic velocity measurements can provide various shear and longitudinal modulus values on a single specimen. A mechanical test for one orientation precludes determination of any other.

- The acousto-ultrasonic configuration allows determination of velocity for a chosen (e.g., load bearing) direction when other velocity measurement techniques cannot be applied.

- Both axial and shear velocities in composites have been determined in the same acousto-ultrasonic orientation.

The table is a summary of an investigation carried out to compare plate wave velocities with important mechanical properties of [0] unidirectional SiC fiber/reaction-bonded silicon nitride matrix composites. Similar results have been obtained with SiC fiber/Ti-15-3.

Experimental conditions:

1 SiC/RSBN with SCS–6 fibers, as fabricated
2 SiC/RSBN with SCS–6 fibers, as fabricated (HIPed)
3 SiC/RSBN with SCS–0 fibers, as fabricated
4 SiC/RSBN with SCS–6 fibers, after 100 hr in O_2 at 600 °C

Change in experimental conditions	Does the variable change?			
	Axial modulus	Interfacial shear strength	Velocity, V_1	Velocity, V_2
From 1 to 2	+	No	+	No
From 1 to 3	No	+	No	+
From 1 to 4	–	–	–	–

Bibliography

Kautz, H.E.; and Bhatt, R.T.: Ultrasonic Velocity Technique for Monitoring Property Changes in Fiber-Reinforced Ceramic Matrix Composites. Ceram. Eng. Sci. Proc., vol. 12, July-Aug. 1991, pp. 1139–1151. (Also NASA TM–103806.)

Lewis contact: Harold E. Kautz, (216) 433–6015
Headquarters program office: OAST

Micromechanical Modeling and Failure Behavior Studied for SCS–6/RBSN Ceramic Composites

Monofilament silicon carbide fiber (SCS–6) in a reaction-bonded silicon nitride matrix (RBSN) is a promising candidate material for engine components in the High Speed Civil Transport plane. For these materials to be used, their overall mechanical behavior and failure mechanisms during loading must be fully understood. It is also necessary to have micromechanical models that account for the observed failure behavior and allow composites to be tailored for optimal properties. The goals of this work are to study failure behavior in this composite system, to evaluate the effects of fiber/matrix interface debonding, to identify the occurrence and nature of damage mechanisms, and to validate and improve micromechanical models.

Damage accumulation and various failure processes induced by mechanical tests were monitored in situ by using various nondestructive evaluation techniques (acoustic emission,

x-radiography, optical microscopy, and edge replication). Acoustic emission results indicate that some fiber breakage, transverse matrix cracking, and fiber/matrix interface debonding had occurred during the linear portion of their stress-strain curves. Matrix cracking was confirmed with optical microscopy and edge replication. Radiography detected cracks and broken fibers only in the nonlinear zone.

Tests of samples with various fiber fractions show that the transition from catastrophic to noncatastrophic failure occurs when fiber content exceeds approximately 16 to 19 vol %. The interfacial shear strengths measured by the pushout test and the matrix crack spacing method were low. This low strength is the main reason for the extensive interface debonding or splitting and the reduction in the work of pullout. This debonding or axial splitting is most undesirable. For composites with high strength and toughness the interfacial shear strength should be high enough to prevent interface splitting but low enough to allow steady-state cracking and substantial fiber pullout lengths for graceful failure.

Micromechanical models incorporating residual stresses to predict the critical matrix cracking strength, the ultimate strength, and the work of pullout were used, and the predictions were compared with measured values. These models were derived by the fracture mechanics approach and the energy balance concept. The fiber Weibull modulus is an important parameter for both the ultimate strength and the work of pullout. When variation in fiber strength is low, the ultimate strength is high: Comparing predictions from these models with experiments shows that they

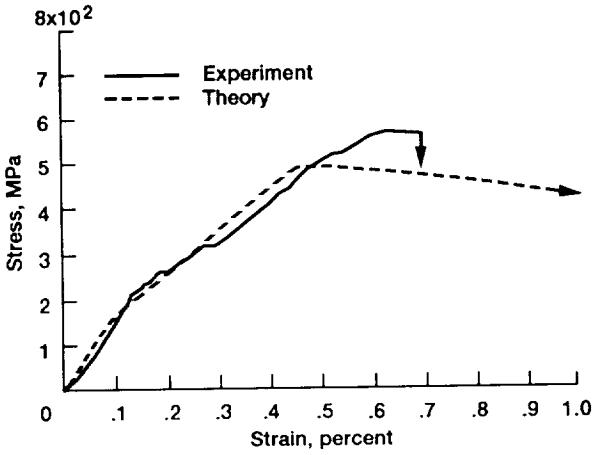

Comparison of theory and experiment for tensile stress-strain curves of SiC/RBSN.

are valid only if steady-state conditions occur and fiber breakage is minimized, at least for loads below the critical matrix cracking condition. From parametric studies and experimental observations the optimum SiC/RBSN composite should meet the following requirements: fiber content as high as permitted by processing considerations (above 30 percent), fiber radius less than 35 mm for optimum critical matrix cracking strength, slightly higher coefficient of thermal expansion for the fiber than for the matrix, and fiber Weibull modulus between 8 and 20 for ultimate strength.

Bibliography

Chulya, A.; and Gyekenyesi, J.P.: Mechanics of Interfaces in Fiber Reinforced SiC/RBSN Ceramic Matrix Composites. Mechanics of Composites at Elevated and Cryogenic Temperatures, S.N. Singhal, et al., eds., ASME, New York, 1991, pp. 217–229.

Lewis contact: Dr. Abhisak Chulya, (216) 433–8523
Headquarters program office: OAST

Interfacial Oxidation Damage in Ceramic Matrix Composites Ultrasonically Assessed

Ceramic matrix composites (CMC) reinforced with continuous fibers are being developed to meet high-temperature performance needs in aerospace and commercial areas because of their superior strength/density ratios at elevated temperatures relative to monolithic materials. One major concern about CMC materials is their high-temperature stability, especially in an oxidizing environment, which depends on the composition of the CMC constituents. In general CMC materials are composed of matrix, fiber, and interface layers (mainly fiber coatings, reaction product layers, or both). It is known that the properties of CMC materials are dominated by the interface, which allows material scientists to optimize the composites by varying the interface properties. However, this interface often suffers from oxidation reactions caused by oxygen diffusion through the matrix.

At NASA Lewis a new approach to characterizing oxidation damage in ceramic matrix composites by using ultrasonic techniques has been proposed. In this approach the elastic constants of the composite are determined nondestructively by measuring the angular dependence of both

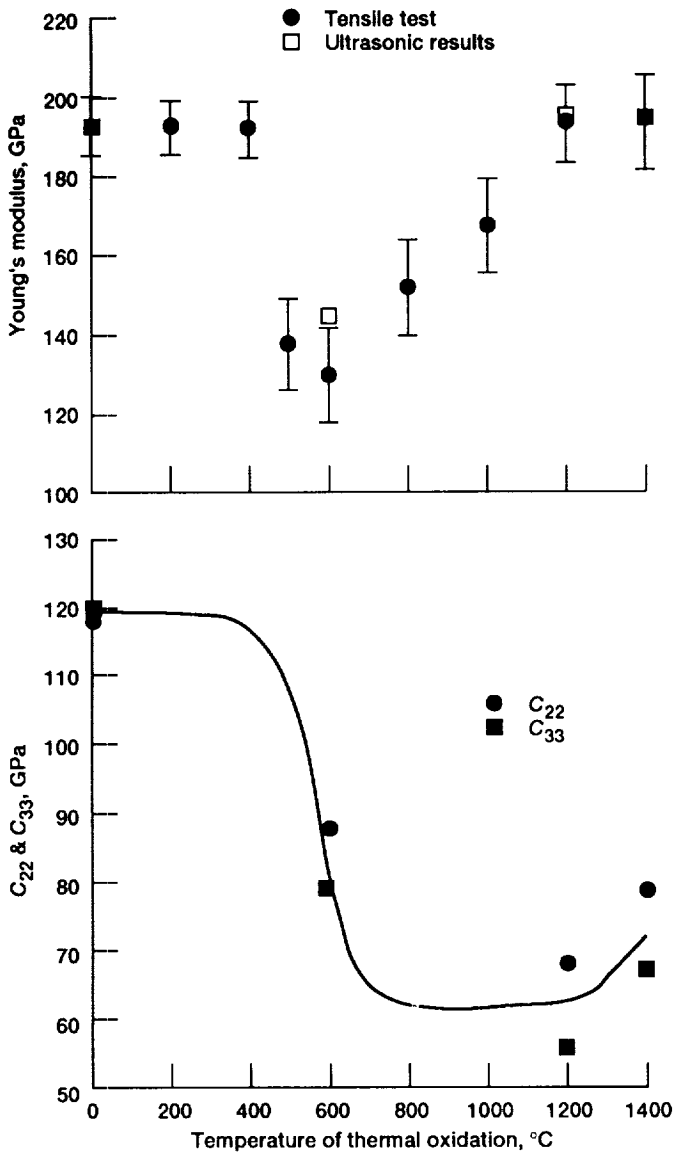

Composite longitudinal Young's modulus and transverse stiffnesses C_{22} and C_{33} as function of oxidation temperature.

longitudinal and transverse wave velocities. A micromechanical model for composites with anisotropic constituents is used to find the anisotropic properties of an effective fiber that is a combination of the fiber and the interface. Interfacial properties are extracted from the properties of this effective fiber by analyzing the difference between effective and actual fiber properties. Unidirectional $[0]_{28}$ SiC/Si_3N_4 composites with 30-percent fiber volume fraction and 30-percent matrix porosity are used. The samples are exposed in a flowing oxygen environment at elevated temperatures, up to 1400 °C, for 100 hours and then measured by ultrasonic methods at room temperature. The Young's modulus in the fiber direction of the sample oxidized at 600 °C decreased significantly, but it was unchanged for samples oxidized at temperatures above 1200 °C. The transverse moduli obtained from ultrasonic measurements decreased continuously up to 1200 °C. The shear stiffnesses behaved like the transverse moduli.

The behavior of different elastic constants obtained by ultrasonic measurements suggests that the dominant mechanism for the reduction of the transverse and shear properties of composites is oxidation of the carbon interfacial layer, whereas the reduction of the longitudinal stiffness could be due to SiC fiber degradation. The reduction of fiber/matrix interfacial stiffnesses due to oxidation damage has been determined quantitatively from the ultrasonic measurements.

Bibliography

Chu, Y.C.; Rokhlin, S.I.; and Baaklini, G.Y.: Ultrasonic Assessment of Interfacial Oxidation Damage in Ceramic Matrix Composites. To appear in ASME Journal of Engineering Materials and Technology.

Lewis contact: Dr. George Y. Baaklini, (216) 433–6016
Headquarters program office: OAST

Space Propulsion Technology

Spectroscope Analyzes Rocket Engine Plumes

As rocket engine components experience wear or degradation, anomalous materials may be entrained in the exhaust plume. Emissions from these materials can be used as indicators of impending failure. Historically, visible plume anomalies have preceded many rocket engine failures. These anomalies result from eroded particulates burning along with the propellants in the combustion chamber. Typically, particulates that have eroded from internal engine components are carried by the propellants into the combustion chamber, where they are dissociated into

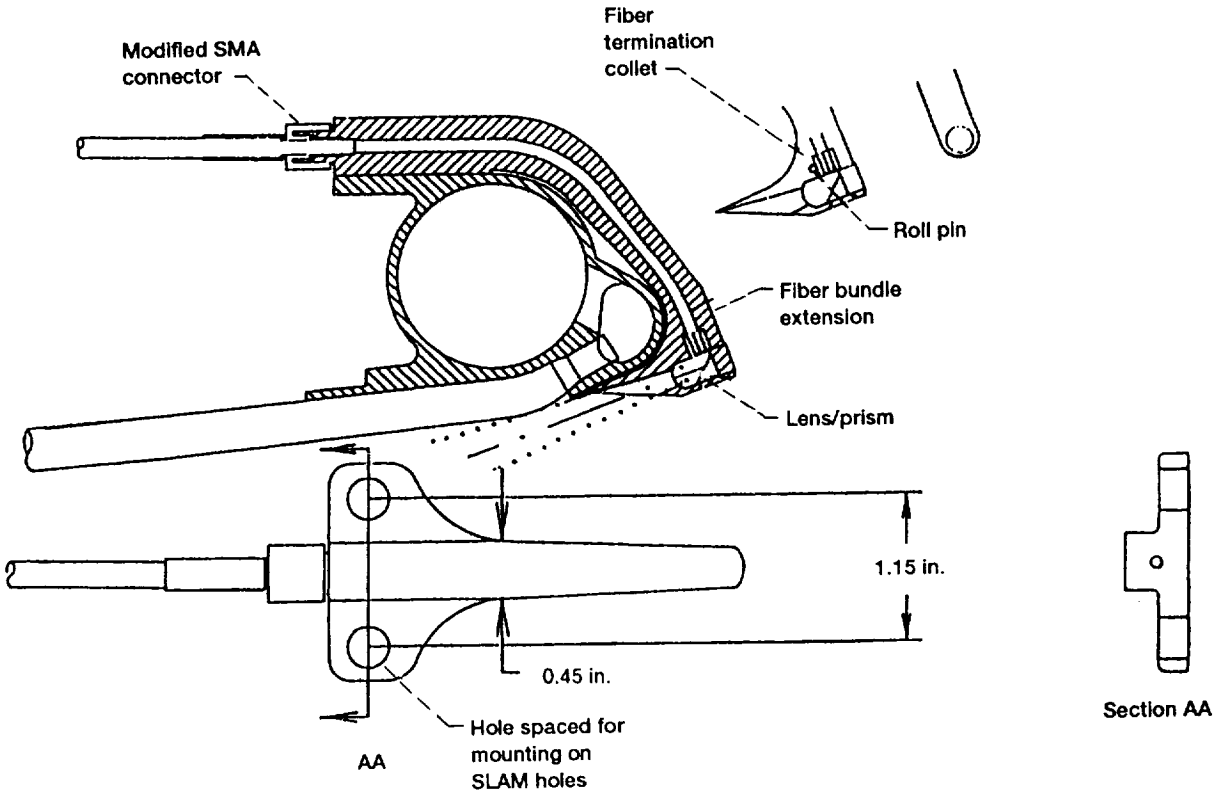

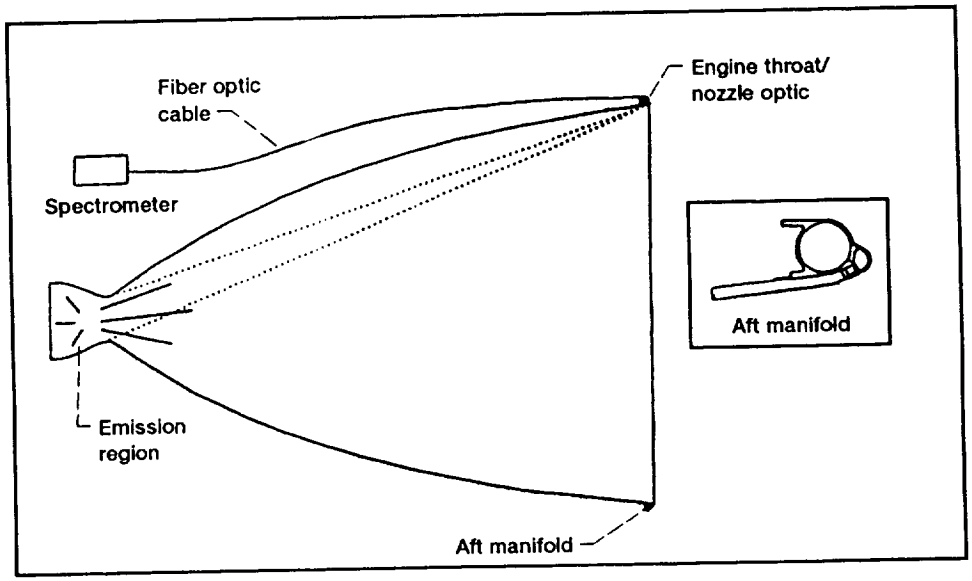

Nozzle-mounted optic assembly.

their elemental species and thermally excited during the combustion process. The excited species emit their characteristic spectra (the visible plume) and can readily be identified because all elemental species have unique spectral signatures.

Plume spectroscopy is the implementation of optical spectroscopic techniques for analyzing the exhaust plume. The emission and/or absorption of spectral radiation by the exhaust gases is used to determine their content. From the identification and quantification of plume content, engine

health and performance can be assessed. Knowledge of material erosion from internal components provides insight into the engines' current health and remaining life.

NASA Lewis is actively developing instrumentation for plume spectroscopy. These instruments consist of an optical device to collect the spectral emissions and a spectrometer to separate the plume emissions into their characteristic spectra. An optic assembly mounted to the aft manifold of the engine nozzle collects spectral emissions from within the combustion chamber. Analysis has shown that the optics are capable of viewing the combustion chamber throughout a typical flight envelope, thereby enabling observation of spectral emissions during all critical phases of the launch.

The light from the spectral emissions is transferred from the nozzle-mounted optic assembly to the Fabry-Perot interferometric (FPI) spectrometer through a fiber-optic cable. An FPI-based spectrometer was selected for its small size, high resolution, and high-speed spectral acquisition capabilities. Engineering an appropriate housing for the interferometer resulted in a rugged, compact, lightweight spectrometer.

Capabilities of the plume spectroscopy system will include real-time measurement of material erosion for engine safety monitoring, determination of performance parameters for feedback into the engine controller, and recording of high-resolution, high-speed spectral data for postfiring engine analysis. The instruments being developed by Lewis are flight compatible and can be retrofitted to the Space Shuttle main engines.

Bibliography

Madzsar, G.C.; et al: An Overview of In-Flight Plume Diagnostics for Rocket Engines. AIAA Paper 92-3785, July 1992.

Lewis contact: George C. Madzsar, (216) 977-7434
Headquarters program office: OAST

Foil Bearing Computer Code Developed

Foil bearings are considered to be a potential alternative to rolling-element bearings for turbopump applications because of their inherent operating characteristics including virtually infinite life, tolerance of debris and misalignment, reduced thermal distortion, and the potential for enhanced dynamic performance. Therefore, NASA Lewis is sponsoring a grant effort to develop predictive analysis tools for the design and performance evaluation of foil bearings.

Funded by the grant, Pennsylvania State University developed **F**oil **LUB**rication, a finite-element-based code capable of predicting the steady-state performance of foil bearings. The code requires coupling fluid and structural analysis. The fluid model is a Reynolds-equation-based solution and can model both incompressible and compressible fluids. An Ng-Pan turbulence model is included as well as a simple cavitation model. The structure model incorporates foil bending, membrane, and elastic foundation effects. In addition, foils with a broad range of initial curvatures, mountings, and interactions are addressed.

The code calculates clearances, pressure distributions, deflections, load capacities, and viscous frictional losses on the basis of geometry, design parameters, and operating parameters. A pre- and postprocessor facilitate the use of the code.

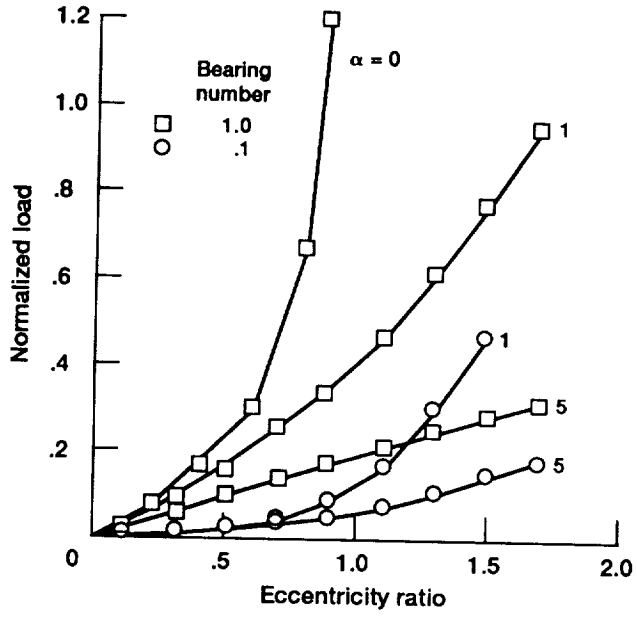

Effect of design and operating parameters on foil bearing load capacity (bearing compliance, 0).

The preprocessor significantly reduces the input required to set up a bearing model, and the postprocessor includes a graphics package that generates plots of clearance and pressure contours.

A modular and flexible approach was used for both the analysis and the code development to facilitate changes and extensions to the code. Already, there are plans to enhance the code's capabilities through a follow-on effort. A three-year program to completely develop the bearing code was jointly defined by Pennsylvania State University and Akron University. Under separate grants each university will work on different aspects of the analyses. Akron University will develop a thermal model and a Navier-Stokes-based fluid model. Pennsylvania State University will develop an analytical perturbation technique for predicting the dynamic performance of foil bearings.

Lewis contact: James F. Walker, (216) 977–7465
Headquarters program office: OAST

Advanced Seal Codes Developed for Aerospace and Industrial Applications

A seven-year contract was established between NASA Lewis and Mechanical Technology Incorporated in 1990 to develop verified computational techniques and codes for designing and analyzing seals. This effort aims to produce improved concepts and modeling tools capable of generating advanced seal designs that will provide greater rotordynamic stability and less leakage in future engine systems. The scope includes a series of two-dimensional codes for a variety of seal configurations, including but not limited to cylindrical, bushing and ring, face, labyrinth, tip, damping, and brush seals, and one three-dimensional computational fluid dynamics code. The final codes will be delivered with a knowledge base encompassing the expertise of code developers and the knowledge of industrial experts in seal dynamics and designs.

Three codes have been produced and disseminated to the user community through NASA Lewis workshops. All codes are two-dimensional codes and modifications of prior industrial codes.

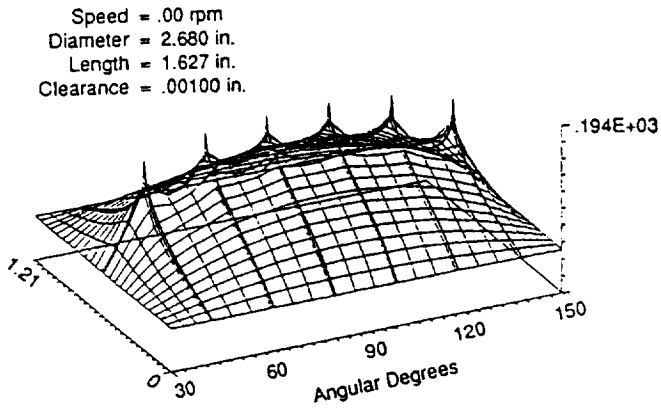

Pressure distribution of hydrostatic sectored cylindrical seal by GCYL.

They are designated SPIRALG for spiral-grooved gas seals, GCYL for cylindrical seals in compressible fluids, and ICYL for cylindrical seals in incompressible fluids. These codes are being evaluated by potential industrial users for accuracy, efficiency, and usefulness. Altough they are currently executable on high-performance personal computers, provisions are being made to transport these codes to workstations.

SPIRALG is used to predict performance characteristics of gas-lubricated, spiral-grooved cylindrical and face seals. Its inclusion of eccentricity and misalignment in the prediction extends the present state of the art. The code produces seal loads and moments, minimum film thickness, axial flow, power loss, and up to 32 frequency-dependent, cross-coupled spring and damping coefficients. It is also coupled to an optimization code that allows optimum groove geometry to be determined on the bases of stiffness, pumping capacity, and flow.

Both the ICYL and GCYL codes are used to analyze cylindrical seals in plain circular, hydrostatic, multilobe, tapered, or Rayleigh step geometries. Each code produces seal loads, righting moments, flows, power loss, clearance, and pressure distributions, and up to 32 dynamic spring and damping coefficients. With its incorporation of roughness on the seal housing or rotating shaft, ICYL has the added capability of analyzing damping seals, which are finding favor in advanced cryogenic turbomachines.

Bibliography

Liang, A.D.: Seals Flow Code Development. NASA CP–10070, 1991.

Liang, A.D.; et al.: Development of a Knowledge Based System for Turbopump Seals. Advanced Earth-to-Orbit Propulsion Technology Conference, NASA CP-3174, 1992, pp. 440–446.

Lewis contacts: Anita D. Liang, (216) 977-7439; Robert C. Hendricks, (216) 977-7507
Headquarters program office: OAST

Plasma Contactors Chosen for Space Station *Freedom*

Space Station *Freedom* will use high-voltage (~160 V) solar arrays in order to optimize system and mission characteristics. Analyses and tests have recently indicated that the selected overall space station configuration will interact with the plasma environment in a number of ways which raised concerns for the overall system life and integrity. "Plasma contactors" were defined and were found in ground testing to eliminate the known deleterious interactions. These ground tests at NASA Lewis supported solar array plasma interactions testing. On the basis of these test results the plasma contactor was chosen to control the electrical potentials of surfaces in order to eliminate or mitigate damaging interactions with the space environment.

Plasma contactors are devices that efficiently provide the negative (electron) and positive (ion) current emissions required to control the electrical potentials of space station surfaces. The key plasma contactor technologies, including hollow cathodes, power processor and control units, and storage and management of xenon gas, are directly traceable to the NASA Lewis electric propulsion program, which has sponsored their advancement for use in ion thruster systems.

A program is now under way in the Space Propulsion Technology Division to evaluate and optimize plasma contactors for Space Station *Freedom*. Specific efforts include design optimizations for contactors and configurations, validations of required lifetimes, and studies of contactor plumes and electromagnetic interference. Under this program prototype plasma contactors have demonstrated in the laboratory the emission current requirements necessary for potential control of space station surfaces. These include electron emission currents from 1 to 10 A and ion

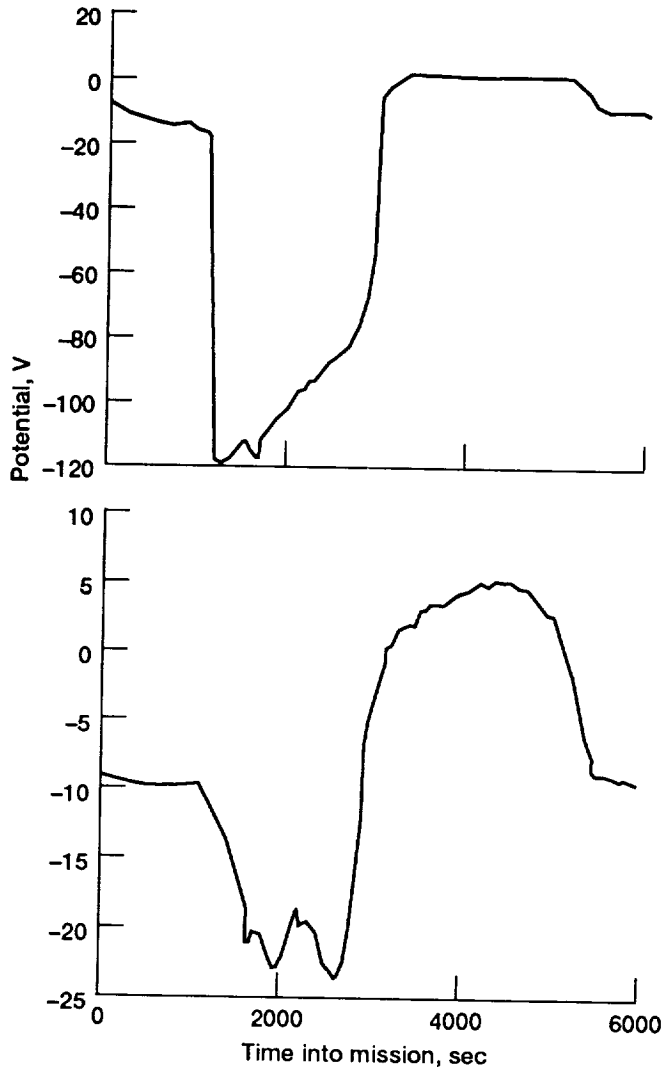

Electrical potential (a) without and (b) with plasma contactor.

emission currents to 100 mA at potentials less than 20 V. Activities are now focused on minimizing contactor consumables (power and xenon) and demonstrating the required lifetimes. A lifetime of at least 3 years is anticipated for the contactor system, and with redundancy, individual plasma contactor unit lifetimes of 12,000 to 15,000 hours will be required. Life tests of contactor components are under way and will culminate in breadboard system demonstrations and life tests under conditions simulating Space Station *Freedom*'s operational and environmental parameters.

These efforts are being conducted in parallel with complementary studies on plasma contactor interactions with the space environment conducted in the Power Technology Division. Overall program management and integration is provided

through the Systems Engineering and Integration Division.

Lewis contact: Michael J. Patterson, (216) 977-7481
Headquarters program office: OAST

Laser Diagnostics Applied to Small Rockets

Small chemical rockets involve a number of complex phenomena, such as mixing, heat transfer, and low-Reynolds-number flows. At present, no localized data on small rocket flows are available, and existing small rocket codes (such as RPLUS) can be evaluated only through comparison with global parameters. In order to better evaluate rocket performance and to verify existing predictive codes, an experimental program was started to measure localized thermodynamic and fluid dynamic properties by nonintrusive laser scattering methods.

Rayleigh scattering was used to characterize the plumes of two full-scale, 110-N gaseous hydrogen-oxygen thrusters installed inside a high-altitude chamber. Propellant temperatures and velocities were extracted from the spectral shift and spectral broadening of scattered narrowband laser light. Comparison with computational results from state-of-the-art codes showed acceptable prediction of radial velocity measurements but large discrepancies for axial velocities and translational temperatures. These discrepancies are believed to result largely from inhomogeneous combustion, incomplete mixing, and injector streaking within the combustion chamber.

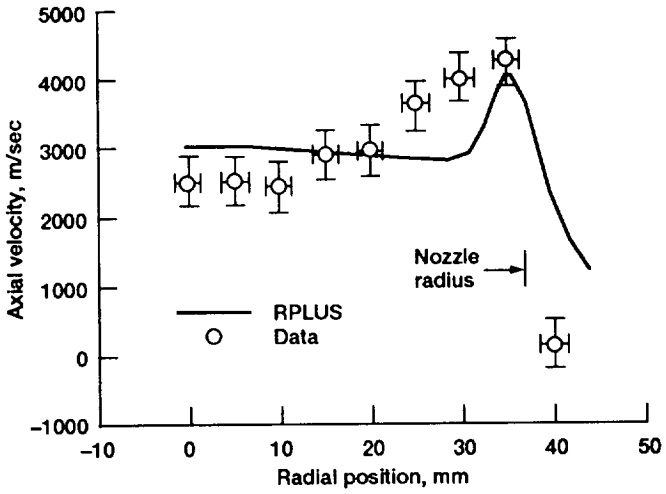

Comparison of axial velocity measurements with RPLUS predictions.

Raman spectroscopy was used to extract the species number densities and vibrational temperatures in the plume of a low-area-ratio rocket with the same combustion chamber and injector as the full-scale thrusters. The Raman technique is useful at higher molecular densities than Rayleigh spectroscopy. Comparison with computational results from a fully viscous Navier-Stokes code showed large discrepancies in both temperature and number densities, which are believed to be caused by inaccurate assumptions of initial conditions at the injector exit. These results show that characterization of the injector performance is critical for predictive codes to be reliable indicators of performance and that the discrepancy caused by viscous effects cannot be quantified as long as injector performance has not been characterized.

The extensive use of optical fibers for accessing hostile environments makes both these diagnostic techniques versatile and reliable. Continuous development of the Rayleigh scattering technique as a prime diagnostics tool for many nozzle and plume flow fields is ongoing. Further Raman measurements will be focused on diagnosing the thermodynamic and fluid dynamic parameters inside the combustion chamber and characterizing the injector performance. Results will be used to improve modeling of mixing and heat transfer processes.

Bibliography

de Groot, W.A.; and Weiss, J.M.: Species and Temperature Measurement in H_2/O_2 Rocket Flow Fields by Means of Raman Scattering Diagnostics. AIAA Paper 92-3353, 1992.

Seasholtz, R.G.; Zupanc, F.J.; and Schneider, S.J.: Spectrally Resolved Rayleigh Scattering Diagnostics for Hydrogen-Oxygen Rocket Plume Studies. J. Propul. Power, vol. 8, no. 5, Sept.-Oct. 1992, pp. 935-942.

Zupanc, F.J.; and Weiss, J.M.: Rocket Plume Flowfield Characterization Using Laser Rayleigh Scattering. AIAA Paper 92-3351, 1992.

Lewis contacts: Frank J. Zupanc, (216) 977-7483;
Wim A. de Groot, (216) 977-7485
Headquarters program office: OAST

New Magnetoplasmadynamic Thruster Facility Developed and Life Limiters Identified

High-power electric propulsion is under development to support advanced near-Earth and planetary orbit transfer missions. Potential benefits include greatly reduced launch costs, shorter trip times, and enhanced payload capabilities. Magnetoplasmadynamic (MPD) thrusters offer the capability of processing a large amount of power in a simple and robust engine configuration. However, considerable improvements are needed in engine performance and lifetime before MPD thrusters can successfully compete with chemical engines.

In order to improve MPD thruster testing capability, a new facility was constructed incorporating a 40-m^2 gaseous helium cryopump. This new facility permits continuous testing of argon propellant thrusters at power levels of about 400 kW and incorporates diagnostics for electrode heat transfer, cathode surface temperature, and plume characteristics, as well as the capability for extended thruster testing. More than 15 thruster geometries have been evaluated, including hollow cathodes and a variety of anode and cathode lengths and radii. In addition, alternative cathode materials have been tested, including 2 percent thoriated tungsten and 4BaO-CaO-Al_2O_3 impregnated porous tungsten. The impregnated material was found to operate at a much lower temperature than the thoriated tungsten and thus should improve thruster lifetime.

Extended thruster testing resulted in the identification of a new MPD thruster lifetime limiter. For specific impulses of interest, over 2000 sec, thrusters using argon propellant suffer severe sputtering of the anode electrode. The sputtering rate can approach 0.1 mm/hr near the thruster exit plane and has caused the failure of an extended test after 30 hours of continuous operation at 60 kW. The erosion rates of the other thruster components, including the cathode and rear chamber insulator, were low enough to permit operation for several hundred hours. A potential solution of the anode sputtering problem is to operate the thruster on either hydrogen or lithium propellants, for which the propellant

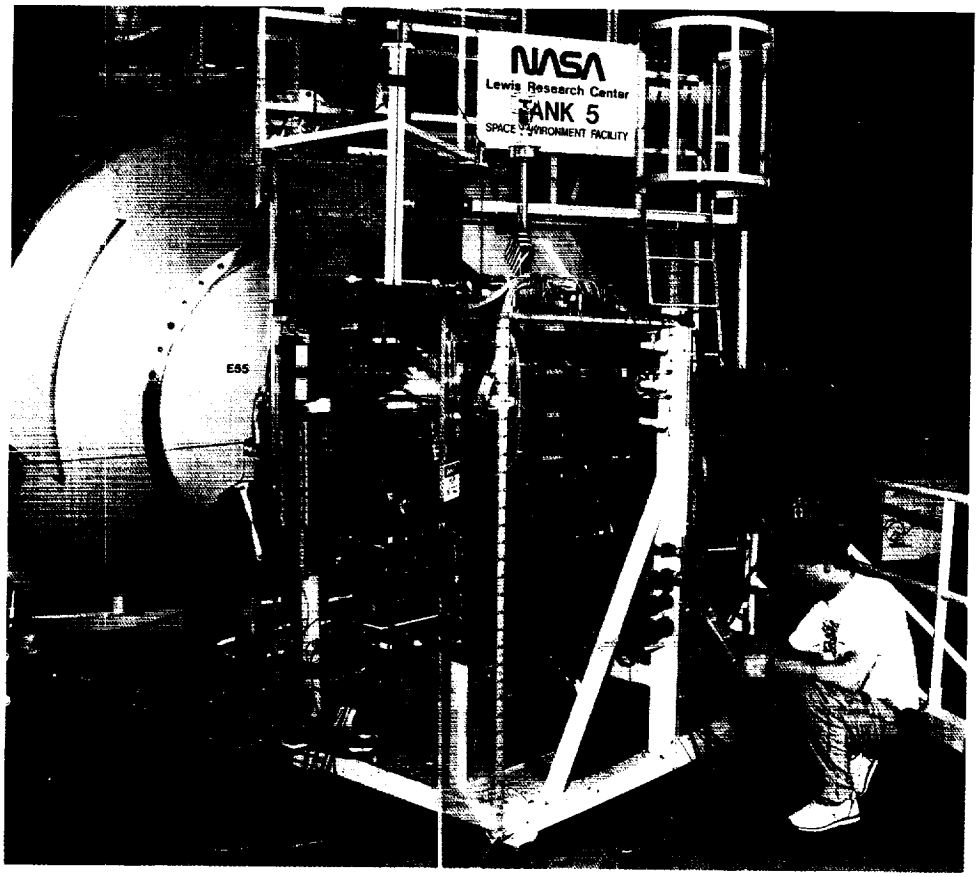

MPD thruster test cart at NASA Lewis tank 5 vacuum facility.

energy will not exceed the sputtering threshold at the specific impulses required for the missions considered.

Lewis contacts: Dr. Roger M. Myers, (216) 977-7426; Maris A. Mantenieks, (216) 977-7460
Headquarters program office: OAST

Water Vaporizer Demonstrated for Resistojet Application

Resistojets operating on water propellant have been proposed to augment the current Space Station *Freedom* propulsion system of high-thrust hydrazine rockets and low-thrust waste gas resistojets. Prior to use as a resistojet propellant, water stored as a liquid must be vaporized. This process must occur in the low-gravity environment on orbit without propellant recycling (i.e., only one pass through the vaporizer heat exchanger). The vaporizer exhaust stream must be dry vapor to avoid possible migration of liquid droplets to the thruster nozzle throat, where the rapid expansion of the propellant could cause freezing, throat closure, and thruster failure.

NASA Lewis has begun an effort to develop technology for water resistojets. The early goals are to identify and characterize candidate resistojet water vaporizer concepts, to identify and implement water vaporizer and thruster power control strategies, and to evaluate life-limiting issues associated with water vaporizer technology.

Two water vaporizers employing packed-bed heat exchangers were constructed and tested. The first vaporizer was characterized in a ground test facility to evaluate the impact of orientation with respect to gravity, to measure the thermal efficiency as a function of flow rate, and to measure the thrust performance of a water vaporizer/multipropellant resistojet assembly (ref. 1). Power was controlled by using propellant flow rate feedback to maintain a constant ratio of power to mass flow rate. This ensured sufficient power to process all flow entering the vaporizer while avoiding heater overtemperature during dynamic flow conditions. Steady, stable vaporizer operation was observed. Vaporizer flow rate and outlet pressure and temperature showed negligible sensitivity to orientation with respect to gravity

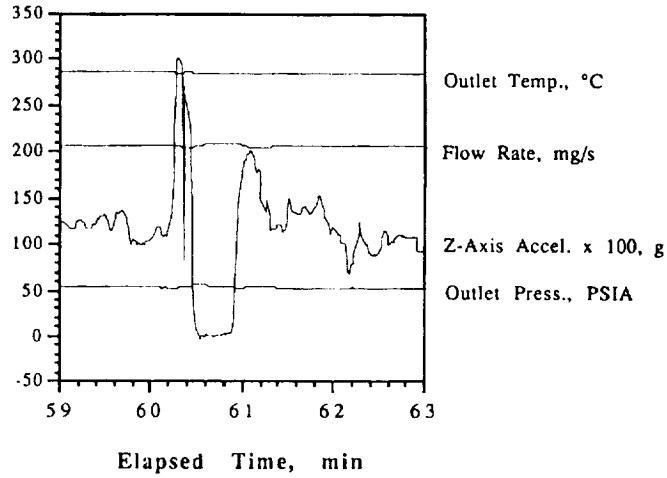

Test results for low-gravity resistojet water vaporizer.

when the operating vaporizer was rotated about a horizontal axis. Vaporizer thermal efficiency was in excess of 0.88 over the range of flow rates tested. The maximum demonstrated specific impulse of the vaporizer/thruster assembly, 234 sec, was limited by the capacity of the available thruster heater power supply.

The second vaporizer, a slightly modified version of the first, was tested at selected operating conditions in the Learjet low-gravity test aircraft. As before, power was controlled to maintain a constant ratio of power to mass flow rate. Preliminary results indicate that the distribution of the liquid phase along the vaporizer axis was somewhat sensitive to the high (2.5 to 3 g) pullups proceeding the low-gravity portions of the aircraft trajectories. However, operation appear to approach a steady condition during the 20- to 25-sec low-gravity period. Outlet conditions were nearly steady at all times, particularly during the low-gravity portions of the trajectories. These results indicate that the packed-bed technology incorporated in the vaporizer tested may be compatible with the low-gravity environment of Space Station *Freedom* and other tended platforms. Additional tests to expand the low-gravity data base of this concept are ongoing.

Reference

1. Morren, W.E.: Preliminary Characterizations of a Water Vaporizer for Resistojet Applications. AIAA Paper 92-3533, 1992.

Lewis contact: W. Earl Morren, (216) 977-7425
Headquarters program office: OAST

Laser Beams Used to Study Metallized Propellants

Technologies for using metal additives in gelled liquid fuels are being developed (refs. 1 to 3) in the Metallized Propellant Program. The metal increases the engine specific impulse, the propellant density, or both to increase space vehicle payloads. Propellant handling is also safer with gelled propellants because fuel spills are smaller and the propellant is less likely to combust during an accidental release. Typically, aluminum particles are suspended in gelled hydrogen, RP-1, or monomethyl hydrazine fuels. Ongoing research will quantify vehicle and engine performance and propellant chemistry and production.

Better combustion and performance of metallized propellants is being sought by reducing metal agglomeration, or "clumping," in the rocket exhaust. Laser beams are being used to determine the size and speed of metal particles as they exit from a low-pressure combustor using RP-1/aluminum fuel.

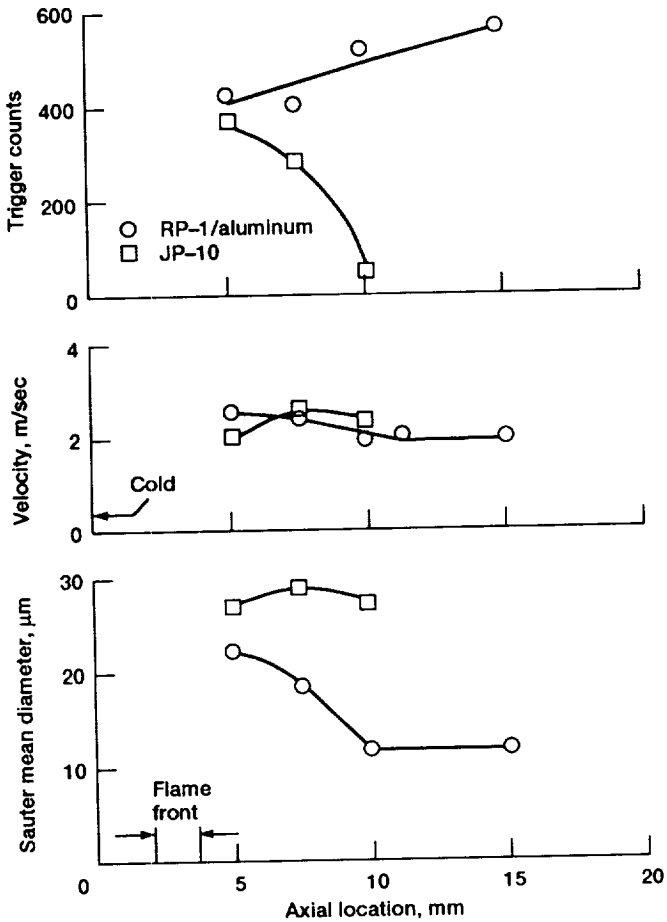

Comparison of metallized and unmetallized propellants.

Measurements show that whereas JP-10 (unmetallized fuel) droplets are consumed soon after exiting the combustor, the metallized droplets persist for an extended distance after all of the nonmetallized fuel is consumed. This implies that the metallized droplets have a greater resistance to combustion. Techniques are being developed at Pennsylvania State University to enhance "secondary" breakup of the metallized droplets in order to accelerate the combustion of the metal particles in the droplets and increase the combustion efficiency. This research may overcome one of the major stumbling blocks to metallized propellants' successful applications in future NASA missions.

References

1. Palaszewski, B.; et al.: Launch Vehicle Performance Using Metallized Propellants. AIAA Paper 91-2050, 1991. (Also NASA TM-104456.)

2. Palaszewski, B.; et al.: Design Issues for Propulsion Systems Using Metallized Propellants. AIAA Paper 91-3484, 1991. (Also NASA TM-105190.)

3. Palaszewski, B.: Upper Stage Using Liquid Propulsion and Metallized Propellants. NASA TP-3191, 1992.

Lewis contact: Bryan A. Palaszewski, (216) 977-7493

Headquarters program office: OAST

Mars Indigenous Propellants Demonstrated

The exploration of Mars will require large masses to be lifted into Earth orbit. A significant portion of this mass will be propellants. If the propellant for the return trip can be manufactured at Mars, the amount of mass lifted into low Earth orbit is reduced not only by the mass of the return propellant, but also by the mass of propellant normally used to push the return propellant out to Mars. The atmosphere of Mars is more than 95 percent carbon dioxide. Potential propellants that can be produced from this indigenous resource include oxygen, carbon monoxide, and methane.

NASA Lewis has a program to establish the technology data base for developing rocket engines

that can use indigenous martian propellants. Because the oxygen/carbon monoxide option has the advantage of needing no hydrogen, the Lewis program has focused on this combination. Experimental investigations have been performed in ignition, combustion, and heat transfer. Additionally, analytical studies have investigated the likely engine cycles and cooling methodologies.

The ignition tests were designed to test the ability to ignite a dry carbon monoxide and oxygen mixture in a standard spark torch igniter. The results indicated that 0.0062 wt % hydrogen added to the carbon monoxide at a mixture ratio of 0.35 catalyzed the ignition process. A mixture ratio range was established where the carbon monoxide and oxygen would ignite and sustain combustion, and this range was dependent on the inlet temperature of the oxygen. The carbon monoxide and oxygen propellants have also been tested in a calorimeter chamber to evaluate the combustion and heat transfer characteristics. The experimental C* efficiency was between 95 and 96.5 percent over a mixture ratio range of 0.3 to 1.0. Using the location of maximum heat flux as an indication of combustion, the end of the combustion zone occurred between 2.7 and 6.5 cm downstream of the injection.

Six expander cycle engines were evaluated analytically by varying the turbine working temperature limit and the turbine working fluid mass flow. The study showed that either type of working fluid was feasible for a Mars ascent engine, although carbon monoxide as the working fluid resulted in the best engine characteristics. Another analytical study investigated the possibility of developing a single engine that could use hydrogen fuel for the outbound trip and then refuel with carbon monoxide or methane for the return portion of the trip.

Six expander cycle engines were evaluated analytically by varying the turbine working temperature limit and the turbine working fluid mass flow. The study showed that either type of working fluid was feasible for a Mars ascent engine, although carbon monoxide as the working fluid resulted in the best engine characteristics. Another analytical study investigated the possibility of developing a single engine that could use hydrogen fuel for the outbound trip and then refuel with carbon monoxide or methane for the return portion of the trip.

Mission studies have continued to show significant reductions in mass in low Earth orbit with the use of Mars indigenous propellants. Experimental and analytical studies are advancing the technology data base for the development of a carbon monoxide/oxygen engine that can be used in sample-return missions and in future human exploration of Mars.

Bibliography

Linne, D.L.: Performance and Heat Transfer Characteristics of a Carbon Monoxide/Oxygen Rocket Engine. NASA TM-105897, 1992.

Pelaccio, D.; et al.: Engine System Assessment Study Using Martian Propellants. AIAA Paper 92-3446, 1992.

Wadel, M.F.: and Roncace, E.A.: Propulsion Systems Using in Situ Propellants for a Mars Ascent Vehicle. AIAA Paper 92-3445, 1992. (Also NASA TM-10574, 1992.)

Lewis contact: Diane L. Linne, (216) 977-7512
Headquarters program office: OAST

Post-Test Diagnostic System Devised for Rocket Engines

The safe and reliable operation of a rocket engine depends on the proper functioning of each component. To ensure successful engine operation, many engineers and technicians test, troubleshoot, and where possible monitor critical components during operation. The Civil Space Technology Initiative's Earth-to-Orbit Program has funded the development of several post-test, postflight diagnostic techniques that are being incorporated into a post-test diagnostic system (PTDS). With this system engineers have an expedient means of reducing and interpreting the large amounts, 20 megabytes and more, of data, and less time and manpower are required after engine tests and flights.

The PTDS aids engineers by providing a fast first-pass data analysis. Its analytical methods are modeled after these engineers' analysis strategies. The PTDS' generic framework allows for easy application to any rocket engine. Its modular architecture has both procedural and non-procedural knowledge-based components. This

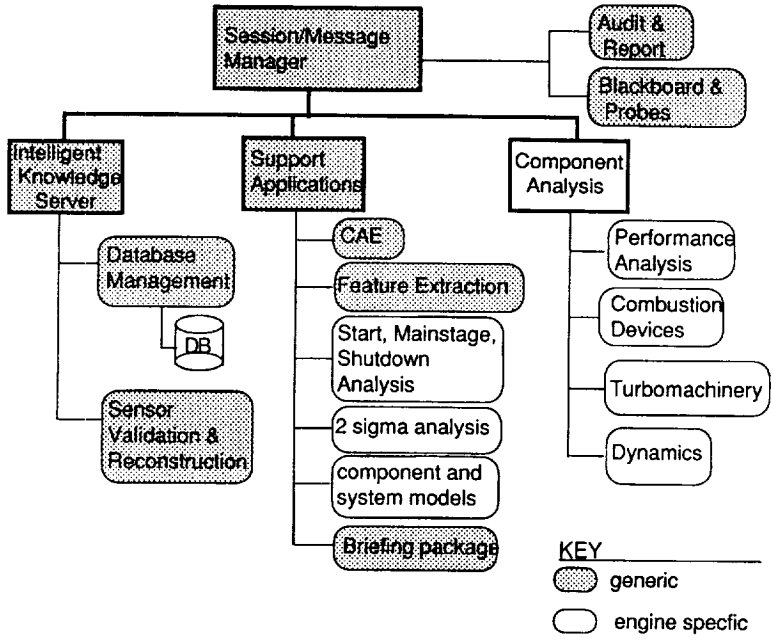

Framework for a post-test diagnostic system.

combination allows conventional algorithms as well as heuristic expert information to be included. Currently, this architecture has been implemented with the expert modules that analyze the high-pressure oxidizer turbopump for the Space Shuttle main engine.

All data being analyzed are time-series data. Interaction between cooperating expert modules must incorporate the time dependence of features. A simple representation of time dependence is employed. The system allows multiple "snapshots" of the domain at different times, explicitly handling points in time and time intervals. It also handles specific time dependence over an interval of an individual sensor trace.

The PTDS has been in testing at NASA Marshall Space Flight Center for several months. Limit table entries have been chosen and the system is producing observations. The initial test results have proven the system's usefulness. It has correctly identified drifting sensors and anomalous shaft motion. It has also detected a subtle case of preburner pump bistability on a nonflight turbopump that was missed initially by human analysts. The system allows easier access to data in a user-friendly atmosphere.
After this initial success the PTDS has been expanded to cover the performance, or system, analyses. This expansion includes additional sensor validation techniques, as well as model-based reasoning techniques. This work is being primarily performed by NASA Lewis and Marshall personnel.

Bibliography

Surko, P.; and Zakrajsek, J.F.: PTDS: Space Shuttle Main Engine Post-Test Diagnostic Expert System for Turbopump Condition Monitoring. Presented at the SAE Aerotech '92 Conference, Anaheim, CA, Oct. 5–8, 1992.

Zakrajsek, J.F.: The Development of a Post-Test Diagnostic System for Rocket Engines. AIAA Paper 91–2528, 1991.

Lewis contact: June F. Zakrajsek, (216) 977–7470
Headquarters program office: OAST

C-2

Feedforward Neural Networks Provide Analytical Redundancy for SSME Sensor Validation

Recent condition-monitoring activities at NASA Lewis have focused on validating Space Shuttle main engine (SSME) sensor measurements. Sensors fail at a much higher rate than any other component class on the SSME. As advanced safety algorithms are tested, validation of a large number of performance sensors has become necessary to prevent erroneous engine shutdowns due to sensor failures. Sensor validation is also a vital component of an automated post-test diagnostic system because failed sensors must be identified before engine health assessments can be made.

Neural network models provide sensor validation capability through analytical redundancy. Analytical redundancy involves the approximation of functions relating observed system variables. Neural networks are attractive for approximating complex nonlinear systems such as the SSME because they can uniformly approximate any continuous function. The differences, or residuals, between the actual values and the neural-network-model-predicted values provide information on the health of the sensor suite under consideration. Feedforward neural networks with two hidden layers were used to approximate two redlined parameters: the high-pressure fuel turbine (HPFT) and the high-pressure oxidizer turbine (HPOT) discharge temperatures during main-stage operation of the engine. Network inputs were selected from knowledge of the engine cycle and the availability of instrumentation. The HPOT discharge temperature was a model input for the HPFT discharge temperature. Procedures for the systematic selection of an optimal or near-optimal set of input sensors have also been developed.

A backpropagation algorithm was used to train the feedforward networks on actual SSME data from two nominal firings. Trained networks were then validated with data from five additional nominal firings. Maximum errors were within 6.2 percent for the HPOT discharge temperature and within 2.5 percent for the HPFT discharge temperature. The behavior of the trained networks in the event of an input sensor failure was also characterized. Only hard sensor failures were considered. A hard failure of any input sensor had an immediate effect on the parameter being modeled. In the case of the HPFT discharge temperature model, a synthesized value for the HPOT discharge temperature was available for substitution from the HPOT discharge temperature model. The prediction accuracy of the HPFT discharge temperature model with a synthesized HPOT discharge temperature input was comparable to using actual nominal test data. Thus, the models continue to provide accurate predicted values for sensor fault detection and isolation after the identification of a failed sensor.

Issues concerning engine-to-engine variations and test-stand-specific characteristics are being addressed. Residual processing techniques must also be formalized.

Bibliography

Lin, C.S.; Meyer, C.M.; and Guo, T.H.: Neurocomputing Techniques for Selecting Measurements for Sensor Validation. Submitted to IEEE International Joint Conference on Neural Networks, San Francisco, March 28–April 1, 1993.

Meyer, C.M.; Maul, W.A.; and Dhawan, A.P.: SSME Main-Stage Sensor Signal Approximation Using Feedforward Neural Networks. Presented at the Fourth Annual Space System Health Management Technology Conference, Cincinnati, OH, Nov. 17–18, 1992.

Lewis contact: Claudia M. Meyer, (216) 977–7511
Headquarters program office: OAST

Power Technology

Fluid Dynamics of Liquid Sheet Radiators Investigated

The mass of a space radiator can be significantly reduced by eliminating the walls that contain the working fluid. Using a flowing, thin (~200 μm) liquid sheet as the radiating surface results in a low-mass space radiator immune to micrometeoroid damage. In order minimize evaporation losses that will occur in the vacuum of space, low-vapor-pressure ($\leq 10^{-8}$ torr) silicone oils and liquid

metals must be used as the working fluid. A unique characteristic of thin-sheet fluid flow is that the flow coalesces to a point, resulting in a triangular-shaped sheet. Surface tension forces at the edges of the sheet cause cylinders to form that grow in diameter in the flow direction. As the cylinders grow, the sheet narrows to satisfy mass continuity. The end cylinders eventually meet at a point. This coalescing of the flow to a point is ideal for flow collection in a space radiator.

Initial experimental and theoretical studies were made of the fluid dynamics of thin liquid sheets. The dependence of the sheet length on the sheet properties was calculated and experimentally verified in a large (0.4-m diameter by 3 m long) vacuum facility at Lewis. A two-dimensional model was used to calculate the shape of the edge cylinders and predicted a nearly circular shape. However, photographic experimental results show that the edge cylinders change shape in the flow direction. The edge cylinder shape oscillates back and forth between a nearly circular cross section and a highly elongated cross section as the flow progresses toward the coalescence point. A three-dimensional theoretical model will probably be required to predict the highly elongated cross sections. It is important to know the edge cylinder shape because where the edge cylinder joins the main sheet an instability can occur that will produce a hole in the sheet flow.

A linear stability analysis predicted that instability depends primarily on the ratio of sheet width W to sheet thickness τ. In order to determine the limit on W/τ that allows flow without instability, an experiment with variable sheet thickness was constructed. The experiment used water as the fluid and was run in atmosphere. Up to the largest W/τ (~4850) that was experimentally attained, no instability was observed. This is an important result because for a practical liquid sheet radiator $W/\tau \approx 5000$ is desirable.

Currently, the large vacuum facility is being prepared to measure the emissivity of the sheet flow. The first measurements will be done with Dow Corning 705 silicone oil, which is a candidate working fluid for a space radiator. Calculated emissivities are greater than 0.8 for sheet thicknesses greater than 100 μm and temperatures between 300 and 400 K.

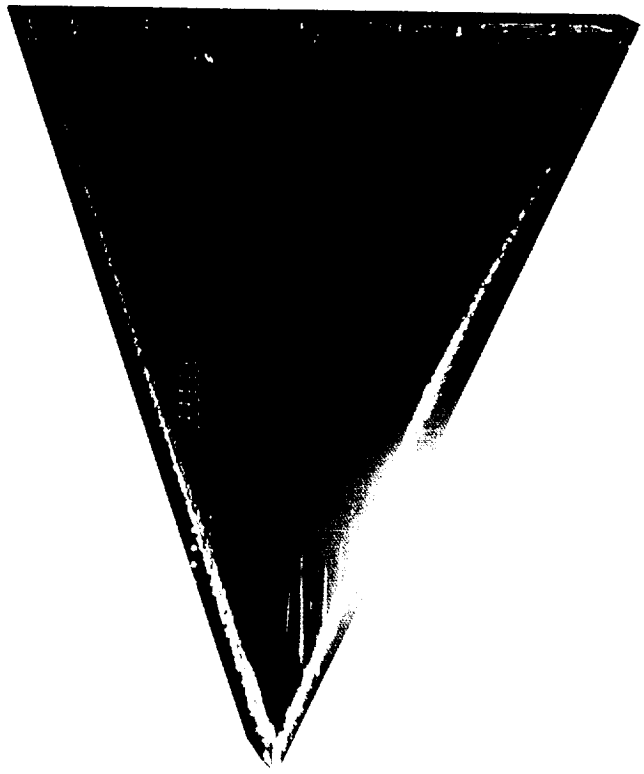

Sheet flow of water in atmosphere.

Bibliography

Chubb, D.L.; and Calfo, F.D.: Scaling Results for the Liquid Sheet Radiator. IECEC '89; Proceedings of the Twenty-Fourth Intersociety Energy Conversion Engineering Conference, W.D. Jackson and D.A. Hull, eds., Vol. 1, IEEE, New York, 1989, pp. 45–50. (Also NASA TM–102100, 1989.)

Chubb, D.L.; and White, K. A.: Liquid Sheet Radiator. AIAA Paper 87–1525, 1987. (Also NASA TM–89841, 1987.)

Juhasz, A.J.; and Chubb, D.L.: Design Considerations for Space Radiators Based on the Liquid Sheet (LSR) Concept. IECEC '91; Proceedings of the 26th Intersociety Energy Conversion Engineering Conference, Vol. 6, American Nuclear Society, LaGrange Park, IL, 1991, pp. 48–53.

Lewis contact: Donald L. Chubb, (216) 433–2242

Headquarters program office: OAST

Titanium Precursors Chemically Vapor Deposited

Titanium and its alloys (i.e., TiAl, $TiSi_2$, TiN, TiC, or TiB_2) are critical for numerous aerospace applications because of their high specific strength

at elevated temperatures, hardness, and resistance to wear and corrosion. It is anticipated that the titanium processes developed will have a tremendous effect on aerospace technologies, primarily propulsion, power, communications, and sensors. Other uses include coatings for metal cutting tools, coatings for medical implants, and thin-film metallization and buffer layers for electronic devices. Metallization is critical for yield and reliability of VLSI and ULSI (very large-scale and ultra-large-scale integration) devices. It is estimated that by the year 2000 increased demand for consumer electronics and personal computers will drive worldwide demand for semiconductors past $200 billion. In particular, these processes will be incorporated in multilevel metallization schemes for emerging submicrometer and smaller generations of ULSI electronic devices (>64 m). As a major user of computer and communication technologies, NASA stands to benefit substantially from the development of such processes.

Of all metal and metal alloy deposition processes, chemical vapor deposition (CVD) is perhaps the most suitable for forming the reliable and reproducible multilevel structures required. A key advantage of CVD is its ability to involve the substrate surface in the deposition reaction, leading to a conformal and planarized growth. This feature is essential to producing three-dimensional multilevel structures, such as those found in contacts for electronic devices or coatings for engine components. Another important characteristic of CVD is that it can produce films on complex-shaped substrates and with growth rates that match or exceed industrial requirements. In addition, films can be grown at reduced temperatures (LTCVD), as low as 150 °C, with no need for postdeposition annealing in some cases. Low temperatures minimize the effects of interdiffusion and allow the growth of abrupt multilayered structures. CVD is relatively simple and controllable and leads to good adherence, high uniformity over a large area, and reduced susceptibility to interfacial mixing and cross-contamination. These unique features have made CVD the technique of choice for depositing electronic materials of high quality and reproducibility. This technology is therefore readily transferable to aerospace components and devices.

The current program focuses on LTCVD of titanium and all its alloys by using a series of novel precursors through thermal and plasma-assisted CVD. The precursors are being synthesized at NASA Lewis with assistance from Cleveland State University. The State University of New York at Albany is depositing and characterizing the films. Further characterization using surface and analytical instrumentation and electrical and mechanical testing of CVD-deposited films is being conducted at IBM and Motorola. Initial results show that high-quality conducting titanium films with low carbon and oxygen content can be deposited from titanium sandwich compounds onto 5-in.-diameter silicon wafers. The deposition process involves plasma-assisted CVD below 400 °C. Current work involves the development of alternative precursors for LTCVD by using only a thermal process.

Lewis contact: Dr. Aloysius F. Hepp, (216) 433–3835
Headquarters program office: OAST

Robust, Lightweight Stirling Engine Heater Head Fabricated

A technological milestone has been achieved during 1992 by the successful fabrication of the Starfish heater for the 12.5-kWe component test power converter (CTPC). The objective of the work was to develop a lightweight, strong, high-performance heat exchanger that would be more reliable than conventional heat exchangers. The resulting design was a sodium-vapor-to-helium-gas heat exchanger, called Starfish, that is machined from a solid block of Inconel 718 superalloy material by electrochemical methods, thereby eliminating all braze joints. The name Starfish reflects the radial configuration of the heat exchanger fins. This work is part of an overall effort to develop all the technology necessary to design, fabricate, and test a high-efficiency, low-specific-mass, 12-kWe Stirling space power converter (SSPC) capable of long-life (60,000 hr) operation. The CTPC and SSPC will operate with the Starfish heater at 1050 K and the converter cold end at 525 K. The work is being performed under NASA contract by Mechanical Technology Inc. of Latham, New York.

The Starfish heater design was selected from a number of possible concepts because it had the lowest specific mass, was easiest to inspect, and was less subject to thermal distortion than any of

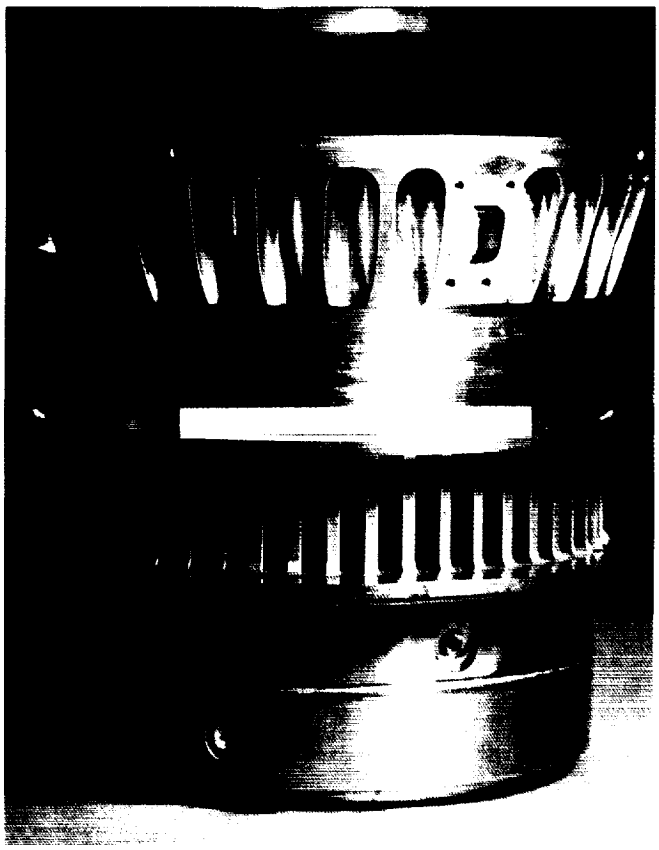

Starfish heater head.

the other concepts. Most importantly, the design completely eliminated braze joints. In comparison, a conventional tube-in-shell heat exchanger would have required 3800 braze joints. Superalloy materials are very difficult to braze. The only question that remained was whether the heater could, in fact, be fabricated.

The 50 heat exchanger fins for the CTPC Starfish heater were formed by using electrical discharge machining to remove material between the fins. The wedge-shaped slots between the fins become the condenser region of a sodium heat pipe. The heat pipe evaporator, when welded in place, is an annular, concentric section that extends radially outward from the condenser region. In the laboratory the evaporator is heated by electrical radiant heaters. During operation, sodium vapor will condense on the fin surfaces. Heat given up by the condensing sodium will be transferred to flowing helium in gas passages within each fin. These 1900 helium gas passages, each about 6 cm in length, have been drilled axially through the fins by shaped-tube electrochemical machining.

After the Starfish heater has been welded to the adjoining CTPC structure and final, conventional machining of the heater is completed, the CTPC will be assembled for performance testing. The Starfish heater for the final power converter of this contract, the SSPC, will be fabricated from Udimet 720 to provide the 60,000-hour creep life needed for this converter. The electrochemical machining processes developed for the CTPC Starfish heater will be directly applicable toward fabrication of the SSPC Starfish heater.

Fabrication of the CTPC Starfish heater has demonstrated the use of machining methods for making heat exchangers that do not require braze joints. These heat exchangers have a low specific mass and should be stronger and potentially more reliable than brazed heat exchangers.

Lewis contact: Donald L. Alger, (216) 891-2927
Headquarters program office: OAST

Udimet 720LI Alloy Electron-Beam Welded

Udimet 720LI alloy has been chosen as the material for the heater head of the 12.5-kWe Stirling space power converter (SSPC). A Udimet 720LI heater head can be designed to operate at 1050 K for the 60,000-hour design life of the SSPC. A unique, electrochemically machined heater head had been developed for the SSPC that eliminated all braze joints, but there remained three weld joints that needed development. Electron-beam welding is the preferred method of joining these joints because it offers repair after fabrication. However, no successful electron-beam welding of Udimet 720LI had been reported. Mechanical Technology Inc. (MTI) of Latham, New York, has since experimented with various heat treatments of Udimet 720 and has successfully electron-beam welded the material. Thus far, specimens that simulate one of the welds required for fabrication of the SSPC have been successfully welded. The work is being performed under NASA contract by MTI.

According to Special Metals Corporation, the maker of Udimet 720LI, the alloy has a relatively high gamma-prime volume fraction. Gamma prime is an intermetallic face-centered-cubic

phase that has the basic composition $Ni_3(Al,Ti)$. During solidification of the alloy the rapid rate of gamma-prime precipitation makes it prone to microcracking during welding and to cracking during the postweld heat treatment. Some general welding success had been achieved, but such welding required a lengthy preweld treatment as well as a closely controlled welding cycle and postweld heat treatment.

MTI metallurgists felt that developing the heat treatment and weld cycle control necessary to achieve a good electron-beam weld was important. The only viable alternative joining method for the SSPC was transient liquid-phase bonding (TLP). However, only electron-beam welding offered the ability to repair a joint in the event of a weld failure. In addition, the TLP bonding processes for joining Udimet 720LI also required considerable development.

Initial electron-beam welding tests performed by MTI demonstrated that Udimet 720LI could be successfully welded and heat treated in an unrestrained assembly. However, the unrestrained assembly did not simulate the actual SSPC welds. Subsequent welds in highly restrained geometries, modified circular patch test welds, were found to be sensitive to cracking during postweld heat treatment. Since that time, the processes been have modified such that several successful electron-beam welds have been achieved in various geometries and under varied degrees of constraint. The complete simulation of one SSPC weld, a radial-butt weld that joins two, approximately 0.4-in.-thick, cylinders has been successfully completed.

Development of an electron-beam welding process for Udimet 720LI has been an important advance in the welding field.

Lewis contact: Donald L. Alger, (216) 891-2927
Headquarters program office: OAST

Component Test Power Converter Cold End Tested at 525 K

A significant milestone of the 12.5-kWe Stirling space power converter (SSPC) technology development program was achieved during 1992 with the successful testing of the 12.5-kWe component test power converter (CTPC) cold end at design operating conditions. The power converter was

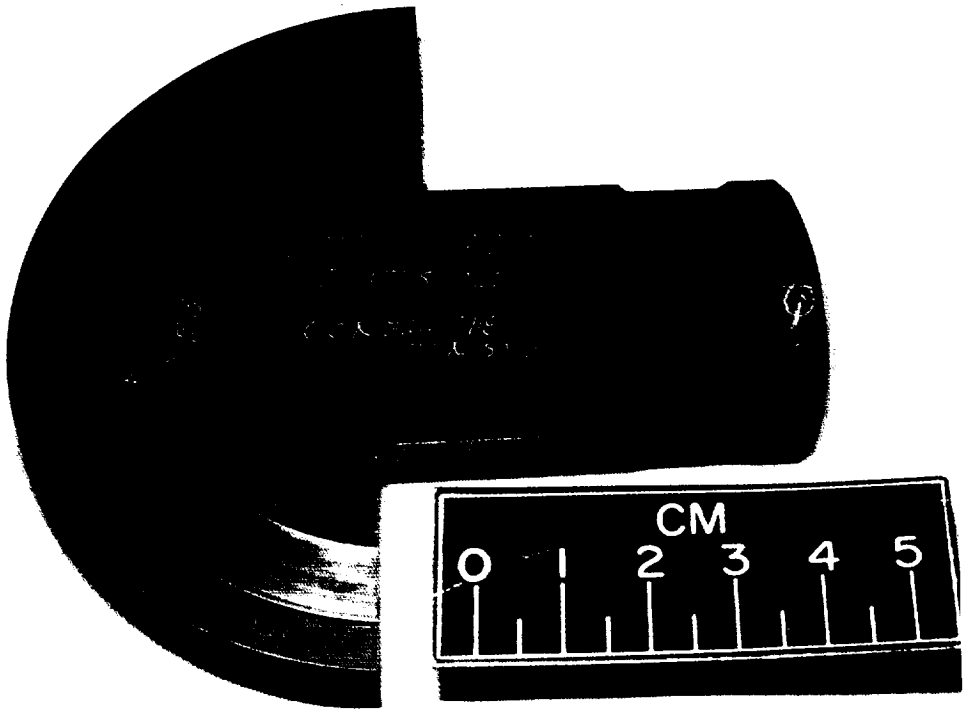

Successful electron beam weld of Udimet 720LI.

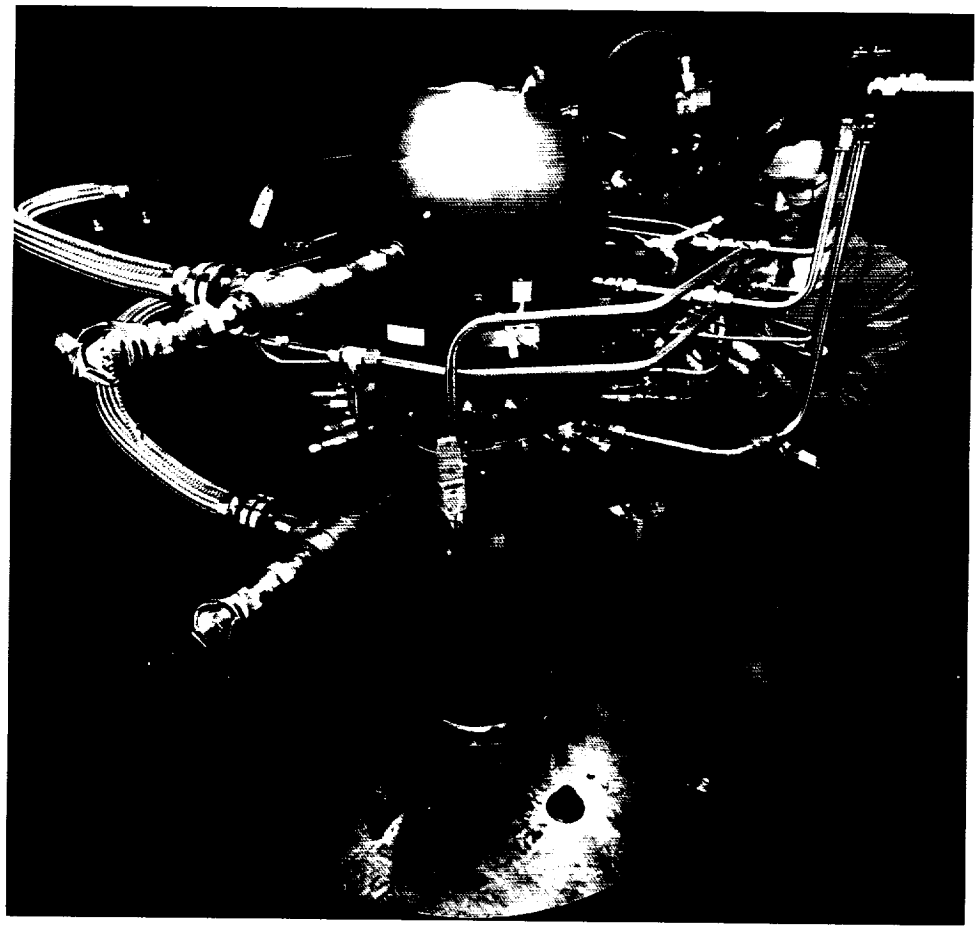

CTPC cold end.

operated at a temperature of 525 K, a working gas pressure of 150 bar, and a frequency of 70 Hz and with power piston and displacer strokes at 28 mm. Movement of the piston and displacer was caused by applying an electrical voltage to the alternator, which then functioned as a linear motor. The CTPC cold end contained all of the CTPC parts except the hot-end heat exchangers. The CTPC is being developed by Mechanical Technology Inc. (MTI) of Latham, New York.

The CTPC was fabricated for developing all the technology necessary to design, fabricate, and test a high-efficiency, low-specific-weight, 12.5-kWe SSPC capable of long-life (60,000 hr) operation. During normal operation both power converters, the CTPC and SSPC, operate with the hot end at 1050 K and the cold end at 525 K.

Operation at the elevated 525 K cold-end temperature is a major technical accomplishment that required breakthroughs in the following areas:

- Alternator stator coil and insulation materials able to operate with a minimum performance penalty at temperatures above 525 K
- Permanent-magnet linear alternator design capable of operating at 525 K
- Power piston and displacer supported on internally supplied hydrostatic gas bearings, capable of dry starting and smooth mechanical operation at temperature levels from ambient to 525 K

Most of the insulating materials of the alternator are polyimide or fiberglass. The stator laminations are coated with an oxide. The permanent magnets are samarium cobalt (Sm_2Co_{17}).

The internally supplied hydrostatic gas bearing is a simple, passive system that relies on the piston gas springs to supply gas to bearing supply and drain plenums located within the pistons. The gas springs are part of the spring-mass system

that causes the pistons of the free-piston Stirling engine to oscillate. The plenums are charged through ports in the piston and cylinder walls that open at appropriate times as the piston traverses its cycle.

An early concern during the design of the CTPC was that the extremely close clearance between the power and displacer pistons and their cylinders, of the order of 0.0005 in., be maintained during operation at 525 K. For this reason, relatively soft carbon graphite sleeves were used to line the interior surface of the cylinders. The mating cylinder surface was coated with hard chromium oxide. It was expected that thermal gradients might cause contact between the pistons and their cylinders. However, such contact has not occurred and the gas bearing system has performed flawlessly.

Successful testing of the CTPC cold end completed the first phase of the CTPC test program. The objective of this phase of testing was to identify and correct problems associated with the CTPC mechanical operation. The next phase of the program is currently in progress and involves incorporating the heat exchangers (heater, cooler, and regenerator) and testing the CTPC as a complete power converter for evaluation of power output and efficiency.

Successful operation of the CTPC cold end at 525 K is important because all developed technology is directly applicable to the 12.5-kWe SSPC, the final power converter to be fabricated and tested under the current contract with MTI.

Lewis contact: Donald L. Alger, (216) 891-2927
Headquarters program office: OAST

Lightweight Nickel/Hydrogen Cells Developed

As part of the nickel/hydrogen (Ni/H_2) cell technology program at NASA Lewis an advanced Ni/H_2 cell design was developed. A goal was to improve the specific energy of the state-of-the-art Ni/H_2 cell from 50 to 100 W-hr/kg. One of the components necessary to accomplish this goal is a lighter weight nickel electrode. The use of lightweight nickel plaque in place of heavy sintered nickel plaque will lessen the weight of the nickel electrode. These plaques (fiber and felt) are fabricated into nickel electrodes by electrochemically impregnating them with the nickel hydroxide active material. After preliminary experiments the Fibrex fiber plaque from National Standard, Niles, Michigan, was selected as one of the most promising support candidates for the active material. The plaque consists of 50 percent nickel fiber, 35 percent nickel powder, and 15 percent cobalt powder. The porosity and thickness of nickel electrodes affect the specific energy, performance, and life of the Ni/H_2 cell. The lightweight plaques can easily be manufactured with much larger porosities than heavy sintered plaques. For example, Fibrex plaques are commercially available in porosities up to 98 percent, but commercial state-of-the-art plaques are available in porosities of only 80 to 85 percent. In addition, use of thicker Fibrex nickel electrodes (e.g., 80 mils) will reduce the required number of electrodes and separators and thereby reduce total cell weight. Highly porous and thick Fibrex plaques are attractive potential candidates for a lightweight Ni/H_2 cell.

Boilerplate nickel/hydrogen cell.

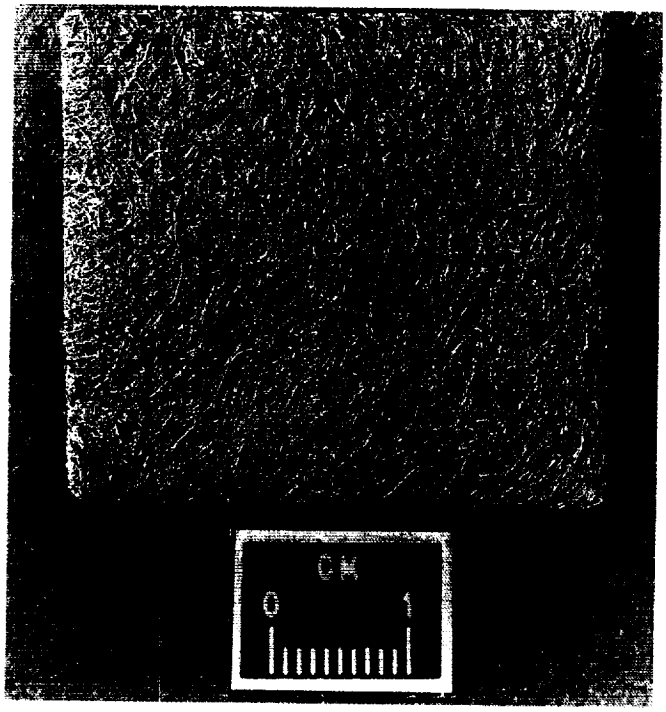

Fibrex nickel fiber plaque.

A major accomplishment in nickel electrode development at NASA Lewis occurred during the cycle life testing of the Ni/H_2 cell. A boilerplate Ni/H_2 cell with a Fibrex nickel electrode was fabricated in-house and cycled at 40 percent depth of discharge. The cell has accumulate 10,000 cycles so far.

The lightweight nickel/hydrogen cell program is a combined effort. A contract with Hughes Aircraft Company to improve the capacity and initial performance of the Fibrex nickel electrode is currently under way. A grant with the Space Power Institute (Auburn University) to develop high-performance electrochemical systems utilizing composite electrode structures is in progress. These electrodes will be tested in an Ni/H_2 cell both at Hughes and NASA Lewis.

Improving the lightweight Ni/H_2 cell will benefit NASA's mission office (exploratory platforms and rovers) and the commercial aerospace companies (communications satellites). It will also benefit commercial battery companies that utilizes nickel-based electrodes (e.g., nickel/metal hydride and nickel/cadmium systems).

Lewis contact: Doris L. Britton, (216) 433–5246
Headquarters program office: OAST

Living Color Frame Maker Solves Graphics Generation Problems

Computer graphics are often applied for better understanding and interpretation of data under observation. These graphics become more complicated when animation is required during run time, as in many typical modern artificial intelligence and expert systems. Living Color Frame Maker (LCFM) solves many of these real-time graphics problems.

With this new tool graphics frames can be generated and then displayed in real time. Video colors and intensities can be altered and objects can be moved during run time. For some applications these images can display a system hardware diagram and the real-time status of components and systems. The tool permits zooming in and out of the object images at any level of detail.

LCFM is user friendly, having graphical interfaces and providing on-line help instructions. All options are executed by using mouse commands and are displayed on a single menu for fast and easy operation. The software is written in C-language by using the Borland C++ 2.0 (registered trademark of Borland International, Inc.) compiler for IBM personal computers and compatible computers running MS–DOS (registered trademark of Microsoft Corp.).

With LCFM, graphics programming is largely eliminated and applications are handled with ease. In addition to the significant benefits of fast and easy graphics generation and modification, the open structure of the saved graphics files suggests many new possibilities for real-time graphics applications in commercial and aerospace markets.

LCFM was developed in-house at NASA Lewis and has been approved by the Technology Utilization Office (LEW–15554) for commercial distribution. The first version of LCFM, including source codes, will be available through NASA's Computer Software Management and Information Center at the University of Georgia ((706) 542–3265) at a cost of $100.00 per copy.

Bibliography

Truong, L.: PC Graphics Generation and Management Tool for Real-Time Applications. NASA TM–105749, 1992.

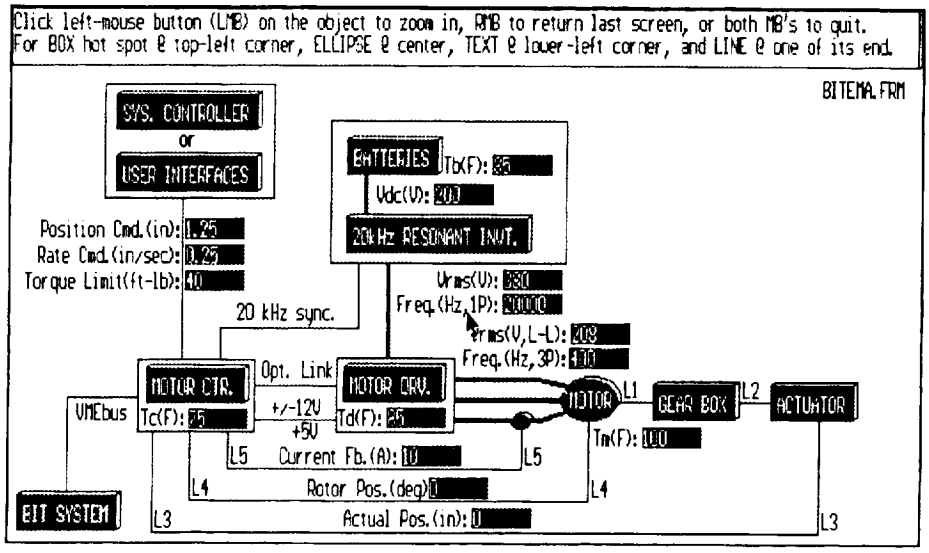

Top-level diagram for monitoring and diagnosis of an electromechanical system.

Truong, L.: LCFM—Living Color Frame Maker: PC Graphics Generation and Management Tool for Real-Time Applications. NASA/COSMIC, The University of Georgia, Athens, GA, 1992.

Lewis contact: Long V. Truong, (216) 433-6153
Headquarters program office: OAST

New Method Enables Optimal Choice of Subsystem Reliability and Redundancy to Minimize Cost

How does a design engineer or a systems engineer choose between one subsystem and another subsystem that is more reliable but costs more? NASA Lewis has developed new techniques and an associated computer program that consider reliability, redundancy, and cost in a combined manner. With the new technique a design, systems, or project engineer who is considering a number of alternative subsystems (each with its own level of reliability and cost) will be able to choose an optimal subsystem and level of redundancy (if any).

Fundamentally, the engineer/analyst must balance the cost needed to obtain reliability and the expected cost due to failure. This can be done by minimizing the total cost function, which is the sum of two costs: the cost of the subsystem itself and the expected cost due to its failure. This expected failure cost is defined as {the cost that will be incurred if the subsystem fails} times {the probability of subsystem failure} times {the reliability of the main system for other than failure of the subsystem under study}. Multiplication by the last factor discounts the cost due to failure of the subsystem because the main system may fail for some other reason.

Through an ongoing grant to California State University at Fullerton, five models have been developed to cover a multiplicity of situations:

1. Simplest model. The subsystem consists of n modules, of which k are required for success. If fewer than k modules are good, a loss occurs. In model 1, k is fixed.

2. Same as model 1, but k can vary. The $g(k)$ cost function is available to cover nonlinear subsystem cost increase with increased redundancy.

3. Expands on models 1 and 2. If fewer than k modules are good, some loss occurs but not necessarily the full loss.

4. Considers the time domain in the loss function. Modules in the subsystem fail exponentially with rate λ.

5. Similar to model 4, but subsystem loss below some critical fraction causes a loss that is not time dependent.

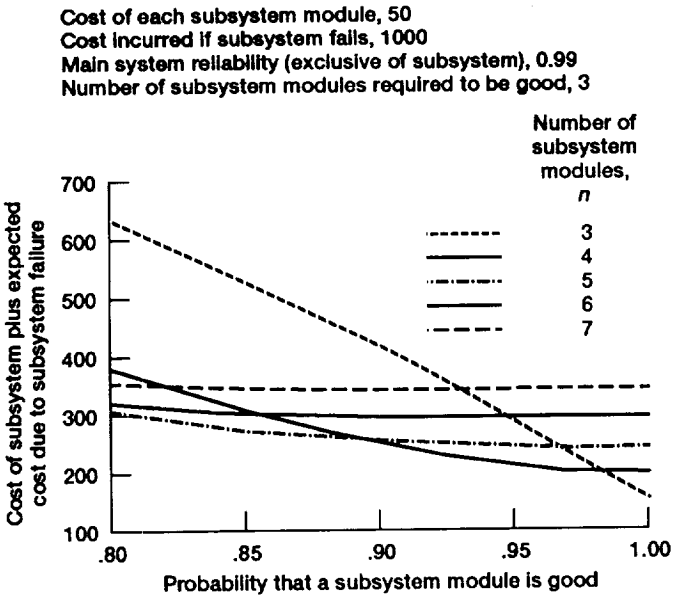

Graphical output from CARRAC software for model 1.

Software called CARRAC (for combined analysis of reliability, redundancy, and cost) was written to execute these models. CARRAC runs on IBM personal computers and clones and has a graphical output that allows an engineer to do sensitivity analyses.

The CARRAC software has been distributed to 20 NASA organizations and to many industry and university groups.

Bibliography

Suich, R.; and Patterson, R.: K-out-of-n:G Systems: Some Cost Considerations. IEEE Trans. Reliab., vol. 40, no. 3, Aug. 1991, pp. 259–264.

Suich, R.; and Patterson, R.: Reliability and Cost: A Sensitivity Analysis. NASA TM–105293, 1991.

Lewis contact: Richard L. Patterson, (216) 433–8166
Headquarters program office: OAST

Space Power Technology Applied to Long-Endurance Unmanned Aerial Vehicles

A solar electric model airplane is being built at NASA Lewis. This airplane is similar to battery-operated electric model airplanes built by hobbyists, but it incorporates an array of high-efficiency photovoltaic cells in its wing. The cells convert sunlight that falls onto the wing into electric power, which is used for propulsion and to recharge the battery in flight. The airplane is representative of the high-altitude, long-endurance unmanned aerial vehicles contemplated by NASA for various monitoring and surveillance applications, such as Earth resources monitoring, remote sensing, and communications relay for the Mission to Planet Earth.

The project is to demonstrate the benefits of space power technology for long-endurance aircraft propulsion. It is not an aeronautics demonstration. The ultimate goal is to enable continuous power for sustained flight at 65,000 to 75,000 ft. Conventionally powered aircraft cannot operate in this regime because airbreathing propulsion, which becomes progressively more difficult at higher altitudes, requires fuel to remain aloft. On the other hand, a solar electric aircraft, flying in the thin air and intense sunlight above the clouds, would not require refueling or resupply. The wing area for low-speed flight at high altitudes about equals the area of a photovoltaic array to power the aircraft. Therefore, solar electric power could keep the airplane on-station indefinitely—as long as it can gather and store enough energy during the day to keep flying through the night. Studies indicate that solar electric flight could be sustained during the night with better electric power and energy storage technologies, particularly the energy storage density achievable by batteries and fuel cells.

The solar electric model airplane is a joint project between NASA Lewis and the Air Force's Wright Aeronautical Laboratories. Lewis will build the aircraft and its power/propulsion system; Wright will furnish the solar cells. The cells, a product of the Air Force's Manufacturing Technology Program, consist of preproduction prototype and first-production qualification run cells to be used on the next generation of Air Force spacecraft. These 6- by 6-cm thin-film devices with an air mass 1 efficiency greater than 20 percent are based on gallium arsenide cell technology originally developed by NASA.

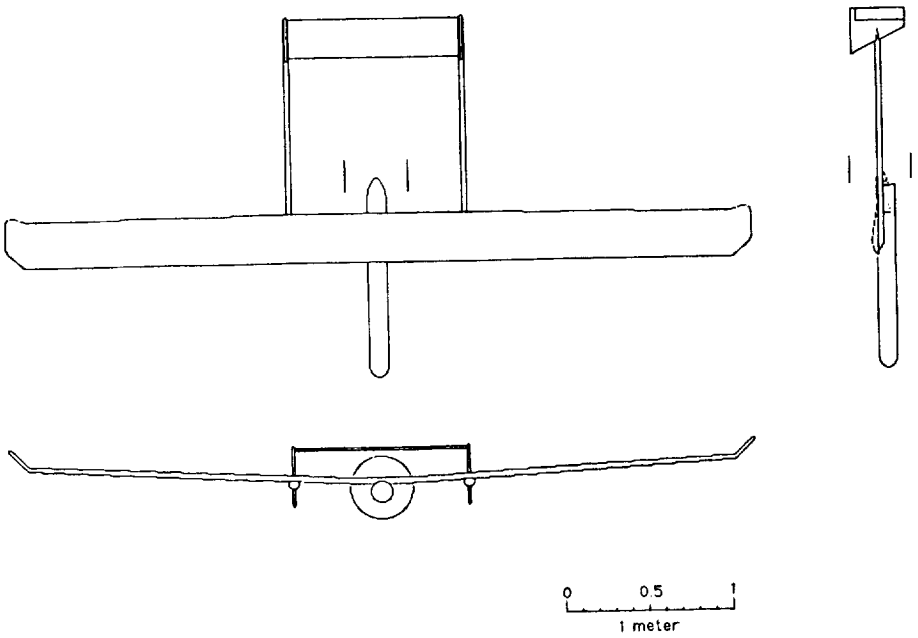

Solar electric airplane.

These improved cells should supply about twice the power of previous solar-powered aircraft, which have flown with array efficiencies of about 8 to 10 percent. It will be capable of flying continuously during solstice at very high latitudes, such as the South Pole, despite the low Sun angles.

The aircraft is being constructed in-house at NASA Lewis. Two identical airframes are being constructed. The first is a battery-powered "precursor" aircraft containing distributed wing weights to simulate the solar array and wiring mass. This aircraft will be subjected to low-power flight and durability testing. The second will be the solar-powered demonstration article. Attempts will be made to achieve new records for solar-powered aircraft, including time in flight, distance covered over a measured course, and altitude achieved from takeoff. Thermal soaring, previously relied on to achieve these records, will specifically not be used.

The aircraft will remain at Lewis for a period of test and demonstration, but the solar cells (and aircraft) will then be returned to Wright Aeronautical Laboratories for further testing and evaluation by the Air Force.

Lewis contact: David J. Bents, (216) 433–6135
Headquarters program office: OAST

2-kWe Solar Dynamic Ground Test Demonstration Program Begins

Solar dynamic systems focus the Sun's light into a chamber, heating a fluid that powers a turbine-alternator combination to produce electricity. The fluid is then cooled by a radiator that rejects waste heat to space. A major benefit of solar dynamic systems in space is their high efficiency, about four times that of current solar-cell power systems. This lets them be more compact, which decreases atmospheric drag. They are, therefore, candidates for the growth Space Station *Freedom* power systems.

On April 1, 1992, NASA Lewis awarded a 42-month, $18 million contract to an aerospace contractor team led by Allied-Signal Aerospace Company from Tempe, Arizona. The team will design, develop, and fabricate system components for a 2-kWe solar dynamic system to be tested in a ground space facility with simulated solar energy at NASA Lewis.

The contractor team includes Harris Corp. for the solar concentrator, Allied-Signal Aerospace Company for the heat receiver and gas cooler and the turbine-alternator-compressor assembly, Loral Vought Systems Corp. for the radiator, and Rockwell International Corp. for system integration. Work began April 1, 1992, at the prime contractor's plant in Tempe, Arizona.

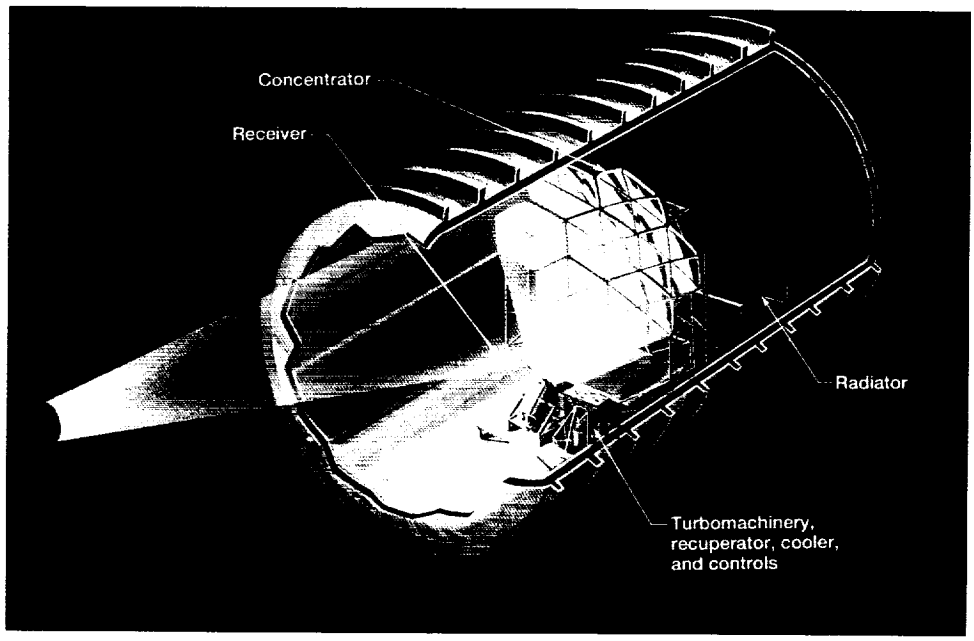

Artist's concept of 2-kWe solar dynamic system in vacuum facility.

Existing turboalternator-compressor and recuperator components will be used from previous programs, minimizing component design, fabrication, and development effort. NASA, with active participation from the contractor, will conduct the major subsystem and integrated system tests at Lewis.

Lewis contacts: Richard K. Shaltens, (216) 433–6138; Carol M. Tolbert, (216) 433–6167
Headquarters program office: OAST

Plasma Contactor Will Control *Freedom* Electrical Potentials

Interactions between the space plasma environment and space systems frequently result in potential differences between system reference ("ground") potential and plasma potential. These system floating potentials become a problem when the voltages involved are large enough to cause unwanted electrical effects, such as arcing or sputtering, or when system potential must be controlled to satisfy scientific requirements. Passive potential control is sometimes possible and has been employed on some scientific spacecraft. In other cases active potential control measures are needed. Hollow-cathode-based plasma contactors are an efficient and effective active potential control technology. Plasma contactors control spacecraft potentials by providing a low-impedance path for exchange of charged-particle "currents" between the spacecraft and the ambient plasma, in effect grounding some part of the spacecraft to the ambient plasma. This compensates for the lack of a naturally occurring good electrical ground in space.

Space Station *Freedom* uses high-voltage (160 V) solar arrays in combination with a negatively grounded direct-current power distribution system. Analysis of the plasma interactions and effects for this configuration indicated a need for active control. Therefore, the Space Station *Freedom* Program has baselined a hollow-cathode-based plasma contactor to control its structure potentials and thereby eliminate the anticipated arcing hazards. Without such a contactor the station structure would attain negative potentials of more than 100 V relative to the local ionospheric plasma during parts of each orbit. This could place excessive electrical stress on anodized surface coatings of some subsystems, notably the laboratory and habitation modules. Coating breakdown and destruction would result, with consequent degradation of thermal performance. The contactor, now being designed at NASA Lewis, will maintain the structure potentials

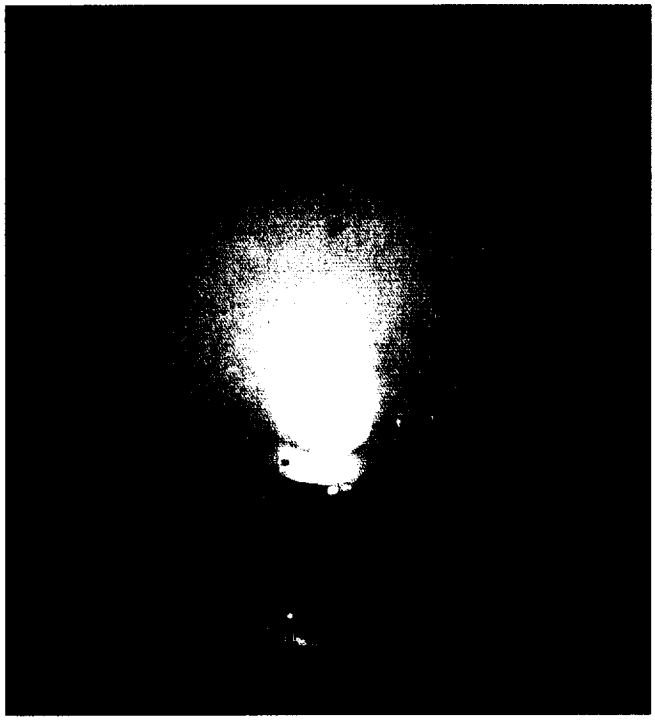

Ignited-mode operation of plasma contactor for electrodynamic tether.

within 40 V of plasma potential. This is expected to require maximum electron emission capability in the 10-A range. A similar device of opposite polarity (electron collecting) was recently flown on the ATLAS mission as part of the SEPAC experiment and successfully controlled the Shuttle potential during operation of the SEPAC electron gun at ampere current levels.

Hollow-cathode devices were originally developed as basic elements of ion thruster systems. Their application to controlling space system potentials on orbit has resulted from the understanding of system-plasma interactions developed in the Lewis environmental interactions technology programs through a combination of in-house, contract, and grant efforts. Models of the plasma contactor are being incorporated into the Environments Work Bench (EWB) computer code being developed for assessing *Freedom*'s plasma environment by S-Cubed Corporation (a division of Maxwell Laboratories) under contract to NASA Lewis.

Lewis contact: Dr. Carolyn K. Purvis, (216) 433-3567
Headquarters program office: OAST

Low-Earth-Orbit Environmental Effects Simulated on Spacecraft Radiator Surfaces

Radiators are necessary to eliminate waste heat from spacecraft systems and maintain desirable operating temperatures. Radiator surfaces for Space Station *Freedom*'s photovoltaic power systems must have high thermal emittance to reject large amounts of waste heat and low solar absorptance to absorb a minimal amount of the Sun's incident energy. Such optical properties must be maintained over the required 30-year life of the power system in low Earth orbit. Candidate radiator coatings for *Freedom* include Z–93, a white paint consisting of zinc oxide pigment in potassium silicate binder; YB–71, a white paint containing zinc orthotitanate pigment in potassium silicate binder; anodized aluminum; and silicon-dioxide-coated silvered Teflon. However, their optical properties may be altered by exposure to atomic oxygen, vacuum ultraviolet radiation, temperature cycling, and other environmental effects of low Earth orbit as well as by contamination from nearby spacecraft surfaces.

NASA Lewis has tested these radiator coating materials to characterize their optical property degradation upon exposure to such environments or from silicone contamination. Samples exposed in a radiofrequency plasma asher to a 30-year equivalent atomic oxygen fluence showed end-of-life solar absorptances below 0.3, which is within the requirements, and only slight emittance degradation. Other radiator samples were exposed to a combined atomic oxygen and silicone contamination environment by using an atomic oxygen beam source and placing radiator samples near silicone-containing samples. White paint radiator coatings exposed in this environment darkened due to silicone contamination, resulting in significant solar absorptance degradation.

A new facility at NASA Lewis can characterize the total hemispherical reflectance in situ (i.e., without breaking vacuum) for samples exposed to an environment containing combined atomic oxygen and vacuum ultraviolet (VUV) radiation. This in-situ characterization capability is important because oxygen in the air has been found to "bleach," or oxidize, damage due to ultraviolet radiation exposure. Proposed new formulations of the Z–93 coating are being tested in this facility. (The original components of Z–93 are not available.) Because the new formulation has had

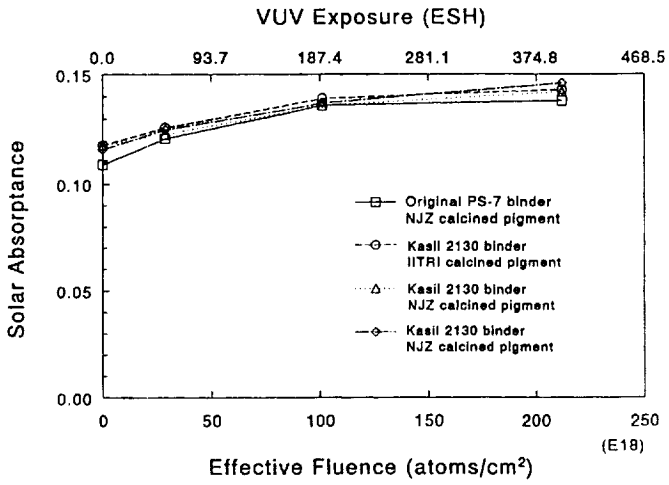

Effects of combined atomic oxygen and vacuum ultraviolet radiation on Z-93 coatings.

no long-term flight history as the original formulation had, requalification of the new Z-93 coating will rely on extensive ground-based laboratory testing. Tests of this nature are important in accurately predicting long-term, on-orbit performance of radiator coatings.

References

1. Dever, J.A.; et. al.: Evaluation of Thermal Control Coatings for Use on Solar Dynamic Radiators in Low Earth Orbit. AIAA Paper 91-1327, 1991. (Also NASA TM-104335, 1991.)

2. Dever, J.A.; and Bruckner, E.J.: The Effects of RF Plasma Ashing on Zinc Orthotitanate/Potassium Silicate Thermal Control Coatings. AIAA Materials Specialist Conference—Coating Technology for Aerospace Systems; A Collection of Technical Papers, 1992, pp. 109-118. AIAA, Washington, DC. (Also AIAA Paper 92-2171, 1992.)

Lewis contact: Joyce A. Dever, (216) 433-6294
Headquarters program office: OSSD

Coatings Protect Retroreflectors Against Atomic Oxygen

Atomic oxygen is the predominant species in low Earth orbit at altitudes between 180 and 650 km. It is highly chemically reactive and will attack most polymers and some metals utilized on spacecraft and orbiting satellites. The reaction of atomic oxygen with these materials can form volatile products or nonadherent surface oxides, reducing mechanical and structural properties or producing undesirable optical and thermal properties. Polymers that will be used as the structural support for the solar cells and circuitry on Space Station *Freedom* and for the alignment and tracking retroreflectors on the Eureka satellite and the Explorer platform are highly susceptible to detrimental changes in mass and optical properties upon exposure to atomic oxygen. Retroreflectors, which are used for satellite location and autonomous docking, are generally composed of acrylic or poly(methyl methacrylate). These materials form a matte surface texture after less than 40 hours at typical Shuttle altitudes. This matte surface absorbs laser light rather than reflecting it, making it impossible to utilize laser-range-finding retrieval techniques.

A thin-film silicon dioxide coating or a silicon dioxide coating with a small fluoropolymer content developed at NASA Lewis has been applied in-house to protect the retroreflectors for both the Eureka satellite and the Explorer platform. Ground-based environmental exposure tests as well as in-space experiments show that they provide adequate protection to these surfaces. Because this metal oxide coating is already in its highest oxidation state, it is resistant to atomic oxygen attack, and only a 100-Å-thick film is needed. This provides a lightweight solution to the durability problem without changing the polymer optical properties. Both sets of coated reflectors are currently in use. The coating is also the primary candidate for protecting the polyimide Kapton solar array blankets on Space Station *Freedom*. An array blanket has been successfully coated commercially and has passed durability evaluation testing. The coated material is currently being evaluated after lamination and array manufacturing to assess its ability to survive these processes. Use of protective coatings of this type can extend the useful life of spacecraft and their power systems operating in low Earth orbit.

Lewis contact: Sharon K. Rutledge, (216) 433-2219
Headquarters program office: OAST

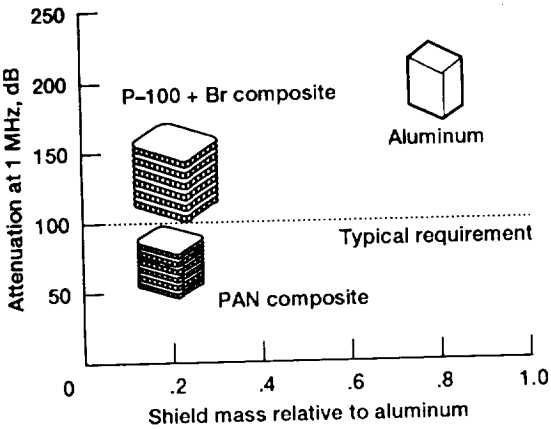

Comparison of composite mass and aluminum with respect to attenuation of signal at 1 MHz.

Intercalated Graphite Fiber Composites Make Lightweight EMI Shields for Aerospace Structures

The requirements for electromagnetic interference (EMI) shielding are more complicated in aerospace structures than in ground structures because of weight limitations. Thus, the best EMI shielding materials must blend low density and high strength and stiffness with high shielding effectiveness. Present technology utilizes aluminum, which has high shielding effectiveness but rather low strength and stiffness relative to materials like graphite/epoxy.

The conductivity of graphite/epoxy composites is too low to make them an effective shield, but the conductivity of certain grades of graphite can be enhanced by intercalation, the inserting of guest atoms or molecules between the graphene planes. When bromine is used as the intercalate, the result is a stable intercalation compound with a conductivity comparable to that of stainless steel but with the strength, stiffness, and low density of graphite.

Calculations show that effective EMI shields can be fabricated from intercalated graphite fiber/epoxy composites that would have less than 12 percent of the mass of conventional aluminum shields. Preliminary experiments support the calculations and prototype development is now under way.

Lewis contacts: James R. Gaier and Bruce A. Banks, (216) 433-2308
Headquarters program office: OAST

Facility Developed to Simulate Low-Earth-Orbit Environment

A world-unique facility for simulating the low-Earth-orbit environment has been developed at NASA Lewis to investigate the effects of this environment on spacecraft materials. Spacecraft operating in low Earth orbit must be designed to withstand the effects of solar radiation (particle and electromagnetic), micrometeoroids, deep thermal cycles, plasma interactions, and neutral atomic oxygen.

Atomic oxygen, the predominant species between the altitudes of 180 and 650 km, results from the dissociation of molecular oxygen by solar ultraviolet radiation. The relative velocities of spacecraft with respect to this atomic oxygen environment make the impacting atomic oxygen sufficiently energetic (~4.5 eV) to break many chemical bonds. Organic polymers are readily oxidized, and some metals form protective oxide layers. The synergistic effects of atomic oxygen, thermal cycling, and ultraviolet radiation exposure may degrade the performance of space power system components. Surface optical properties, such as solar absorptance and thermal emittance, are important to the thermal control of low-temperature radiators and other system components. Changes in these properties will result in penalties on component performance. Therefore, these components require ground-based evaluation of their low-Earth-orbit-environment durability prior to use in space.

The Atomic Oxygen/VUV Radiation Environment Simulation Facility at NASA Lewis is unique in that it provides accelerated rates of exposure to a directed oxygen beam, simultaneous with vacuum ultraviolet (VUV) radiation, as well as in-situ reflectance characterization. Adding to the facility's uniqueness is its ability to evaluate large samples and components. For example, a solar array coupon can be mounted under operational loads while exposed to the simulated low-Earth-orbit environment. A rotary stage can simulate on-orbit motion, such as that experienced by a solar tracking array.

An electron-cyclotron resonance plasma source generates a low-energy, high-flux oxygen beam. Deuterium lamps provide VUV intensity levels, in the 115- to 200-nm range, of four to five equivalent suns. The reflectance measurement system integrated into the facility can measure in situ

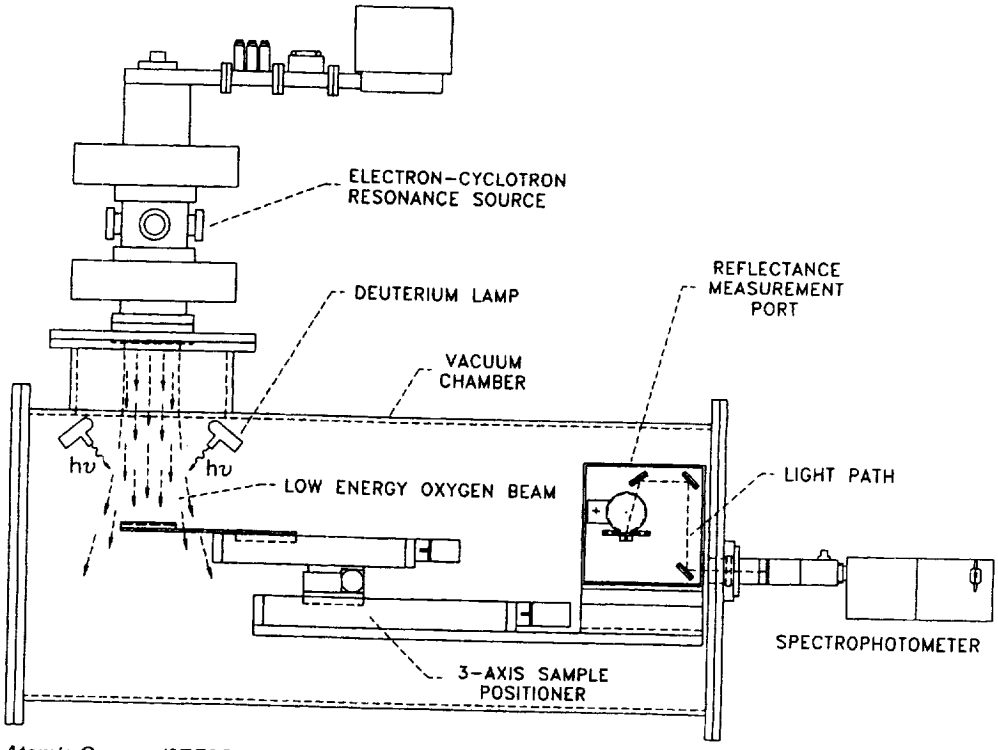

Atomic Oxygen/VUV Radiation Environment Simulation Facility.

total hemispherical spectral reflectance over the wavelength range 300 to 2500 nm. A three-axis, computer-controlled, sample-positioning system provides accurate and highly repeatable positioning for translation from the exposure region to the reflectance measurement position while maintaining the sample in the vacuum environment.

This facility has been developed in-house at NASA Lewis with support from Sverdrup Technology, Inc. It is used extensively by NASA Lewis and its contractors in evaluating space power system component materials for Space Station *Freedom*. The success of Space Station *Freedom* and other missions operating in low Earth orbit will depend on environmental durability evaluations that lead to the selection of durable materials for spacecraft design.

Lewis contact: Bruce A. Banks, (216) 433–2308
Headquarters program office: OAST

Solar Concentrator Materials Evaluated for Low-Earth-Orbit Durability

Solar dynamic power modules (SDPM) have been considered for additional electric power delivery during the growth phases of Space Station *Freedom*. In the SDPM a solar concentrator mirror reflects and focuses incident sunlight into a receiver to operate a heat engine. For efficient operation the solar concentrator must maintain a high solar specular reflectance in the low-Earth-orbit environment. The environment includes atomic oxygen, ultraviolet radiation, thermal exposures (such as thermal cycling), and a vacuum of ~10^{-8} torr. This harsh environment can cause considerable damage to vulnerable spacecraft materials, and susceptible materials must be protected when used in low Earth orbit. NASA Lewis is evaluating the low-Earth-orbit durability of SDPM solar concentrator materials.

The solar concentrator coupons evaluated had a sandwich structure of two sheets of graphite epoxy bonded to an aluminum honeycomb core. A multilayer reflective and protective system was applied to this sandwich structure. Silver was chosen as the reflective material for its high solar specular reflectance. Because silver does not adhere well to graphite epoxy, an adhesion-

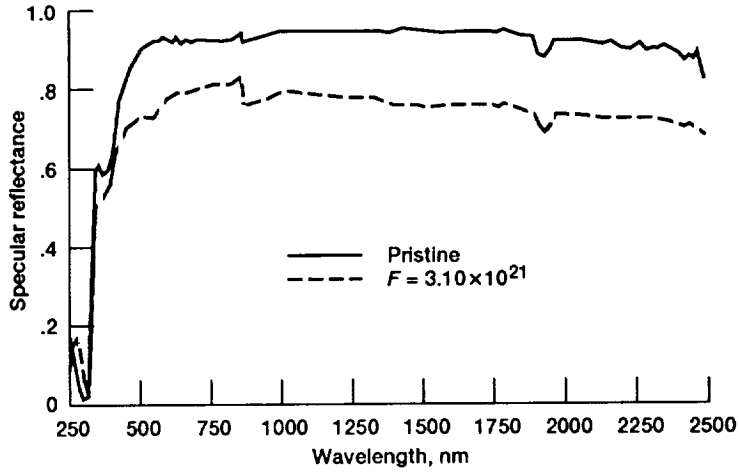

Specular reflectance, pristine and atomic oxygen exposed.

promoting layer of copper (200 Å) was first deposited onto the graphite epoxy facesheet, followed by silver (1000 Å). Two atomic oxygen protective coatings were deposited on top of the silver: aluminum oxide (200 Å) followed by an outer coating of silicon dioxide (700 Å). Concentrator coupons were subjected to iterative and continuous atomic oxygen exposures, vacuum thermal cycling, vacuum ultraviolet (VUV) radiation, and vacuum thermal cycles combined with VUV. The coupons were characterized before and after environmental exposures for surface features, optical properties, and analytical analysis.

The results indicate that the solar concentrator materials tolerate VUV radiation, vacuum thermal cycling, and combined VUV–thermal cycling, but not long-term atomic oxygen exposure. Thermal cycling and VUV–thermal cycling exposure resulted in a negligible change in the integrated solar specular reflectance although VUV radiation alone decreased solar specular reflectance. Coupons exposed to VUV radiation experienced spectral changes in the wavelength range from 250 to 500 nm with an associated yellowing of the surface. The change in spectral reflectance was attributed to ultraviolet darkening.

Atomic oxygen erosive oxidation was observed at defect sites in the protective coatings. Extensive atomic oxygen undercutting and curling of reflective and protective coatings were found to be promoted through an undercutting-tearing propagation process. Iterative atomic oxygen exposure appeared to accelerate this process, revealing the importance of choosing simulation techniques and of interpretation.

The primary cause of solar concentrator degradation was found to be atomic oxygen undercutting erosion occurring at defect sites in the protective coatings. The extent of optical damage experienced after continuous ashing to 1.08 equivalent Space Station *Freedom* years was found to be unacceptable when linearly extrapolated for the needed 15-year lifetime of the solar concentrators. This research provided evidence of the need to decrease the number of defect sites.

On the basis of the results from this completed program the SDPM concentrator contractor (Harris Corporation) plans to investigate using leveling coatings and other fabrication techniques (such as one based on replication) to produce ultrasmooth surfaces so that defects sites would be fewer. These results are relevant to photovoltaic systems currently being developed.

Bibligraphy

de Groh, K.K.; Terlep, J.A.; and Dever, T.M.: Atomic Oxygen Durability of Solar Concentrator Materials for Space Station Freedom. NASA TM–105378, 1990.

de Groh, K.K.; et al.: Low Earth Orbit Durability Evaluation of Solar Concentrator Materials. Solar Eng., vol. 2, 1992, pp. 775–782.

Lewis contact: Kim K. de Groh, (216) 433–2297
Headquarters program office: OAST

Phase Change During Thermal Energy Storage Investigated

Thermal energy storage is a critical element in solar dynamic systems. It provides the system with constant-temperature energy for those missions where solar energy is received sporadically, as in near-Earth orbits. Fluoride salts, such as lithium fluoride (LiF), are considered the best candidates to fulfill this function. Their fusion temperature values are in the optimal range for dynamic systems, and their heats of fusion are high. However, such salts change density and hence volume in going from the liquid to the solid phase. These salts also have poor thermal conductivity. This can vary the heat flow rate to the system's working fluid as the salt freezes and thaws continuously during orbit.

NASA Lewis instituted an analytical program to characterize the behavior of salt during melting and freezing. Because a prime application for thermal energy storage is under microgravity and there is no history of materials undergoing phase change under microgravity, a flight experiment is being designed to validate the analysis.

Thermal tests have been conducted on a canister containing lithium fluoride as part of the procedure leading to the flight test. Temperature profiles on the canister surface showed the effect of the void inside the canister as the salt changed phase. As the liquid froze, the voids became larger. Because these tests were conducted on Earth, the void was known to occupy the upper part of the canister. Temperature profiles showed the effect of the phase-changing salt and the accompanying changing void volume on the canister wall.

The heat flux imposed on the canister was in the same orientation as the canister would be in a solar receiver. Temperatures obtained in the terrestrial test are expected to exceed those obtained during the microgravity test. More detailed predictions of the canister temperatures will be obtained when the analytical computer code is completed.

Lewis contact: David Namkoong, (216) 433-6301
Headquarters program office: OAST

Space Electronics

Lewis Baseband Processor Technology Spurs Iridium Satellite System

In the early 1980's NASA Lewis began developing baseband processor technology envisioned to enable thousands of Earth terminals to communicate simultaneously with one another through a communications satellite. The baseband processor architecture selected by Lewis for proof-of-concept development was designed to switch, on a demand-assigned basis, individual voice, video, and data messages from any location to any other location within a fixed or scanning spot beam. This alleviates the need for message distribution on the ground and essentially moves the switchboard from the ground to space. Motorola was selected as the prime contractor for the proof-of-concept development. This effort established the feasibility of the baseband processor, perhaps the most complex communications payload component ever contemplated for a satellite. This pioneering effort, coupled with other advanced technologies developed by Lewis and its contractors—particularly the multiple-narrow-beam scanning antenna, set the stage for the development of the Advanced Communications Technology Satellite (ACTS). Motorola developed the baseband processor for ACTS, which is scheduled to be launched in 1993.

In a classic example of technology transfer Motorola's intimate knowledge of the baseband processor technology coupled with their position as a world leader in communications equipment led to their vision of a new class of communications satellites in low Earth orbit to provide personal communications to anyone, virtually anywhere in the world. Motorola's concept, called Iridium, consists of 77 satellites in low Earth orbit. Their payload architecture is a direct heritage from the baseband processor technology developed for Lewis. Motorola has filed an application to the Federal Communications Commission for construction and operation of a multibillion dollar satellite system consisting of 87 satellites (77 active, 10 spares). It is expected that the first satellite would be launched in 1996 and that the system will reach full operational capability by 1999.

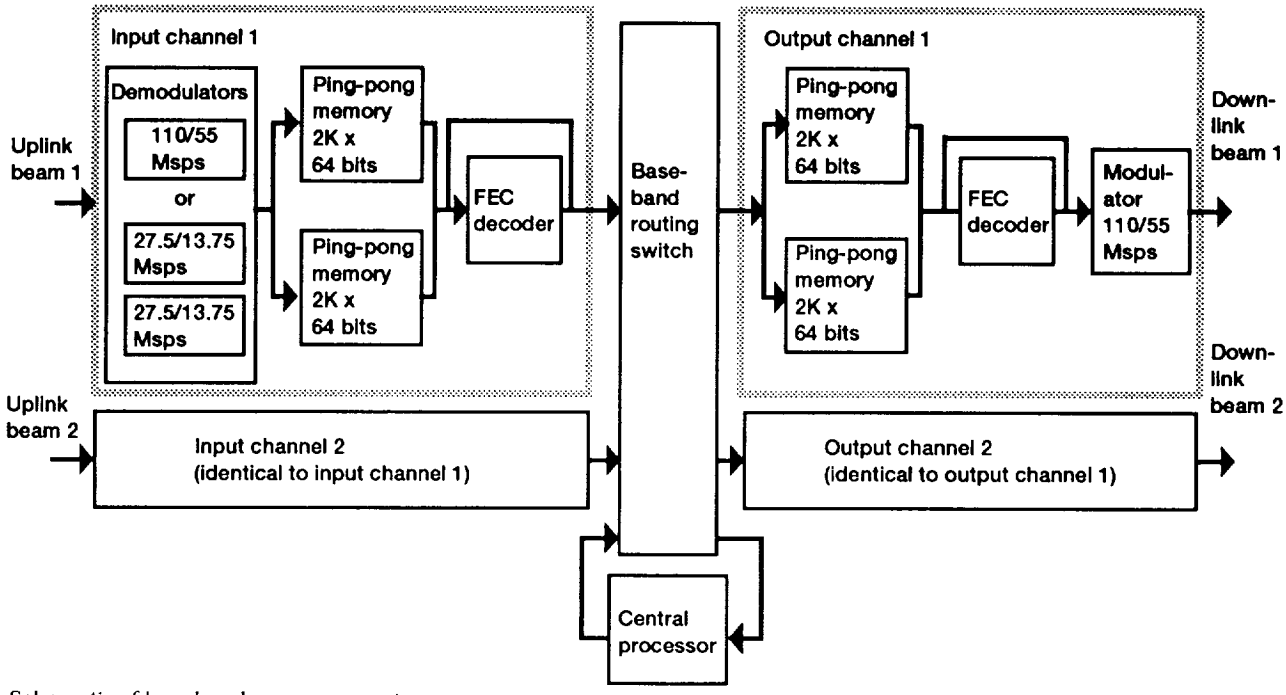

Schematic of baseband processor system.

Lewis contact: James R. Ramler, (216) 433-3475
Headquarters program office: OSSA

New Satellite Communications Frequency Allocations Gained

At the 1992 World Administrative Radio Conference (WARC-92), NASA Lewis played a key role in obtaining new frequency allocations to benefit the U.S. communications satellite industry. WARC-92 considered new frequency spectrum allocations for a wide range of satellite communications services to be offered through a vast array of new technologies and systems. WARC-92 decisions will affect satellite communications systems and services during the remainder of this century and beyond.

The International Telecommunications Union (ITU) convenes World Administrative Radio Conferences to construct international agreements on use of the radiofrequency spectrum for communications. Agreements are incorporated in the ITU Radio Regulations and constitute international law. WARC-92 addressed issues ranging from frequency allocations for low-Earth-orbit mobile satellite services to allocations for new space services above 20 GHz.

U.S. satellite communications industry issues included establishing new allocations at 19.7 to 20.2 and 29.5 to 30.0 GHz to provide for a new generation of commercial communications satellites building upon NASA Advanced Communications Technology Satellite (ACTS) developments to provide a flexible mix of fixed and/or mobile applications and establishing suitable broadcast satellite service (sound) frequency allocations for digital audio broadcasting.

Under the auspices of NASA's Office of Commercial Programs, NASA Lewis participated in a comprehensive series of domestic and international WARC preparatory activities. Lewis participated on behalf of the United States in the International Radio Consultative Committee, contributing critical technical studies on viable frequency allocations for the broadcast satellite service (sound), on interference between the broadcast satellite service (sound) and other communications services, and on modulation and coding for satellite broadcasting of high-definition television. Lewis also prepared U.S. position papers for the Organization of American States (OAS) on the broadcast

satellite service (sound) and new 20/30-GHz satellite service allocations and sent a U.S. delegate and spokesperson to OAS WARC preparatory meetings. These activities culminated in Lewis participation in the U.S. WARC–92 delegation to Torremolinos, Spain, and active involvement in international negotiations to secure new satellite communications service allocations.

WARC–92 established new mobile satellite service allocations within the ACTS frequency bands. This will pave the way for commercial use of ACTS technologies in a mixture of fixed and mobile satellite service applications. WARC–92 also allocated three frequency bands to be used by the broadcast satellite service to provide digital audio broadcasting. These allocations open new opportunities for the U.S. commercial communications satellite industry to offer new services and technologies to a global marketplace.

Bibliography

Reinhart, E.; et al.: WARC's Last Act?—Frequency Allocations. IEEE Spectrum, vol. 29, Feb. 1992, pp. 20–33.

Lewis contact: Ann O. Heyward, (216) 433–3484
Headquarters program office: OCP

Direct-Broadcast-Satellite Radio Demonstrated

Direct-broadcast-satellite radio offers listeners and service originators many benefits not previously available in the audio broadcast medium. Satellites can broadcast on a single channel to a national, regional, or continental audience. Wider coverage presents new opportunities for audience access to a variety of programming. Such programming might include educational, cultural, national, or target-audience-oriented broadcasts that may not be economically attractive to offer in any other way. Commercial radio broadcasting has not seen a more dramatic possibility for change since the introduction of frequency-modulated (FM) stereo broadcasting.

NASA is committed to developing technology that will enable new commercial applications for communications satellites. The Direct Broadcast Satellite–Radio (DBS–R) Program, a joint effort between NASA's Office of Commercial Programs and the United States Information Agency/Voice of America (VOA) Office of Engineering, is designed to achieve this objective. The program will provide service and technology definition and development for a new direct-to-listener, satellite, sound-broadcasting service. Managed by Lewis, the DBS–R program also involves the cooperative efforts of the Jet Propulsion Laboratory. Major

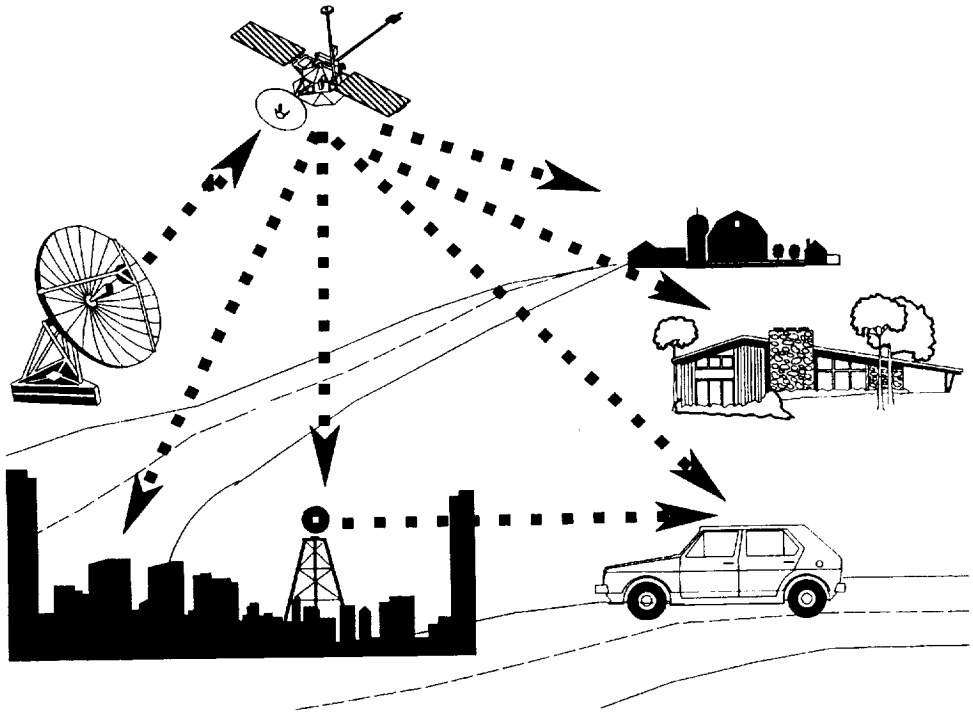

Broadcast satellite service (sound).

program efforts are directed toward frequency planning, hardware and service development, service demonstration, and experimentation with new satellite and receiver technology.

The evolution of digital and mobile satellite communications technologies has enhanced the potential quality and availability of a DBS–R service well beyond original expectations. DBS–R satellite systems can cover a range of desired broadcast areas, depending upon the satellite antenna size used and the power required at the receiver. DBS–R will also offer audio signals with various levels of sound quality—ranging from robust amplitude-modulated (AM) quality through FM monophonic and FM stereo quality to compact disk quality. DBS–R digital signals will reach a variety of radio receiver types (fixed, portable, and mobile) in various environments (indoor/outdoor, rural, urban, and suburban). Studies have shown that DBS–R systems can deliver programming economically for wide area coverage.

In September 1991, NASA Lewis and the Jet Propulsion Laboratory (JPL) conducted the first mobile, direct-broadcast-satellite radio experiments. Using the satellite capacity provided by Inmarsat, NASA/VOA uplinked an audio signal from Comsat's Coast Earth Station in Southbury, Connecticut, to Inmarsat's MARECS–B satellite, which transmitted the audio signal to a van traveling the highways of Connecticut. The experiments verified the feasibility of satellite sound broadcasting to a mobile receiver and permitted collection of system technical data in a mobile environment, establishing the basis for later demonstrations.

During November and December 1991, NASA's Office of Commercial Programs, Lewis, JPL, and VOA conducted the world's first live, public, mobile demonstrations of direct-broadcast-satellite radio, in Washington, DC, and Cleveland, Ohio. Observers from U.S. government departments and agencies and the U.S. communications industry, representatives of various embassies in Washington, DC, and media representatives from Washington, DC, and Cleveland, Ohio, participated in the series of demonstrations.

The 1992 World Administrative Radio Conference established three frequency allocations for the broadcast satellite service (sound) within which DBS–R systems may be implemented. These

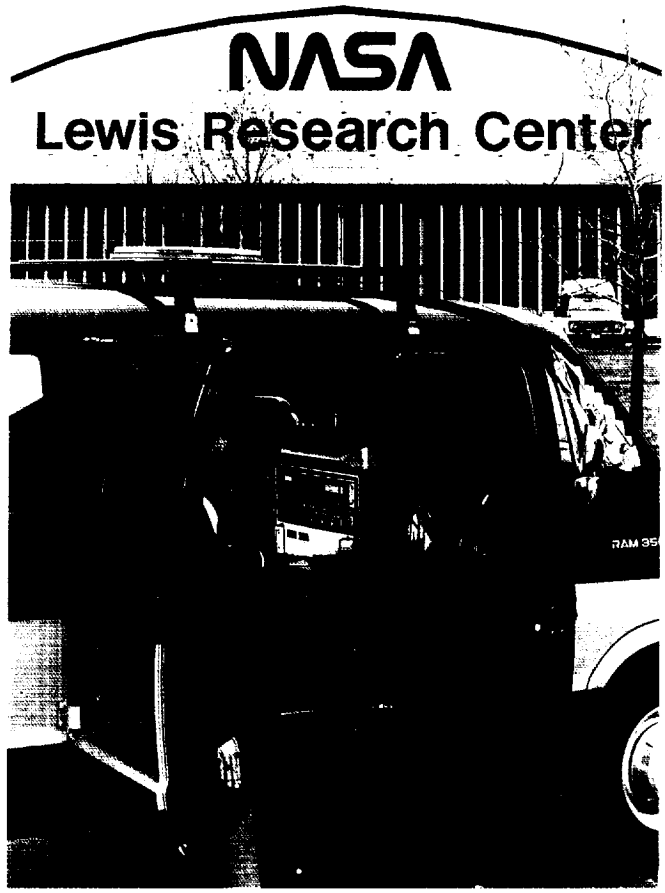

DBS–R demonstration mobile receiver.

allocations represent a major step toward commercial implementation of DBS–R. Research and technology development by NASA, the VOA, and industry can now proceed in much more specific directions in areas affected by the choice of operating frequency. Satellite system and receiver manufacturers can now embark on end-to-end DBS–R system development efforts tailored to the appropriate operating frequencies. NASA's objective is to assist in developing such systems through technology transfer—helping to shape a new satellite communications service.

Lewis contact: James E. Hollansworth, (216) 433–3458
Headquarters program office: OCP

New Spread-Spectrum Technique Offers Superior Spectrum Efficiency

Under contract to NASA Lewis, Stanford Telecommunications has completed a study of a new spread-spectrum technique called code-phase-division multiple access (CPDMA) and its applicability to networking of very-small-aperture terminals (VSAT's) by satellite. Like traditional spread-spectrum techniques CPDMA provides a measure of interference protection and enables multiple users to simultaneously use the same spectrum. CPDMA is unique, however, in that all users use the same code but are each assigned a unique time offset. By this alternative, CPDMA offers superior isolation properties between users and significant improvements in spectrum use and also enables a simple despreading operation in the form of a proposed multichannel module having 255 simultaneous user outputs.

Preliminary evaluation by a combination of analytic and simulation techniques indicated that the combined effects of timing errors and channel filtering should not degrade channel performance more than 2.6 dB, in spite of the mutual interference among the many simultaneous users that is inherent with spread-spectrum techniques. In addition, there should be a significant improvement in spectral efficiency—the channel's ability to carry a specific number of bits per unit of bandwidth. For differential quadrature phase shift keying (DQPSK) this efficiency was estimated to be 8/9 for uncoded operation and 2/3 for coded operation. This is far superior to conventional spread-spectrum techniques, which might achieve ~7 percent of this value.

With these promising indicators a more detailed simulation effort was undertaken to more precisely evaluate timing methods and channel capacity, as well as to examine the possibility of rain fade alleviation through power boost of individual users in the channel. This latter feature was added when the inherent interference rejection properties of spread spectrum were recognized, as well as the possibility that the rejection might allow adjacent users with widely different power levels. Performance was evaluated by using Comdisco SPW simulation software. The more detailed simulation confirmed previous estimates of channel performance, indicating less than 2.6-dB degradation in spite of the mutual interference among 170 simultaneous users, provided that timing errors were held to less than 0.2 chip

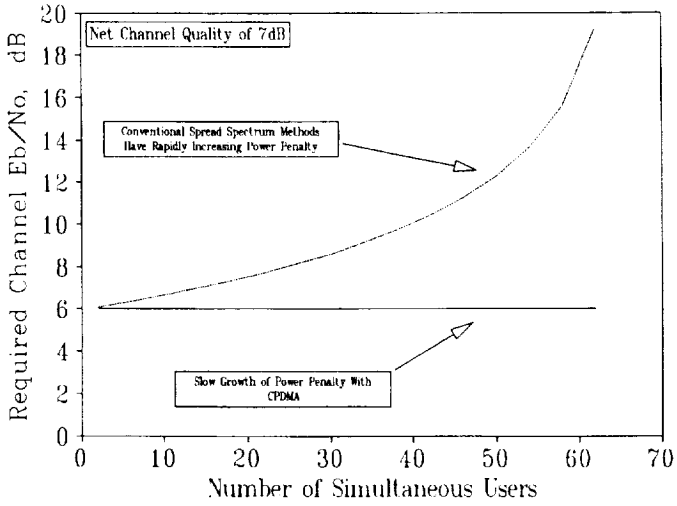

Comparative power penalty associated with spread-spectrum methods.

times. In addition, the rain fade alleviation simulation indicated that 15-dB power boosting of 10 percent of the user channels could be accommodated with 6 dB of power margin, provided that low-power channels were protected by one time slot on either side. Thus, the satellite high-power amplifier need only be oversized by a factor of 4 to accommodate a 32-times power boost of 17 simultaneous users. Timing simulations show that users would typically require about 2 sec to achieve synchronization. This suggests that a separate acquisition channel may be needed to avoid this penalty for random accessing.

A very-large-scale integrated circuit (VLSIC) correlator and its supporting mother-board have been obtained from Lincoln Laboratory to be used by NASA Lewis in testing CPDMA with 16-kbps voice.

Lewis contact: Grady H. Stevens, (216) 433-3463
Headquarters program office: OCP

Capability Developed for Measuring Angular Distribution of Scattered Electrons

Secondary electron emission properties of electron collectors are important in designing many types of electron beam devices. Ideally, an electron collector should behave like a blackbody, absorbing all incoming electrons. However, secondary electrons with a wide range of energies are emitted by collector surfaces. The behavior of

elastically scattered electrons is of particular importance for these devices because these electrons have the same energy as primary electrons and can retrace the primary trajectory back into the tube. This process can make tube operation unstable and reduce tube efficiency. Complex collector designs have evolved from attempts to maximize collector efficiency and to minimize the distortion introduced into the electron tube by scattered electrons.

Research conducted at NASA Lewis includes studies of the angular distribution of the secondary electrons with different energies from materials that are used to manufacture collectors for electron beam devices. These materials are treated to simulate conditions in a real collector. One recent development in collector technology includes the technique of treating surfaces by ion bombardment. This process drastically changes the surface morphology of the bombarded material and its secondary electron emission properties.

A special experimental apparatus has been designed and built at Lewis to measure the angular distributions of scattered electrons. The apparatus includes a small energy analyzer mounted on a rotating arm that is driven by a computer-controlled stepping motor. Measurements are made in an ultra-high-vacuum chamber. The experimental results are analyzed and curve-fitted to linear combinations of Gaussian and Lorentzian distributions. Results are then calibrated and fed into the Herrmannsfeldt computer code, and ray tracing of a particular collector design is conducted.

Currently, Lewis is investigating two kinds of surfaces: polished and ion-textured copper. The measurement of the secondary electron angular distribution will be extended to a variety of other surfaces that show promise in future collector designs.

Lewis contact: Dr. Isay L. Krainsky, (216) 433–3509
Headquarters program office: OAST

High Secondary Electron Emission Discovered From Diamond Films

NASA Lewis, at the request of the United States Navy, has been studying the secondary electron emission properties of thin diamond and diamond-like films deposited on various substrates. These films were prepared at Auburn University. During testing at Lewis it was discovered that thin diamond films deposited on molybdenum exhibit a high secondary electron emission yield σ as high as 27 (σ is the number of secondary electrons produced by each primary one). To put this value of σ in perspective, many practical devices utilize secondary emission materials with σ of less than 3.

It is difficult to underestimate the importance of a material with such a high secondary yield, particularly a material like a diamond film, which is relatively easy to manufacture and has outstanding physical properties. Possible applications include electron multiplier tubes, channeltrons, channelplates (night vision devices), secondary emission cathodes, crossed-field amplifiers, gated-emission amplifiers, and magnetrons.

Preliminary studies show that an excess of hydrogen on the surface of these films is important in keeping the value of the yield high. Such high yields of secondary electrons indicate that these thin diamond films can exhibit negative electron affinity. Initial measurements showed that the secondary yield of these films can be unstable and decay when the film is exposed to an electron beam. Nevertheless, Lewis has discovered that this process can be reversed and the yield even increased if the film is heated in vacuum or is exposed to a relatively low residual hydrogen pressure.

Although the use of large, cleaved single-crystal diamond surfaces is hardly viable for many applications, the technology is now available for growing epitaxial oriented films of diamond on suitable substrates. Various chemical vapor deposition methods of polycrystalline diamond synthesis have been developed successfully over the past 13 years. The ability to produce a diamond film with such high secondary electron emission yield may turn a new page in improving a variety of devices requiring these materials.

Lewis contact: Dr. Isay L. Krainsky, (216) 433–3509
Headquarters program office: OAST

New Computer Models Enable New Design Approaches for Traveling-Wave-Tube Circuits

An ongoing NASA Lewis in-house program has significantly improved the capability of designing traveling-wave-tube (TWT) circuits with computer simulation models. A new three-dimensional electromagnetic circuit analysis computer model has been implemented. With it TWT designers can accurately obtain circuit characteristics that previously were available only from time-consuming and expensive experimental testing. These characteristics are used as input data for a Lewis-developed, coupled-cavity TWT model. This model simulates the interaction of an electron beam with a coupled-cavity TWT circuit. Together these two models can accurately simulate the performance of conventional and advanced TWT circuit designs.

The electromagnetic circuit analysis computer model SOS (for self-optimized sector), which was developed by Mission Research Corporation, solves the full set of three-dimensional Maxwell equations. SOS has been used to analyze three different types of coupled-cavity TWT circuits. It has determined the radiofrequency (RF) phase shifts and beam-RF interaction impedances per cavity, respectively, to within 1 and 3 percent of experimental values. One circuit analyzed was that of a 29-GHz TunneLadder TWT.

This new simulation capability will enable NASA Lewis to create and explore new circuit designs that will enhance performance of TWT characteristics, such as RF output power, efficiency, frequency bandwidth, and signal distortion. Because the design procedures will not require experimental input, they can be performed much more quickly and cheaply than was previously possible.

Bibliography

Connolly, D.; and O'Malley, T.: Computer Program for Analysis of Coupled-Cavity Traveling-Wave Tubes. NASA TN D–8492, 1977.

Kory, C.; et al.: Simulation of Cold-Test Dispersion and Interaction Impedances for Coupled-Cavity Tube Slow-Wave Circuits. Presented at the 1992 IEEE International Electron Devices Meeting, San Francisco, CA, Dec. 13–16, 1992.

Wilson, J.: Revised NASA Axially Symmetric Ring Model for Coupled-Cavity Traveling-Wave Tubes. NASA TP–2675, 1987.

Lewis contact: Jeffrey D. Wilson, (216) 433–3513
Headquarters program office: OAST

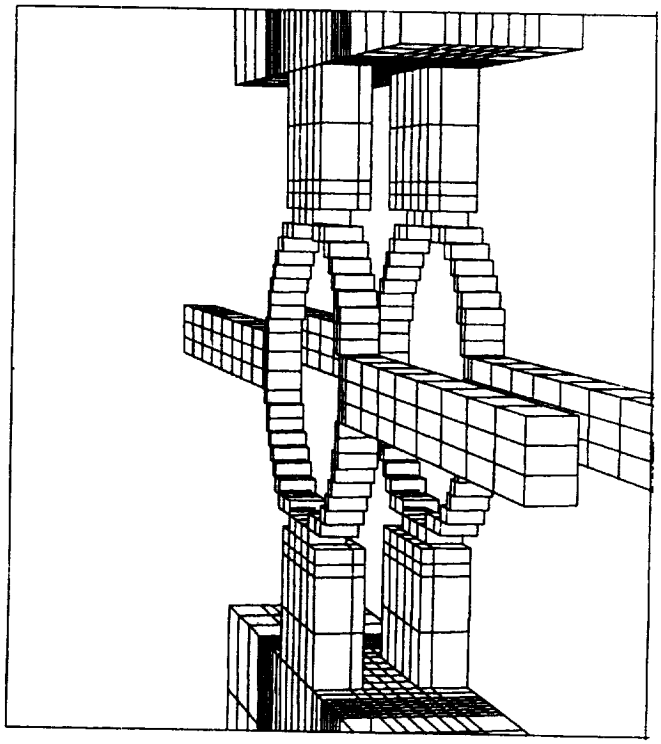

Three-dimensional grid for TunneLadder TWT.

High-Efficiency Traveling-Wave-Tube Amplifier Developed for Cassini

NASA Lewis continues to develop advanced technologies to provide high-efficiency, millimeter-wave, traveling-wave-tube amplifiers (TWTA's) for planned NASA missions to deep space. A TWTA consists of a traveling-wave tube (TWT) and a power supply or electronic power conditioner. Currently, a very efficient low-power TWTA that operates in the Ka frequency band (32 GHz) is being developed for use in the Cassini mission planned for launch to the environment of Saturn in 1997. The program is being conducted in a cooperative effort with the Electron Dynamics Division of the Hughes Aircraft Company. In coordination with the Jet Propulsion Laboratory, which is responsible for the Cassini mission, Lewis has included packaging and testing requirements that will permit the use of TWT's directly from this program as mission flight hardware and the electronic power conditioner as an

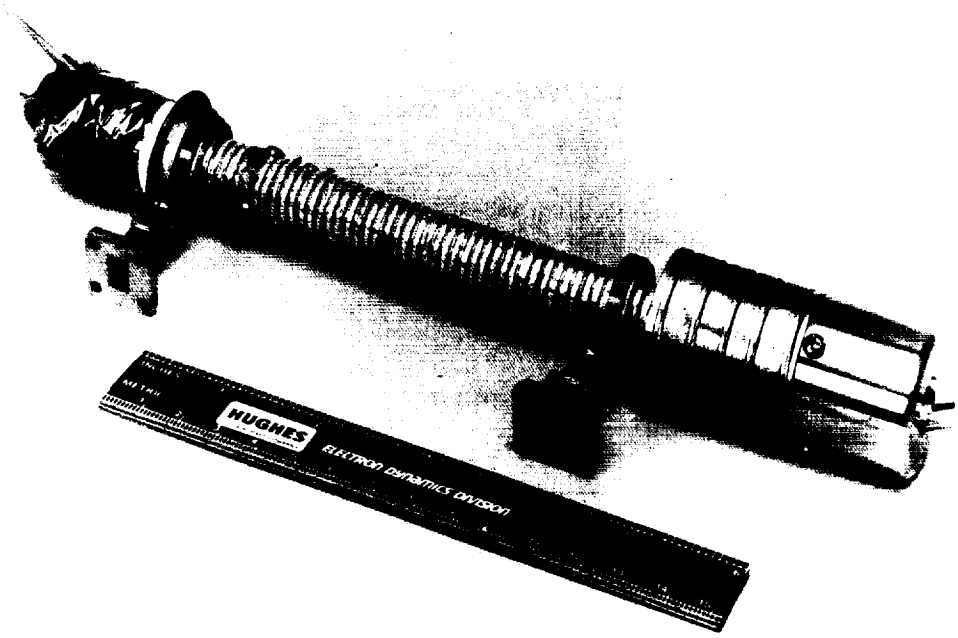

30-GHz Cassini traveling-wave tube. (The multistage depressed collector assembly is at the right end of the tube.)

immediate predecessor for the development of a flight unit.

The Cassini mission requires that the radio-frequency (RF) power output of the TWTA be 10 W, but the direct-current input power to the electronic power conditioner is limited to about 30 W. This level of performance requires more than twice the efficiency of Ka-band TWTA's presently available at this power level. Therefore, several key performance-enhancing innovations developed at Lewis have been applied in the TWTA design. A Lewis-designed advanced helix dynamic velocity taper greatly improves the interaction between the tube's electron beam and electromagnetic wave and thus enhances efficiency. Another Lewis-developed design feature, an advanced multistage depressed collector and spent-beam refocusing section, efficiently recovers spent-beam energy. To further support spent-beam energy recovery, Lewis is treating the multistage depressed collector's electrode surfaces in-house to suppress secondary electron emission. Performance-improving features introduced by Hughes include a closely spaced interaction section magnet assembly to improve beam quality and a power-conserving cathode heater design. The electron gun utilizes an isolated focus electrode for electron beam control, enabling the beam to be turned on and off with a voltage swing of only 150 V rather than full cathode potential of more than 5000 V. This feature enhances electronic power conditioner efficiency and also reduces its mass by eliminating the need for additional transformers and circuitry.

Tests with development TWT's have verified the basic dynamic velocity taper and multistage depressed collector designs. Recent test data indicate measured saturated RF output power of 10.6 W in continuous operation at the design frequency and at design conditions of 5200-V cathode potential with 14-mA helix current at 40.8-percent TWT overall efficiency. With additional scheduled design modifications a TWT efficiency of 43 percent is expected to be achieved.

This effort will conclude with the delivery of six fully functional engineering model TWT's and one engineering model electronic power conditioner that has been integrated and tested with one of the TWT's. Three of the TWT's will be selected for flight and flight backup hardware, and the

electronic power conditioner will be utilized to guide the final development by JPL of a flight version.

Bibliography

Curren, A.; et al.: A Low-Power, High Efficiency Ka-Band TWTA. AIAA Paper 92-1822, 1992.

Lewis contact: Arthur N. Curren, (216) 433-3519
Headquarters program office: OAST

Integration of Peeled-Off Semiconductor Demonstrated

In the past decade gallium arsenide (GaAs)-based technology, including complex multilayer structures, has been developed for a wide range of high-speed electronics for both analog and digital applications. For analog applications the frequency range above 20 GHz is completely dominated at present by GaAs-based circuits, mainly receivers and transmitters. These frequencies will be used by all advanced radars and NASA deep space and commercial communications systems. In all these applications GaAs multilayer devices are fabricated on a semi-insulating GaAs substrate and integrated into a complete circuit. However, the GaAs substrate has several serious problems (e.g., very low thermal conductivity limiting the circuit's density and power dissipation; losses of the electromagnetic signal at high frequencies, and relatively fragile and expensive material).

In recent research at NASA Lewis a layer of aluminum arsenide (AlAs) was added just above the substrate during the growth of the multilayer structures needed for the GaAs-based devices. After the devices were fabricated, the AlAs layer was used as a parting layer (i.e., an acid was used to chemically etch this layer). The whole multilayer structure needed for the device applications was peeled from the GaAs substrate undamaged and was transferred to another substrate. This process, called epitaxial lift-off, allows the substrate to be optimized for a particular application. Several devices were transferred to sapphire, a high-thermal-conductivity material, to achieve higher thermal dissipation. No degradation in the device performance was encountered in all the transfers performed.

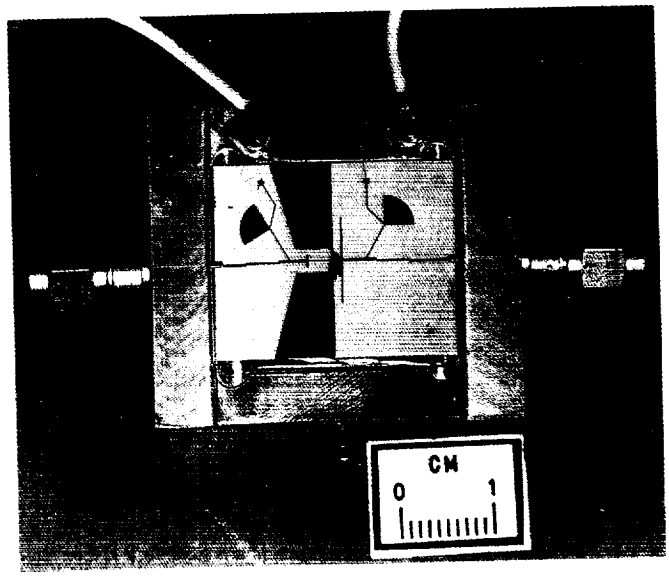

Amplifier in test fixture.

In the most important result of this work the peeled-off device was transferred to a low-loss substrate (alumina) and integrated into a one-stage amplifier without the use of bond wires. This was the first successful integration of a peeled-off device. The amplifier showed a 8.5-dB gain at 9.3 GHz, which compares very well with the design goals of 12-dB gain at 9.2 GHz. The return loss was −12 dB.

This process may have a variety of applications in optimizing substrates to requirements of the microwave circuit designers. NASA Lewis is now investigating a high-dielectric-constant substrate (vs the regular GaAs substrate) that will miniaturize the complete circuit.

Lewis contact: Dr. Samuel A. Alterovitz, (216) 433-3517
Headquarters program office: OAST

Ka-Band 64-Element Superconducting Array Demonstrated

When microstrip antenna designs are extended to microwave frequencies above 30 GHz, certain difficulties become apparent. Offsetting losses due to surface waves and radiation means drastically reducing circuit dimensions. The required narrower lines have high resistive losses when

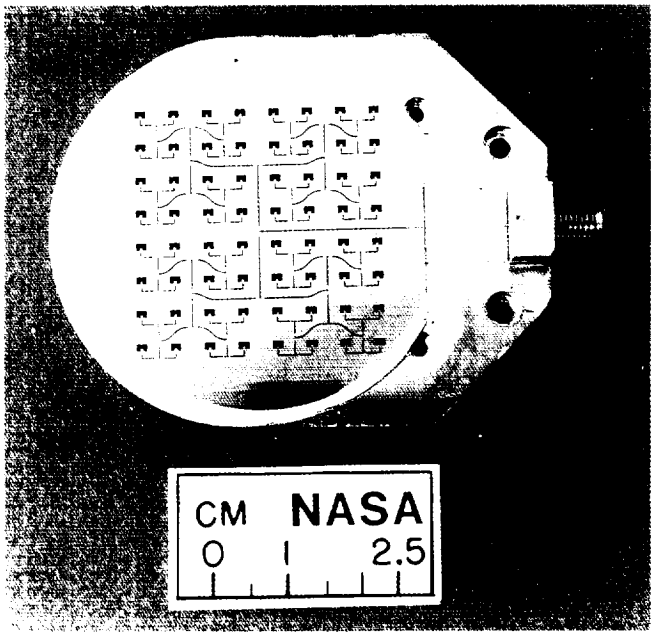

64-Element (consisting of 8 × 8 patches) superconducting antenna array along with corporate feed network required to distribute signal to all patch elements.

conventional metals are used. These losses can be reduced by using high-temperature-superconducting (HTS) materials to form the feed networks for high-gain, phased-array antennas. NASA Lewis has investigated the benefits of applying high-temperature superconductivity to new areas of microwave circuit and system design where performance is limited by passive (i.e., normal metal) circuit loss. In this case the loss is primarily in the feed network of the antenna.

In order to demonstrate these benefits, two 64-element, 30-GHz, microstrip superconducting antenna arrays with corporate feed networks were developed. One array was fabricated from gold film, and a second had a thallium film high-temperature superconductor. Both antennas used gold ground planes deposited on the reverse side of a lanthanum aluminate substrate. Gain and radiation patterns were measured for both antennas at room temperature and at cryogenic temperatures. Observations agreed well with simple models for loss and microwave beam width, with a gain on the boresight of 20.3 dB and a beam width of 15° for the superconducting antenna. The HTS antenna displayed an overall gain approximately 2 dB greater than that of the equivalent gold circuit at the same temperature.

Ball Aerospace Corporation, along with Superconducting Technologies Inc., under contract to NASA Lewis, designed and fabricated the two 64-element arrays. Final testing of the two antenna arrays was performed at NASA Lewis.

The successful implementation of HTS circuits in this relatively low-gain antenna supports the position that high-gain millimeterwave antennas would benefit from using the new superconductors. For example, a larger array, with a directivity of 40 dB at this frequency, would exhibit a feed network loss of 25 dB if implemented in copper. The identical circuitry, fabricated from an HTS film, would have a loss of only 3 dB.

Lewis contact: Dr. Kul Bhasin, (216) 433-3676
Headquarters program office: OAST

High-Temperature-Superconducting Space Experiment Will Use Lewis-Designed Receiver

High-temperature superconductivity promises miniaturization and improved sensitivity for microwave receivers, perhaps to frequencies as high as 60 GHz, because of extremely small signal attenuation. The potential to operate such subsystems at high temperatures, relative to conventional superconductors, will enable practical implementation of superconductor technology. Space will be an attractive arena for its debut. Prototype high-performance and/or miniaturized bandpass filters, phase shifters, local oscillators, and amplifiers have already been demonstrated. Hence, microwave applications of these materials are no longer considered speculative.

NASA Lewis, in collaboration with the Jet Propulsion Laboratory, is designing a hybrid superconducting/semiconducting microwave receiver for the Naval Research Laboratory's (NRL's) High-Temperature Superconductivity Space Experiment (HTSSE–II), to be launched in 1996. NRL's host satellite will perform radiofrequency testing of a limited number of superconducting subsystems or advanced components in space. The ultimate goal is early demonstration of this technology under the severe design restrictions imposed by the space environment to accelerate development of the technology from proof-of-concept to flight-qualified hardware. It is hoped that this overall effort will assist U.S. industry to assume a leadership role in worldwide commercialization of superconductivity and that the

manyfold benefits promised by superconductivity will be realized expeditiously.

The low-noise (sensitive) receiver that is under development filters and amplifies a 7.25-GHz radiofrequency signal and downconverts it to a 1-GHz intermediate-frequency signal for further processing. The Jet Propulsion Laboratory is developing the preselect filter and low-noise amplifier sections of the receiver. NASA Lewis is designing, fabricating, and testing a low-phase-noise, superconducting-ring-resonator-stabilized local oscillator (LO) and a cryogenic mixer that operates with a very low LO power level. The 8.4-GHz LO uses a high "Q" superconducting microstrip ring to stabilize the field-effect-transistor oscillator and provide low phase noise (i.e., excellent short-term stability). Because the LO is inherently an inefficient device, the mixer is designed to operate with as little LO drive power as possible while providing a minimum of conversion loss. The total heat load placed on the cryogenic cooler by all receiver components is expected to be less that 75 mW. A prototype receiver will be delivered to NRL in January 1993.

Lewis contacts: Dr. Kul Bhasin, (216) 433-3676; Robert R. Romanofsky, (216) 433-3507
Headquarters program office: OAST

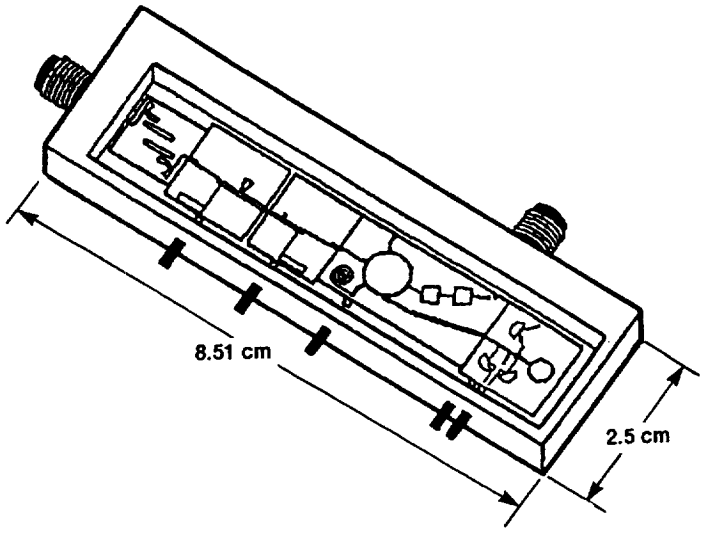

Example layout of proposed superconducting/semiconducting 7.25-GHz receiver.

Monolithic Optical Receiver Created on a Chip

Future communications applications require antenna systems with electronic steering and multifrequency and multibeam capabilities. Much effort is being directed to developing arrays and array feeds at Ku band, Ka band, and higher frequencies that use monolithic microwave integrated circuits (MMIC's) for amplitude and phase control. The close spacing of phased-array elements required at these frequencies can only be achieved by developing MMIC integration technologies that minimize both the space used per element and the number of signal connections to each element.

Using fiber optic links for distributing control information to MMIC phase shifters and amplifiers is a key integration technology for large, high-frequency MMIC arrays. The broad fiber bandwidth allows multiple control lines to be multiplexed on a single fiber, reducing the number of interconnections. The mechanical flexibility of the optical fiber supports simpler, space-conservative array configurations. Fiber links eliminate much of the weight and volume associated with conventional signal distribution media, such as coaxial cable or other metal conductors. Optical fiber has extremely low crosstalk and electromagnetic interference.

The key component of a fiber optic link is the optical receiver. This type of optoelectronic interface circuit (OEIC) converts the incoming optical signal (light) to an electronic signal (radio-frequency). Typically, it consists of a photodetector, a low-noise amplifier, and a demultiplexer circuit. Ideally, these circuits are monolithically integrated on a single gallium arsenide substrate, creating a monolithic optical receiver on a chip.

In 1989 a hybrid OEIC device was developed by Honeywell for NASA Lewis, proving the feasibility of integrating a photodetector and a radio-frequency amplifier in a single monolithic circuit. This achievement was recognized with an R&D 100 award. Three years of subsequent development by Lewis and Honeywell resulted in a system-ready monolithic chip with a demultiplexer and added advanced digital capabilities, including built-in clock recovery and addressability. The bandwidth is broad, with the data rate variable from 10 to 400 Mbps. The new chip redefines the state of the art for optical data link applications. Honeywell now offers the fully

monolithic, foundry-compatible circuit as a commercial product (part number, OEIC Rx–400) and is marketing it for a variety of optical fiber data link applications. In addition to optical control of MMIC arrays for commercial communications systems and NASA missions, the OEIC will support spacecraft and aircraft optical signal distribution systems, including robotics.

OEIC devices delivered by Honeywell will be integrated and demonstrated in a optically controlled phased array at NASA Lewis in early fiscal 1993. The next challenge, already being addressed at Lewis, is to develop a high-frequency (K/Ka band) monolithic OEIC that will enable distribution of radiofrequency signals through optical fiber links.

Lewis contact: Richard R. Kunath, (216) 433–3490
Headquarters program office: OAST

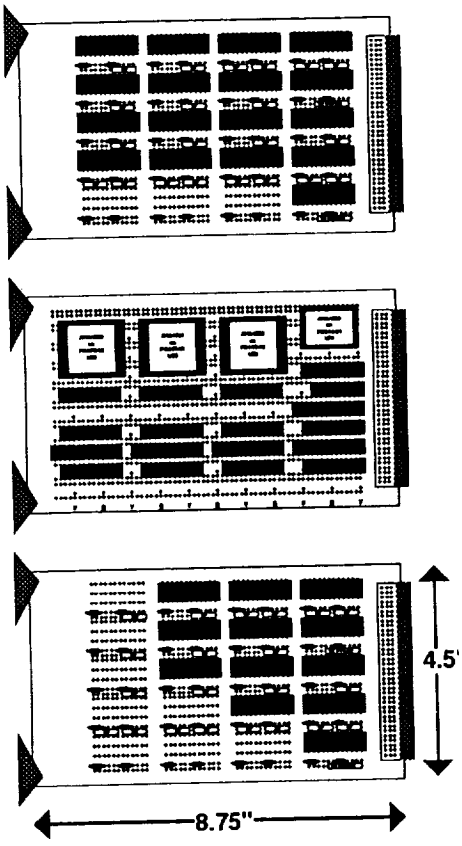

Board layout of least-reliable-bits codec.

Least-Reliable-Bits Codec Demonstrated

One measure of the overall efficiency of a satellite communications system is the number of users that can access the satellite at any given time. In the domain of digital communications this efficiency is directly related to the number of bits per second the satellite can accommodate. Thus, given that all other parameters remain the same, any method that increases the number of bits per second will directly increase the efficiency. For example, a doubling of the number of bits per second doubles the number of users that can access the satellite. This would in turn double the revenue the satellite could earn or halve the cost per user in a commercial application. Alternatively, it would double the amount of science data acquired through NASA systems, such as the Tracking and Data Relay Satellite System, Space Station *Freedom*, the Earth Observing System, and other space platforms.

NASA Lewis' experience in advanced modulation and coding has enabled the accelerated in-house development of a low-cost, high-performance coding scheme called least-reliable-bits coding (LRBC) that can more than double a satellite's capacity. Because its architecture is less complex, LRBC is applicable to data, voice, and video communications at aggregate rates of several hundred megabits per second. It uses the NASA Consultative Committee on Space Data Systems (CCSDS) standard Reed-Solomon error-correcting code on the least reliable bit in a specially mapped 8-phase-shift-keyed (8PSK) digital modulation format. Soft-decision multistage decoding is used to make decisions on unprotected bits through corrections made with the CCSDS compatible decoder.

The performance of LRBC when matched to the 8PSK digital modulation format has been extensively studied at Lewis through analysis and computer simulation. The results indicate that, at a bit error rate of 1×10^{-6}, LRBC offers 2.87 times the capacity of a traditional modulation format, such as binary phase shift keying (BPSK), while requiring approximately 25 percent less transmitted power. A hardware prototype has been implemented that exhibits high-data-rate operation at up to 225 Mbps with low-complexity hardware consisting of only 51 digital integrated circuits. The already completed hardware will be integrated and tested in the fall of 1993 with the

scheduled delivery of a programmable digital modem being developed for Lewis by Comsat Laboratories.

Bibliography

Vanderaar, M.; Budinger, J.; and Wagner, P. : Least Reliable Bits Coding (LRBC) for High Data Rate Satellite Communications. AIAA Paper 92–1868, 1992. (Also NASA TM–106531.)

Lewis contact: James M. Budinger, (216) 433–3496
Headquarters program office: OAST

Fault-Tolerant Onboard Switching Demonstration Testbed Developed for Communications Satellites

Future meshed, very-small-aperture terminal (VSAT) satellite communications systems will provide direct-to-user commercial communications services for the transmission of data, voice, facsimile, and teleconferencing information. These meshed VSAT systems will enhance current communications services as well as enable new services. Through an in-house effort, aided by multiple study contracts and inputs from industry, NASA Lewis has developed an architecture of the meshed VSAT satellite network and continues to study and develop critical enabling subsystems of this architecture. One such enabling subsystem is an information switching processor (ISP) that switches and routes user data onboard the satellite. Fault tolerance is a critical issue in the development of the ISP circuitry to provide and maintain reliable communications services. In order to evaluate candidate circuit and packet-switched architectures and to demonstrate fault-tolerance techniques, NASA Lewis has developed an in-house baseband switching demonstration testbed.

The switching demonstration testbed consists of three elements: a baseband switch, fault-tolerant memory, and special test equipment. A 4 × 4 single-stage memory switch was chosen for the

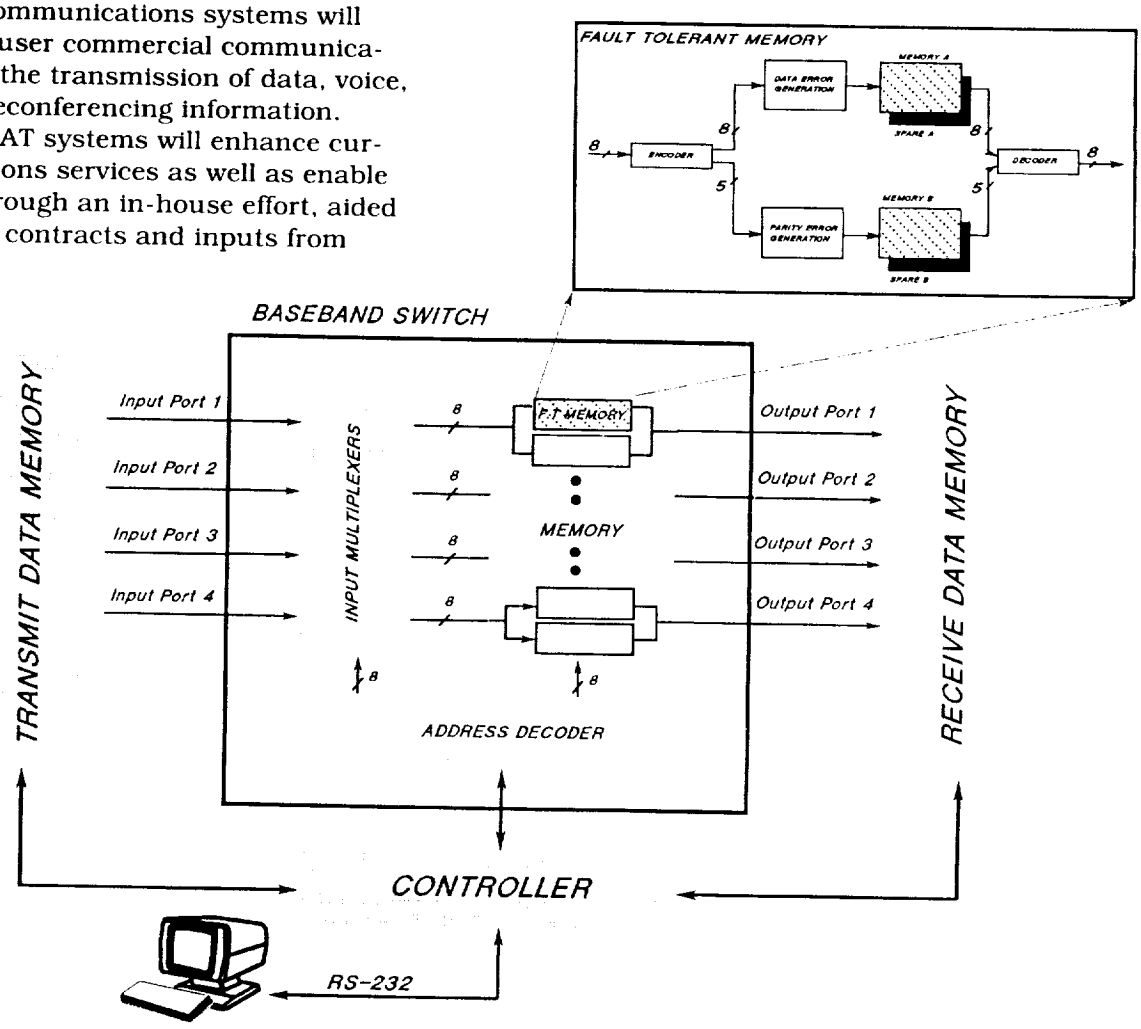

Switching demonstration testbed containing a 4 x 4 single-stage memory with fault-tolerant memory.

switching demonstration testbed because it has simple architecture, a low memory requirement, and ability to support both circuit and the packet switching. The switch contains four time-division multiplexed (TDM) input ports and four TDM output ports. Switching is performed by multiplexing data from each input port onto a TDM bus and then storing the data into the correct memory location according to the destination downlink beam and the time slot. The memory is read sequentially on the output side. The baseband switch supports both point-to-point and broadcast connections.

The baseband switch receives its input data from the special test equipment (STE) and sends its output data back to the STE for verification of proper routing. The STE is also responsible for control and operation of the switching testbed and for reporting the system status.

One memory component in the baseband switch is protected with fault tolerance. The fault-tolerant memory protects the data by using a Hamming error correction code capable of correcting one-bit errors and identifying two-bit errors. In order to simulate faults occurring in the baseband switch memory, errors are induced at the input to the memories in either the data bits or the parity bits. When two or more bit errors are detected at the memory output, a memory failure has occurred, and the circuit automatically reconfigures to a redundant memory device.

This testbed has been utilized to successfully demonstrate fundamental satellite baseband switching architectures and fault-tolerance techniques. Lewis is currently developing the conceptual design for candidate baseband switching architectures for the information switching processor. Once the best switch architecture is selected, Lewis will develop a proof-of-concept information switching processor that will include the baseband switching system and onboard controlling processors. The proof-of-concept model, which will be designed and built in-house, will include advanced fault-tolerant components where necessary. The ISP architecture will ultimately be demonstrated in a meshed VSAT satellite network simulation.

Bibliography

Shalkhauser, M.; et al.: Fault-Tolerant Onboard Digital Information Switching and Routing for Communications Satellites. To be published as NASA TM, 1993.

Ivancic, W.; et al.: Destination-Directed Packet Switch Architecture for a Geostationary Communications Satellite Network. Presented at the World Space 43rd Congress, International Astronautical Federation, IAF Paper 92-0413, Sept. 1992.

Lewis contacts: Mary Jo Shalkhauser, (216) 433-3455; William D. Ivancic, (216) 433-3494
Headquarters program office: OAST

Hi-LITE Prototype Modem Nears Completion

Project Hi-LITE (for high-speed laser integrated terminal electronics) is the communication electronics portion of a free-space optical communications program led by NASA Goddard Space Flight Center. The three racks of Hi-LITE system electronics comprise modulators-demodulators (modems), sources and sinks for both video and test data, interface and test equipment, and a control computer. Signals between the modems will be transmitted optically through laser links being developed by Goddard.

The prototype communications electronics (PCE) modem, constructed at NASA Lewis with discrete high-speed components mounted on approximately 15 special circuit boards and housed in three chassis, is expected to be completed by the end of 1992. These chassis (PCE transmitting and PCE receiving) are mounted in the electronics rack.

The PCE will provide proof of concept of the design and serve as a forerunner to a demonstration model that will use application-specific integrated circuit technology to incorporate the attributes required for flight-qualifiable size, mass, and power consumption. Ultimately, the Hi-LITE system will include two demonstration model modems.

The modems have full duplex capability, allowing them to communicate with each other in both directions simultaneously. At any given time, one or both modems may process one 650-megabit-per second (Mbps) data source or some combination (data or video) of two 325-Mbps data sources. Transmitting 650 million bits per second is equivalent to transmitting 8.9 volumes of the Encyclopedia Britannica every second!

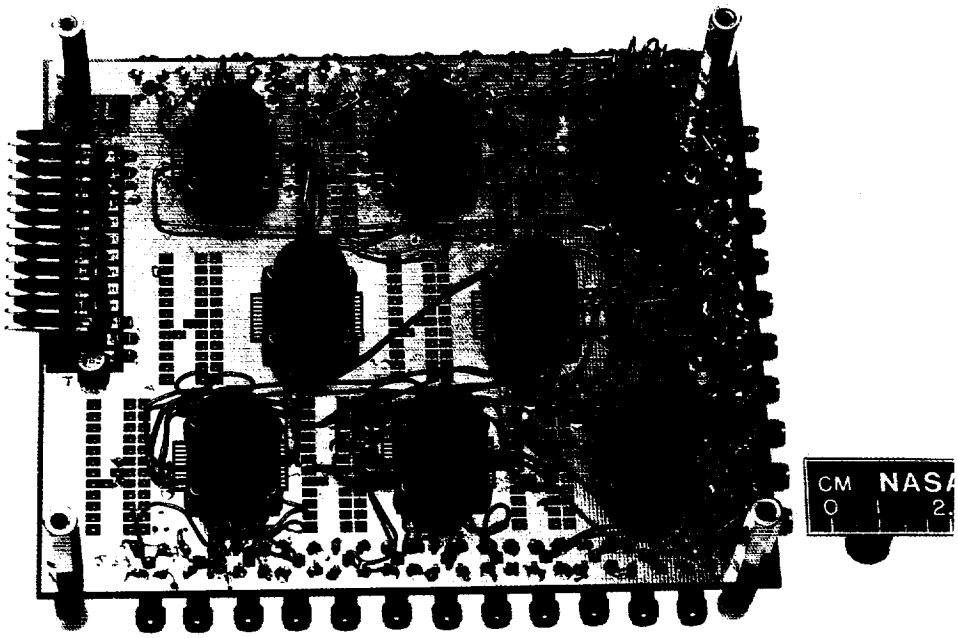

Hi-LITE digital circuit board.

At these data rates, digital logic design takes on aspects of radiofrequency circuit design, where interconnection of signals is subject to transmission line considerations. Coaxial cables, terminations, multiplanar circuit boards, and surface-mount components must be employed. Signal propagation delay is of extreme importance. Every centimeter of coaxial cable, corresponding to 50 picoseconds (trillionths of a second) of signal delay, must be taken into consideration in the design. In addition, the inherent inductance and capacitance associated with cables and components drastically affect signal quality.

In order to combat these effects, special circuit boards are used for mounting the gallium arsenide (GaAs) digital integrated circuits, chip resistors, chip capacitors, and semi-rigid coaxial cables in much of the Hi-LITE subsystem fabrication. About half of the boards for the PCE modem were fabricated in-house from these boards.

Lewis' Hi-LITE Project has conducted three major design reviews for Goddard and supported a peer review of the optical program at Goddard. Some significant changes in performance requirements have necessitated rather extensive design modifications. Project Hi-LITE has met these challenges and has a projected delivery date to Goddard of December 1993.

Lewis contact: Lawrence A. Nagy, (216) 433-3453
Headquarters program office: OAST

First 300-Mbps BCH Codec Developed on Single Chip

Future processing satellites with high-data-rate throughput, multiple-beam time- or frequency-division multiple access (TDMA/FDMA) hybrid uplinks, and multiple-beam, high-data-rate time-division-multiplexed (TDM) downlinks will require high-speed burst data encoding, decoding, and error correction. Planned NASA missions such as the evolutionary Space Station will require high-reliability voice, data, and video communications with several hundred megabits per second of throughput. High-performance coding can reduce the transmitting power requirements and the antenna and radiofrequency subsystems' size, weight, and costs for a given bit-error-rate performance and bandwidth conservation requirement.

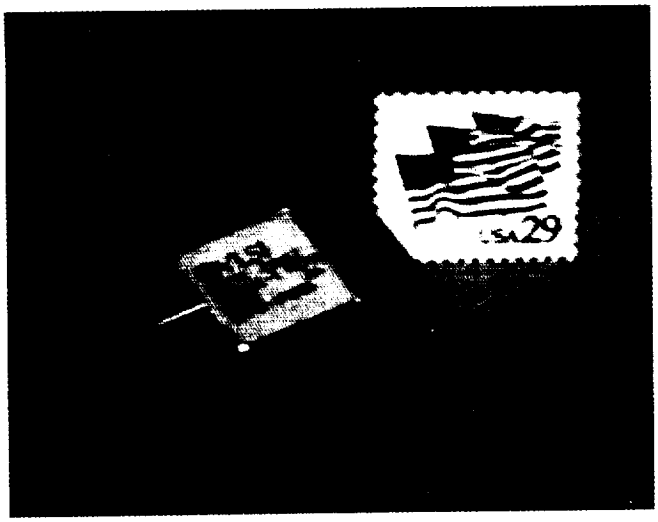

Application-specific integrated circuit BCH codec.

Coding may also be used to adaptively compensate for rain attenuation on a burst-by-burst basis. Further advancement of the implementation of flexible, high-speed coding technology is required to enhance the performance and efficiency of existing and future communications systems and to reduce both the development risk and costs for Government and commercial space communications applications.

Under a contract with Harris' Government Communications Systems Division, NASA Lewis has developed a coder/decoder (codec) application-specific integrated circuit (ASIC) with associated test and demonstration hardware. Testing of the contract hardware deliverable has been completed at Harris' facility, and they plan to demonstrate the ASIC's capability to their other internal divisions. This will aid in maximizing technology transfer to other product lines within Harris and could lead to implementation of this product as one of Harris' standard "off-the-shelf" commercial offerings.

The ASIC is a low-power, complementary metal-oxide semiconductor, triple-error-correcting Bose-Chaudhuri-Hocquenghem (BCH) block codec capable of data rates from DC to 300 Mbps. The device can accommodate a data source of 1, 2, 4, or 8 bits at a time. Some other unique features of the chip include the encoder and decoder on a single chip, up to 4 dB of hard-decision coding gain at 10^{-8} bit error rate, bursted and continuous data format capability, and flexible accommodation of various data rates, code rates, and modulation formats. These features make the chip attractive for a variety of applications in present and future space and ground segments of communications systems, including terrestrial links, compressed high-definition television data, or just about any data application up to 300 Mbps that could utilize block coding. Lewis has immediate application plans for the codec, including the multichannel-error-decoder project and the least-reliable-bit coding project.

A preliminary product data sheet has been developed by Harris for the ASIC. The ASIC chip will be available in a 132-lead pin-grid-array commercial packaging format.

Lewis contact: Rober E. Jones, (216) 433-3457
Headquarters program office: OAST

High-Efficiency Gallium Arsenide Modules May Improve SARSAT Distress Beacons

The Search and Rescue Satellite-Aided Tracking (SARSAT) Program has been credited with the successful rescue of more than 1700 persons worldwide since the first satellite carrying the SARSAT package was launched in 1982. The SARSAT system currently comprises four Russian and U.S. satellites that continuously monitor several international distress frequencies. All four satellites are polar orbiting and accurately predict position location by using the Doppler shift of a distress beacon's transmitted frequency as the satellite passes over the beacon's area. The internationally allocated emergency distress frequency assignment of 406.025 MHz, coupled with technical performance specifications for 406-MHz beacons, significantly improves the accuracy of position location prediction, saving precious time for rescue teams to arrive.

The 406-MHz SARSAT beacon transmitters are self-contained, battery-powered units containing a 5-W transmitter, a digital controller, a bi-phase modulator, and a high-stability amplifier. Only a few companies currently manufacture 406-MHz beacons. Several technical barriers impede the availability of low-cost, highly efficient beacons suitable for the pleasure boating and general aviation market. One of these barriers is the availability of small, inexpensive and safe

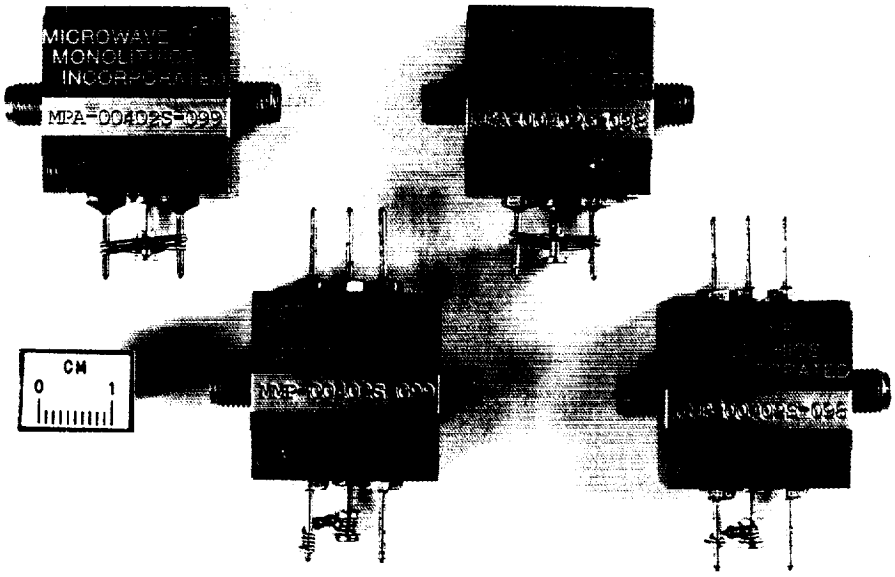

High-efficiency gallium arsenide modules.

batteries with adequate capacity to power the beacon at low temperatures.

NASA, under a contract with Microwave Monolithics, Inc., developed a highly efficient gallium arsenide monolithic-integrated-circuit (MIC) amplifier and modulator that will reduce the size and change the type of batteries required for beacons. Present high-capacity lithium batteries—which under certain circumstances pose a hazard—may be replaced by less expensive nonhazardous types. An additional benefit is frequency stability improvement due to reduced heat dissipation. The development of the MIC-based bi-phase modulator improved the phase accuracy and manufacture of the modulator and lowered the maintenance costs by eliminating the need for periodic phase adjustments.

Lewis contact: Michael A. Cauley, (216) 433-3483
Headquarters program office: OAST

Unique High-Data-Rate Terminal Developed

In support of NASA's Advanced Communications Technology Satellite (ACTS) Program, NASA Lewis has developed a high-burst-rate link evaluation terminal (HBR LET). This unique and versatile experimental Earth terminal will support various ACTS technology experiments.

The terminal is a critical element in the ACTS Experiments Program because it provides the unique capability to evaluate the operation of certain ACTS systems, such as the microwave switch matrix and the adaptive uplink power control. In addition to component and system characterization, the terminal also has an experimenter interface, which will permit users to connect various modulators and demodulators for use in specific applications experiments.

The entire terminal can be operated manually or under computer control. Software to control the LET and to assist end users is being developed and will be delivered with the terminal to the ACTS Project. The software employs artificial intelligence techniques to provide user-friendly assistance in operating the terminal, documentation about the terminal, and an intelligent tutor to train users on the system.

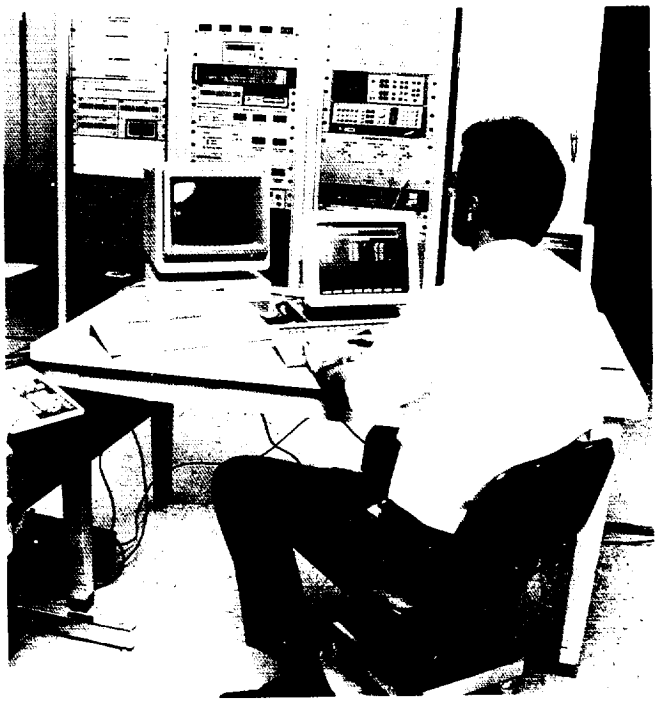

Engineer at controls of link evaluation terminal.

The terminal completed systems testing and was shipped to General Electric in Princeton, New Jersey, for testing with the ACTS spacecraft. This testing was completed successfully. The terminal will be returned to Lewis for installation at its permanent location.

Lewis contact: Gerald J. Chomos, (216) 433–3485
Headquarters program office: OAST

30-GHz Power Amplifier Being Developed for Earth Terminals

Successful development of a low-cost, 30-GHz Earth terminal power amplifier will provide a critical component for NASA's objective of developing low-cost Earth terminals.

NASA Lewis is developing a solid-state power amplifier that can be produced at one-third to one-half the cost of a traveling-wave tube and will make this technology available to U.S. manufacturers of commercial Earth terminals. The salient features of the amplifier are a power output of 10 W, a frequency from 29 to 30 GHz, an efficiency greater than 30 percent, and a gain of 40 dB.

A contract for this effort has been awarded to Avantek Incorporated in Santa Clara, California. During the past year Avantek has concentrated on developing 30-GHz field-effect transistors. The best result to date has been a device that develops 400 mW of output power at 28-percent efficiency. Avantek is also working on developing thin-film combining techniques.

Lewis contact: Gerald J. Chomos, (216) 433–3485
Headquarters program office: OSSA

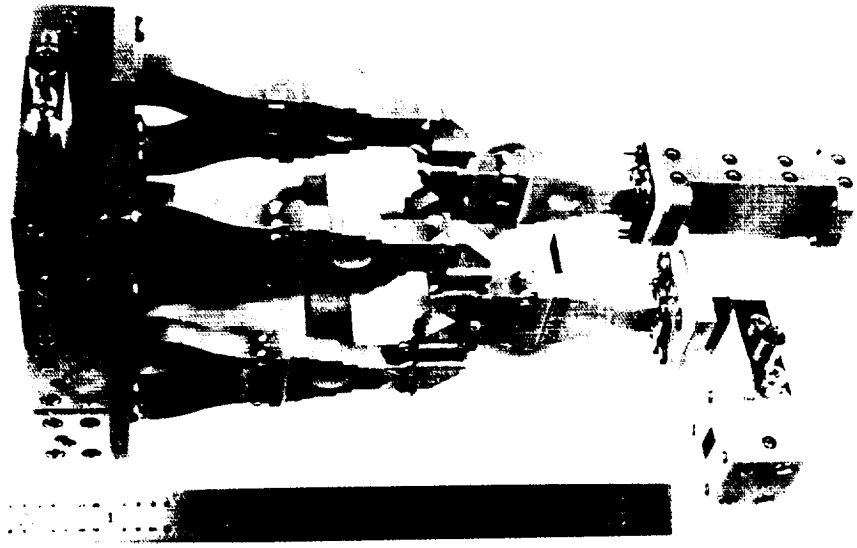

30-GHz Earth terminal power amplifier.

Space Flight Systems

Space Experiments

GaAS Crystal Growth Experiment Flies Again

Gallium arsenide (GaAs) substrates and devices are considered a leading contender for a new generation of electronics technology offering greater speed and durability than existing silicon-based systems. High-quality GaAs crystals are difficult to produce and the commercial crystal growth of this material is of significant interest. The effect of gravity-induced, buoyancy-driven convection on the types and distribution of defects and dopants in GaAs is the focus of a study begun by GTE Laboratories, Inc., of Waltham, Massachusetts, and now continued at the Lewis Research Center. Through the course of the project, the work has been cost shared by GTE, the Air Force Materials Laboratory, and NASA. NASA manages the project, has implemented numerical modeling of the furnace and fluid flow, and will characterize selected samples from the study. The addition of the principal investigator, Dr. David Matthiesen, to the Lewis staff as a support contractor now brings the primary science program to the laboratory.

The study, as proposed by the originators (Dr. James Kafalas and Dr. Brian Ditchek of GTE Laboratories, Inc.), consists of a systematic investigation of how buoyancy-driven fluid flow affects GaAs crystal growth. It includes GaAs crystal growth in the microgravity environment of the Space Shuttle. The program also involves a comparative study of crystal growth under a variety of Earth-based conditions with variable orientation (to change the direction of the gravity vector) and applied magnetic field (to partially damp flow). Earth-based growth will be performed under stabilizing as well as destabilizing temperature gradients. The boules grown in space and on Earth will be fully characterized to correlate the degree of convection with the distribution of impurities. Both macro- and microsegregation of dopant will be determined.

In June 1991 the experiment was flown on the Space Shuttle *Columbia* as part of STS–40. That experiment was a qualified success as the hardware, software, electronics, and control routines all performed as designed. However, there was insufficient power in the primary battery supply to complete the two regrowth experiments as planned in the dual-furnace payload. The shortfall was determined to be caused primarily by the reduced temperature of the batteries at the start of the second experiment. The boule from the successful experiment has been sectioned and analyzed during the past year.

In March 1992 the refurbished payload was reflown on the Space Shuttle *Atlantis* as part of STS–45. This mission was configured to include a single sample. The furnace again successfully completed the regrowth (although the presence of desired interface demarcation indicators has not been confirmed to date). Sample characterization will continue during the coming year with ongoing chemical and electrical measurements and correlation of measured data with theoretical and numerical predictions.

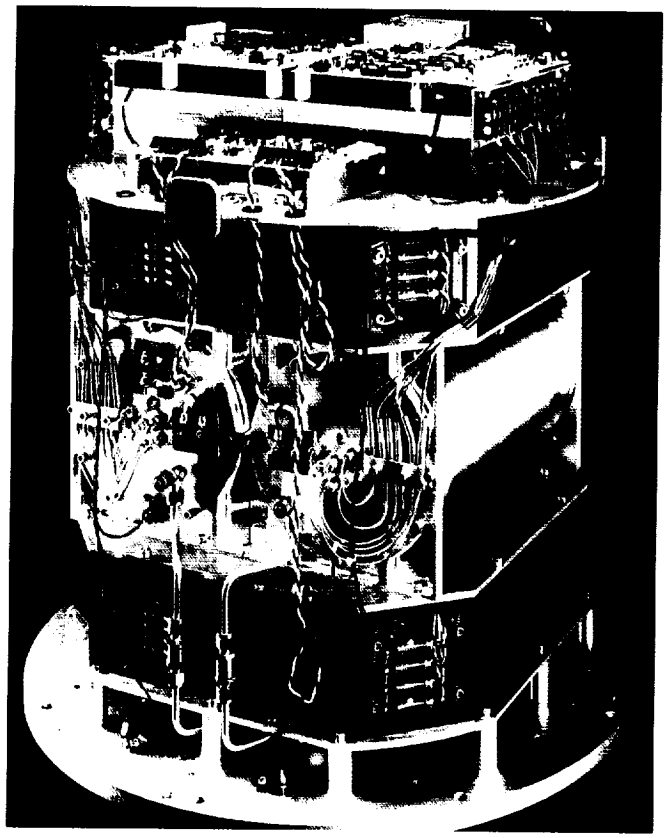

Self-contained dual furnace payload for GaAs crystal growth experment.

Bibliography

Matthiesen, D.: Growth of Electronic Materials in Microgravity. AIAA/IKI Microgravity Science Symposium, 1st, Moscow, USSR; Proceedings, AIAA, Washington, DC, 1991, pp. 111–118.

Matthiesen, D.; and Bellows, A.: Microgravity Acceleration Measurements Aboard the GAS Bridge during STS–40. AIAA Paper 92–0355, 1992.

Matthiesen, D.M.; et al.: Interface Demarcation in GaAs by Current Pulsing. AIAA Paper 90–0319, 1990.

Steiner, B.; et al.: High Resolution Synchrotron X-Radiation Diffraction Imaging of Crystals Grown in Microgravity and Closely Related Terrestrial Crystals. J. Res. Nat. Inst. Stand. Technol., vol. 96, May-June 1991, pp. 305–331.

Lewis contact: Dr. Richard W. Lauver, (216) 433–2860
Headquarters program office: OSSA

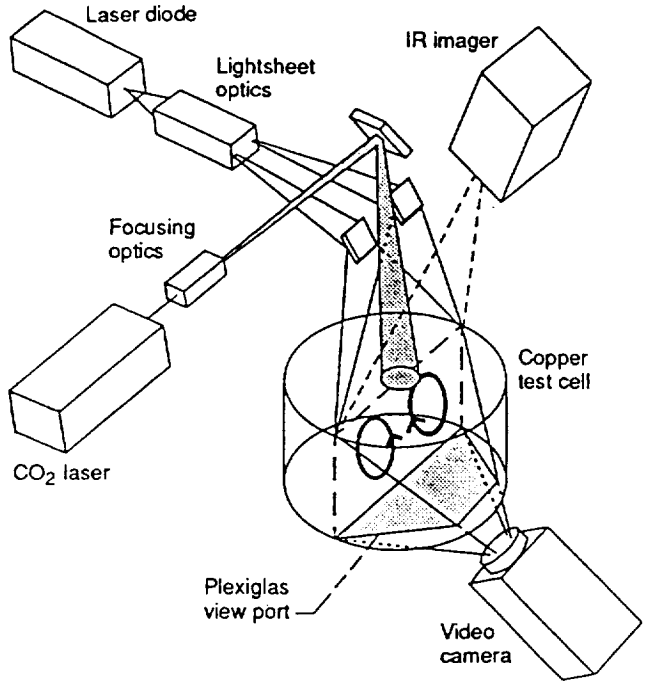

Optics module for STDCE.

Surface-Tension-Driven Convection Experiment Proves Theory

Materials processing that involves solidification and crystal growth is generally expected to be dramatically improved in the microgravity environment of space because natural convection and buoyancy effects are eliminated. However, convection currents due to surface tension forces are still present. These thermocapillary flows result from the fluid motions generated by the surface-tractive force that is caused by surface tension variations due to the temperature gradient along the free surface.

In order to complete an understanding of the physical process and develop an accurate numerical model, experimental data must be obtained in an extended low-gravity environment. Therefore, the Surface-Tension-Driven Convection Experiment (STDCE) was proposed by investigators from Case Western Reserve University (CWRU) for the Space Shuttle.

The design and development of the STDCE for the United States Microgravity Laboratory (USML–1) mission in June 1992 was an in-house project at NASA Lewis. Major components were developed under contract: an infrared thermal imager for mapping the surface temperature gradients, a carbon dioxide laser for surface heating, and a laser diode system for illumination. These components were integrated with the mechanical, optical, electrical, electronic, and structural systems that were designed, fabricated, and tested at Lewis.

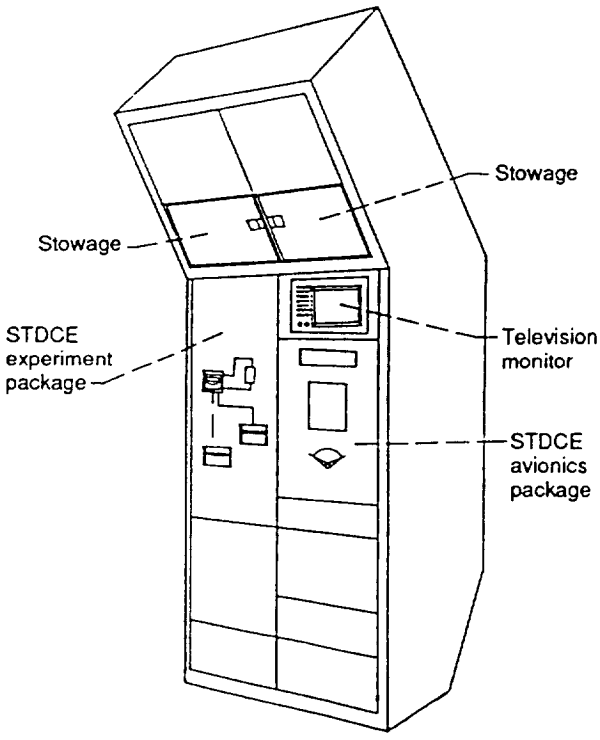

STDCE experiment package in Spacelab rack.

The basis of STDCE is a copper test cell, 4 in. in diameter by 2 in. deep, filled on orbit with silicone oil to provide both a flat and a curved free surface. It can be centrally heated either externally by a carbon dioxide laser or internally by an immersion heater. The cross section is illuminated by a 1-mm-thick sheet of light, which scatters from small aluminum oxide particles mixed into the oil, allowing observation of the axisymmetric flow velocities.

A significant milestone was achieved with the successful completion of 38 tests of STDCE, operated for the first time in orbit, during the USML–1 mission. A total of 12.5 hours of thermocapillary flow data were obtained. The flight hardware provided better video data than expected, some of which was downlinked for observation by the scientists and engineers. Preliminary evaluation corroborates the CWRU theory that oscillatory flows require lower viscosity liquids and smaller test chambers. Operations were controlled by a team of Lewis engineers located in the Payload Operations Control Center at NASA Marshall Space Flight Center. Operations were monitored at Lewis in a remote operations center in the Development Engineering Building.

Bibliography

Kamotani, Y.; and Ostrach, S.: Design of a Thermocapillary Flow Experiment in Reduced Gravity. J. Thermophys. Heat Trans., vol. 1, no. 1, Jan. 1987, pp. 83–89.

Ostrach, S.: Surface Tension Gradient Induced Flows at Reduced Gravity. NASA CR–159799, 1980.

Pline, A.D.; et al.: Hardware Development for the Surface Tension Driven Convection Experiment. J. Spacecr. Rockets, vol. 27, no. 2, May-June 1989, pp. 312–317.

Pline, A.D.; and Butcher, R.L.: Spacelab Qualified Infrared Imager for Microgravity Science Applications. Thermosense XII: Proceedings of the International Conference on Thermal Sensing and Imaging Diagnostic Applications (SPIE Proceedings, Vol. 1313), S.A. Semanovich, ed., SPIE, Bellingham, WA, 1990, pp. 250–258.

Wernet, M.P.; and Pline, A.D.: Particle Displacement Tracking Technique and Cramer-Rao Lower Bound Error in Centroid Estimates from CCD Imagery. Presented at the Thirteenth Symposium on Turbulence, University of Missouri-Rolla, Rolla, MO, Sept. 21–23, 1992.

Lewis contacts: Thomas P. Jacobson, (216) 433–2860; Robert L. Thompson, (216) 433–3321; Alexander D. Pline, (216) 433–6614

Headquarters program office: OSSA

Critical Fluid Light Scattering Experiment Nears Testing

The Critical Fluid Light Scattering Experiment (dubbed Zeno by the principal investigator in honor of the ancient Greek philosopher noted for descriptions of paradoxes of infinity) will use dynamic light-scattering spectroscopy and correlation analysis to study the density fluctuations of xenon at temperatures near (within 100 microkelvin) the critical temperature for the vapor/liquid phase transition of this ideal fluid. These data will test transport property theories describing such phase changes in realms that are theoretically interesting (strong divergence of dynamic properties such as compressibility, thermal conductivity, and viscosity are predicted) but inadequately tested to date at the temperatures of most interest. Such measurements are severely limited on Earth because large density gradients are created by normal gravity acting on the fluid as the compressibility of the sample increases (diverges) near the critical temperature. The ultimate impact of such theories will be far reaching because the theories provide "universal" descriptions of many transitions, such as ferromagnetization, superconductivity, and binary fluid miscibility limits.

The principal investigator is Prof. Robert W. Gammon of the Institute for Physical Science and Technology at the University of Maryland, College Park. Prof. Gammon has assembled a team of 10 at the university including graduate research assistants, postdoctoral scientists, project engineers, and program/contract administrators.

This team is responsible, under NASA contract, for defining the science requirements and developing the flight instrument. The flight hardware engineering, fabrication, integration, and testing is subcontracted to the Ball Aerospace Group, of Boulder, Colorado.

Although the implementation of the experiment is fully contracted, a significant team of NASA Lewis personnel support the effort: project management and scientific oversight for the experiment is provided by the Space Experiments Division (SED); engineering oversight is matrixed from SED and the Engineering Directorate; product assurance support is provided by the Office of Mission Safety and Assurance; and contract management and financial management is provided by the Office of the Comptroller.

During 1992 the flight hardware fabrication and integration/testing neared completion. The process was slowed by challenging technical issues related to maintaining precise alignment of the optics and to fabricating the high-pressure sample cell. However, at year's end the electronics module was complete and ready for testing, and the optics module was integrated and checked out awaiting the flight thermostat. Flight acceptance testing should be complete by early 1993.

The flight instrument is currently identified on the manifest for STS–67 in February 1994 as part of the second United States Microgravity Payload mission.

Bibliography

Boukari, H.; et al.: A Very High-Resolution Thermostat for Observing Fluids in Space. IAF Paper 92–0924. Presented at the World Space Congress, Joint COSPAR/IAF Symposium on Gravity Dependent Phenomena in Fluid and Material Sciences, Washington, DC, Aug. 28–Sept. 5, 1992.

Boukari, M.; et al.: Thermal Equilibration of a Critical Fluid in Low Gravity. IAF Paper 92–0925. Presented at the World Space Congress, Joint COSPAR/IAF Symposium on Gravity Dependent Phenomena in Fluid and Material Sciences, Washington, DC, Aug. 28–Sept. 5, 1992.

Briggs, M.E.; Gammon, R.W.; and Shaumeyer, J.N.: Measurement of the Temperature Coefficient of Ratio Transformers. To be published in Rev. Sci. Instrum., 1993.

Gammon, R.W.: Zeno: Photon Correlation Spectropscopy of Critical Fluctuations in Microgravity on the Space Shuttle. Invited Paper MA4. Presented at the National Institute of Science and Technology Conference, Photon Correlation and Scattering: Theory and Applications, Boulder, CO, Aug. 24–26, 1992.

Gammon, R.W.: The Zeno Experiment: Photon Correlation Light Scattering From Critical Density Xenon. Invited COSPAR paper G.1–S5.1 Presented at the World Space Congress, Joint COSPAR/IAF Symposium on Gravity Dependent Phenomena in Fluid and Material Sciences, Washington, DC, Aug. 28–Sept. 5, 1992.

Segre, P.N.; et al.: Rayleigh Scattering in a Liquid Far From Thermal Equilibrium. Phys. Rev. A., vol. 45, 1992, pp. 714–724.

Shaumeyer, J.N.; et al.: Statistical Fitting Accuracy in Photon Correlation Spectroscopy. Invited Paper WA5. Presented at the National Institute of Science and Technology Conference, Photon Correlation and Scattering: Theory and Applications, Boulder, CO, Aug. 24–26, 1992.

Shaumeyer, J.N.; and Gammon, R.W.: Locating the Critical Temperature of a Pure Fluid to ~10 μK. IAF Paper 92–0926. Presented at the World Space Congress, Joint COSPAR/IAF Symposium on Gravity Dependent Phenomena in Fluid and Material Sciences, Washington, DC, Aug. 28–Sept. 5, 1992.

Zhang, K.C.; Briggs, M.E.; and Gammon, R.W.: The Susceptibility Critical Exponent for a Nonaqueous Ionic Binary Mixture Near a Consolute Point. To be published in J. Chem. Phys., 1993.

Lewis contact: Dr. Richard W. Lauver, (216) 433–2860
Headquarters program office: OSSA

Space Acceleration Measurement System Maximizes Science Return

Many experiments are flown on the Space Shuttle to utilize the reduced levels of gravity during orbital operations. The actual levels of acceleration and vibration experienced by the experiments quite often need to be measured to enhance the analysis of the experimental results. The Space Acceleration Measurement System (SAMS) Project has designed and fabricated an instrument to measure acceleration at or near experiments on the Shuttle. The data are provided to the experimenter after the mission or, in some cases, in near real time at a payload operation center. A data base of this acceleration environment will also be developed and maintained to facilitate future analyses and predictions of expected environments.

The SAMS project in fiscal 1992 delivered two flight units to the NASA Kennedy Space Center (KSC) for integration into STC–52, the first United States Microgravity Payload (USMP) mission. These units were of a new design for operation in the Shuttle cargo bay. Additional disk drives and data downlinking are utilized in this SAMS configuration to increase the data capacity for the mission because crew disk changeout is not possible.

The integration of three other flight units, which were delivered in 1991, was also worked with KSC in 1992. These efforts culminated in the third flight of a SAMS unit on STS–42 in January 1992 as part of the first International Microgravity Laboratory (IML) mission. The fourth flight occurred from June 25 to July 9 as part of the highly successful United States Microgravity Laboratory (USML) mission. The fifth flight occurred from September 12 to 20 as

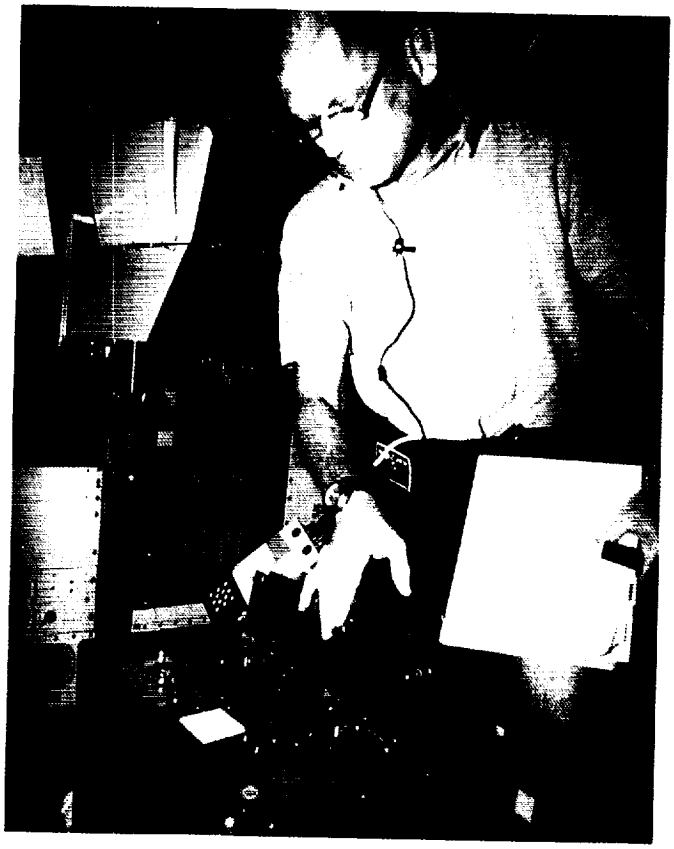

Mission specialist Norman E. Thagard performs a disk change operation for the Space Acceleration Measurement System during the first International Microgravity Laboratory mission in January 1992.

part of the Spacelab J mission. The sixth flight occurred from October 22 to November 1 as part of the first USMP mission.

SAMS data from the USML–1 mission have been prepared onto compact disk read-only memory (CD–ROM) for distribution to the principal investigators associated with the science experiments. SAMS data from all the missions will be distributed in CD–ROM format in the future.

The two principal investigators for the two science experiments on the USMP–1 mission utilized the SAMS downlink data for their operations at the NASA Marshall Space Flight Center's Payload Operations Control Center. This near-real-time examination of microgravity data permitted the principal investigators to adjust their experiment operations to maximize the science return.

The six SAMS flight units will be flown on numerous Shuttle missions in the coming years in the Shuttle middeck and cargo bay and in the Spacelab module. SAMS will average about four or five flights per year. This flight rate is expected to continue until Space Station *Freedom* is operational. A new-style SAMS will be among the first user experiments aboard *Freedom*.

The work is being performed at NASA Lewis by a team composed of NASA and Sverdrup Technology Inc., engineers and NASA technicians. The component parts have been fabricated by the NASA Lewis team and also by commercial companies. Missions involving international participation with the European, Japanese, and Canadian space agencies are also supported.

Bibliography

DeLombard, R; and Finley, B. D.: Space Acceleration Measurement System Description and Operations on the First Spacelab Life Sciences Mission. NASA TM–105301, 1991.

DeLombard, R.; Finley, B. D.; and Baugher, C. R.: Development of and Flight Results From the Space Acceleration Measurement System (SAMS). AIAA Paper 92–0354, 1992. (Also NASA TM–105652, 1992.)

Foster, W. M., II: Thermal Verification Testing of Commercial Printed-Circuit Boards for Spaceflight. NASA TM–105261, 1992.

Thomas, J. E.; Peters, R. B.; and Finley, B. D.: Space Acceleration Measurement System Triaxial Sensor Head Error Budget. NASA TM–105300, 1992.

Lewis contact: Richard DeLombard, (216) 433–5285
Headquarters program office: OSSA

Glovebox Experiments Produce Surprises

As part of the United States Microgravity Laboratory (USML)–1 Space Shuttle mission (June 1992), five small-scale experiments in microgravity combustion and fluid physics were developed and flown. They are entitled:

- Interface Configuration Experiment (ICE), to determine the preferred orientation that contained fluids will take in space

- Smoldering Combustion in Microgravity (SCM), to determine the potential effects of low gravity on the smoldering of common materials

- Wire Insulation Flammability (WIFE), to determine the offgassing, flammability, and flame spread characteristics of overheated wire

- Candle Flames in Microgravity (CFM), to determine and demonstrate the unique burning characteristics of candles in low gravity

- Oscillatory Thermocapillary Flow Experiment (OTFE), a companion to the Surface-Tension-Driven Convection Experiment (STDCE), but OTFE is expected to yield oscillatory flow

The glovebox demonstrations differ from most experiments conducted on the Space Shuttle. They are far less expensive (by 10 to 100 times) and were built and approved for flight in only two years (as compared with the usual 5 to 10 years).

The ICE behaved as hoped for. The free surface of the liquid took the expected asymmetric shape and was exceptionally stable in this configuration. The control container also behaved as expected, yielding a symmetric free interfacial surface. The mathematical theory for equilibrium surface behavior, in existence for several years, was finally verified in this set of experiments.

The SCM experiment studied how the initiation and propagation of smoldering—a most important mechanism for the inception of many accidental fires—is affected by gravity. The hardware was entirely sealed to contain the gases and heat produced in smoldering polyurethane foam. Four separate tests were conducted on USML–1 as a precursor to a Shuttle Get-Away Special experiment in 1994 and 1995. In two tests igniters were buried inside the length of the foam. Both tests produced smoke and combustible, noxious tars even when the smoldering did not visibly degrade the outside of the foam. The other two tests with an igniter at one end of the sample produced a type of smolder never seen on Earth in identical samples. In space the smolder front, as evidenced by black char, was visible on the outside of the foam.

The WIF experiment studied how flames spread along wire insulation material in the presence of a small fan-driven flow of air over an overheated wire. These were the first studies in space of such low-speed flows at levels similar to those produced by the ventilation systems of the orbiter and Space Station *Freedom*; they are very relevant to NASA's spacecraft fire safety program. The tests directly examined the effects of airflow direction (with or against the direction of the spreading flame). Some results were expected: The wire insulation did not drip in space as it had on Earth, and the flame supported by airflow spread faster than the one opposed by airflow. However, as with the smoldering experiment, there were significant surprises: The microgravity flame produced much more soot and was much brighter than expected or observed in tests conducted in drop towers or aircraft.

The CFM was both a fundamental investigation and a demonstration for young students of physics, chemistry, and engineering. On Earth the familiar candle flame is bright, yellow, soot producing, and teardrop shaped. In microgravity, as expected, the flames were dim blue, nonsooting, and hemispherical. However, there were three surprises. First, the flames spontaneously oscillated several times, extremely small oscillations at first but with large amplitude just before extinguishing. There is no clear explanation for this because similar oscillations observed on Earth were believed to be due to gravity-induced buoyant flows. Second, two candles could not be ignited in close proximity in space. The distance

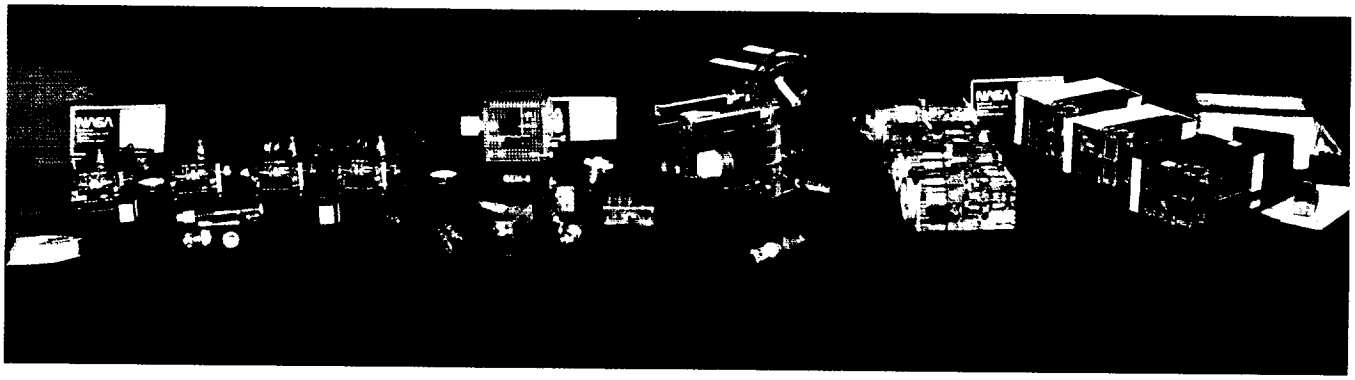

Lewis USML–1 glovebox flight hardware.

between these candles would have produced strong, in fact near-optimal, burning on Earth. In space the flame from the first candle seemed to prevent the second from being ignited, perhaps because it used the available oxygen near both. Third, vernier thruster firings caused the flames to suddenly flare up and produced soot—at levels of 10^{-4} g.

The OTFE produced flow oscillations in one of its four containers, behavior that was previously hypothesized as possible in space but never before observed. The other containers produced some bubble formation prior to the onset of oscillations, for reasons that are still being explored. An important byproduct of this set of tests is the bubble formation result, which will be factored into the planned full-scale testing in the STDCE for USML–2 in May 1995.

Lewis contact: John B. Haggard, Jr., (216) 433–2832
Headquarters program office: OSSA

Experiments Simulate Low-Gravity Flame in Normal Gravity

An innovative approach is used to simulate a low-gravity (spacecraft) diffusion flame in normal gravity by applying scaling laws and similarity between buoyant and forced flow. Diffusion flame structure and extinction characteristics are studied at a low stretch rate representative of a reduced-gravity environment. The flame configuration chosen was that of the forward stagnation-point region of a cylindrical fuel sample. A low-gravity experiment would utilize a low forced flow to obtain the low stretch rate, but a normal-gravity experiment must use extremely large radii of curvature to obtain low stretch, as buoyant flow dominates for low forced flow velocities.

Both experimental and theoretical investigations are being conducted. In the experiment a normal-gravity simulation of a low-stretch-rate diffusion flame is generated by using a fuel sample with an extremely large radius of curvature. The normal-gravity setup enables the detailed measurements needed for flame structure studies (temperature, flow, species fields, radiative heat loss, and local mass burning rate). The

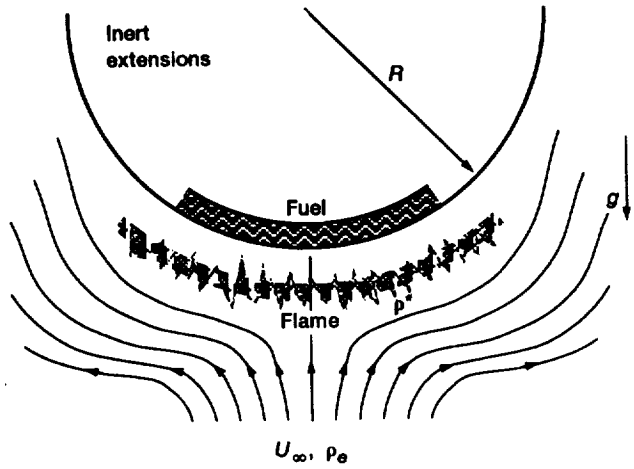

Geometry of low-stretch-rate, stagnation-point diffusion flame.

experimental apparatus has been fabricated, and the ignition, extinguishment, and diagnostics systems have been developed during this year. Testing is planned for much of next year.

Theoretical modeling has focused on how gas-phase and surface radiation affect the energy balance of the flame at low stretch rates. Decreased stretch rate amplifies the radiation effects with respect to the other energy transfer mechanisms. Numerical simulation has shown that including radiation effects leads to lower temperature flames and extinction at higher stretch rates than would otherwise be the case.

Detailed comparison between theory and experiment should delineate the unique features of diffusion flames at low stretch rates, including the extinction mechanisms. This program has the potential for significant knowledge that can be applied to new, more appropriate methods of evaluating the flammability of spacecraft materials in normal gravity. Ultimately, a space experiment will be proposed to verify the simulation. The space experiment will benefit from the normal-gravity work in that it can verify the simulation with fewer, simpler diagnostic measurements.

Lewis contacts: Sandra L. Olson, (216) 433–2859;
Jennifer L. Rhatigan, (216) 433–8330
Funding source: Director's discretionary fund

Pool Boiling Experiment Yields Preliminary Data

The Pool Boiling Experiment (PBE) is designed to fly onboard the Space Shuttle in a Get-Away Special canister. This experiment for studying nucleate boiling under microgravity conditions was conceived by Dr. Herman Merte, Jr., of the University of Michigan and built by NASA Lewis. Its objective is to improve understanding of the fundamental mechanisms that constitute nucleate pool boiling. These mechanisms include nucleation, or the onset of boiling; dynamic growth of vapor bubbles near the heater surface; and subsequent motion and collapse of the vapor bubbles. A pool of liquid that is initially at a precisely defined pressure and temperature will be subjected to a step-imposed heat flux from a semitransparent thin-film heater that forms part of one wall of the container. This will allow boiling to be initiated and maintained for a defined period of time at a constant pressure level. Transient temperature measurements of the heater surface will be made, noting especially the conditions at the onset of boiling. Motion photography will record the boiling process in two simultaneous views, one from beneath the heater surface, and one from the side. The control of the experiment and data acquisition will be completely automated.

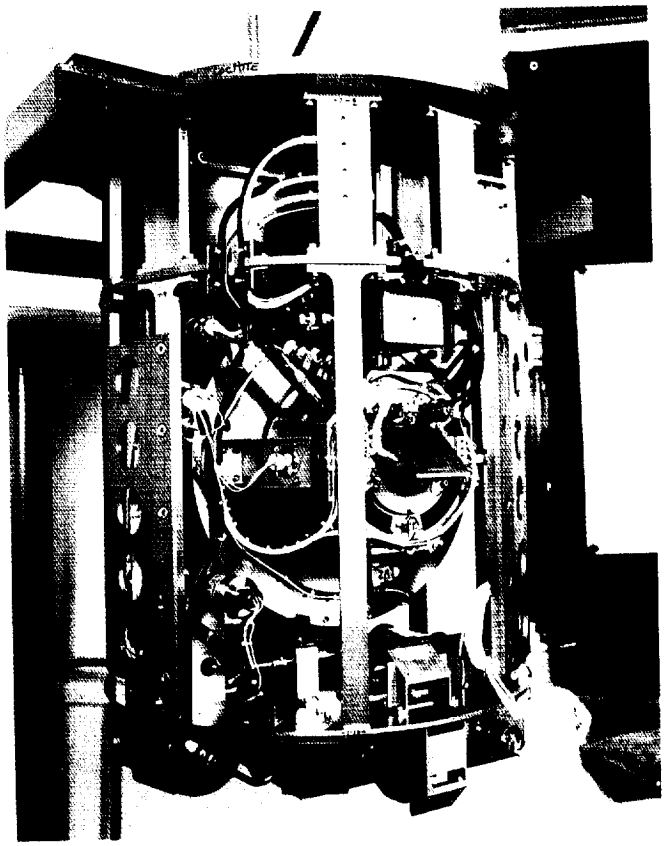

Pool Boiling Experiment.

This experiment will provide an understanding of how heat flux, initial subcooling, and time affect the growth and motion of vapor bubbles; will correlate the liquid vapor behavior with observed heater surface temperature variation; will use initial liquid temperature distribution at nucleation to compute the vapor bubble growth rate for comparison with observations; and will measure delay time to nucleation for correlation with nucleation theory by using heat flux, surface temperature, and liquid temperature distribution.

The information obtained from this experiment will be invaluable in designing equipment for use in space station modules and on space platforms for temperature control, power generation, energy dissipation, and the storage, transfer, control, and conditioning of fluids, including cryogenic fluids.

The pool boiling prototype system was flown on STS–47 in September 1992. The considerable amount of scientific data from the STS–47 flight was reviewed by the project team. The expected boiling pattern was observed in all high-heat-flux cases, but a different pattern was observed in the low-heat-flux cases. These differences appear to be caused by the rewetting of the heater surface. The film data indicate that the saturated cases experienced a more activated boiling process (more vapor than expected was generated).

The data from the STS–47 flight will be used to improve the science return on the pool boiling flight unit, which will fly on STS–57 early in 1993.

Lewis contact: Angel M. Otero, (216) 433–3878
Headquarters program office: OSSA

Solid Surface Combustion Experiment Performs Well

The Solid Surface Combustion Experiment (SSCE) is the first combustion experiment to fly in the Space Shuttle and the first such experiment in the NASA spaceflight program since Skylab. It was conceived by Professor Robert A. Altenkirch, Dean of Engineering at Mississippi State University, and built by NASA Lewis. The SSCE completed its fourth and fifth flights this year and the sixth is planned for late in the year. The STS–50 (USML–1) and STS–47 Spacelab tests were conducted in 35 percent oxygen, the lowest oxygen concentration specified in the science matrix. With these flights the ashless filter paper portion of the flight test matrix was completed. Aboard the orbiter *Endeavour* during STS–54 late this year the SSCE is scheduled to conduct its first tests of polymethylmethacrylate (PMMA).

The purpose of the SSCE is to study the physical and chemical mechanisms of flame spread over solid fuels in the absence of gravity-driven buoyant or externally imposed airflows. Because the controlling mechanisms of flame spread are different in low gravity than in normal gravity, the SSCE results have a practical application in evaluating spacecraft fire hazards. In these first five flights the fuel sample—ashless filter paper instrumented with three thermocouples—was mounted in a sealed chamber filled with a 50 percent or 35 percent mixture of oxygen in nitrogen at pressures of 1.0, 1.5, and 2.0 atmospheres. The sample was ignited with an incandescent wire. Two 16-mm motion picture cameras photographed the combustion process from perpendicular perspectives. Temperature (chamber and fuel sample) and pressure measurements were recorded with a digital data acquisition and control system. The SSCE is self-contained and battery operated and can be flown either in the Shuttle middeck or in the Spacelab module. Because of environmental requirements, only one ashless filter paper fuel sample is tested in each chamber during a mission. The chamber provides adequate volume to test two PMMA fuel samples. Reference 1 provides more information concerning the hardware configuration.

NASA Lewis designed and built the SSCE payload and also performed engineering, testing, scientific, and flight operations support. The SSCE project was supported in some way by nearly every major element of the Lewis organizational structure.

The SSCE hardware was activated and performed without incident on STS–50 and STS–47 flights, igniting the test specimen and recording the instrumentation data as designed. The crew continued to provide exceptional experiment support

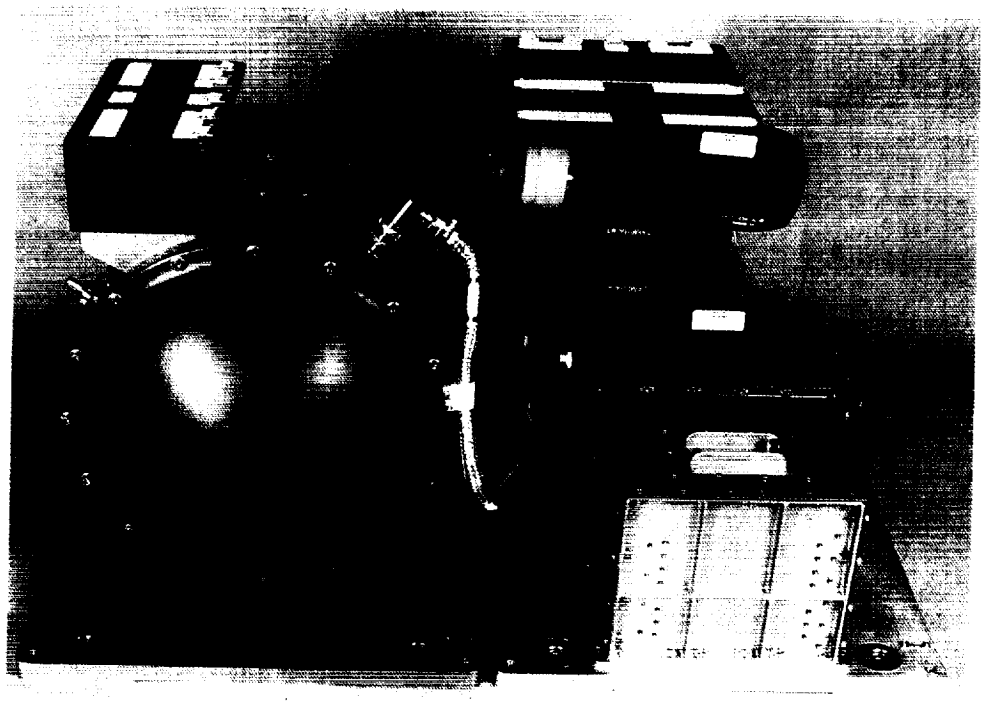

SSCE hardware for polymethylmethacrylate fuel—middeck configuration.

with the unplanned addition of downlinked video coverage of the combustion test. The flame spreading process exceeded the predefined camera run time during the STS–50 flight. The crew obtained additional run time on STS–47 by operating one of the cine cameras in the manual mode. The flame spread rate for 35 percent oxygen was determined to be approximately 1/3 of the slowest test at 50 percent oxygen. The 35-percent-oxygen test also had a considerable amount of burnt fuel remaining, which will provide an additional comparison with the computer simulation of the flame-spreading process.

The principal investigator, Professor Altenkirch, has developed a numerical simulation of the flame-spreading process from first principles (of fluid mechanics, heat transfer, and reaction kinetics). The spread rates, flame shape, and thermodynamic data from the SSCE flights are being compared directly with the results of the computational model. The flight temperature data indicate that the solid-phase kinetics parameters commonly used to model normal-gravity fuel pyrolysis do not reproduce the fuel regression rates observed. The results from the five flights of ashless filter paper will be used to formulate an improved solid-phase pyrolysis model.

Integrated analysis of the temperature, pressure, and imaging data is being performed for this year's flights. The analysis of the first three flights, which was completed last year, has been submitted for publication in three archival journal articles. The data were presented by Professor Altenkirch at the 24th International Symposium on Combustion, in Sydney, Australia, and at the Second International Microgravity Combustion Workshop in Cleveland, Ohio.

The SSCE project is currently scheduled for a total of eight flights. Polymethylmethacrylate fuel will be tested on STS–54 and on two additional flights planned for 1993.

Reference

1. Vento, D.M.; et al.: The Solid Surface Combustion Space Shuttle Experiment Hardware Description and Ground Based Test Results. AIAA Paper 89–0503, Jan. 1989.

Lewis contact: John M. Koudelka, (216) 433–2852
Headquarters program office: OSSA

Tank Pressure Control Experiment/Thermal Phenomena Obtains Objectives

An important issue in microgravity fluid management is controlling pressure in on-orbit storage tanks for cryogenic propellants and life support fluids, particularly liquid hydrogen, oxygen, and nitrogen. The purpose of the Tank Pressure Control Experiment/Thermal Phenomena (TPCE/TP) was to provide some of the data required to develop the technology for pressure control of subcritical cryogenic tankage. TPCE/TP was a reflight of the highly successful Tank Pressure Control Experiment (TPCE), which flew onboard STS–43 in August 1991 in a Get-Away Special (GAS) container.

TPCE, which used Freon 113 as a test fluid in a 0.5-ft^3 tank, was designed to provide data on jet-induced mixing for controlling tank pressure in low gravity. It met all of its objectives and significantly increased the knowledge base in fluid mixing. In addition, it gave some limited insight into the thermal phenomena involved in the stratification and self-pressurization of subcritical fluids and the boiling phenomena occurring during heating in a low-gravity environment. TPCE also gave some surprising results on pressure rise rates depending on ullage location and heat source location. Pressure spikes, on the order of 30 percent of the nominal tank pressure, were encountered under certain conditions during self-pressurization. This represents a potentially hazardous condition for the long-term storage of cryogenic fluids for future NASA missions. The purpose of the reflight, TPCE/TP, was to focus on the thermal phenomena involved in the heating and self-pressurization of subcritical tanks in a low-gravity environment. The Space Shuttle *Columbia* (STS–52), launched on October 22, 1992, carried the TPCE/TP experiment onboard.

The software for the flight computer was modified to provide more tests where the pressure spikes are likely to occur and to provide extended video coverage during the heating process. Additional data on fluid mixing at very low flow rates were also acquired to supplement the data provided by the previous TPCE flight. A total of 21 tests, over a 16-hour period, were planned. Heating time and power level were varied as well as the jet flow rate (low flows only) during the subsequent mixing process. Temperature, pressure, flow, heater power, and acceleration data were taken along with 4 hours of video.

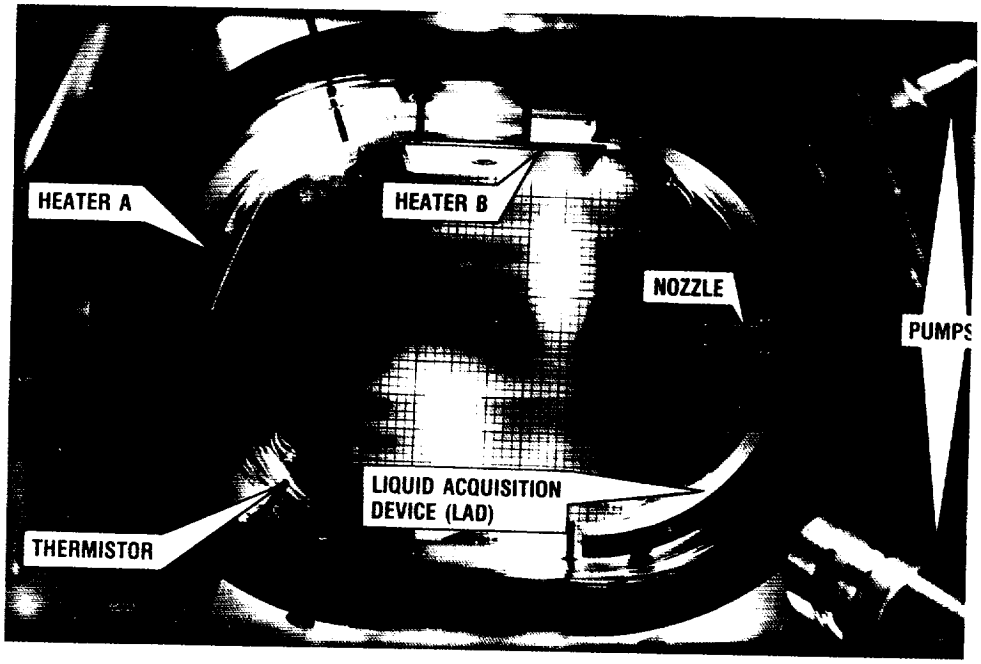

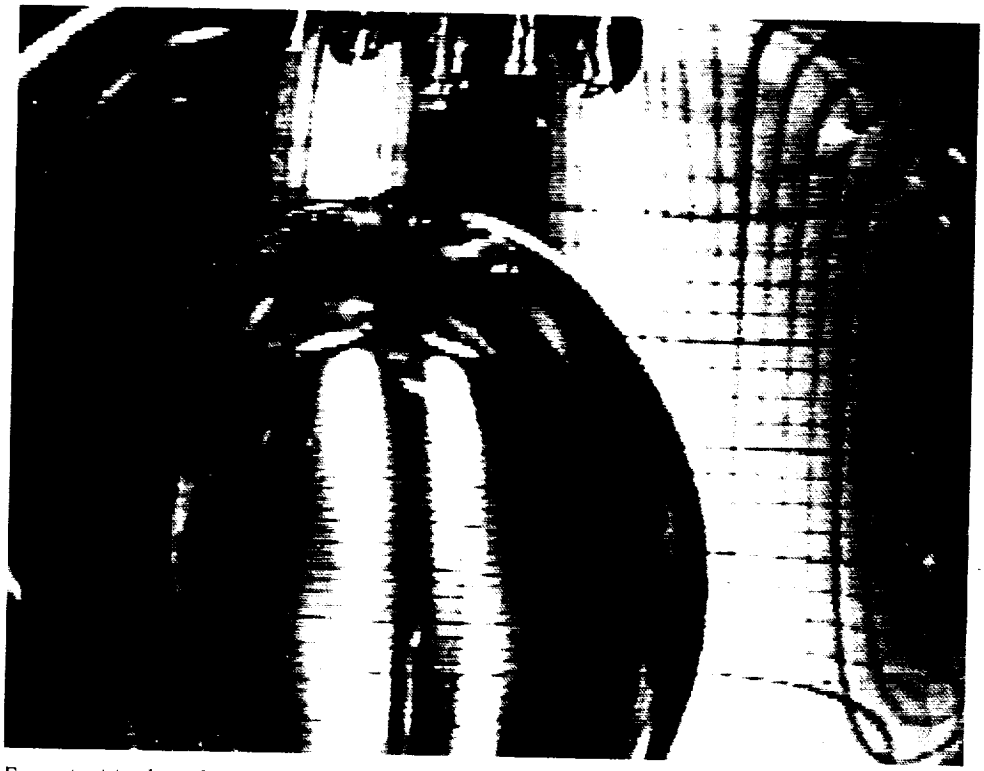

Freon test tank and typical fluid configuration during low-gravity heating.

The video and digital data show that all test objectives were obtained. Besides showing the thermal processes at work when a subcritical liquid is heated in low gravity, the video graphically illustrates the fluid dynamics associated with jet mixing at low flow rates. The pool boiling process at extremely low heat fluxes (~0.1 W/cm^2) is shown from inception to full boiling at the heater surface. For some test conditions explosive boiling occurred at these low heat fluxes, resulting in significant pressure spikes.

The experimental data obtained are of direct relevance to the design of space-based cryogenic fluid systems.

Lewis contact: Dr. M.M. Hasan, (216) 977-7494
Headquarters program office: OAST

Solar Array Module Plasma Interactions Experiment (SAMPIE) Prepares for Flight

The Solar Array Module Plasma Interactions Experiment (SAMPIE) is a Space Shuttle-based flight experiment with a scheduled launch date in January 1994. SAMPIE will determine the environmental effects of the low-Earth-orbit (LEO) space plasma environment on state-of-the-art solar modules biased to high potentials relative to the plasma. In addition, specially modified solar cell modules will be tested to demonstrate the possibility of arc suppression during operation at highly negative potential levels. Finally, several metal test specimens will be included to study the basic nature of these interactions and to validate computer models. The experiment is being developed at NASA Lewis.

Heretofore, space power systems in LEO have operated at low voltages and have not suffered from the effects of plasma interactions. High-power, photovoltaic-based systems now under development for space applications will operate at higher voltages in order to increase system efficiency. High-voltage systems suffer from adverse interactions with the LEO space plasma. The interactions, which are incidental results of power system operation, include arcing, which occurs when exposed metal surfaces attain a negative potential, and parasitic current collection, which occurs at a positive potential level. These interactions can damage power system components and decrease power system efficiency. SAMPIE will provide information concerning the interaction of system components with the LEO plasma.

SAMPIE will consist of a metal enclosure with the experiment plate fixed to the top surface and two small probes. The metal enclosure will mount directly to the top plate of a Hitchhiker carrier in the Shuttle cargo bay. The electronics will include a programmable, high-voltage power supply that will provide direct-current bias to the test specimens. A transient current detector will detect arcing and measure the arc rate as a function of negative bias voltage. An electrometer will measure parasitic current collection versus voltage for both positive and negative bias potentials. An onboard data acquisition system will record and store the information to solid-state nonvolatile memory. The probes for plasma data collection will be mounted on a Hitchhiker side plate. Data collected from the probes will be sent to a set of plasma diagnostic instruments.

The experiment plate includes solar cell samples of standard silicon cells, Space Station *Freedom* cells, advanced photovoltaic solar array (APSA) cells, and cells modified for arc suppression tests. Standard silicon cells will function as a baseline for comparison with the other cell modules. A four-cell module of *Freedom* cells, with copper interconnects, will allow a test of this technology. A 12-cell module of APSA cells, modified for LEO operation, will test the behavior of this relatively new, very thin (60 μm) technology. The APSA cells were modified because ground testing here at Lewis indicated that the type of Kapton used for the cells was not suitable for LEO applications. The TRW Corporation has provided the SAMPIE project with APSA cells that have a suitable Kapton for LEO application; the SAMPIE flight data will validate this design. Several solar modules will be modified in accordance with two arc suppression techniques under investigation as part of the ground-based testing effort. Both of these techniques will be explored using modified *Freedom* solar cells.

Various metal samples will be tested to investigate the effects of both current collection and arcing with the LEO plasma. These tests will provide design information for the *Freedom* plasma contactor program and will be used to

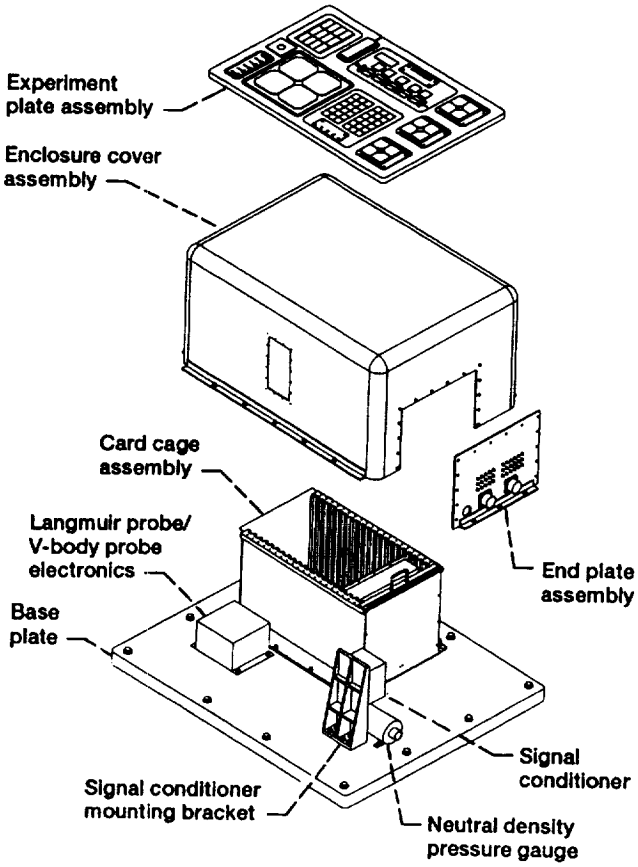

Exploded view of SAMPIE electronics enclosure and experiment plate.

help validate computer modeling codes developed at Lewis.

Roughly 18 hours will be devoted to experiment operation on orbit. During operation one module is biased to a particular voltage for a preset time while arcing and current collection effects are measured and recorded. In addition, measurements of the plasma environment are made with the onboard diagnostic instruments, and this information is recorded. The procedure is repeated at the other bias voltages until all measurements are completed. Vehicle orientation is critical because ram and wake effects are known to be significant. Accordingly, during the experiment, the orbiter will be oriented such that one entire set of measurements is made with the payload bay held in the ram direction and a second set with the bay in the wake direction.

A team of Lewis and Sverdrup engineers is currently building the SAMPIE flight hardware for the OAST–2 mission. Phase 0/1 safety reviews have been successfully completed and the data packages have been submitted for the phase 2 safety reviews. The critical design review was held in October 1992.

Lewis contacts: Lawrence W. Wald, (216) 433–5219; Dr. Dale C. Ferguson, (216) 433–2298; Dr. G. Barry Hillard, (216) 433–2220
Headquarters program office: OAST

Vibration Isolation Technology Demonstrated for Microgravity Science Experiments

An advantage of doing materials and fluid physics in space is that the gravity-driven forces are greatly reduced. However, experience has shown that the spacecraft environment is disturbed by vibrations from crew motions, thruster firings, and onboard machinery. These disturbances can detrimentally affect sensitive science experiments that require a microgravity environment. Sensitivity analyses on selected experiments were done to develop acceptable levels of vibrations. These analyses indicated that the critical regime for maintaining a microgravity environment is the subhertz frequency regime. The technology to achieve this regime had not been demonstrated at that time, so the Vibration Isolation Technology Project was begun.

Early in the project a workshop was held to assess the current state of the art and to define user needs. As a result of this workshop the project was designed to develop and demonstrate an actively controlled magnetic isolation system in six degrees of freedom (DOF) in a low-gravity environment on an aircraft. Technology development was conducted in-house at NASA Lewis. Magnetic actuator concepts and control strategies were evaluated in one DOF and three DOF. From this effort a laboratory six-DOF actively controlled magnetic isolation system was developed and evaluated under normal-gravity conditions. Position and inertial feedback controller schemes were evaluated. The concept of using position feedback in conjunction with inertial feedforward was found to yield excellent isolation capability.

Concurrent with technology development, the development of a suitable testbed for the NASA Learjet was undertaken. The initial phase in this development was to characterize the vibroacoustic environment of the Learjet. Using these

data a passive isolation testbed system was developed with a self-contained data acquisition system. This system was flown on the Learjet to validate testbed system performance. The data from these flights were then used to develop a testbed system for evaluating the actively controlled six-DOF magnetic isolation system. The active isolation system consisted of 12 electromagnetic actuators, in three sets of four actuators, that suspended the isolated plate assembly. The entire isolation system was mounted in a trunnion-supported assembly. The trunnion assembly ensured that residual gravity vector orientation remained constant with respect to the frame of reference as the aircraft flew a parabolic trajectory. The trunnion assembly was mounted in a standard Learjet rack.

Performance data for the active magnetic isolation system were obtained during approximately 60 parabolic trajectories under varying conditions (e.g., trunnion locked, trunnion free, position control feedback only, and position control feedback with inertial feedforward control). Because a limited amount of low-gravity time was available during a trajectory (less than 15 sec), evaluation in the very-low-frequency regime is not feasible using an aircraft. The isolation system natural frequency was set at 0.6 Hz so that time-averaged data could be obtained. The performance of the system in the laboratory with position control indicated a rolloff of about 40 dB/decade. Incorporating inertial feedforward improved rolloff to about 110 dB/decade. Comparable results were observed in the Learjet. The Learjet vibroacoustic environment is extremely harsh relative to that seen in a spacecraft, so the resulting system performance is encouraging. The principal limitation on system performance was found to be the sensor noise floor. This means that isolation performance can only be as good as sensor resolution. A full verification and technology demonstration of this system in the frequency range 0.01 to 0.1 Hz can only be done during orbital flights, but the results obtained to date indicate that isolation in the very-low-frequency regime is possible.

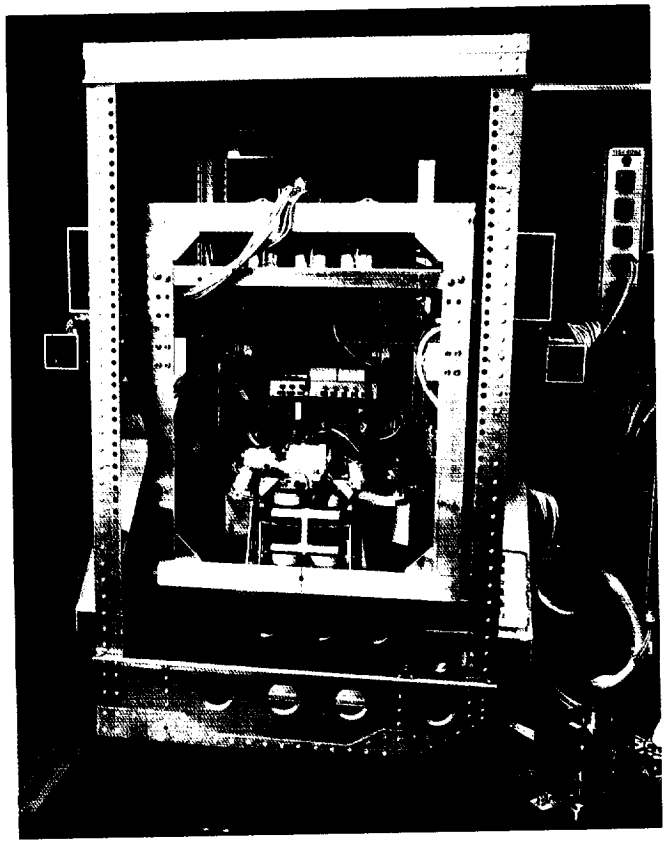

Actively controlled six-degree-of-freedom magnetic isolation system testbed.

Bibliography

Grodsinsky, C.M.: Development and Approach to Low Frequency Microgravity Isolation Systems. NASA TP–2984, 1990.

Grodsinsky, C.M.; and Logsdon, K.A.: Development and Design of a Magnetic Inertially Referenced Isolation System for Microgravity Experimentation. Proceedings of the Workshop on Aerospace Applications of Magnetic Suspension Technology, Pt. 2, N.J. Groom and C.P. Britcher, eds., NASA CP–10066, 1990, pp. 643–654.

Grodsinsky, C.M.; and Sutliff, T.J.: The Vibro-Acoustic Mapping of Low Gravity Trajectories on a Learjet Aircraft. NASA TM–103103, 1990.

Lewis contact: Carlos M. Grodsinsky, (216) 433–2664
Headquarters program office: OSSA

Space Station *Freedom*

Systems Engineering and Integration

Electric Power System Performance Model Enhanced

As the design and development of the Space Station *Freedom* electric power system (EPS) continues, more accurate predictions of its performance are needed in order to assess new operating scenarios and updated resource allocations. To meet these needs, NASA Lewis has enhanced SPACE, its computer code that models EPS performance.

SPACE was developed to predict the amount of power that the EPS can produce on orbit throughout its life under a wide variety of orbital conditions and on-orbit configurations. The code includes an orbital mechanics section, which determines the orbit parameters, including the sunlight and eclipse times. Models of the solar arrays and nickel/hydrogen batteries predict the amount of power that can be produced during the sunlight and eclipse portions of the orbit. These source models are coupled with a detailed load-flow model of the power management and distribution system to determine the amount of power that can be delivered to the housekeeping and user loads. SPACE uses a numerical iteration procedure to predict the highest power level that can be sustained throughout the specified orbit, taking into consideration any hardware constraints. SPACE also contains a model of the photovoltaic power module's thermal control system that predicts the temperatures of the batteries and other components under active thermal control.

The latest version of SPACE has been enhanced with several new capabilities. In addition to predicting the power level that the EPS can produce, a new load-driven version of SPACE can assess the ability of the EPS to supply a specified load demand versus time. The model assesses the load demand by checking that no hardware operating limits are violated. The code also determines if the solar arrays and batteries are able to supply the required power levels and whether the

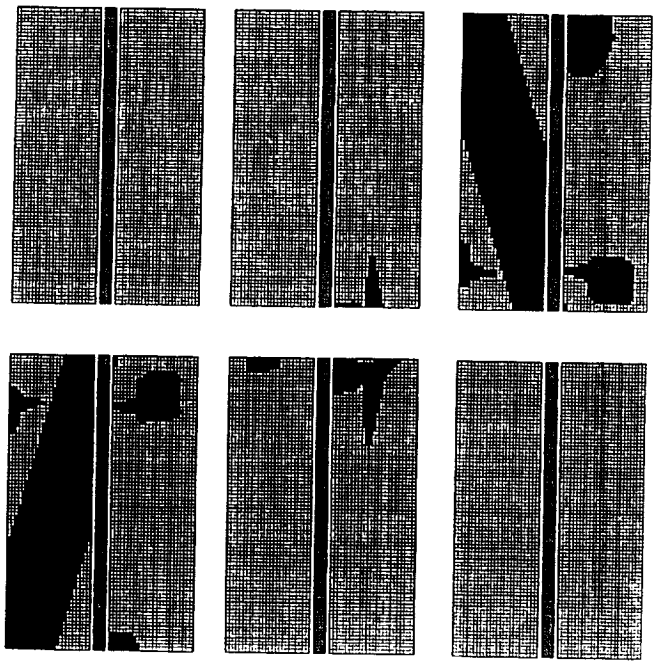

Shadow patterns on photovoltaic (solar) arrays during Tomahawk flight mode with Shuttle attached.

EPS can fully recharge the batteries. This version of SPACE has been used in the past year to assess a proposed load profile that would occur during a Space Shuttle rendezvous in *Freedom*'s human-tended phase.

Also, a detailed model of the secondary and tertiary distribution system has been added to SPACE. This system distributes power inside the habitable elements and along the integrated truss assembly to individual electrical loads. This portion of the model is designed to predict the losses that will occur in the remote power controller modules and the secondary and tertiary cabling.

Efforts are continuing to expand the capabilities of SPACE by adding the ability to assess how shadowing by other station structures would affect the solar arrays. Also, SPACE is continually being updated with the latest information on the performance of various EPS components as the design progresses and higher fidelity information becomes available.

Lewis contacts: Jeffrey S. Hojnicki, (216) 433-5393; David B. McKissock, (216) 433-6304; Robert D. Green, (216) 433-5402
Headquarters program office: OSSD

Penetration Analyses Use BUMPERII Computer Code

The threat to Space Station *Freedom* from micrometeoroid and orbital debris is an important issue. An impact from one of these particles can damage a space station component. Both NASA and its contractors are developing shield configurations to protect *Freedom* from such impacts. NASA Lewis is responsible for *Freedom*'s electric power system. The integrated equipment assembly is a structure that includes various components of the electric power system. These components generate heat and require a cooling system. The cooling system fluid circulates through a serpentine arrangement of stainless steel tubing. Because the cooling system is vital to the operation of the electric power system, the tubes must be protected from micrometeoroids and orbital debris.

NASA Lewis is using a computer code called BUMPERII to perform penetration analyses on this tubing. BUMPERII is maintained by NASA Marshall Space Flight Center's contractor Boeing Defense and Space Group. The code requires as input a geometric output file from a finite element model that is created with plate elements by using a preprocessor such as PATRAN or IDEAS. The model is analyzed to determine which meteoroid and debris particles impact on each element of the model. The wall configuration, shield and wall thickness, standoff distance, and material are also required. Three types of wall configurations are available: single wall, double wall, and multiwall. Single wall uses a single sheet of aluminum. Double wall uses two aluminum plates separated by a specified standoff distance. Multiwall uses single or double aluminum plates with additional layers of Nextel, Kevlar, or Spectra. The integrated equipment assembly is currently designed with double-wall shielding.

The penetration function to be used in the analysis is then chosen. A penetration function is an analytical formulation that calculates the critical (smallest) particle diameter that will penetrate the specified wall configuration at a given velocity and impact angle. Lewis is using the Richardson penetration equations for this analysis. One advantage of the Richardson method is that it is valid for stainless steel–aluminum wall shield configurations. The other double-wall methods in the code are accurate for aluminum-aluminum configurations only. A probability of no penetration value for both debris and meteoroids is calculated from the geometry input and critical diameter array calculated previously. This value is then compared with the probability of no penetration calculated by the contractor.

BUMPERII is also used to determine the shielding required to protect the integrated equipment assembly from particles of a certain diameter.

Lewis contact: Christopher A. Gallo, (216) 433–8808
Headquarters program office: OSSD

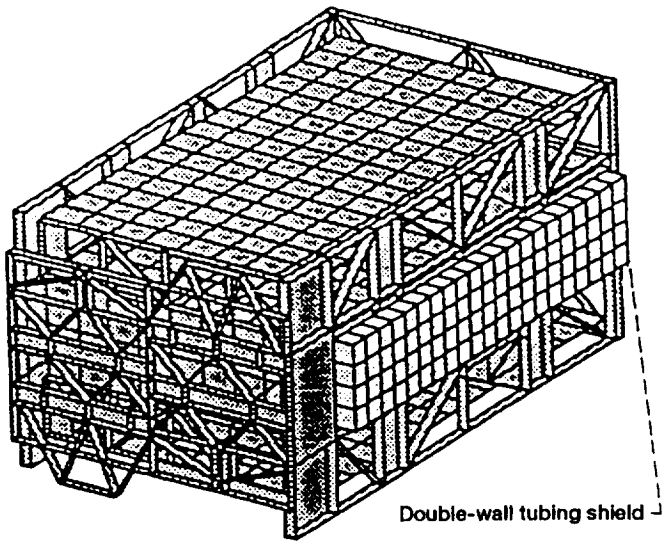

Integrated equipment assembly.

Photovoltaic Power Modules

Photovoltaic Power Module Tested in Neutral Buoyancy

In December 1991, following the Space Station *Freedom* restructuring design activity, a neutral buoyancy test of the photovoltaic power module was conducted to verify the compatibility of the preliminary design with extravehicular activity (EVA). The test was conducted in the Weightless Environment Training Facility at NASA Johnson Space Center.

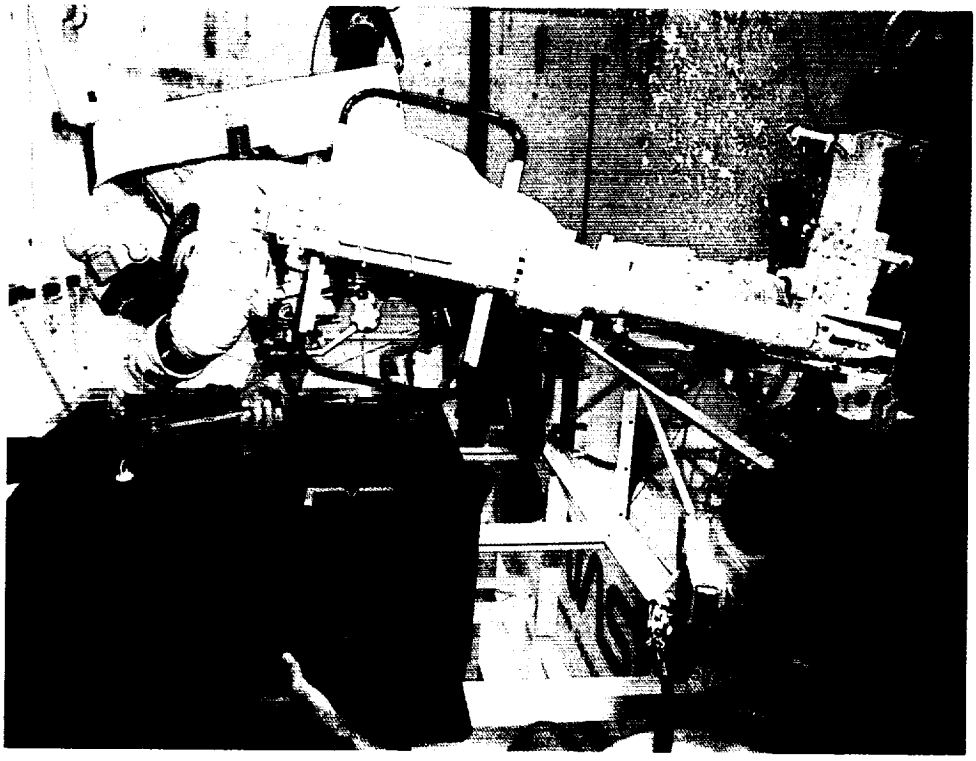

Astronaut performing changeout of battery orbital replacement unit.

In order to minimize the effects of drag, the mockups consisted primarily of aluminum-frame construction using polyvinyl chloride tubing to provide buoyancy and nylon mesh to represent solid surfaces. The hardware included high-fidelity mechanisms to realistically represent critical EVA interfaces and operations.

The flight hardware represented was in varying stages of development. Test hardware included a volumetric mockup of the photovoltaic power module built by NASA Lewis, a high-fidelity mockup of a solar array mast canister and blanket box provided by Lockheed Missiles and Space Company (LMSC), and high-fidelity mockups of a battery orbital replacement unit and an electronics control unit built by Rocketdyne. Space Station *Freedom* tools and EVA equipment were provided by NASA Johnson Space Center and McDonnell Douglas Space Systems Company.

The test involved simulating assembly and maintenance tasks for the photovoltaic power module. Test subjects wore extravehicular mobility units (EMU's, otherwise known as Shuttle space suits) and were members of the astronaut core. Test objectives included evaluating EVA crew and tool accessibility to launch restraint release locations and maintenance worksites; EVA translation routes for all tasks; EVA solar array deployment operations; and orbital replacement unit alignment, installation, and removal operations.

Key findings from the many test results include:

- Solar array blanket box changeout could be accomplished with two crewmembers; one mounted on the end of the remote manipulator system, and the other at the mast canister aiding alignment of the orbital replacement unit (ORU).
- The swingbolt design for the solar array blanket box is susceptible to damage.
- Because the soft docking mechanism does not rigidly capture the solar array blanket box, soft docking redesign is required.
- Screw disengagement was difficult to verify on the electronics control unit (ECU) and the battery.
- ECU coarse alignment, soft docking, and keying features worked well; ECU connector shells bound during removal of the ORU.

- Some portable foot restraint sockets must be relocated to permit access to launch restraint release locations.

- Additional handholds and handrails are required to improve the outboard translation route to the mast canisters.

The test results and conclusions were based on the observations noted during the tests and during post-test debriefings with astronaut test subjects; from reviews of video recordings and still photographs of the test; and from consultation with test observers and hardware designers.

Test results have been factored into numerous preliminary design reviews of the orbital replacement units for the photovoltaic power module, including that for the integrated equipment assembly in February 1992. Both design changes and assembly and maintenance procedure changes have been implemented on the basis of the test results. As hardware design continues, tests are planned to verify the design and EVA operations required to assemble and maintain the photovoltaic power module throughout the life of Space Station *Freedom*.

Lewis contacts: Monica I. Hoffmann, (216) 433–6765; Robert D. Draper, (216) 433–6779
Headquarters program office: OSSD

Thermal Cycle Testing of Solar Array Coupons Successfully Completed

NASA Lewis has conducted thermal cycle tests to demonstrate the durability or operational life of the welded-interconnect design for a solar array in a low-Earth-orbit thermal cycling environment. Secondary objectives included identifying potential failure modes and determining electrical performance degradation over the design life.

Power for Space Station *Freedom* will be generated by six large photovoltaic, or solar, arrays. Each array will contain 164 active solar cell panels. An active solar cell panel contains 200 solar cells, each connected to the underlying copper circuit by 10 welded contact points. These solar-cell-to-circuit interconnects are subjected to thermally induced stresses during the temperature excursions experienced in every orbit. *Freedom* will orbit the Earth once every 90 min—equaling 6000 thermal cycles a year or 90,000 thermal cycles over the 15-year design life.

Each test coupon contains four 8- by 8-cm silicon solar cells connected in series and a bypass diode that is used for circuit protection on orbit. The *Freedom* solar cells are an N- on P-type of silicon with a boron backsurface field and a 10-Ω-cm nominal base resistivity. Four holes in each cell bring the front N contacts through to the back side of the cell, where they are welded to the copper circuitry along with the six back P contacts. The cells and circuitry are bonded to a polyimide substrate with a silicone adhesive to form the completed solar array test coupon.

Lewis has completed a series of tests on development blanket coupons in a thermal cycling (–90 to 70 °C) chamber containing a dry nitrogen environment. The coupons were cycled at an accelerated rate and removed at set intervals for electrical performance measurements and visual inspections.

Five different designs have been supplied by the Lockheed Missiles and Space Company throughout the development program. Twelve four-cell coupons have completed 90,000 thermal cycles.

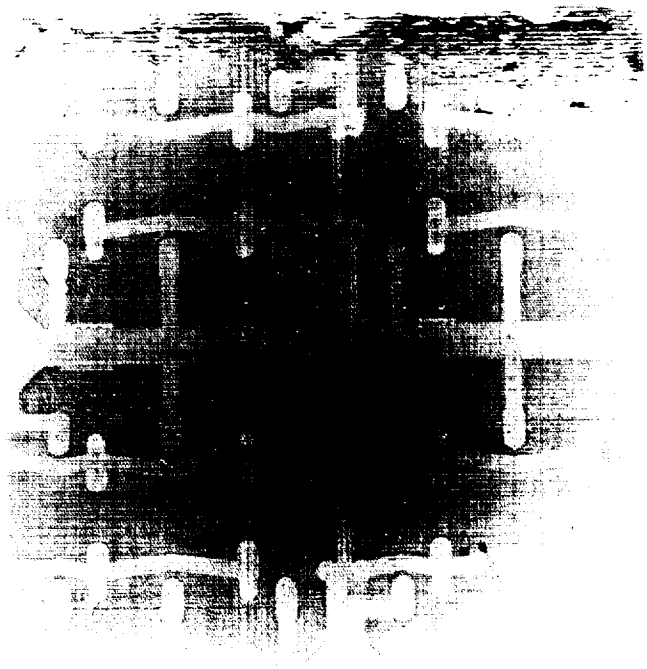

Solar array test coupon used in thermal cycling tests.

Results of these tests have produced modifications to the panel design, the circuit layout, and the manufacturing process that have led to the selection of a final design for the Space Station *Freedom* solar array panel.

This final blanket design has been tested to its 15-year design life without significant mechanical degradation or changes in electrical output. The successful test results have provided confidence in the ability of the solar arrays to withstand the low-Earth-orbit thermal cycling environment over the design life.

Lewis contact: Bryan K. Smith, (216) 433-6703
Headquarters program office: OSSD

Nickel/Hydrogen Battery Cells Undergo Life Testing

NASA Lewis and its contractors are responsible for designing and fabricating the electric power system for Space Station *Freedom*. *Freedom* will circle the Earth every 90 min in a low Earth orbit (LEO). Approximately 55 min of this orbit will be in sunlight and 35 min will be in the Earth's shadow (eclipse). In order to supply continuous power over the orbit, the electric power system must not only provide power during the sunlight portion by means of solar arrays, but must also store energy for use during eclipse. Nickel/hydrogen (Ni/H_2) cells were chosen as the energy storage system for *Freedom*. Because of the limited Ni/H_2 data base on life and performance characteristics in a LEO regime, NASA Lewis began two test programs: one in-house and one at the Naval Surface Weapons Center (NSWC) in Crane, Indiana.

For the in-house test program Lewis has built a computer-controlled Ni/H_2 cell laboratory with a data acquisition system to screen a large number of cell designs. Cells were purchased from three vendors through existing Lewis contracts with Yardney Technical Products, Eagle-Picher Industries, and Hughes Aircraft Company. The resulting 39-cell test matrix consists of 13 different cell designs including both 50- and 65-Ahr-capacity cells. All cells have successfully completed acceptance, vibration, and characterization testing and are currently undergoing LEO life testing at a 35-percent depth of discharge (DOD) and at either −5 or 10 °C. As of September 1992, 22 cells have successfully completed over 3 years of life testing (17, 520 cycles); the rest have completed over 2 years. From 16, 000 to 20, 500 life cycles have been completed.

The Naval Surface Weapons Center was contracted by Lewis through an interagency order to characterize and life test a statistically significant number of Ni/H_2 cells for the purpose of verifying the Space Station *Freedom* requirement of 5-year life at 35-percent DOD. The test matrix consists of 130 Ni/H_2 cells from each of three vendors: Yardney Technical Products, Eagle-Picher Industries, and Gates Aerospace Batteries. Each vendor supplied 50 "standard" 65-Ahr cells that represent a low-risk, state-of-the-art LEO design. They also supplied 20 "advanced" 65-Ahr cells and 60 "advanced" 81-Ahr cells. For the advanced design the vendors were directed to include at least two recent technology developments that improve cycle life and electrical performance. The 20 advanced 65-Ahr cells from Gates were canceled and 30 additional standard 65-Ahr cells were purchased. All cells were procured through separate Lewis contracts. All life testing is performed in either 10-, 8-, or 5-cell series-connected test packs, at 35- or 60-percent DOD, and at 10 or −5 °C. The charge scenario used is a two-step, constant-current profile.

As of September 1992, all cells have been delivered to NSWC and have completed acceptance, vibration, and characterization testing. Eighty Yardney cells (40 standard 65 Ahr, 20 advanced 65 Ahr, and 20 advanced 81 Ahr) have started life testing and have accumulated between 800 and 12,500 cycles. Four test packs at 60-percent DOD have failed, with the longest one lasting 4,700 cycles. One hundred and eight Eagle-Picher cells (48 standard 65 Ahr, 20 advanced 65 Ahr, and 40 advanced 81 Ahr) have started life testing and have accumulated between 500 and 7,000 cycles. The 48 standard 65-Ahr cells are undergoing a special charge control study. Some of the cells are being charged using a *Freedom* baseline charge profile that incorporates a constant current charge followed by a taper charge to 100-percent state of charge. The others are being charged at a constant current terminating at 90- or 94-percent state of charge. Forty advanced 81-Ahr Gates cells have started life testing and have accumulated between 600 and 2,300 cycles.

The 30 additional standard 65-Ahr Gates cells will be used for assessing the effect of electrolyte concentration with various charge management techniques. The balance of the 308 cells scheduled for life testing should be on test by the end of 1992. The NSWC will also perform storage tests on cells from each vendor.

Lewis contact: David T. Frate, (216) 433–8329
Headquarters program office: OSSD

Nickel/Hydrogen Battery Cells Tested for Hypervelocity Impact

The energy storage system on Space Station *Freedom* will utilize nickel/hydrogen (Ni/H_2) batteries. *Freedom* will have 18 batteries in a fully loaded configuration. Each battery consists of two orbital replacement units (ORU's) that each contain 38 Ni/H_2 cells. During normal operation each of these cells can reach a hydrogen pressure of 900 psi inside the 0.024-in.-thick pressure vessel. The 38 cells in an ORU are mounted in a 0.148-in.-thick aluminum thermal sleeve, affixed to a finned baseplate, and arranged inside a 1/2-in.-thick aluminum honeycomb box. One of the concerns surrounding these cells is their response to a micrometeoroid or orbital debris impact while in orbit on *Freedom*. Speculation was that the batteries may fragment or explode, damaging other batteries, hardware, or possibly crew members. NASA Lewis therefore developed a test program to investigate this scenario using Gates Aerospace Batteries cells built under the *Freedom* development program. The tests were conducted at the NASA Johnson Space Center's White Sands Test Facility in New Mexico in January and February 1992. A 7.6-mm (0.30-caliber), two-stage, light gas hypervelocity gun was used for all the tests.

The test matrix consisted of five combinations of cell impact location and particle velocity. The first cell was impacted with a 3/16 in. aluminum sphere at 7 km/sec into the cylindrical portion of the cell through the thermal sleeve, simulating a particle penetration through the side of the ORU box. The Ni/H_2 cell withstood this impact without a puncture to the vessel. It was later retested with a 1/4-in. particle at 6 km/sec. This was at the top end of the gun's performance level. Another cell was impacted with a 1/4-in. aluminum sphere at 3 km/sec into its cylindrical portion. Two cells were impacted in the hemispherical dome region, simulating a particle penetration through the top of the ORU box. One of these was at a particle velocity of 3 km/sec and the other at 7 km/sec. Both particles were 3/16-in. aluminum spheres.

Each test simulated the operating environment of the Ni/H_2 cells while on *Freedom*. The cells were electrically charged to 900-psi hydrogen pressure. They were placed behind a piece of the ORU honeycomb box cover and mounted in thermal sleeves to the test fixture, duplicating the structural arrangement in the ORU. The test chamber was also pumped down to about 0.5 psi, closely simulating the vacuum of space. Witness plates of aluminum and Inconel were placed around each cell to characterize the debris generated from the impacts. Cell pressure, voltage, and temperature were monitored during the test. Also, a high-speed camera filmed each impact at 10,000 frames per second.

Four out of five tests resulted in penetration of the Ni/H_2 cells. All tests resulted in benign failures. No explosion or fragmentation of the pressure vessels occurred. The holes in the cells were clean and did not lead to rapid crack growth. The debris that resulted from each impact was limited to small particles traveling at relatively low velocities. No damage to any of the witness plates occurred. Under the conditions tested, Lewis has shown that the *Freedom* batteries can survive a micrometeoroid impact without causing any secondary damage to neighboring batteries or hardware.

Lewis contact: David T. Frate, (216) 433–8329
Headquarters program office: OSSD

Nickel/Hydrogen Battery Cells Short-Circuit Tested

Nickel/hydrogen (Ni/H_2) batteries will be used as the energy storage system on Space Station *Freedom*. Each battery consists of 76 Ni/H_2 cells connected electrically in series. Each cell has a capacity of 81 Ahr. An important design

consideration in determining the electric power system's fault protection is to characterize the Ni/H_2 battery response to a short-circuit fault. As a result, NASA Lewis designed the hardware and carried out a test to determine the current obtained when a charged Ni/H_2 cell was short circuited. From these data the internal cell resistance was calculated. A model was developed for estimating the characteristics of a 76-cell battery.

Two Eagle-Picher 65-Ahr cells were used for this test. Both one-cell and two-cell series tests were performed. The tests consisted of charging the cells to a full charge and introducing a short circuit of approximately 1 mΩ for 180 msec in duration. Short-circuit currents and voltages were measured. Tests were also performed after discharging the cells to 35-percent depth of discharge (DOD), which is the nominal *Freedom* state of charge at the end of the eclipse.

The one-cell test showed that a 65-Ahr cell had a short-circuit current of 770 A when fully charged and 660 A when at a 35-percent DOD. The two cells in series had a short-circuit current of 987 A when fully charged and 856 A when at a 35-percent DOD. The internal resistance of the 65-Ahr cells was determined to be approximately 1.06 mΩ per cell. Predictions for a 76-cell battery of 81-Ahr cells yielded a short-circuit current of 1753 A.

Lewis contact: David T. Frate, (216) 433–8329
Headquarters program office: OSSD

Electrical Systems

Diagnostic Expert Systems Developed for Electric Power System

NASA Lewis is developing expert systems to help the ground-based operations team diagnose failure causes in Space Station *Freedom*'s electric power system. To date, prototype expert systems have been developed for power generation (solar conversion and energy storage) and for power distribution (switchgear and voltage conversion). Two approaches have been used.

The first approach, used for the distribution system and the solar conversion equipment, incorporates the failure knowledge into data tables, a technique known as set covering. Using set covering rather than a series of if-then rules to encode the failure knowledge makes the diagnostic program extremely flexible. The program uses a standard reliability tool—the failure modes and effects analysis—to produce the symptom and failure data base. Symptoms are detected by using rule-based classifiers. Symptoms are then linked, by using antecedent-driven rules, to all related systems failures. This linkage generates failure-cause hypotheses. Hypotheses are ranked primarily by the number of observed symptoms; the more symptoms, the more likely the failure cause. Explanations are provided for the failure causes and their symptoms, making the reasoning process readily understood by a power system operator.

The second, used for the nickel/hydrogen battery energy storage system, compares actual measurements with the values predicted by analytic models and with tabulated aging characteristics to discern incipient failures. The system displays these health trends and alerts the system operator should there be any deviations from the expected. Three trends are maintained: short term, medium term, and long term.

The short-term trend data (three orbits) address battery current and voltage, cell pressure and temperature, and depth of discharge. The data are smoothed. Trends are identified and compared with results from an empirical analytic model of the battery. Deviations are used to detect events such as sensor failure, cell short circuit, and cell rupture.

Medium-term (100 orbits) and long-term (3000 orbits) data address cell pressures and voltages at the end of the charging period and at the end of the discharging period, recharging ratio, watt-hour efficiency, depth of discharge, and cell temperatures. These data are smoothed and trends are identified and compared with the batteries' expected aging characteristics. The comparisons detect the anomalies that develop over many orbits, such as cell soft short, slow cell leak, high internal resistance, internal corrosion, excessive overcharge, abnormally high operating temperature, and gradual loss of charge-carrying capacity.

These two prototype expert systems will be evaluated for use in Space Station *Freedom*'s control center complex and for use in Lewis' mission evaluation center.

Lewis contact: James L. Dolce, (216) 433–8052
Headquarters program office: OSSD

Large Paralleled Direct-Current-to-Direct-Current Converters Operated Successfully

The Space Station *Freedom* Program requires that direct-current-to-direct-current converter units (DDCU's) be paralleled at their output terminals to serve loads larger than the 6.25-kW nominal power rating of a single unit. NASA Lewis has modified existing TRW DDCU breadboards and tested them, in parallel, in the Lewis electric power system (EPS) testbed to assess any technical issues arising from the need to parallel converters. Results showed that both parallel control methods tested work well.

Four TRW series-resonant, 6.25-kW DDCU's were modified to incorporate control schemes designed for parallel operation. Two schemes were implemented: "droop" and "master-slave." In the droop configuration a finite direct-current regulation gain is employed to achieve a relationship between bus voltage and output current. This method allows stable paralleling of two or more DDCU's without interconnecting cables. Using an adjustable error-to-output gain in each DDCU allows controlled uneven power sharing. The master-slave connection uses an interconnecting harness to let one of the DDCU's regulators control the other DDCU's output. This arrangement preserves the low steady-state voltage error of a single DDCU at the expense of the additional cable between the DDCU's. Uneven power share is achieved through an analog multiplier in each DDCU between the regulator output and the current stage input.

The paralleled DDCU's were tested in the EPS testbed, supplying a secondary load composed of constant-power load converters and other loads. The paralleled DDCU's operated stably and met performance expectations in both paralleling modes. Measurements of DDCU output impedance show that adjustments in the current share setpoints in either mode affect the output impedance of the combined converters. Further investigation is required to determine the impact of varying source impedance on secondary system stability; it is believed that setpoints can be chosen to affect the desired current share while keeping a consistent output impedance.

The modified DDCU's remain as an integral part of channel A of the EPS testbed and will serve in upcoming investigations into EPS stability and power quality.

Lewis contact: Robert M. Button, (216) 433–5335
Headquarters program office: OSSD

Operator Interface System Designed for Power Testbed

A computer-graphics-based operator interface system (OIS) was designed in-house for the Space Station *Freedom* power management and distribution testbed. The OIS was attached to the testbed and is used to easily display data from the testbed and to easily control the testbed. The OIS is designed to accommodate two testbed operators, each working with his or her own computer console. Other testbed users can connect through the OIS and use the testbed for developing and evaluating control algorithms that reside outside the testbed environment (such as those that will run on ground-based computers with Space Station *Freedom*).

The OIS consists of three computers added to the testbed. Two of the computers are the operator consoles; the third is the integrated data interface system (IDIS) computer that permits multiple computers to connect to the testbed simultaneously. The IDIS connects to the operator consoles and any additional ground-based computers with an Ethernet network. The IDIS connects to the testbed through an 802.4 network.

The OIS console computers present data in a hierarchical, windowed, graphical format. Schematic diagrams of testbed subsystems are displayed on the screens, and the pictures are animated to convey information about the state of the testbed. Numerical data are superimposed over the pictures. The operators can change the

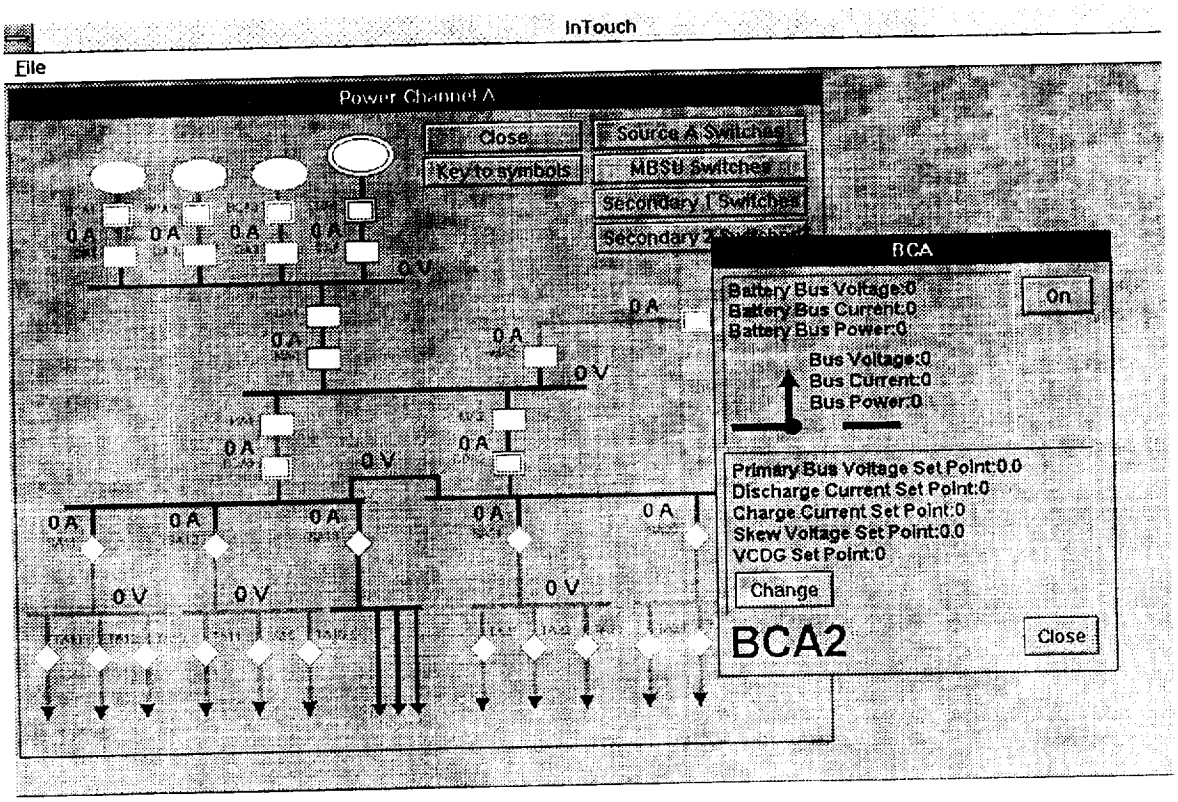

Typical screen display on OIS console.

state of testbed components by using a mouse to click on buttons displayed on the screen. The mouse is also used for moving through the hierarchy of screens, so that the appropriate data are displayed. In addition to the graphical interface the OIS consoles provide a terminal window where commands to testbed components can be typed. Results from these commands show up in the terminal window.

Along with enabling multiple computers to connect to the testbed, the IDIS computer provides some data acquisition services. OIS console computers or ground-based computers that require periodic data can ask the IDIS computer for the data by name. The IDIS computer looks up the name in a data base of available periodic data and determines how to retrieve the data from the testbed. The IDIS then notifies the appropriate computer in the testbed to send the data. The testbed computer will retrieve the required data and send it to the IDIS approximately once per second. The IDIS routes the data to the computer that requested it. When the data are no longer needed, the IDIS notifies the proper testbed computer to stop sending the data. The IDIS will not send requests for data it is already getting, even if it is requested by another computer. One-time commands to the testbed and responses from those commands are passed through the IDIS and routed to the pertinent OIS console.

In order to support the periodic data updates required by the OIS, several software tasks were added to the Ada software running in the testbed computers. These tasks retrieve requested data and send the data periodically to the IDIS. The retrieval is usually done from the data base on the testbed processor in which the task is running. If the data are not in the data base, they can be requested from the testbed processor that has the required data. All requesting and routing is handled behind the scenes and is not apparent to the testbed operators.

Work on the IDIS is complete, but there are ongoing efforts to improve the efficiency of the OIS console computers. New graphics screens are being generated for the OIS console computers so that they track the actual configuration of the testbed. Work also continues on the data acquisition part of the software that runs in the test- bed computers.

Lewis contact: Anastacio N. Baez, (216) 433–5318
Headquarters program office: OSSD

Operations

Data System Developed for Electric Power System Testbed

The power management and distribution (PMAD) data system was developed to provide a lower cost, effective data and control system that will support testing in the PMAD systems testbed. The PMAD systems testbed represents a portion of the Space Station *Freedom* electric power system. The testbed contains sources including a 30-kW solar array field, power distribution switchgear, power-conditioning devices, and loads—all representative of the hardware to be used on *Freedom*. The PMAD data system controls the facility and collects data from the testbed hardware and from the external transducers to verify the testbed hardware data.

The PMAD data system is based around a control and data acquisition software package called GENESIS from Iconic's Inc. GENESIS provides a real-time multitasking environment that runs on IBM personal computers and compatible systems. Device drivers are installed that tie the GENESIS system to data collectors. The data may be displayed, trended, plotted, or saved to history files. Alarm and operator events may be logged to disk. GENESIS allows for the development of an unlimited number of displays that may include dynamic shapes which expand or contract in proportion to the value of the data points they are connected to. GENESIS also provides the capability, via the ARCNET or NETBIOS compatible networks, to network a number of personal computers together and provide data to all nodes.

The PMAD data system consists of four ARCNET-networked 386 AT&T, IBM-compatible personal computers running GENESIS. A device driver was developed under contract with SDI and enhanced in-house to allow the connection of a non-GENESIS (remote) personal computer running any data collection algorithm written in C to a GENESIS node through an ARCNET interface. This driver is used to collect data from seven Analog Devices uMAC-6000's. The uMAC's currently collect analog data from 396 voltage, current, pressure, and temperature sensors and control and monitor 232 digital channels. Two remote personal computers collect the data from the uMAC's with an IEEE-488 direct memory access and organize the data in a data array for transfer to the GENESIS node. Two additional remote personal computers collect MIL-STD-1553 data from 1553 monitors built in-house, decode the data, and transfer them to GENESIS nodes. Currently, three hundred and sixty-four 1553 data words are collected. All of the PMAD data system data are scanned every 0.25 sec.

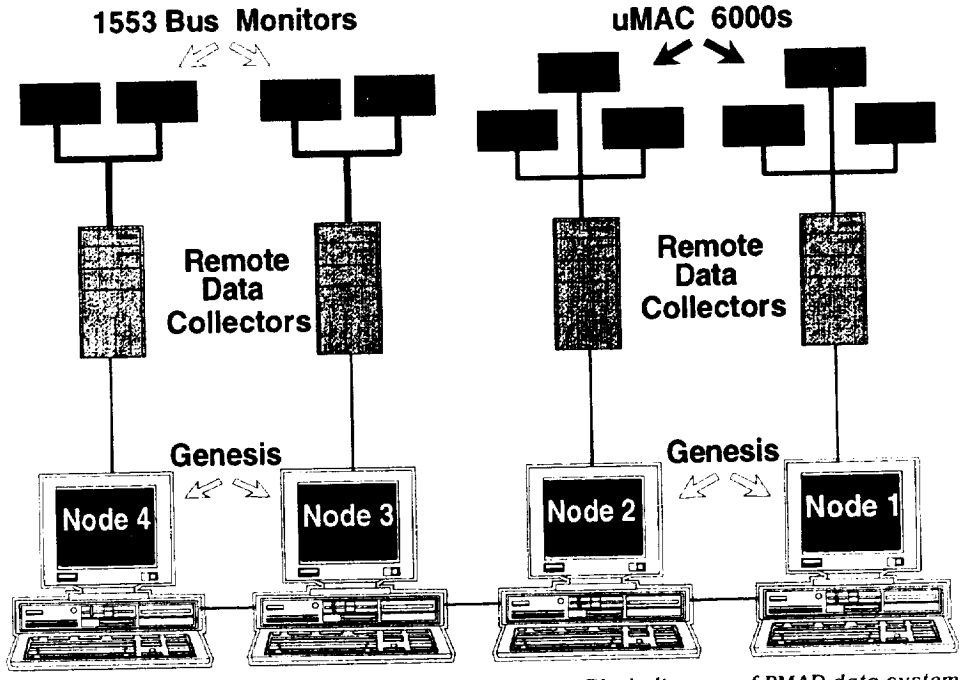

Block diagram of PMAD data system.

The remote driver that was developed for the PMAD data system has proven to be effective and flexible. Work is under way to connect a Colorado Data Systems instrument-on-a-card system to the uMAC's remote personal computers that will provide additional transistor-transistor logic control interfaces and additional 1553 control and data acquisition capabilities. The driver will not have to be modified to support this addition. The freedom to have any data collection process running on a personal computer and the ability to utilize the GENESIS data collection and display functions make the PMAD data system flexible and easily adaptable to changing test requirements.

Bibliography

Trase, L.M.; et al.: Description of the PMAD Systems Testbed Facility and Data System. Proceedings of the 27th Intersociety Energy Conversion Engineering Conference: IECEC '92, Vol. 6, T. Bland and B. McFadden, eds., Society of Automotive Engineers, Warrendale, PA, 1992, pp. 6.61–6.65.

Lewis contact: Larry M. Trase, (216) 433-5347
Headquarters program office: OSSD

Robots Change Out Electric Power System Components

A major Space Station *Freedom* goal is to maximize the use of telerobotic manipulators for assembly and maintenance operations. NASA Lewis, with Rocketdyne Division of Rockwell International, is attempting to make this goal a reality.

The majority of the orbital replacement units (ORU's) are being designed for robotic maintenance. The soon-to-be developed Canadian special-purpose dextrous manipulator (SPDM) will be used to change out these ORU's. The SPDM is a 14-joint robot, with two seven-degree-of-freedom dexterous arms.

Several robotic changeout tests have taken place in 1992, involving a battery, an electronics control unit, a remote power control module, and a sequential shunt unit. These ORU's have been designed as modular replacement items, are box shaped, and vary in size from shoe box to well over breadbox. The battery was the largest ORU tested, measuring 36 by 40 by 19 in.

These remove-and-replace tasks are well planned, beginning with a known set of robotic requirements, including definitions of standard robotic interfaces, standard robotic tools, established camera views, loading capabilities, and robotic alignment guides. Following a first cut at designing the robotic features of each ORU, specially trained NASA Lewis Operations personnel analyzed the complete maintenance task, from start to finish. The Computer Graphics and Simulation Laboratory at Rocketdyne houses unique silicon graphics simulation tools to provide insight regarding camera views, lighting, clearances, etc. Geometric and kinematic simulations have proven to be quite helpful in determining the design and location of the robotic enhancements to the hardware and the surrounding system. Finally, lightweight mockups were built, incorporating the concepts for robotic compatibility.

The tests have taken place in two locations: Loral Space Systems, Palo Alto, California, and Oceaneering Space Systems, Houston, Texas. Both facilities have provided early insight into the proposed capabilities of the Canadian SPDM robot. The Oceaneering facility has a unique capability to use the robot under water, allowing higher fidelity (and greater weight) mockups to be tested. All of the tests were successful. Robotic changeout concepts have been demonstrated for these ORU's. Thermal and electrical contacts were mated robotically in all cases. Without exception, it has been shown that camera views are critical for the task. In each test, in addition to the manipulation and positioning of the ORU, a screw was actuated to complete the changeout. This part of the testing helped to provide insight into the need for fastener status indication (i.e, some method for determining that the fastener is engaged). In one case a "picture frame" type of alignment guide proved to be optimal for insertion of the box into its footprint. In another test a unique concept for a robotic tool was tested with success.

Continued testing will ultimately verify complete compatibility with the planned Space Station *Freedom* robotic system. At this time the concepts appear to be viable. As Lewis and Rocketdyne move toward first element launch in 1996, the electric power system will be setting the standards for robotic operations.

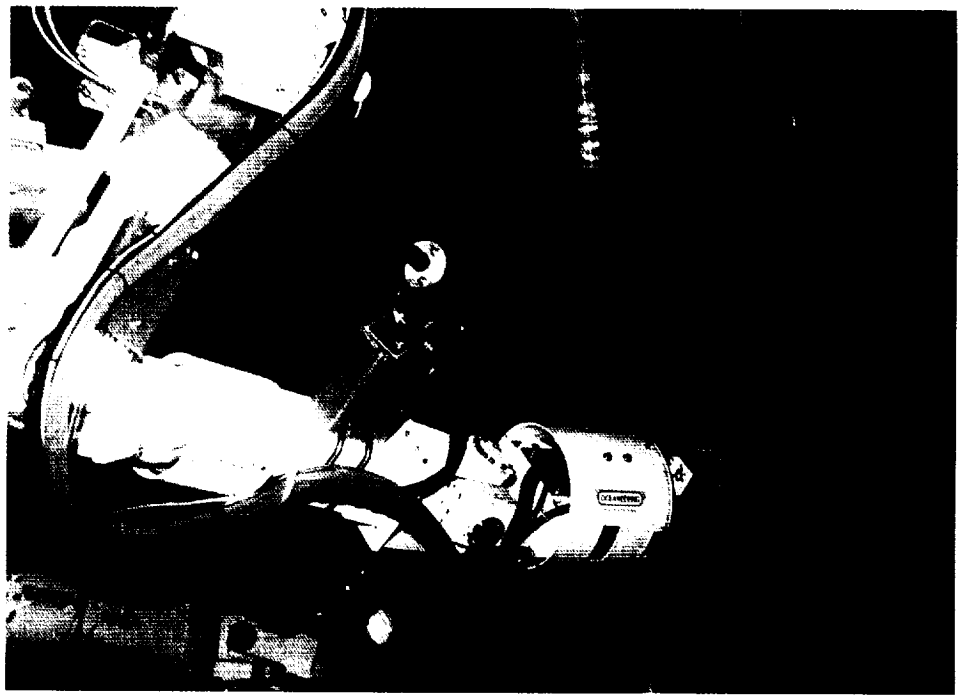

Robotic installation of remote power control module underwater at Oceaneering Space Systems.

Lewis contact: Robert D. Draper, (216) 433–6779
Headquarters program office: OSSD

Engineering Drawing Review System Devised

The design of the NASA Lewis electric power system (EPS) for Space Station *Freedom* will result in the creation of several hundred thousand drawing sheets. Traditionally, the mailing, storage, retrieval, and review of these sheets would be done with paper. However, the amount of drawings involved in EPS calls for a new approach to handling and reviewing engineering drawings. The new approach is to design an electronic analog of the paper method that preserves basic functionality while adding efficiencies that only a computerized system can provide. The result is Lewis' Drawing Review and Annotation System (DRAS).

The analogy is effected as follows: EPS drawings are generated for Lewis by Rocketdyne and its subcontractors on computer-aided design (CAD) systems in a vector format. Space Station *Freedom* Directorate engineers for the most part do not have CAD workstations, which are mandatory for viewing CAD drawings. They do, however, have personal computers that can deal with raster-format drawings. As suggested by Lewis, Rocketdyne converts the vector-format CAD drawing files directly into raster-format drawing files without creating paper copies as an intermediate step. In any event paper copies would require scanning (a cumbersome task) to convert them into raster format, and DRAS eliminates that step. Department of Defense, computer-aided acquisition and logistics system (CALS) headers and delivery report files are added to the raster drawing files and the entire set is "mailed" via a computer network to NASA Lewis. The "storage" at Lewis consists of a data base that tracks all the received drawings and physically keeps them on a laser storage system. The laser system can store 500,000 drawings in the same floor space in which flat files would hold 500 drawings. Another advantage of laser storage is that, unlike magnetic media, laser disks are not susceptible to moisture or electrical disturbances and thus provide longer, safer storage. The computerized data base allows engineers to search for drawings and "retrieve" copies directly from laser storage. Dozens of engineers can search and obtain copies at the same time and without the need to leave their offices. Once copied to their personal computers the drawings can be "reviewed" on screen electronically with red-lining tools. In those instances where paper copies are needed, they can be made of either the original

drawings or their red-lined versions. The red-lines, or engineering annotations, can then be shared over the local Lewis network or over the wide network with Rocketdyne, other NASA centers, or Space Station headquarters.

DRAS is an operational system. It was developed at Lewis by NASA, Boeing, and Analex personnel. The data-base coding and the laser storage coding were done by Boeing, and the network setup and routines were developed by Analex. Both groups worked under NASA direction. Beyond its day-to-day role as a delivery, storage, and review mechanism, DRAS will serve as the source for the official drawing deliveries to Space Station headquarters. DRAS is currently being used at NASA's Johnson Space Center, Marshall Space Flight Center, and Kennedy Space Center and at Space Station headquarters to obtain these drawings. It will fulfill the requirement to have all Space Station *Freedom* drawings available for the 30-year life of the program through the longevity of the laser storage system. Engineers will not have paper copies of drawings cluttering their offices. DRAS will result in a paper-less environment.

Lewis contact: Israel Greenfeld, (216) 433–5305
Headquarters program office: OSSD

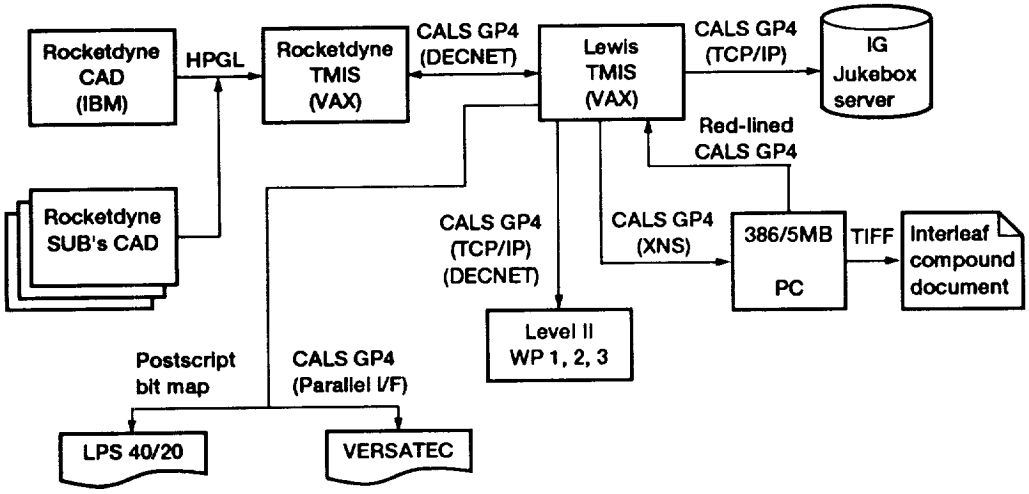

Architecture of DRAS system.

Engineering and Computational Support

Electronic and Control Systems

Launch Vehicle Flight Data Analyzed by Wavelet Transforms

In-depth analysis of flight data is becoming increasingly important in launch vehicle work, where design renovations often approach technology limits. Until recently, the classical windowed Fourier transform (e.g., power spectral densities of flight-data "snapshots") has been the standard spectral analysis tool for reassessing vehicle vibrations, transient loads, stability, and attitude control performance. However, this classical tool is often inadequate for handling high levels of dynamic coupling and transients. Modern time-frequency analysis methods, such as the wavelet transform, now have proven to perform better in these situations. In particular, wavelet methods have yielded remarkably accurate, useful results in analyzing fundamental characteristics of rapidly varying mechanical systems and environments, such as Atlas-Centaur launch vehicles in flight.

In short, a wavelet time-frequency signature, or "scalogram," of a band-limited time sequence (e.g., a recorded sequence of rate-gyro outputs) is a certain coherent way of expressing how its power spectrum changes with time. The scalograms are created by a finite decomposition using a particular set of compact waveforms, called analyzing wavelets, all having the same shape but with different scale factors and time shifts.

In applications using Atlas-Centaur flight data the contour maps of a three-dimensional scalogram over the time-frequency domain for rate-gyro outputs showed

- A very strong correlation with NASTRAN-predicted frequency curves
- Separable layers of both coarse features and fine details revealing important modal characteristics as well as transients and anomalies
- Decisive information on the interactions between attitude control mechanisms and vibration dynamics

In consequence, many critical areas in autopilot design, sensors, and dynamical modeling were identified for further review.

A personal-computer-compatible, signal-processing toolbox based on wavelet transform theory has been recently developed at NASA Lewis. This toolbox has been applied successfully in analyzing Atlas-Centaur telemetry data, providing reliable results on vehicle dynamics and control responses. This toolbox includes an extensive wavelet library, algorithms, and automated criteria for scalogram generation, reconstruction of selective modal components, frequency-versus-time curves for vibration modes, wavelet selection, and filtering with wavelets.

This analysis tool is useful in studying launch vehicle attitude stability, control performance, component loads, and control structure interaction or in sensor outputs from space experiments. Furthermore, a similar workbench for processing two-dimensional signals can be developed with the same principle and structure. This future workbench can be used to improve related technologies in space experiments, flow research data, medical imaging, and computer-assisted diagnosis.

This work was performed in-house at NASA Lewis, with contract support by Analex Corporation.

Bibliography

Rioul, O.; and Vetterli, M.: Wavelets and Signal Processing. *IEEE Signal Processing Magazine*, Oct. 1991, pp. 14–38.

Lewis contacts: Dr. Dzu K. Le, (216) 433–5640; Dr. Rick Lalonde, (216) 433–0162
Headquarters program office: OAST

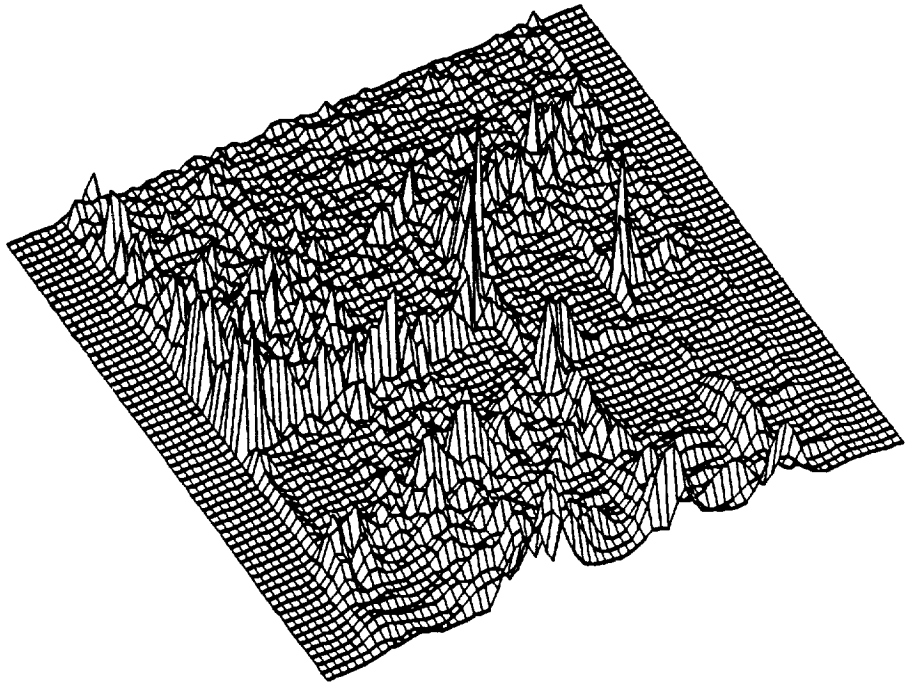

Scaleogram of AC102 forward-pitch-rate gyro.

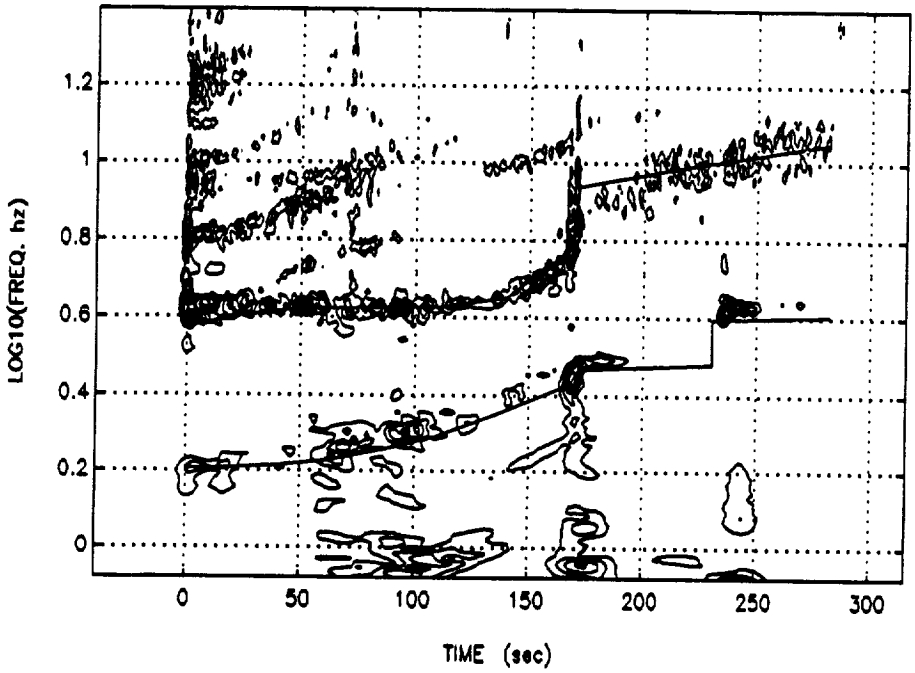

Level contour plot of scaleogram (with NASTRAN overlay). NASTRAN frequency curves are of first and second modes.

Electric-field-radiated susceptibility testing of a space experiment.

Electromagnetic Interference Test Facility Installed

The Engineering Directorate has completed installation of a new electromagnetic interference (EMI) test laboratory to support the Center's needs for electronic systems development and qualification. The EMI test facility contains a 12- by 16- by 8-ft shielded enclosure and adjacent control room for performing standardized conducted and radiated emissions and susceptibility testing over a frequency range of 20 Hz to 18 GHz, depending on the test.

The laboratory can qualify flight hardware to MIL-STD-461/462 derived tests. Of equal importance it can assist electronics designers in evaluating prototype circuit boards and engineering models at a developmental stage, where fixes may be most effectively implemented. This approach improves overall system design margins and hence the probability of passing flight qualification tests when required.

Computer-automated instrumentation is utilized to provide accurate and repeatable tests in the shortest time. This is advantageous for autonomous space experiments when EMI measurements must be synchronized to an operational time line. By using broadband electric field sensors in a closed-loop control system, for example, output leveling of the radiofrequency power amplifiers can produce a preprogrammed electric field profile as a function of frequency. Radiated susceptibility electric field levels of at least 20 V/m can be achieved from 14 kHz to 18 GHz.

Lewis contact: Noel B. Sargent, (216) 433-2398
Headquarters program office: OAST

Structural Systems

Finite Element Method Developed for Dynamically Analyzing Preloaded Beam in Space

Space structures, such as the Space Station *Freedom* photovoltaic arrays, are large, lightweight, flexible structures. Accurate prediction of the natural frequencies and mode shapes is essential for determining the structural adequacy of components and designing a controls system. The tension preload in the "blanket" of photovoltaic solar collectors, as well as the free/free boundary conditions of a structure in space, causes serious reservations about the use of standard finite element solution techniques. In particular, a phenomenon known as "grounding" or false stiffening of the stiffness matrix occurs during rigid-body rotation.

The "grounding" phenomenon was examined in detail for a beam element. Numerous stiffness matrices developed by existing methods were examined for rigid-body rotation capability and found lacking. Various techniques were then used for developing new stiffness matrices from the rigorous solutions of the differential equations, including the solution of the directed-force problem. A new directed-force stiffness matrix was developed that provides all the rigid-body capabilities for a beam in space.

Lewis contacts: Damian Ludwiczak, (216) 433–2383; Marsha Nall, (216) 433–5374; Dr. Paul Bosela, (216) 433–6508
Headquarters program office: OSSD

Random Vibration Environment Predicted for ACTS

Properly qualifying spacecraft components to the dynamic environment of their launch vehicle is essential to mission success. Normally, component random vibration tests are performed at the box level at test levels expected to envelop flight vibration. Later these same components are often exposed to a spacecraft system acoustic test that represents the expected flight acoustic environment.

The Advanced Communications Technology Satellite (ACTS) is scheduled to be launched by the Space Shuttle in June 1993. A computer program called VAPEPS (for vibroacoustic payload environment prediction system) has been used to predict the vibration that the ACTS components would see when exposed to the expected acoustic environment of the Space Shuttle. VAPEPS, which is based upon statistical energy analysis, is managed by the Jet Propulsion Laboratory and is currently sponsored by NASA Lewis.

NASA Lewis performed a VAPEPS analysis of ACTS in 1988. The analysis indicated that 83 percent of the ACTS components were satisfactorily qualified by their box-level random vibration test. The remaining 12 components were predicted to have spacecraft acoustic test responses that would exceed their box qualification vibration test levels. In March 1992 the ACTS spacecraft acoustic test was performed and this prediction was confirmed. Thirteen components had exceedances, including all 12 named in the

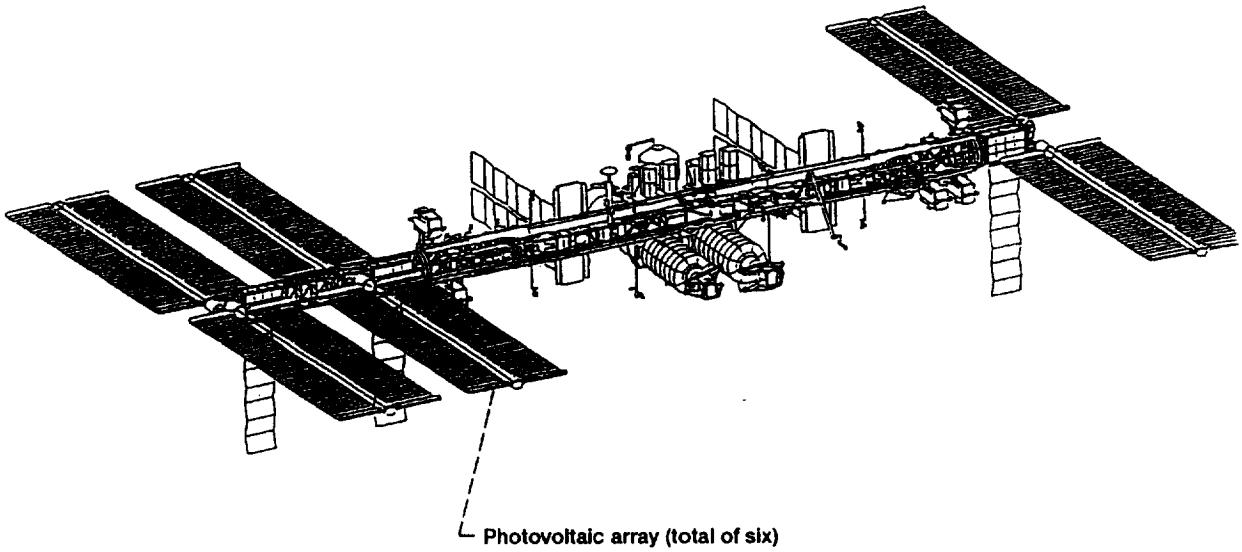

Finite element model uses 100 beam elements.

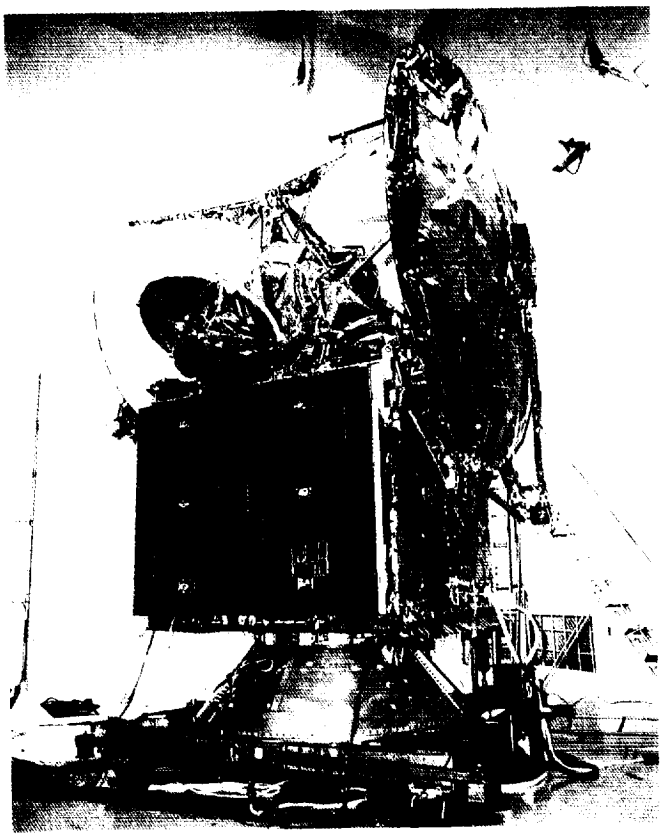

ACTS acoustic test configuration.

earlier test. These components are now being analyzed to determine if they are suitable for flight.

The VAPEPS prediction methodology utilized for the ACTS program has proved to be an accurate prediction tool that may be used early in a program to properly qualify spacecraft components. This tool may be applied to missions flying on either the Space Shuttle or on expendable launch vehicles.

Bibliography

Hughes, W.O.; and McNelis, M.E.: Summary of ACTS Component Random Vibration Specification Analysis. Presentation to ACTS Project Office, June 19, 1992.

Lewis contact: William O. Hughes, (216) 433-2597
Headquarters program office: OSSA

Computational Support

Computer Software Testbed Will Aid Structural Design

A major task assigned to structural engineers is the design of a structural component or piece of equipment. A salient design feature is reducing the cost while ensuring that all required specifications are met. This process is referred to as optimal design. Examples abound in aerospace and other disciplines.

Consider the structure needed to hold in place solar array panels on Space Station *Freedom*. The panels must remain separated from each other, as well as from other modules, such as the habitation modules. The major cost involved with, for example, the long spacer and the short spacer is usually the cost to transport them to low Earth orbit, where the space station will be located. Major cost savings can be gained by reducing the weight of the structure. The structure must be strong enough, however, to hold the panels in place and must survive the stresses and vibrations induced during launch and ascent to orbit without excessive deformations, which could damage itself or the cargo bay of the Space Shuttle.

Airframes of commercial aircraft are another example. Consider airplane wings, which undergo stress and displacement (i.e., relative movement) during flight. Specifications are imposed to restrict the amount of stress in the wing in order to prevent collapse, as well as the amount the tips of the wings rise relative to the fuselage. Reducing the weight of the wing is often an important component of cost reduction.

Traditional engineering design techniques for these kinds of structures include a method known as the fully stressed design. This method attempts to reduce the weight of each component (e.g., each bar) until its stress matches the stress specification. During the 1960's the mathematical optimization techniques of nonlinear programming came into use in structural engineering. Many different mathematical algorithms have been developed and implemented in computer programs. But until now, there has been no easy means of comparing these different algorithms

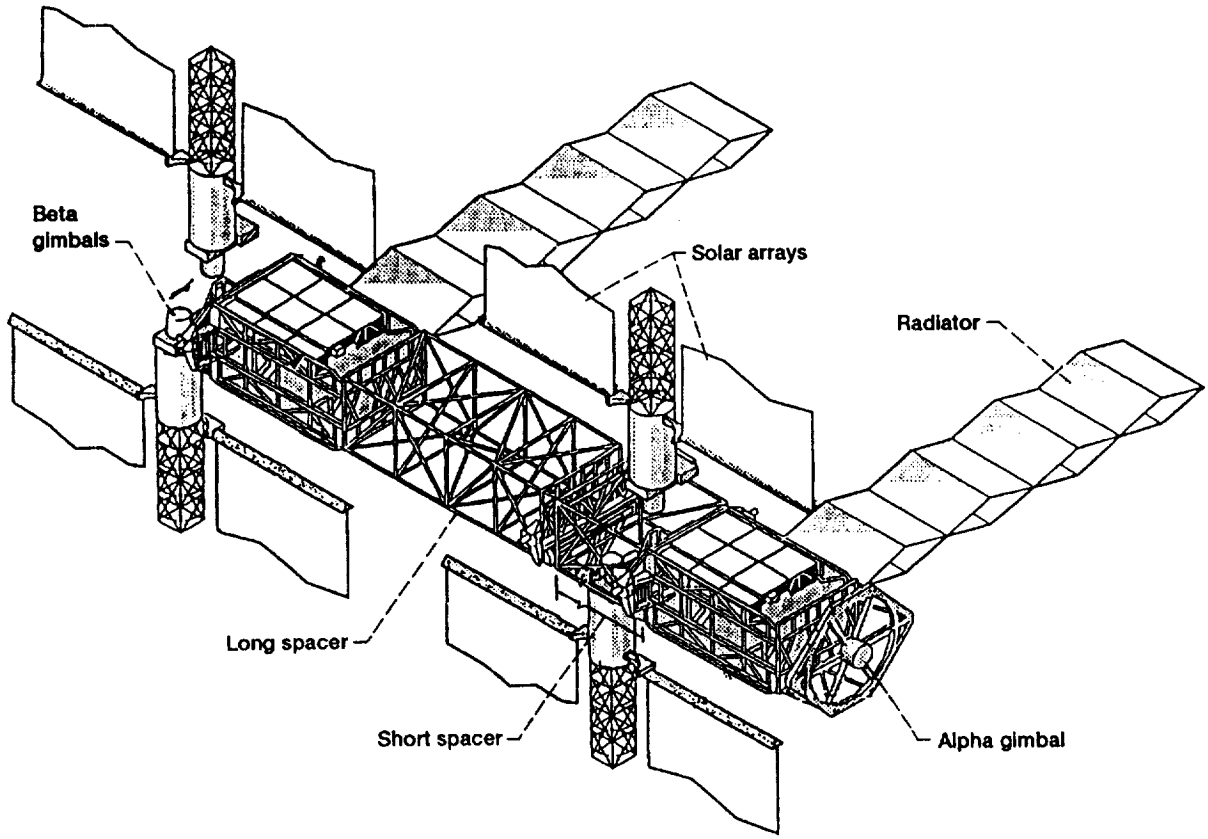

Space station conceptual design configuration near solar array panels.

and techniques to determine which perform best for optimal design of these kinds of structures.

To help fill this need, NASA Lewis, in collaboration with the Ohio Aerospace Institute, is developing a computer software testbed called CometBoards. This acronym stands for a comparative evaluation testbed of optimization and analysis routines for the design of structures. It is essentially a collection of optimization routines, analysis routines, data input routines, and interface routines. The data input routines provide the ability to build a computer model of the structure and allow structural specifications to be declared. The analysis routines use the computer model to calculate the stresses, displacements, and other important characteristics of the structure. The optimization routines provide the design algorithms, and the interface routines link them together. These routines are being developed and modified so that they can be easily interchanged. For example, one will be able to choose a particular set of data with any one analysis routine and use it with any or all of the optimization techniques available in the testbed. Similarly, the same data with the same choice of analyzer and optimizers could be run on a variety of computer systems. A simple command is used to run CometBoards.

The initial release of the testbed software for use on a variety of Posix (i.e., Unix-like) computers, as well as computers using the IBM VM/CMS operating system, is scheduled to be available through the NASA Computer Software Management and Information System (COSMIC) in early 1993.

Lewis contacts: Dr. James D. Guptill, (216) 433–45213; Dr. Surya Patnaik, (216) 433–8368
Headquarters program office: OAST

Lewis Research Academy

Flow Modeling Aids Turbomachinery Research

A mathematical analysis has yielded a set of equations governing the conceptual flow model currently used to design turbomachinery blading. These equations govern the time-averaged flow state within a typical passage of a blade row embedded in a multistage configuration. This mathematical exercise has been transformed into a number of computer simulation models and has aided in the formulation of two turbomachinery research programs.

The first research program was jointly conducted with the Massachusetts Institute of Technology (MIT). This research effort used a Lewis-developed viscous turbomachinery flow code to uncover the flow physics associated with axial skew grooved casing treatment. This form of treatment has been found to be effective in increasing the stable operating range of fans and axial-flow compressors. A series of experiments performed at MIT showed that this form of casing treatment greatly altered the character of the end-wall flow. It was believed that this was the primary reason for the increase in the stable operating range.

The numerical simulations executed with the viscous code revealed the details of the flow in the end-wall region, including the interaction between the clearance flow and the flow entering and exiting the casing treatment. It was found that this interaction led to the observed increase in operating range. This work was presented at the 1992 ASME Gas Turbine Conference and accepted for publication in the ASME Journal for Turbomachinery.

The second research project involved the design of an advanced axial-flow multistage compressor. This project was jointly conducted with Allison Gas Turbine. The design consists of two stages with a combined pressure ratio of 5. A three-dimensional viscous flow code developed at Lewis that simulates the flow within a typical blade row passage of a multistage configuration was used to examine the aerodynamic interactions of the blade rows and access the stall stability boundary.

Over a dozen multistage configurations were examined at their design settings. Of these, four were analyzed to determine their stall limits at design speed. The design phase of this activity has been completed, and the fabrication of the final design is under way. This compressor will be tested at Lewis in fiscal 1993.

Lewis contact: Dr. John J. Adamczyk, (216) 433-5829
Headquarters program office: OAST

Numerical Solutions Show Sensitivity of Turbulence to Initial Conditions

Most fluid flows (those made by humans and those occurring in nature) are turbulent. In spite of considerable progress over the last century, our understanding of turbulence is still incomplete. Much of our inability to predict turbulent flows stems from that lack of understanding. In order to better characterize turbulence, numerical solutions of the unaveraged Navier-Stokes equations have been obtained at NASA Lewis.

We have shown (ref. 1) that a basic characteristic of forced turbulence is sensitive dependence on initial conditions; that is, a small change in initial conditions completely changes the values of the instantaneous velocity components a short time later. More recently (ref. 2), that has been shown to be a characteristic of decaying turbulence as well as of forced turbulence. In order to determine whether sensitive dependence on initial conditions, or chaos, is a characteristic of the turbulence itself, rather than a characteristic of the numerical method used (i.e., to rule out spurious chaos), the effect of numerical resolution on the chaos was investigated.

The results are shown in the three graphs, where u_1 is a component of the velocity fluctuation at the numerical grid center and at time t, u_0 is the initial velocity fluctuation, the overbar indicates a space average, ν is the kinematic viscosity, and x_0 is the initial scale of the fluctuations. The effect of spatial resolution on the indicated sensitivity of the flow to small changes in initial conditions can be seen by comparing the initially perturbed (dashed) curves to the unperturbed (solid) curves.

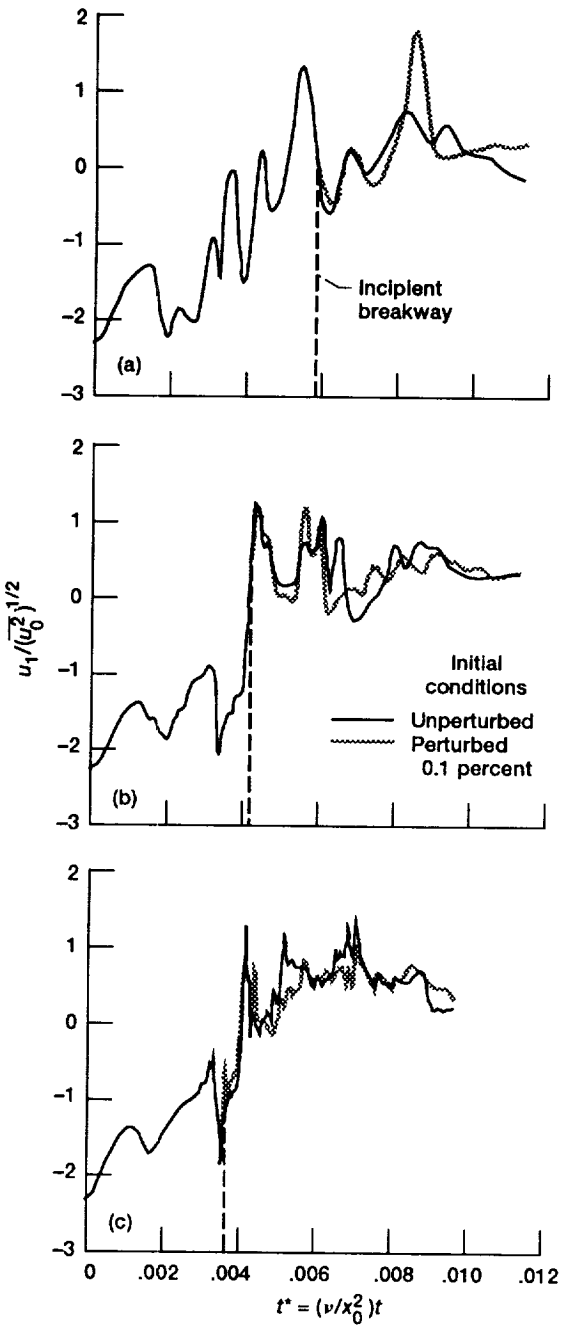

Calculated evolution of velocity fluctuations for (a) 32^3 grid points, (b) 64^3 grid points, and (c) 128^3 grid points.

Take as a measure of that sensitivity the value of t^* at which a perturbed solution first shows a definite break with the unperturbed one (the incipient breakaway time). It is clear that improved resolution increases the sensitivity of the solution to small initial-condition changes: The perturbed solution breaks away from the unperturbed one sooner for the more highly resolved cases with more grid points. Similar results were obtained for other velocity components and at other grid points. These are comforting observations because, if the results were otherwise, the observed chaos in the solutions might be due to inadequate numerical resolution. Further details of this work are given in reference 2.

References

1. Deissler, R.G.: Is Navier-Stokes Turbulence Chaotic? Phys. Fluids, vol. 29, no. 5, 1986, pp. 1453–1457.

2. Deissler, R.G.: Effect of Spatial Resolution on Apparent Sensitivity to Initial Conditions of a Decaying Flow as It Becomes Turbulent. J. Computational Phys., vol. 100, no. 2, 1992, pp. 430–432.

Lewis contact: Dr. Robert G. Deissler, (216) 433–5823
Headquarters program office: OAST

Analysis of Adverse-Pressure-Gradient Boundary Layer Transition Extended

The prediction of boundary layer transition is a major unresolved issue in aircraft design. This phenomenon is commonly studied experimentally by artificially introducing relatively two-dimensional, small-amplitude, single-frequency disturbances in the flow. An excitation device, such as a vibrating ribbon or an acoustic speaker, is used. These disturbances are initially well described by linear stability theory, and their two-dimensional linear behavior can persist over a long streamwise distance when the excitation levels are sufficiently small. However, the disturbances usually become three-dimensional and nonlinear at sufficiently large downstream distances. The initial nonlinear stage is reasonably well understood and is associated with a resonant-triad interaction between a basic fundamental two-dimensional mode and a pair of oblique subharmonic modes. This stage is effectively a parametric resonance regime because the oblique modes do not affect the plane wave. However, a nonlinear stage ultimately will develop where the waves in the resonant triad are fully interacting.

Most experiments are carried out on a thin, flat plate carefully aligned with the upstream flow. Transition in technological devices, however, often occurs in regions with adverse pressure gradients, and the onset of transition usually occurs about four or five wavelengths upstream of

the resulting transition point. In an adverse-pressure-gradient situation the linear instability waves are essentially inviscid instabilities of the Rayleigh type. As previously worked out (ref. 1), asymptotic analysis of the fully interactive nonlinear stage for this flow situation has now been extended. Viscosity effects have been incorporated and the fundamental disturbance has a larger initial amplitude so that it becomes strongly nonlinear before or just as the parametric resonance stage occurs. In the previous inviscid case the nonlinear self-interaction of the oblique modes completely dominated the downstream development and caused an explosive growth. The effects of these extensions on those interactions are now being evaluated numerically.

Reference

1. Goldstein, M.E.; and Lee, S.S.: Fully Coupled Resonant-Triad Interaction in an Adverse-Pressure-Gradient Boundary Layer. J. Fluid Mech., vol. 245, Dec. 1992, pp. 523–551.

Lewis contacts: Dr. Marvin E. Goldstein, (216) 433–5825; Dr. Lennart S. Hultgren, (216) 433–6070
Headquarters program office: OAST

Radiation Heat Transfer Effects Studied in Semitransparent Materials

Heat transfer becomes complex in materials that are partially transparent to radiant energy. Infrared and visible radiation from hot surroundings penetrate into the material, heating it internally. This is similar to the way in which food is heated in a microwave oven. When the temperature in the material is elevated, internal energy emission becomes significant. There is also internal transmission, absorption, and scattering of radiant energy. The energy transport within the material depends on these effects combined with heat conduction. Radiant energy transfer can affect internal temperatures of some ceramic engine parts and coatings because they are often partially transparent to radiation in some portions of the wavelength spectrum. This is also true of some crystals being grown in microgravity experiments.

Research is being done to develop improved analytical and numerical methods for predicting internal temperature distributions and heat flows

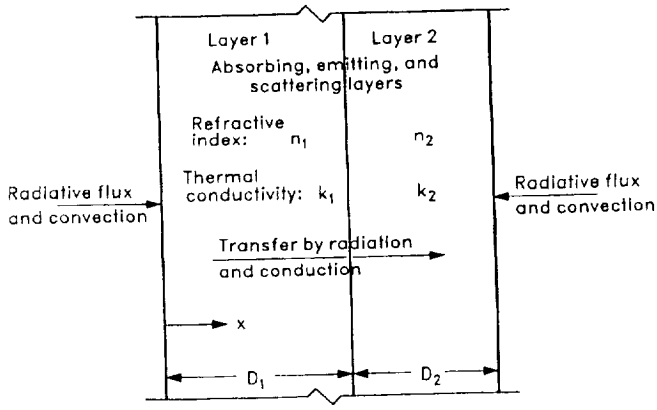

Radiation heat transfer in heated semitransparent laminate with two layers.

in partially transparent materials. This in-house research is a continuing effort. In references 1 to 5, radiation combined with heat conduction has been analyzed in plane layers with refractive indices typical of ceramic materials. The materials partially absorb, emit, and scatter internal radiant energy. Each boundary is heated by differing amounts of radiation and convection, and the effect of interface reflections is included. Because the refractive index is larger than 1, there are total internal reflections at the boundaries for some energy directed outward from within the layer. The reflections distribute energy within the layer and considerably alter the temperature distribution as compared with having a refractive index of 1 and no internal reflections.

Results have been obtained for a single layer that is either gray or has a two- or three-band spectral variation of the absorption coefficient. Various amounts of isotropic scattering are included to simulate internal reflections within the ceramic due to a granular or reinforcing structure. The solutions provide temperature distributions that show thermal performance and can be used to examine thermal stresses. The radiant energy leaving the layer was considered to see if it can be used to measure the surface temperature. The prediction can be inaccurate when scattered energy from the interior of the material is not characteristic of the surface temperature.

The solution is being extended to a two-layer laminate, and an additional layer will then be included. This will simulate a ceramic layer with internal reinforcement by another material. An analytical solution has been found for the special case of pure radiation in a plane layer composed of an arbitrary number of laminated sublayers.

This solution is approached when there is small heat conduction and small convection at the external boundaries. Each sublayer can have a different refractive index, thickness, and set of optical properties. Each interface is assumed to be diffuse, and all internal interface reflections are included. This special solution is being compared with results from the current computer program being developed for a two-layer laminate with internal conduction and external convection.

References

1. Spuckler, C.M.; and Siegel, R: Refractive Index Effects on Radiative Behavior of a Heated Absorbing-Emitting Layer. J. Thermophys. Heat Trans., vol. 6, no. 4, 1992, pp. 596–604.

2. Siegel, R.; and Spuckler, C.M.: Effect of Index of Refraction on Radiation Characteristics in a Heated Absorbing, Emitting and Scattering Layer. J. Heat Trans., vol. 114, no. 3, Aug. 1992, pp. 781–784.

3. Spuckler, C.M.; and Siegel, R.: Refractive Index and Scattering Effects on Radiative Behavior of a Semitransparent Layer. To be published in J. Thermophys. Heat Trans., 1993.

4. Siegel, R.; and Spuckler, C.M.: Refractive Index Effects on Radiation in an Absorbing, Emitting, and Scattering Laminated Layer. To be published in J. Heat Trans., 1993.

5. Siegel, R.; and Spuckler, C.M.: Variable Refractive Index Effects on Radiation in Absorbing, Emitting and Scattering Multilayered Regions. To be published in J. Thermophys. Heat Trans., 1993.

Lewis contact: Dr. Robert Siegel, (216) 433–5831

Headquarters program office: OAST

New Computational Techniques Developed for Material Science

A great deal of progress has been made in developing quantum mechanical techniques for calculating the mechanical properties of real materials for static geometries. However, these techniques have not reached the point where configurational energy minimization, dynamic effects, and thermal effects can be accomplished in reasonable computing time. Consequently, NASA Lewis has been developing new semiempirical methods that accurately predict the energy of defects and can be used efficiently to accomplish the latter goals.

Different classes of materials, such as metals, semiconductors, and ceramics, require different approaches because of bonding differences. Lewis is developing techniques that build on our previous discoveries of the universal binding energy equation and on the similarities between these different classes. At this point, many properties of metals and semiconductors have been successfully predicted and the approaches have been used to calculate alloy properties. Current research in extending the techniques has concentrated on methods for including thermal effects, which will also enable the prediction of phase diagrams in alloys and the development of configurational energy minimization techniques. The initial stages of this work, examining surface segregation in binary alloys, is presented in reference 1.

The second phase of this effort is to build on the methods in order to predict the properties of ceramics. This problem has been approached by adding a Coulomb term to the universal binding energy relation. This approach had been shown to predict the binding energy relation of alkali halides, which have an approximate charge transfer of 1.0. In order to be useful in predicting the properties of ceramics, the methods must be able to predict material properties with a wide range of charge transfers. Thus, the methods were applied (ref. 2) to predicting the equation of state for the ceramic compound magnesium oxide, which has a charge transfer of approximately 2.0. The theoretical prediction agreed accurately with the experimental data. This alloy theory is being extended to predict the properties of ceramics.

References

1. Bozzolo, G.; Good, B.; and Ferrante, J.: Heat of Segregation of Single Substitutional Impurities. Submitted for publication to Surface Science.

2. Schlosser, H.; and Ferrante, J.: A High Pressure Equation of State for Partially Ionic Solids. Submitted for publication to Physical Review B.

Lewis contact: Dr. John Ferrante, (216) 433–6069

Headquarters program office: OAST

Author Index

REPORT DOCUMENTATION PAGE

Form Approved
OMB No. 0704-0188

1. AGENCY USE ONLY (Leave blank)	2. REPORT DATE	3. REPORT TYPE AND DATES COVERED
		Technical Memorandum

4. TITLE AND SUBTITLE

Research & Technology 1992

5. FUNDING NUMBERS

None

6. AUTHOR(S)

7. PERFORMING ORGANIZATION NAME(S) AND ADDRESS(ES)

National Aeronautics and Space Administration
Lewis Research Center
Cleveland, Ohio 44135-3191

8. PERFORMING ORGANIZATION REPORT NUMBER

E-7425

9. SPONSORING/MONITORING AGENCY NAMES(S) AND ADDRESS(ES)

National Aeronautics and Space Administration
Washington, D.C. 20546-0001

10. SPONSORING/MONITORING AGENCY REPORT NUMBER

NASA TM-105924

11. SUPPLEMENTARY NOTES

Responsible person, Walter S. Kim, (216) 433-3742

12a. DISTRIBUTION/AVAILABILITY STATEMENT

Unclassified - Unlimited
Subject Category 01 and 31

12b. DISTRIBUTION CODE

13. ABSTRACT *(Maximum 200 words)*

This report selectively summarizes the NASA Lewis Research Center's research and technology accomplishments for the fiscal year 1992. It comprises approximately 200 short articles submitted by the staff members of the technical directorates. The report is organized into six major sections: Aeronautics, Aerospace Technology, Space Flight Systems, Space Station *Freedom*, Engineering and Computational Support, and Lewis Research Academy. A table of contents by subject has been developed to assist the reader in finding articles of special interest. This report is not intended to be a comprehensive summary of all the research and technology work done over the past fiscal year. Most of the work is reported in Lewis-published technical reports, journal articles, and presentations prepared by Lewis staff or by contractors. In addition, university grants have enabled faculty members and graduate students to engage in sponsored research that is reported at technical meetings or in journal articles. For each article in this report a Lewis contact person has been identified, and where possible, a reference document is listed so that additional information can be easily obtained. The diversity of topics attests to the breadth of research and technology being pursued and to the skill mix of the staff that makes it possible.

14. SUBJECT TERMS

Aeronautics; Aerospace engineering; Space flight; Space station power supplies; Materials; Structural analysis; Computational fluid dynamics; Computer programming

15. NUMBER OF PAGES

170

16. PRICE CODE

A08

17. SECURITY CLASSIFICATION OF REPORT	18. SECURITY CLASSIFICATION OF THIS PAGE	19. SECURITY CLASSIFICATION OF ABSTRACT	20. LIMITATION OF ABSTRACT
Unclassified	Unclassified	Unclassified	